5TH INTERNATIONAL CONFERENCE
INTERFACES AGAINST POLLUTION 2008

June 1-4 Kyoto, Japan

PROGRAM & ABSTRACTS

IAP2008

5th International Conference
Interfaces Against Pollution 2008

1-4, June 2008

Clock Tower Centennial Hall,
Kyoto University

IAP2008　国内委員会

Auspices:

JSPS (Japan Society for the Promotion of Science) etc.

IAP2008 Office
Yasuhisa Adachi, University of Tsukuba
Tennoudai 1-1-1, Tsukuba-shi, Ibaraki 305-8572, Japan
Tel. +81(0)29-853-4862
Fax. +81(0)29-853-7198
Mail: iap2008@envr.tsukuba.ac.jp
Website: http://www.rs.noda.tus.ac.jp/iap2008/

Cover Design: Miki Yamamoto (Univ. of Tsukuba)
Printed by ISEBU

Contents

IAP2008 Organizing Committee

Chairman
H. Ohshima (Tokyo University of Science)
Co-Chairmen
S. Ooi (National Institute for Rural Engineering)
Y. Adachi (University of Tsukuba)
Secretary General
M. Ishiguro (Okayama University)
Treasurer
K. Nakaishi (Ibaraki University)

International Board

L. K. Koopal (Netherlands)
J. Gregory (UK)
A. Barany (Hungary)
E. Klumpp (Germany)
F. Gonzalez-Caballero (Spain)
A. Delgado (Spain)
Y. Adachi (Japan)
S. Aidarova (Kazakhstan)
P. Behra (France)
M. Blesa (Argentina)
S. Bradford (USA)
A. Dabrowski (Poland)
I. Dekany (Hungary)
M. Elimelech (USA)
F. Frimmel (Germany)
E. Graber (Israel)
R. Kookana (Australia)
R. Kretzschmar (Switzerland)
N. Mishchuk (Ukraine)
K. Musabekov (Kazakhstan)
V. N. Parmon (Russia)
E. Pelizzetti (Italy)
J. Ralston (Australia)
B. Sulzberger (Switzerland)
E. Tombacz (Hungary)
R. van Genuchten (USA)
W. van Riemsdijk (the Netherlands)
H. Vereecken (Belgium)
K. Wilkinson (Canada)
D. Waite (Australia)
S. Ooi (Japan)

Domestic Board

K. Kaneko (Chiba University)
M. Miyahara (Kyoto University)
H. Tamon (Kyoto University)
H. Morisaki (Ritsumeikan University)
S. Wada (Kyushu University)
T. Miyajima (Saga University)
M. Abe (Tokyo University of Science)
A. Tanioka (Tokyo Institute of Technology)
M. Misono (National Institute of Technology and Evaluation)
S. Nakao (The University of Tokyo)
E. Iritani (Nagoya University)
K. Kurihara (Tohoku University)
K. Higashitani (Kyoto University)

Executive Committee

S. Nagasaki (The University of Tokyo)
N. Takisawa (Saga University)
M. Kobayashi (Iwate University)
T. Saito (The University of Tokyo)
M. Fukushima (Hokkaido University)
K. Nakatani (University of Tsukuba)
Y. Takata (Tokyo University of Science)
K. Makino (Tokyo University of Science)
H. Kano (Chiba University)
K. Ooi (National Institute of Advanced Industrial Science and Technology)
K. Kawamura (Tokyo Institute of Technology)
K. Kawamoto (Saitama University)
T. Hatta (Japan International Research Center for Agricultural Sciences)
Y. Yamashita (University of Tsukuba)
T. Tsuru (Hiroshima University)
M. Matsukata (Waseda University)
A. Satsuma (Nagoya University)
S. Nagao (Hokkaido University)
K. Hori (Nagoya Institute of Technology)
N. Ishida (National Institute of Advanced Industrial Science and Technology)
H. Shinto (Kyoto University)
M. Ohtsubo (Kyushu University)
K. Sasaki (Kyushu University)
I. Moriguchi (Nagasaki University)
S. Ozeki (Shinshu University)
T. Iiyama (Shinshu University)
K. Nakamura (Kyoto University)
S. Kawashima (Kyoto University)
C. Tokoro (Waseda University)
T. Makino (National Institute for Agro-Environmental Sciences)
T. Nashima (National Institute of Advanced Industrial Science and Technology)
M. Nanzyo (Tohoku University)
T. Ohmura (Tohoku University)
S. Hiradate (National Institute for Agro-Environmental Sciences)
T. Kanamori (National Institute of Advanced Industrial Science and Technology)
T. Yamaguchi (Tokyo Institute of Technology)
C. Inoue (Tohoku University)
Y. Mori (Doshisha University)
T. Moroizumi (Okayama University)
H.Kodama(Saga University)
Y. Mori (Shimane University)

Auspices and Sponsors

- The International Association of Colloid and Interface Scientists (IACIS)
- Japan Society for the Promotion of Science (JSPS)
- Japan Oil Chemists' Society (JOCS)
- Oreo-nanoscience Division, Japan Oil Chemists' Society
- The Society of Rheology, Japan (SRJ)
- The Society of Powder Technology, Japan (SPTJ)
- The Society of Chemical Engineers, Japan (SCEJ)
- Division of Materials & Interfaces, The Society of Chemical Engineers Japan
- Division of Separation Processes, The Society of Chemical Engineers Japan
- Japan Society on Water Environment (JSWE)
- Japanese Society of Soil Physics (JSSP)
- Japanese Humic Substances Society (JHSS)
- The Japan Society on Adsorption (JSAd)
- The Membrane Society of Japan (MSJ)
- Catalysis Society of Japan (CSJ)
- Japanese Society of Soil Science and Plant Nutrition (JSSPN)
- The Chemical Society of Japan (CSJ)
- The Division of Colloid and Surface Chemistry, the Chemical Society of Japan
- The Society of Polymer Science, Japan (SPSJ)
- The Japanese Society of Irrigation, Drainage and Reclamation Engineering (JSIDRE)
- Kurita Water and Environment Foundation
- Geo-Environmental Protection Center (GEPC)
- National Institute for Rural Engineering (NIRE)
- National Institute of Advanced Industrial Science and Technology (AIST)
- Research Foundation for the Electrotechnology of Chubu (REFEC)
- Hosokawa Powder Technology Foundation
- JSPS Core-to-Core Program Advanced Particle Handling Science
- University of Tsukuba
- Tokyo University of Science

Welcome to IAP2008

IAP is a successful series of conferences that was kicked off in Wageningen (The Netherlands, 1997) and was followed up in Miskolc (Hungary, 2002), Jülich (Germany, 2004) and Granada (Spain, 2006). The aim of these conferences is to provide a forum for scientists working on colloids and surfaces in relation to natural environments, environmental protection and remediation. Insight into fundamental aspects is very useful to broaden the interdisciplinary discussion. Such interaction between scientists is becoming more and more important not only for solving the environmental problems but also to consider the development of colloid and interface science. The Kyoto IAP meeting will be a new milestone in this field.

The organizing committee wishes to express sincere thanks to JSPS and other Sponsors for their financial supports. We also wishes all participants a successful and rewarding communication and to enjoy stay in Kyoto.

Hiroyuki OHSHIMA, Chairman of IAP2008

Plenary Lectures

(1A01) Luuk K. Koopal (Wageningen Univ., The Netherlands)

(2A01) Katsumi Kaneko (Chiba Univ., Japan)

(3A01) Michal Borkovec (Univ. of Geneva, Switzerland)

(4A01) Masao Doi (Univ. of Tokyo, Japan)

Keynote Lectures

(1A02) Kunimitsu Morishige (Okayama Univ. of Science, Japan)

(1A03) Jiuhui Qu (the Research Center for Eco-Environmental Sciences, China)

(2A02) Minoru Miyahara (Kyoto Univ., Japan)

(2A03) Menachem Elimelech (Yale Univ., USA)

(2A04) Hajime Tamon (Kyoto Univ., Japan)

(2A05) Takeo Yamaguchi (Tokyo Institute of Technology, Japan)

(2A06) Tomohisa Yoshioka (Hiroshima Univ., Japan)

(2A07) Koichi Eguchi (Kyoto Univ., Japan)

(2A08) Kei Inumaru (Hiroshima Univ., Japan)

(2A09) Robert S. Bowman (New Mexico Institute of Mining and Technology, USA)

(2A11) Hisao Morisaki (Ritsumeikan Univ, Japan)

(2B11) Taku Iiyama (Shinshu Univ., Japan)

(2E15) Masaru Ogura (Univ. of Tokyo, Japan)

(2E17) Takashiro Muroi (N. E. Chemcat Corp., Japan)

(2E18) Masami Fukushima (Hokkaido Univ., Japan)

(3A02) Nataliya Mishchuk (The National Academy of Sciences of Ukraine, Ukraine)

(3A03) William Ducker (The Univ. of Melbourne, Australia)

(3A04) Ko Higashitani (Kyoto Univ., Japan)

(3A05) Kazue Kurihara (Tohoku Univ., Japan)

(3A06) K. Hori (Nagoya Institute of Technology, Japan)

(3A07) Kenta Ooi (Advanced Industrial Science and Technology, Japan)

(3A08) David Waite (The Univ. of New South Wales, Australia)

(3A11) Marcelo Avena (Universidad Nacional del Sur, Argentina)

(3A15) Katumitu Hayakawa (Kagoshima Univ., Japan)

(4A02) Ryoichi Yamamoto (Kyoto Univ., Japan)

(4A03) Jérôme F. L. Duval (Nancy Univ., France)

(4A04) Toshinori Tsuru (Hiroshima Univ., Japan)

(4A05) Akihiko Tanioka (Tokyo Institute of Technology, Japan)

(4A07) Kaoru Tsujii (Hokkaido Univ., Japan)

(4A08) Arie de Keizer (Wageningen Univ., The Netherlands)

(4A09) Kenichi Sakai (Tokyo Univ. of Science, Japan)

(4A11) Isamu Moriguchi (Nagasaki Univ., Japan)

(4A13) Kiyoharu Nakatani (Univ. of Tsukuba, Japan)

(4A15) Mitsuhiro Fukuda (Hyogo Univ. of Teacher Education, Japan)

(4B13) Erwin Klumpp (Research Centre Jürich, Germany)

(4B15) Scott A. Bradford (US Salinity Laboratory, USA)

IAP-Engineering Forum (in Japanese)

Fundamentals and Frontiers of Environmental Technology

1st June 13:00-16:00 (Room A)

Toyoki Kunitake
Makoto Misonou
Ko Higashitani
Katsumi Kaneko
Takeo Yamaguchi

Interfaces for Beginners

3rd June 13:40-16:40 (Room C)

Hiroshi Maeda
Hiroyuki Ohshima
Setsuo Ooi
Koji Yamanaka
Yasuhisa Adachi

Conference Program

June 1

Room A

16:30 Opening

Chairs: Y.Adachi, K. Kaneko

16:40 1A01 **Plenary:** Luuk K. KOOPAL
HUMICS, SPECIAL COMPONENTS

17:10 1A02 **Keynote:** Kunimitsu MORISHIGE
Capillary Condensation in Ordered Mesoporous Materials

17:30 1A03 **Keynote:** Jiuhui QU, Hong He, Min Yang
Mirco-interface Processes and Application in the Transformation and Control of Environmental Pollutants

Room E & F

18:00 Welcome Mixer

June 2

Room A

Chairs: H. Kanoh, S. Kataoka, L. K. Koopal

9:00 2A01 **Plenary:** Katsumi KANEKO, T. Ohba, C.M. Yang, Y. Tao, N. Kojima, Y. Nobuhara, T. Konishi, T. Fujikawa, M. Yudasaka, S. Iijima, H. Kanoh
Structure of ions and molecules confined in carbon nanospaces

9:30 2A02 **Keynote:** Minoru MIYAHARA
Phase Behavior of Simple Fluid confined in Nanospace
― Finding Phase Diagram and Exploring into MOF Nanospace ―

9:50 2A03 **Keynote:** Menachem ELIMELECH
Antibacterial Effects of Carbon Nanotubes

10:10 2A04 **Keynote:** Hajime TAMON
Control of Morphology and Nanostructure of Carbon Cryogels

10:30 2A05 **Keynote:** Takeo YAMAGUCHI
Micro pore filling membranes and their unique performances
~from Bio-inspired materials to polymer electrolyte fuel cells~

June 2

Room A

10:50 Coffee Break

Chairs: J. Qu, A. Satsuma, H. Tamon

11:10 2A06 **Keynote:** Tomohisa YOSHIOKA
Gas permeation properties through ultra microporous inorganic membranes

11:30 2A07 **Keynote:** Koichi EGUCHI, S. Suzuki, T. Matsui, R. Kikuchi
Reversible NO_x Sorption-Desorption on Pt/mixed oxides

11:50 2A08 **Keynote:** Kei INUMARU
Mesoporous silica-based composite materials as molecular selective photocatalysts for purification of water

12:10 2A09 **Keynote:** Robert Stephen BOWMAN
Surfactant-Modified Zeolite and Its Application to Treatment of Oilfield Wastewaters

12:30 Lunch

Room A

Chairs: K. Hori, W. Lv

14:00 2A11 **Keynote:** Hisao MORISAKI
Consideration about Bacterial Attachment as Soft Colloidal Particles

14:20 2A12 Hiroyuki SHINTO, Y. Aso, J. Tsujimura, Y. Ohta, M. Ito, K. Higashitani
Adhesion, uptake, and cytotoxicity of engineered particles for living cells

14:40 2A13 Taisuke OHTSUKA, D. Nakai, Y. Nakamura, H. Morisaki, I. Yoshinaga, I. Imai
Algal assemblages on submerged reed stems and their influence on microbial activities

15:00 2A14 Melba Padua ORTEGA, T. Hagiwara, H. Watanabe, T. Sakiyama
Factors affecting adhesion of Staphylococcus epidermidis cells on stainless steel surface

Room A

15:20 Coffee Break

Chairs: H. Morisaki, H. Shinto

15:40 2A15 Ji-Zheng HE
Interactions of soil macromolecules and microbial DNA isolation

16:00 2A16 W. Lv, Y. Zhang, Min YANG
The impact of cell surface properties on the stability of inoculated yeast strains in a biological system used for treating high-strength oil-containing wastewater

16:20 2A17 Takehiko TSURUTA, Y. Aiba, T. Hirajima, K. Sasaki
Biosorption of some heavy metals using microorganisms

June 2

Room A

16:40 2A18 L. Fang, P. Cai, X. Rong, W. Liang, Qiaoyun HUANG
Determination of Copper and Cadmium Binding on Bacterial Cells by Chemical Modifications and Potentiometric Titration

Room B

Chairs: K. Ooi, A. Sineva

14:00 2B11 **Keynote:** Taku IIYAMA, S. Ozeki
The Direct Determination of Intermolecular Structure of Pollutants in Micropore Using *in situ* X-Ray Diffraction

14:20 2B12 Mathias FLÖERSHEIMER, K. Kruse, R. Polly, B. Schimmelpfennig, R. Klenze, T. Fanghänel
Speciation and Hydration of Mineral Surfaces Determined at the Molecular Level

14:40 2B13 A. Kondo, H. Noguchi, H. Kajiro, A. Tohdoh, Y. Hattori, W.-C. Xu, M. Inoue, T. Sugiura, K. Morita, H. Tanaka, T. Ohba, K. Kaneko, Hirofumi KANOH
CH_4 Storage and CO_2 Separation through Expansive Modulation of a Porous Coordination Polymer Sample

15:00 2B14 Yan CHENG, A. Kondo, H. Noguchi, H. Kajiro, K. Urita, T. Ohba, H. Kanoh, K. Kaneko
The Change of morphology and CO_2 adsorptivity of a Cu-MOF on Rehydration

15:20 Coffee Break

Chairs: M. Flösheimer, H. Kanda

15:40 2B15 Satoshi WATANABE, S. Mizuta, T. Yamamoto, and M. Miyahara
Stripe Pattern Formation on Hydrophilic Surfaces by Convective Self-Assembly

16:00 2B16 Koji TSUCHIYA, K. Fujiwara, T. Konno, K. Itani, T. Ito, T. Matsuura, K. Ohkawa, K. Tsubone, K. Sakai, H. Sakai, M. Abe
Ultrasound imaging of antibody-labeled microbubbles

16:20 2B17 Alissa V. SINEVA, A.M. Parfenova
Adsorption of Ionic and Non-ionic Surfactants on Shungite

16:40 2B18 K. Sawamura, Y. Sekine, E. Kikuchi, Masahiko MATSUKATA
Adsorption of water and methanol on ZSM-5 zeolite

Room E

Chairs: M. Fukushima, M. Ogura

14:00 2E11 Hisao HIDAKA, H. Honjo, T. Koike, T. Oyama, N. Serpone
Wastewater treatment: TiO_2 Photoassisted Degradation of the Binary Systems of Cationic/Anionic surfactants and their Components in Aqueous Dispersions

June 2

Room E

14:20 2E12 Xu ZHAO, H. Liu, J. Qu
Photoelectrocatalytic Degradation of Organic Contaminants at Novel Electrodes

14:40 2E13 C.-L. Chuang, Ming-Chun LU
Oxidation of trichloroethylene with persulfate in the presence iron oxide-coated sand

15:00 2E14 Chun HU, J. Guo, J. Qu, X. Hu
Photocatalytic degradation of pathogenic bacteria with AgI/TiO_2 under visible light irradiation

15:20 Coffee Break

Chairs: R. S. Bowman, K. Eguchi

15:40 2E15 **Keynote:** Masaru OGURA
K-doped Microporous Tectoaluminosilicate for Soot Combustion

16:00 2E16 Y. Saito, K. Shimizu, T. Nobukawa, N. Miyoshi, Atsushi SATSUMA
In-situ FT/IR Study on Dynamics of Stored Nitrates on Pt/Ba/MOx (M=Al, Zr, Si, Mg)

16:20 2E17 **Keynote:** Takashiro MUROI
Role of Zeolite for Air Pollution Control

16:40 2E18 **Keynote:** Masami FUKUSHIMA
Detoxification of organic pollutant by multi-functionalities of humic substances

Room F

Chairs: M. Barczak, S. Nagao

14:00 2F11 C. Tokoro, Y. Yatsugi, Daisuke HARAGUCHI, A. Otsuki, S. Owada, H. Sasaki
Removal mechanism of dilute As(V) or F(I) in wastewater using Fe(III) or Al(III) hydroxides co-precipitation method

14:20 2F12 Keiko SASAKI, H. Nakano, W. Wilopo, T. Hirajima
SPECIATION OF ARSENIC IN TREATMENT OF GROUNDWATERS SPIKED WITH ARSENITE USING PERMEABLE REACTIVE MATERIALS

14:40 2F13 Biplob Kumar BISWAS, J. Inoue, K. Inoue, H. Harada, K. Ohto, H. Kawakita
Use of orange waste and pectic acid gel for arsenic removal

15:00 2F14 M. Seredych, Teresa J. BANDOSZ
Removal of Ammonia on Graphite Oxides

15:20 Coffee Break

Chairs: K. Sasaki, T. Wajima

15:40 2F15 Olga L. GASKOVA
SURFACE PRECIPITATION MODELS FOR THE SORPTION OF HEAVY METALS ON CALCITE IN DRAINAGE FROM MINING DISTRICTS

June 2

Room F

16:00 2F16 C. Tokoro, S. Owada, A. Otsuki, T. Shiozawa, Sei YUKI
Lead removal from a contaminated soil in shooting range by combining surface grinding and acid leaching

16:20 2F17 Mariusz BARCZAK, A. Dąbrowski, S. Pikus
Removal of mercury ions from wastewaters by SBA-15 organosilicas

16:40 2F18 H. Sakai, Anatoly A. ZINCHENKO, S. Murata
Purification of Heavy Metal Ions from Aqueous Solutions by Incorporation into DNA-Surfactant Complexes

Room C & D

Room C & D

17:30 Poster session

June 3

Room A

June 3

Room A

Chairs: J. F. L. Duval, Mo. Kobayashi, K. Kurihara

9:00 3A01 **Plenary:** Michal BORKOVEC
Colloid Stability: Sixty Years after Verwey and Overbeek

9:30 3A02 **Keynote:** Nataliya MISHCHUK
The state of interface and nearest layers of water and its influence on interparticle interaction

9:50 3A03 **Keynote:** William DUCKER, Chris Honig
Lubrication Forces in Squeeze Films

10:10 3A04 **Keynote:** Ko HIGASHITANI
Molecular-scale Structure on Surfaces and their Interaction, Adhesion and Friction in Solutions

10:30 Coffee Break

Chairs: W. Ducker, M. Elimelech, K. Higashitani

10:50 3A05 **Keynote:** Kazue KURIHARA
Polyelectrolytes at Solid-Liquid Interface Studied by Surface Forces Measurement

11:10 3A06 **Keynote:** Katsutoshi HORI
Bacterial adhesion and cell surface structure

11:30 3A07 **Keynote:** Kenta OOI
Ion-sieve Adsorbents for Selective Removal of Minor Ions from Aqueous Solutions

11:50 3A08 **Keynote:** David WAITE, A. L. Rose, S. Garg, M. Fujii
Generation of the superoxide radical anion at biological interfaces and impact on iron acquisition by aquatic organisms

June 3

12:10 Lunch (Syogoin)

Room A

Chairs: M. Ishiguro, N. Takisawa

14:40 3A11 **Keynote:** M. Brigante, G. Zanini, Marcelo AVENA
The dissolution kinetics of humic acid particles

15:00 3A12 Dongsheng WANG, M. Yan, J. Qu, C. W.K. Chow
Particle-particle interaction in water treatment: Role of Coagulant Speciation and Hydrolysis Kinetic on NOM removal

15:20 3A13 Takumi SAITO, S. Nagasaki, S. Tanaka
Evaluation of the electrostatic potential of a humic acid molecule by a fluorescence quenching technique

15:40 3A14 Krisztina KOVACS, A. Gáspár, Ph. Schmitt-Kopplin, E. Tombácz
Acidic functionality of humic and fulvic acids isolated from deep aquifers

Room A

16:00 Coffee Break

Chairs: M. Avena, D. Wang

16:20 3A15 **Keynote:** Katumitu HAYAKAWA, M. Matsuda, Y. Muroi
Utilization of Surfactant Binding for Characterization of Humic and Fulvic Acids

16:40 3A16 Munehide ISHIGURO, L. K. Koopal
Binding of Surfactants to Polystyrene Sulfonate, Humic Substances and High-Humic Soil

17:00 3A17 Kenichi NAKASHIMA, S. Xing, T. Miyajima
Interaction between humic substances and heavy metals as studied by two-dimensional correlation fluorescence spectroscopy

17:20 3A18 Nao ISHIKAWA, S. Uchida, K. Tagami
Effect of humic acid on radiocesium sorption in illite

Room B

Chairs: K. Nakamura, T. Nashima, D. Waite

14:40 3B11 X. Wu, Xiaopeng GE, D. Wang, H. Tang
Distinct mechanisms of particle aggregation induced by alum and PACl: Floc structure and DLVO evaluation

15:00 3B12 H. Kudoh, Tohru MIYAJIMA, Y. Adachi
Structures of tideland sediment flocs in Ariake sea

RoomB

June 3

RoomB

15:20 3B13 Jr-Lin LIN, C.-J. M. Chin, C. Huang, J. R. Pan, Dongsheng Wang
Coagulation behavior of Al_{13} aggregates

15:40 3B14 Warmadewanthi, C.-J. Chang, J. C. LIU
Precipitation Flotation of Phosphate from Water

16:00 3B15 Qingchun YUAN, R. A. Williams, S. Biggs
Manufacturing Microcapsules for Controlled Release

16:20 3B16 Akira OTSUKI, D. Gjergj, T. Fujita
Effects of particle size and its distribution on size measurements of fine particles by means of interactive force apparatus

Room E

Chairs: S. Lee, T. Muroi

14:40 3E11 S. Wei, Huijuan LIU, J. Qu
Preparation and characterization of a novel silica aerogel as adsorbent of toxic organic compounds

15:00 3E12 Hai ZHANG, G. Pan, K. Kurumada
Hybrid Glass for Removal of Phenol in Wastewater

15:20 3E13 M. D. G. de Luna, WARMADEWANTHI, J. C. Liu
Combined treatment of polishing wastewater and fluoride-containing wastewater from a semiconductor manufacturer

15:40 3E14 Hiroshi SAKAGUCHI, A. Kawai
Essentials for Designing Recovering Materials of Oil in Water

16:00 Coffee Break

Chairs: H. Hidaka, K. Inumaru

16:20 3E15 Gordon C. C. YANG, S.W. Chan, T.C. Peng
REMOVAL OF CHLORINATED HYDDROCARBONS BY NANOSCALE $[Fe_3O_4]$MgO

16:40 3E16 Seung-Woo LEE, N. Takahara,T. Kunitake
Sensitive binding of bisphenol A in TiO_2 ultrathin films: a combination of molecular imprinting and host-guest interaction

17:00 3E17 Takuji YAMAMOTO, Y. H. Kim, T. Ohmori
Synthesis of monodisperse carbon microspheres as adsorbents for detecting aqueous organic pollutants

17:20 3E18 Sho KATAOKA, T. Yamamoto, A. Endo, M. Nakaiwa, T. Ohmori
Synthesis of Mesoporous Carbon Thin Films

Room E

June 3 — Room F

Room F

Chairs: T. Kawanishi, Y. Mori

14:40 3F11 Chih-Hsiang LIAO, J. Anotai, C. Ruangchanikom
Evaluation of complete nitrate removal by Fe^{o}/CO_2, air/water lifted fluidized sand bed reactor, and air stripping in series

15:00 3F12 Abul Hasnat SHAMIM, H. R. Khan, T. Akae
Potentiality of Basic Slag for the Remediation of Soil Acidity and Changes in Exchangeable Cations in Acid Sulfate Soils under Various Moisture Regimes

15:20 3F13 Harunor Rashid KHAN, S. A. Lipi
Assessment, Purification and Phytoremediation Strategies for the Pollution Arising from Lead, Zinc and Cadmium Released through Industrial Effluents

15:40 3F14 Delphine CHARRIÈRE, Z. Pokryszka, P. Behra
Thermodynamic and kinetic processes at coal interface for CO_2 geological storage

16:00 Coffee Break

Chairs: D. Charrière, H. Liu

16:20 3F15 Ken-ichi KURUMADA, H. Okubo, K. Egusa
Nanofoaming in silica glass matrix by instantaneous heating

16:40 3F16 Takeshi UMETSUBO, T. Hayakawa, K. Kurumada
Optimum conditions for hybridization of epoxy resin and silica

17:00 3F17 Toshio SAKAI, H. Enomoto, H. Sakai, M. Abe
Surfactant- and reducer-free metal nanoparticle synthesis in aqueous solutions: Particle size, shape and colloidal stability

17:20 3F18 Yoshihiro KAMIMURA, K. Kurumada, G. Pan
Å-scale droplets of extractant in glass matrix

18:00 Cultural Event (Room A)

18:30 Banquet

June 4

June 4 — Room A

Room A

Chairs: M. Borkovec, H. Ohshima, T. Yamaguchi

9:00 4A01 **Plenary:** Masao DOI
Electrokinetic Boundary Condition Compatible with the Onsager Reciprocal Relation in the Thin Double Layer Approximation

June 4

Room A

9:30 4A02 **Keynote:** Ryoichi YAMAMOTO, S. Yamamori, Y. Nakayama, K. Kim
Direct Numerical Simulations for Electrokinetics of Colloids

9:50 4A03 **Keynote:** Jérôme F. L. DUVAL
Monitoring the electrochemical reactivity of pyrite/humics/electrolyte solution interface by electrokinetics of the second kind

10:10 4A04 **Keynote:** Toshinori TSURU
Permeation and diffusion through nanoporous inorganic membranes

10:30 Coffee Break

Chairs: M. Doi, E. R. Graber, Y. Takata

10:50 4A05 **Keynote:** Akihiko TANIOKA
TRANSPORT PHENOMENA ACROSS MEMBRANES IN SOLUTION

11:10 4A06 Hiroyuki OHSHIMA
Effective viscosity of a suspension of soft particles

11:30 4A07 **Keynote:** Kaoru TSUJII
Fractal Materials and Their Functional Properties

11:50 4A08 **Keynote:** Arie de KEIZER
Antifouling surfaces obtained by adsorption of complex coacervate core micelles

12:10 4A09 **Keynote:** Kenichi SAKAI
Sugar-Based Gemini Surfactants

12:30 Lunch

Room A

Chairs: A. Tanioka, T. Tsuru

14:00 4A11 **Keynote:** Isamu MORIGUCHI, H. Yamada
High-rate Ion-transportable Nanoporous Carbons as a High Performance Electric Double-layer Capacitor Material

14:20 4A12 Yasushi MORI, N. Higashi
Controlling Solute Transport Process in Soils using Dual-Characteristics of Soil Pore System

14:40 4A13 **Keynote:** Kiyoharu NAKATANI
Diffusion in nanometer-sized pores studied by single microparticle injection and absorption microspectroscopy

15:00 4A14 Syuntaro HIRADATE, H. Murano, A. Furubayashi, T. Otani
Adsorption of phenoxyacetates on colloids of a humus-rich Andosol

15:20 Coffee Break

June 4

Room A

Chairs: T. Terao, T. Yoshioka

15:40 4A15 **Keynote:** Mitsuhiro FUKUDA
Interaction of a small molecule with polyisoprene surface studied by molecular simulations

16:00 4A16 Elise ROTUREAU, J. Duval, H. P. van Leeuwen
Dynamic metal sorption by charged polysaccharides

16:20 4A17 Kazuho NAKAMURA, S. Fukada, K. Matsumoto
Fouling monitoring during Microfitration of surface water and humic acid suspension by streaming potential measurement

Room B

Chairs: S. A. Bradford, K. Suto

14:00 4B11 Michikazu TAKAHASHI, D. Kawasaki, T. Saito, I. Shimizu, S. Nagasaki, S. Tanaka
Studies on matrix diffusion of colloid in a fractured medium

14:20 4B12 Philippe LE COUSTUMER, B. Eloifi, F. Huneau, F.v.d. Kammer, M. Baalousha
Physical speciation of mobile trace elements by natural colloids

14:40 4B13 **Keynote:** Erwin KLUMPP
Transport und deposition of Pseudomonas fluorescens in porous media: Role of the cell concentration and morphology

15:00 4B14 Yuki SHIMOJO, Y. Inoue, A. Katayama
Development of Two-Region, Three-Site Model for Bacterial Transport in Saturated Porous Media

15:20 Coffee Break

Chairs: K. Kawamoto, E. Klumpp

15:40 4B15 **Keynote:** Scott A. BRADFORD, S. Torkzaban, F. Leij, N. Toride, J. Simunek
A New Paradigm for Colloid and Colloid-Facilitated Transport and Retention in Porous Media

16:00 4B16 Y. Kamio, K. Tabata, Yuko HATANO
A CTRW Approach to Column Adsorption Tests

16:20 4B17 Ursula ALONSO, T. Missana, A. Patelli, D. Ceccato, N. Albarran, M. García-Gutiérrez
Quantification of heterogeneous colloid retention on the granite surface under varying chemical conditions

June 4

Room E

Chairs: J. K. Lee, A. de Keizer

14:00 4E11 Marta SZEKERES, T. Körtvélyesi, I. Dékány, E. Tombácz, R. Schoonheydt
Investigation of the adsorption of cationic proteins on smectite clays

14:20 4E12 Kazuya MORIMOTO, T. Sato, T. Yoneda
Complexation reactions of inorganic anions on layered double hydroxide surfaces

14:40 4E13 Atsushi NAKAO, S. Funakawa, T. Kosaki
^{137}Cs adsorption on soil clays blocked by hydroxy-Al polymers in acidic forest soils of southwestern Japan

15:00 4E14 Etelka TOMBÁCZ, M. Szekeres
Surface charge heterogeneity of 1:1 and 2:1 type clay particles in aqueous suspension

15:20 Coffee Break

Chairs: T. Saito, E. Tombácz

15:40 4E15 Yu ZHANG, X. Dou, M. Yang, H. He
Arsenate Adsorption on an Fe-Ce Bimetal Oxide Adsorbent: Role of Surface Properties and Surface Complexation

16:00 4E16 Wen-Feng TAN, F. Liu, Y.-P. Wang, L. Koopal
Effect of electrolyte on adsorption/desorption of Cu^{2+} on Mn oxide

16:20 4E17 K. Sasaki, Hitoshi TAKAMORI, H. Yoshizaka, T. Hirajima
SORPTION OF BORIC ACID ON MAGNESIUM OXIDE IN PERMEABLE REACTIVE BARRIERS

Room F

Chairs: N. Mishchuk, T. Ohtsuka

14:00 4F11 Reni DESMIARTI, F. Li, C. Yoshimura, Y. Suzuki
SORPTION AND BIODEGRADATION OF NATURAL ESTROGENS IN SEDIMENT MUD CORES

14:20 4F12 Saule B. AIDAROVA, A. Babayev, A. Sharipova, A. Makhambetova
THE EFFICIENT PURIFICATION OF OIL-CONTAMINATED SOIL BY SURFACTANT

16:40 4F13 Wawan BUDIANTA, C. Salim, H. Hinode, H. Ohta
In situ Washing by Sedimentation Method of Organics-Contaminated Sandy Soil

15:00 4F14 S. Anraku, K. Morimoto, Tsutomu SATO, T. Yoneda
Sorption of Anions and Formation of Minerals at Naturally-occurring Hyperalkaline Condition

15:20 Coffee Break

June 4

Room F

Chairs: S. Hiradate, K. Tsujii

15:40 4F15 Ellen R. GRABER, S. Tagger, R. Wallach
The Role of Divalent Fatty Acids Soaps at Soil Particle Interfaces in Controlling Wetting Kinetics of Water Repellent Soils

16:00 4F16 Anurudda K. KARUNARATHNA, K. Kawamoto, P. Moldrup, T. Komatsu, L.W. de Jonge
Characterizing Soil Water Repellency Properties by Soil Organic Carbon Content, Soil Texture and Sieved-size Fractions

16:20 4F17 Kotaro FUKADA, S. Kawashima, K. Nakamura
A new methodology for measuring continuous soil air content using sound resonance

Room A

Room A

16:45 Farewell

LIST OF POSTERS

P001 Sedimentation and Electrophoresis of Porous Colloids
Yuta UCHIDA, Y. Adachi, K. Aoki

P002 New extractive substances for extraction of boric acid from industrial sewage
M.R. BEISSEMBAEVA, S. Sydykbaeva, M. K. Kalabaeva, M. R. Tanasheva

P003 Dynamic interaction between oppositely charged vesicles
Daisuke SAEKI, S. Sugiura, T. Baba, T. Kanamori, S. Sato, S. Mukataka, S. Ichikawa

P004 Adsorbing Materials Designed for Remediation of Oil-Polluted Water
Akiko KAWAI, H. Sakaguchi

P005 Effects of charge density of polyelectrolyte chain on the flocculation of polystyrene latex particles
Yasuhisa ADACHI, T. Hara, K. Aoki

P006 Diffusion of pesticide in nanometer-sized pores of ODS-silica gel by single microparticle injection and absorption microspectroscopy
Katsumi CHIKAMA, K. Nakatani

P007 THE $A1_2O_3$ NANOFILMS THICKNESS EFFECT ON THE DEPENDENCE OF CONTACT ANGLES
Nazira JADAGAYEVA, S. Aidarova, E. Gribanova

P008 Interface processes of carbonyl sulfide on atmospheric particles
Yongchun LIU, H. He

P009 Complexation of Am with size-fractionated soil humic acids
Seiya NAGAO, M. Aoyama, A. Watanabe, T. Tanaka

P010 Could iron oxide particles generated at the steel/bentonite interface move along the compacted bentonite barrier in a Deep Geological Repository for High Level Nuclear Wastes?
E. Torres, A.L. Morales, M.J. Turrero, P.L. Martín, A. Escribano, Ursula ALONSO

P011 Effect of ionic strength on deposition kinetics of humic acid through columns packed with glass beads
Yuji YAMASHITA, T. Tanaka, Y. Adachi

P012 The effects of humic acid adsorption on the deposition behavior of kaolinite particles in the sand column
Katsuya SHIRATORI, Y. Yamashita, Y. Adachi

P013 Oxidative degradation of 2,4,6-trichlorophenol by an Iron (III)-porphyrin- Humic Acid Supermolecular Catalyst
Satoko SHIGEMATSU, M. Fukushima

P014 Cadmium solidification on clay mineral and Fe oxide using Magnesium Oxide
Shogo OISHI, R. Takamatsu, I. Kitazawa, K. Tanaka

P015 Interfacial and precipitation reactions between soil colloids and water-soluble materials eluted from compost
K. Funada, K. Kakisaka, K. Otsuki, Masami NANZYO

P016 Effects of bound water on the measurement of solid-phase permittivity for volcanic soils
Teruhito MIYAMOTO, K. Kameyama

P017 Effect of an allophone-imogolite on the formation humic-like compounds from catechol and glycine
Akitaka MIURA, M. Fukushima, M. Sasaki, K. Izumo

P018 Effect of humic acid on the water repellency of imogolite membrane
Mitsuhiro KUMAGAI, Y. Watanabe, Y. Adachi

P019 Anion-exchange property of functional charcoal prepared from plant wastes

T. Takahashi, R. Yokoyama, S. Hayashi, Tomoyuki IWATA

P020 Chemical fractionation and behavior of Zn, Cu and Mn in upland fields after long-term application of pig farm manure

Kei ASADA, M. Kato, T. Nishimura

P021 ^{13}C PST/MAS and CP/MAS NMR for estimation of biodegradation properties of environmental organic matters at hydrated and desiccated states
A. SUETSUGU, K. Asakura, T. Miyazaki, K. Hori

P022 Removal of Phenol from Aqueous Solution using Hydrogel Media

Gaofeng PAN, K. Kurumada

P023 Power law tailing in removal of pollutants from water to gas: a invasion percolation and random walk model study

Takuya KAWANISHI, D. M. Rehan, H. Sugiyama

P024 Adsorption of Basic Dye and Reactive Dye by Kaolin Coated with Chitosan

Soydoa VINITNANTHARAT, S. Klankrong

P025 Prediction of plant availability of radioactive ^{137}Cs by using radiocesium interception potential
Hirofumi TSUKADA, A. Takeda, S. Hisamatsu, A. Nakao

P026 Effect of pore size on colloidal transport phenomena in porous media

Koichi SUTO, Y. Yoshino, C. Inoue

P027 Anion Exchange Properties of Hydrous Metal Oxides. Analysis Based on Surface Coordination with Stability Constant Data Base

Kenta OOI

P028 Temperature-Swing Adsorption of Proteins in Water Using Polymer-Grafted Silica Particles

Shintaro MORISADA, S. Suzuki, K. Namazuda, Y. Hirokawa, Y. Nakano

P029 Volatilization of organic compounds from sandy soil

Toshitsugu MOROIZUMI, Y. Sasaki, T. Miura

P030 Microscopic observation of deposition of colloidal particles onto single glass bead: effect of salt concentration

Yasuyuki KUSAKA, Y. Yamashita, Y. Adachi

P031 Prediction of Adsorbed Amounts of Volatile Chlorinated Organic Compounds to Soil

Takeshi KOBAYASHI, Y. Shimizu, K. Urano

P032 Density flow in a porous media caused by salt accumulation

Yasutaka KIHARA

P033 Transport and Straining of Colloid-Sized Materials in Saturated Porous Media

D.T.K.K Chamindu, Ken KAWAMOTO, H. Saito, S. A. Bradford , P. Moldrup, T. Komatsu

P034 Colloid-facilitated and dissolved cadmium transport through layered soils with subsurface cracks

X.-Y. Tang, Hidetaka KATOU, K. Suzuki, T. Ohtani

P035 The effect of soil compaction on solute diffusion in volcanic ash soil

Shoichiro HAMAMOTO , M. S. A. Perera, A. Resurreccion, K. Kawamoto, T. Komatsu, P. Moldrup

P036 Experimental study and modeling of europium adsorption onto smectite clay colloids

T. Missana, U. Alonso, Miguel GARCÍA-GUTIÉRREZ, N. Albarrán, T. López-Torrubia

P037 Calcium hydroxide leaching process modeling for a well-buffered volcanic-ash soil

DaiWen CHEN, N. Toride

P038 Adsorption of selenium on single oxides and natural solids

Charlotte HUREL, N. Marmier

P039 Fluorescence Lifetime Imaging Microscopy applied for Eu(III) adsorbed on Granite
Keisuke ISHIDA , T. Kimura, T. Saito, T. Toraishi, S. Tanaka

P040 Effects of pore-wall on the transport properties of porous media
Setsuo OOI

P041 Two-dimensional Arrays of Gold Colloids and the Function of Ionic Liquid on their Stabilization
Om P. KHATRI, K. Adachi, K. Murase, K. Okazaki, T. Torimoto, N. Tanaka, S. Kuwabata, H. Sugimura

P042 Speciation Characterization of Hydrolyzed Fe(III) during Fenton Reaction by Ferron Assay
Yingxin GAO, M. Yang, D. Wang, Y. Zhang

P043 INTERACTION BETWEEN ENZYME TREATED RED BLOOD CELLS
Atsushi HYONO, J. F. L. Duval, F. Gaboriaud, T. Mazda, H. Ohshima

P044 Effective interaction between colloidal particles with grafted polyampholytes
Takamichi TERAO, T. Kuze

P045 Effect of Counterion on Colloid Vibration Potential in Aqueous Surfactant System
Youichi TAKATA, T. Nagahashi, T. Miyayama, A. Hyono, H. Ohshima

P046 Sorption of U(VI) on granite: Application of a surface complexation model
Jae Kwang LEE, M.H. Baik, S.Y. Lee, Y.C. Seo

P047 Surface Charge and Coagulation of Bentonite Colloids: Effects of the pH and Ionic Strength
M. H. Baik, J. H. Park, Jae Kwang LEE

P048 Initial deposition rate of latex particles in the packed bed of zirconia beads
Motoyoshi KOBAYASHI, H. Nanaumi, Y. Muto

P049 Surface charging, polyanionic coating and colloid stability of magnetite nanoparticles
Angela HAJDÚ, E. Illés, E. Tombácz

P050 Effect of colloid volume fraction on the rate of Brownian coagulation
Tomonori FUKASAWA, Y. Adachi

P051 Dynamic study of colloid retention mechanisms in a granite fracture
Nairoby ALBARRÁN, T. Missana, U. Alonso, M. García-Gutiérrez, T. Lopez-Torrubia

P052 Investigation of Air/solution Interface by a Small Bubble
T. Murata, Masashi SAKAI, K. Mukae, A. Yamauchi, Y. Moroi, Willem Norde

P053 Influence of nanosized bubbles on the stability of disperse systems
Nataliya MISHCHUK, J. Ralston, D. Fornasiero

P054 Physico-chemical properties of functionalised carboxymethyldextran macromolecules in the presence of metallic cations: an electrokinetic and dynamic light scattering study
Jean-Pierre SAGOU, F. Thomas, J. F. L. Duval

P055 Capillary viscosity of Dilute Montmorillonite Suspension under Electrostatically Dispersed State in the Limit of Low Pressure Gradient
Nobuyuki SAKAIRI, K. Saito , Y. Adachi

P056 On-Chip Cell Electrophoresis to Evaluate Cell's Condition
Takanori AKAGI, T. Ichiki

P057 Low-swelling smectite in Ariake marine clay and its role in quick clay development
Masami OHTSUBO, T. Higashi and M. Kanayama

P058 Preparation of W/O/W microcapsule containing enzyme without alcohol

Takayuki NARITA, T. Kishigawa, Y. Tagami, Y. Oishi

P059 Quickened sedimentation for dense suspensions by the formation of vertical-channels

Katsuya NAKAISHI, S. Ooi, Y. Suzuki

P060 THE COAGULATION FEATURES OF LATEX NANOPARTICLES

Saule B. AIDAROVA, N. Tusupbayev, K. Musabekov, A. Sharipova

P061 Adsorption studies for the removal of basic dyes from wastewater by activated sludge biomass

Hawan-Chung CHU, K.-M. Chen

P062 ECOLOGICAL ASSESSMENT OF OIL-GAS PRODUCING AREA IN KAZAKHSTAN ZONE OF CASPIAN SEA AND USING THE BIOTECHNOLOGY FOR CLEANING OF HIGH LEVEL OIL POLLUTED SITES

A.A. Bigaliev, N.E. Ishanova, Aitkhazha B. BIGALIEV

P063 CeO_2 surface induced bromate reduction during ozonation of bromide-containing water

T. Zhang, Zhimin QIANG

P064 Preparation of carbonaceous sulfur-impregnated adsorbent for removal of heavy metal in aqueous solution

Takaaki WAJIMA, K. Sugawara

P065 Adsorption behavior of fluoride ion by titanium hydroxide-derived adsorbent

T. Wajima, Yuta UMETA, K. Sugawara

P066 DNA adsorptions on andosols and allophane minerals

M. Sakai, A. S-I. Wada, Kazutoshi SAEKI

P067 Extraction of PCBs from River Sediment Using Liquid Dimethyl Ether as Extractant

Kazuyuki OSHITA, M. Takaoka, S. Kitade, N. Takeda, H. Kanda, H. Makino, T. Matsumoto, S. Morisawa

P068 Sonochemical reduction of MnO_4^- and formation of MnO_2 particles in aqueous solutions in the presence and absence of alcohols

Kenji OKITSU, M. Iwatani, B. Nanzai, R. Nishimura

P069 Estimation of acoustic cavitation bubble temperatures in aqueous anion surfactant solutions

Ben NANZAI, K. Okitsu, N. Takenaka, H. Bandow

P070 Colloidal behavior of acetate-utilizing methanogens in the anaerobic digester

Toshiyuki NOMURA, A. Yoshihara, Y. Konishi

P071 CROSSFLOW ULTRAFILTRATION OF DISSOLVED HUMIC ACID SOLUTIONS USING COAGULATED HUMIC ACID CAKE FORMED ON POROUS FINE CERAMICS

Hideo NAKAKURA, K. Yamashita

P072 Deoiling and Dewatering Processes for General Purposes by Using Liquefied DME

Hideki KANDA, H. makino

P073 Molecular analysis of a bacterial nanofiber of the highly adhesive bacterium, *Acinetobacter* sp. Tol 5

Masahito ISHIKAWA, S. Takada, K. Hori

P074 Population analysis of denitrifiers inhabit the biofilm on submerged reed surface through molecular biological protocol targeting denitrifying genes, *nir*S and *nir*K

Ikuo YOSHINAGA, T. Nakamura, T. Amano, Y. Sako

P075 Root endophytes isolated from a native species *Clethra barvinervis Sieb.* et Zucc. in Hitachi mine increase the seedling growth and control the heavy metal absorption

Keiko YAMAJI, Y. Watanabe, K. Kobayashi, T. Kozaki

P076 Influence of Biofilm Formation on Stainless Steel Corrosion

Tetsuya URAKAMI, A. Ikoma, H. Morisaki, J. Liao, H. Fukui, K. Hojo

P077 Viable spores on solid surfaces: adhesion characteristics and alkaline cleaning effect
Yusuke NANASAKI, T. Hagiwara, H. Watanabe, T. Sakiyama

P078 Penetration behavior of *Vibrio cholerae* hemolysin into a mixed monolayer of DMPC and Cholesterol
Y. Tagami, T. Narita, H. Ikigai, Yushi OISHI

P079 Microscale Environment and Microbial Flora Inside of Biofilm
Yuki TSUCHIYA, A. Hiraki, T. Arakawa, R. Kusakabe, M. Yamamoto, H. Morisaki

P080 Effect of cathodic protection on biofilm attached to carbon steel
Kazuhiko MIYANAGA, Y. Tanji

P081 Denitrification in the biofilm developed on submerged reed surface
Takahisa NAKAMURA, T. Amano, T. Yamagishi, Y. Suwa, Y. Sako, I. Yoshinaga

P082 Adsorption and desorption of Sulfadiazine on different soil components
N. Meng, H. Lewandowski, H.-D. Narres, Erwin KLUMPP, H. Vereecken

P083 Analysis of Biofilm Formation Process on Reed Surface
Ayami HIRAKI, Y. Tsuchiya, T. Arakawa, R. Kusakabe, H. Morisaki

P084 Morphological analysis of bacterial nanofibers on *Acinetobacter* sp. Strain Tol 5 by electron microscopy
Aisuke HIGUCHI, Y. Hotta, K. Yamamoto, K. Hori

P085 Colloids fractal dimension
Philippe LE COUSTUMER, S. Galaup, M. Masson, J. Schäfers, G. Blan, M. Baalousha

P086 Chemical composition of suspended matter and particulate phosphorus discharged to tile drains in a clayey field
Katsuhiro SUZUKI, K. Adachi, T. Sekiguchi, S. Yoshida, K. Nakano, H. Katou

P087 Effect of water extraction on soil water repellency of a forest soil
Masahiro KOBAYASHI, H. Matsui

P088 Absorption of The Trees and Shrubs to Sulfur Dioxide and Heavy Metal in Greenbelt of Beijing
F. Qian, Yuan TIAN, Q. Wang, and X. L. Liu

P089 FOR PUBLIC ADMINISTRATION ISSUES OF CASPIAN SEA ECOLOGICAL POBLEMS
Yedii ZHANBURSHIN

P090 Influence on concentration and molecular size distribution of uranium in soil solution by plant growth
Akira TAKEDA, H. Tsukada, Y. Takaku, S. Hisamatsu

P091 Simultaneous Measurement of Surface Potential and Viscosity in a Capillary Channel
Takeshi NASHIMA

P092 Surface-Assisted Laser Desorption/ionization Mass Spectrometry of Environmental Pollutants with Nanostructured Surfaces
Hideya KAWASAKI, T. Sugitani, Y. Shimomae, T. Watanabe, R. Arakawa

P093 Contact angle effects of sand on the fingered flow under non-ponding infiltration
Takeyuki ANNAKA, S. Hanayama

P094 Bactericidal activity of Ag-Ce/AlPO4 catalyst using molecular oxygen in water
Q.Y. Chang, Hong HE, J.C. Zhao, M. Yang, J.H. Qu

P095 Complete mineralization of the recalcitrant cyanuric acid substrate by ozonation in aqueous TiO_2 suspensions
Toshiyuki OYAMA, I. Yanagisawa, T. Koike and H. Hidaka

P096 Catalytic properties of Fe-containing imogolite in cyclohexane oxidation

Masashi OOKAWA, Y. Nagamitsu, M. Oda, Y. Takata, T. Yamaguchi, T. Maekawa

P097 Using Fe (III)-substituted hydroxyapatite as an adsorbent and a photo-Fenton catalyst for clarification of stained water

Takeshi MORIGUCHI, S. Nakagawa, F. Kaji

P098 Catalytic Diesel Soot Oxidation – Screening Study and Ag/Ceria Catalyst

Hiroshi KAWACHI, K. Shimizu, A. Satsuma

P099 Simultaneous HDS and HDN over supported PtSn catalysts in comparison to commercial $NiMo/Al_2O_3$

Micheal OKIROR, N. Sarah, F. K. Walulya

P100 Sorption of atrazine (AT) onto humic acids (HAs) coated nanoparticles

J. Lu, Y. Li, B. Shi, H. Tang, Dongsheng WANG

P101 BIODISTRIBUTION OF COLLOIDAL GOLD NANOPARTICLES UP ON INTRAVENOUS ADMINISTRATION: EFFECT OF PARTICLE SIZE

G. S. Sonavane, Keishiro TOMODA, K. Makino

P102 Bridged polysilsesquioxane xerogels functionalized with different groups as sorbents of mercury from wastewaters

M. Barczak, Andrzej DABROWSKI, S. Pikus, Y. L. Zub

P103 Effect of Infiltration Rate on Denitrification in a Ponded Soil Column

Satoko WATANABE, K. Nakamura, T. Hama, S. Kawashima

P104 Characteristics comparison of fulvic acids extracted from mountain streams in different forest forms

Hiroki KODAMA, D. Itoh, N. Higashi, M. Chiwa, K. Otsuki, T. Miyajima

P105 Chemical Structure of humic acids on tideland sediment in Ariake sea

N. Hiromatsu, Tohru MIYAJIMA

P106 Adsorption-desorption behavior of heavy metal ions with colloids in Ariake sea esturian area

D. Itoh, Masashi KAMACHI, T. Miyajima

P107 Unfrozen water in a bundle of capillaries filled with solution

Kunio WATANABE

P108 Restoration of cadmium-contaminated paddy soils by washing with ferric chloride:-An increase of soil sediment volume during washing procedure-

Y. Kodani, Tomoyuki MAKINO, T. Kamiya, H. Takano

P109 Estimation of constrictivity relevant to diffusion in sedimentary rocks based on X-ray CT image

Hiroaki TAKAHASHI, Y. Seida, K. Miyahara, M. Yui

P110 Transport and fate of dissolved organic carbon in the vadose zone and shallow aquifer below an Andisol

Sadao EGUCHI, M. Sawamoto, M. Shiba

P111 Effectiveness and Mechanism of Priority Pollutant Nitrobenzene Adsorption by Incinerated Rice Husks

Zhi-Sheng LIU, Jun Yin, Yu-Juan Yu, Jian-Hui Wang, Gui-Bai Li

P112 Towards a New Conceptualization of Colloid Filtration in Granular Porous Media

Naoyuki OCHIAI, M. Dragila, J. Parke

Oral Presentations
Abstracts

1A01

HUMICS, SPECIAL COMPONENTS

Luuk K. Koopal
Laboratory of Physical Chemistry and Colloid Science,
Dreijenplen 6, Wageningen University,
NL 6703 HB Wageningen, The Netherlands.

Humic substances (HS) are soil and aquatic biomaterials that are part of the natural organic matter. HS can act as redox agents and pH buffer, retain water, bind metal ions, adsorb organic solutes, photosensitize soil reactions, stimulate plant growth and bio-transform toxic pollutants. It is important to know which components of HS are responsible for the mayor processes in soils and waters, and in studies it is desirable to deal with pure components of HS. After isolation of HS from natural organic matter, three main components are considered: fulvic acids (FA), humic acids (HA) and humins. The distinction is based on the solubility in alkaline and acid solutions. FA and HA (higher molar mass and lower degree of oxidation than FA) are best studied. HA nano-particles (see figure) are often considered as open aggregates of building blocks that are structured by physical and chemical interactions. Both HA and FA are aromatic and aliphatic and contain a range of functional groups that make them soluble. The charge characteristics of dissolved HA and FA are mainly derived from the dissociation of carboxylic and phenolic groups. This charge, together with the heterogeneity is very important for the interactions of HA and FA with inorganic ions, organic ions and surfactants, cationic polyelectrolytes and proteins and for their interaction with mineral particles. In the presentation the interaction of these components with HA and FA will be illustrated and discussed.

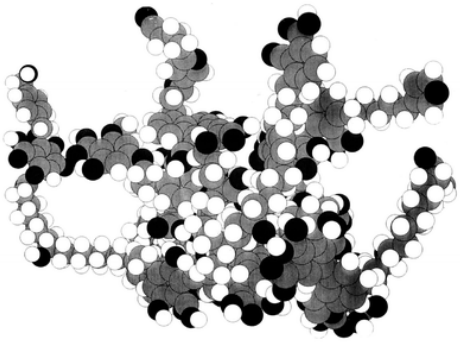

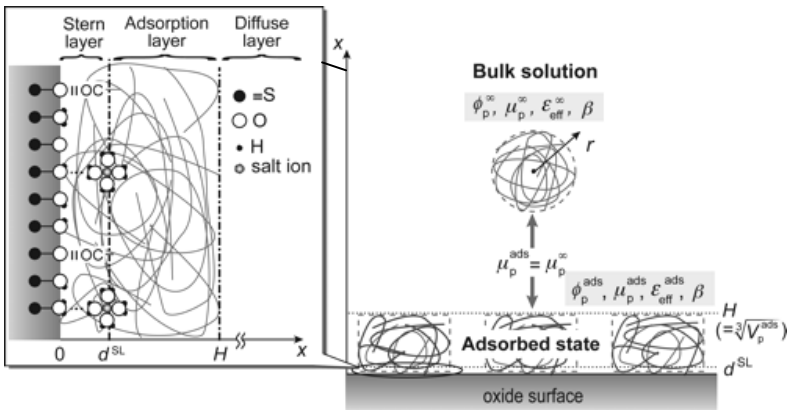

Specific attention will be given to: (1) binding of metal ions and the NICA-Donnan model to describe this interaction as a function of the environmental conditions (pH, ionic strength, presence of competing cations), (2) interaction of negative HA and FA nano-particles with positive metal oxide particles and the model description of this interaction (see figure). This interaction is not only important as such, but also in relation to proton and metal ion binding and vice verse.

luuk.koopal@wur.nl

1A02

Capillary Condensation in Ordered Mesoporous Materials

Kunimitsu Morishige
Department of Chemistry, Okayama University of Science,
1-1 Ridai-chou, Okayama 700-0005, Japan

In order to elucidate the behavior of a fluid in a restricted space and also to establish the fundamentals of pore size analysis by a gas adsorption method, capillary condensation of a fluid in mesoporous materials has been extensively investigated. This phenomenon is a shifted gas-liquid phase transition resulting from the confinement of the fluid. The pressure at which capillary condensation takes place is often larger than that of capillary evaporation. This hysteresis effect depends strongly on pore geometry and temperature and would be closely concerned with the mechanisms of capillary condensation and evaporation. The effects of pore size and geometry on capillary condensation would be most effectively explored using ordered mesoporous materials because of their well-defined porous structures.

We review some recent progress in experimental studies of the capillary condensation of simple molecules in ordered mesoporous materials. We show that the nature of the adsorption hysteresis due to capillary condensation can be examined with less ambiguity by measuring the hysteresis loop for the ordered mesoporous materials with four types of pore geometries (cylindrical, interconnected cylindrical, interconnected spherical, and interstitial between cylindrical rods) over a wide temperature range. The adsorption hysteresis arises from the metastability of a confined phase and the temperature at which the hysteresis disappears is lower than the critical temperature of vapor-liquid equilibrium in pores. The hysteresis occurs mainly on the desorption rather than adsorption branch, irrespective of the pore geometries.

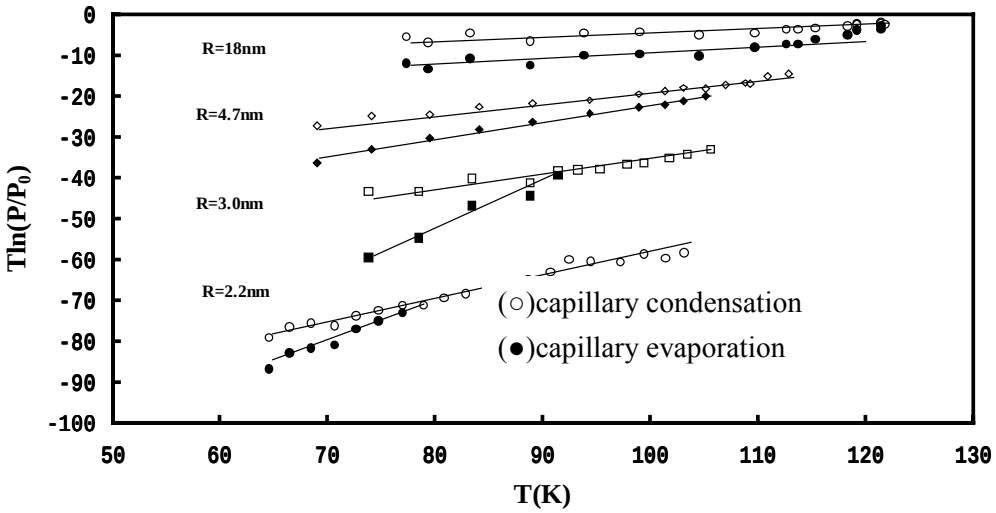

Fig.1 Temperature dependence of capillary condensation and evaporation pressures of nitrogen in cylindrical pores of four kinds of silicas with different pore radii.

morishi@chem.ous.ac.jp

1A03

Mirco-interface Processes and Application in the Transformation and Control of Environmental Pollutants

Jiuhui Qu*, Hong He, Min Yang
SKLEAC, Research Center for Eco-Environmental Sciences, CAS,
POB 2871, Beijing 100085, China

The transfer and transformation of pollutants at environmental micro-interfaces are the basic environmental behaviors of the pollutants, providing an important scientific basis for environmental pollution control. As a Creative Research Group sponsored by National Natural Science Foundation of China, the team is aimed to explore the main mechanisms of the tranfer and transformation of pollutants at the enivromental micro-interfaces and develop suitable pollution control technologies.

On the basis of the establishment of quantitative and qualititative *in-situ* characterization techniques and scientific methdolgies for environmental micro-interfaces under complicated conditions, the general behaviors of pollutants in major environmental media have been investigated in detail. We studied the adsorption and reaction mecahnism of pollutants on the micro-interfaces and the stucturre-efficiency relationship during the process using *in-situ* FTIR and Raman spectroscopy. We built the Knudsen cell-MS and vacuum UV radiation MS systems to obtain the kinetic data of heterogeneous reaction on the micro-interfaces. The construction of AFM and STM palteform is underway to directly observe continuous changes on the microstructure of the micro-interfaces.

For example, the heterogeneous reactions of carbonyl sulfide (OCS) on the typical mineral oxides in the mineral dust particles was investigated using a Knudsen cell flow reactor and an in situ diffuse reflectance infrared Fourier transform spectroscopy (DRIFTS). We found that heterogeneous reactions, which belong to hydrolysis of OCS and succeeding oxidation of intermediate products, readily take place on mineral dust. The global flux of OCS due to heterogeneous reactions on mineral dust was estimated at 0.05-0.64 $Tg \cdot yr^{-1}$, which is comparable to the annual flux of OCS for the reaction with •OH. This result reminds us that the role of heterogeneous reactions in the environmental chemistry cycles of long-life trace gases is remarkable. In addition, the interaction mechanisms of priority pollutants, such as polycyclic aromatic hydrocarbons (PAHs), bio-esseantial elements, and fine particulates at the micro-interfaces of water/particulate/microorganism, soil/plant root/microroganism and air/particulate are elucidated, and their biological, physical and chemical transfer and transformation principles have been investigated as well.

Based on the composite micro-interfacial effects of some representative pollutants, suitable pollution control methods are developed with focal points on adsorption-desorption, catalytic oxidation-reduction, coagulation-flocculation, and biological control techniques etc., such as the binary Fe-Mn oxide preparation, its application and mechanism for arsenic removal, the magnetic powder $MnO–Fe_2O_3$ composite material for the removal of pollutants from water, new electrodes for abatement pollutants in advanced oxidation porcess, the coagulatoin speciation and its affect on the NOM removal efficiency and some micobiology methods for pollutants removal.

* Email: jhqu@rcees.ac.cn

2A01

Structure of ions and molecules confined in carbon nanospaces

K.Kaneko*, T. Ohba, C.M.Yang, Y. Tao, N.Kojima, Y. Nobuhara, T. Konishi, T. Fujikawa, M.Yudasaka[+], S. Iijima[+], and H. Kanoh,

Graduate School of Science, Chiba University , Inage, Chiba 263-8522, Japan
*[+] Department of Physics, Meijyo University, Tenpaku, Nagoya 468-8502, Japan, **JST Agency, NEC Cooperation, Tsukuba, Ibaraki 305-8501, Japan*

The urgent demand for preservation of the global environment has requested to construct environment-friendly technologies. Adsorption on nanoporous solids has contributed to energy storage, highly efficient catalysis, concentration of noble substances, and removal of pollutants, separation of harmful gases or valuable gases, and medical treatments. It is indispensable to characterize nanoporous materials and to understand the structure of molecules and ions confined in nanopore spaces. In particular, nanoporous carbons have contributed to environmental technologies. Recently it was shown that single wall nanocarbons can interact strongly with various organic molecules, which should be applicable to sustainable chemistry. Then, surface chemical properties of single wall nanocarbons should be studied[1-3]. Structure and properties of molecules and ions confined in nanopores of activated carbon fiber (ACF)s and single wall carbon nanohorn (SWCNH) as model nanoporous carbons will be given.

ACFs have slit-shaped nanopores, while SWCNHs have one-dimensional pores. Molecules such as N_2, alcohol, and water confined in these nanopores have ordered structure even at ambient temperature with in situ X-ray diffraction and molecular simulation. In particular, water molecules must form clusters to get great stabilization in hydrophobic nanopores. In situ small angle X-ray scattering elucidated the unique growth of clusters in the nanopores[4].

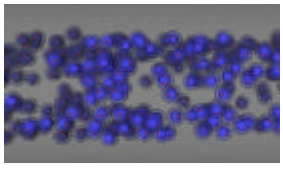

Fig.1. Water cluster in Tube space. Filling=0.4

Ionic solution was confined in hydrophobic carbon nanospaces and the hydration structures were determined with X-ray absorption (EXAFS) technique[5]. As to Rb^+ ions, the hydration number and Rb-H_2O distance decrease remarkably by confinement in the nanospaces of SWCNH and ACF. A significant decrease in the hydration number was also observed in Cu^{2+} and Fe^{3+} nanosolution. A more intensive confinement effect was observed in nanopores of SWCNH than ACF. It was shown that SWCNH is a promising applicant for an efficient ion-selective storage [5].

References

1. K. Urita et al, *Nano Lett.* **6**, 1325-1328(2006),S. Utsumi et al. *J. Phys. Chem.* C. **111**, 5572(2007).
2. S. Gotovac, et al. *Nano Lett.* **7** , 583(2007)
3. H. Honda et al. J. Phys. Chem. C. **111** (8), 3220-3222 (2007).
4. T.Ohba, *et al*. *J. Amer. Chem. Soc.* **126**, 156(2004), *J. Phys. Chem*. B**108**, 14964 (2004). *Nano Lett.*, **5**, 227 (2005), *Euro Chem. J.* **11**, 4890(2005)T. Ohkubo, *et al. J. Am. Chem. Soc*. **124**, 11860 (2002). *J. Phys. Chem. B***107**, 13616 (2003). *Physica Scr.*, T**115**, 685 (2005)
5. C.-M. Yang, et al, *J. Am. Chem. Soc.*, **129**, 20 (2007).

Katsumi Kaneko e-mail:kaneko@pchem2.s.chiba-u.ac.jp

2A02

Phase Behavior of Simple Fluid confined in Nanospace
― Finding Phase Diagram and Exploring into MOF Nanospace ―

M. Miyahara
Department of Chemical Engineering, Kyoto University
Nishikyo, Kyoto 615-8510, JAPAN

The phase behavior of fluid confined in nanospace often significantly differs from those in bulk phase, because of the possible effects of attraction from pore walls and interfaces of nanoscale. Even for such simple geometries as slit and cylinder, much difficulty comes from simultaneous affection of numerous factors onto the phase behavior. As summarized below the authors employed various types of molecular simulation techniques in order to elucidate the influence of each factor, which was to be thermodynamically modeled for prediction of the phase boundaries.

As for capillary condensation (vapor-liquid coexistence), many studies have pointed out the incorrectness of the Kelvin model in the scale of nanometers. A condensation model with simple concept and easy calculation, however, had not been established until done by us in computer experiments employing Molecular Dynamics (MD) techniques and Lennard-Jones (LJ) fluid [1-3], which demonstrated success also in the real pore system of MCM-41 [4].

Also, as for freezing phenomena (solid-liquid coexistence), we have clarified variety of shifts in freezing point. Freezing-point temperature was found to get higher as well as lower than the bulk freezing point, which is thought to have resulted from combination of three factors: i) the elevating effect by the pore-wall potential energy (compressing effect: Fig. 1) [5], ii) geometrical shape of pore (geometrical hindrance effect) [6], and iii) the depressing effect by the tensile condition of the capillary condensate (tensile effect) [7]. Our simple solidification models successfully predicted Grand canonical Monte Carlo (GCMC) and MD results. Triple points of pore fluid can be predicted as the simultaneous solution of our model on vapor-liquid coexistence and that on solid-liquid coexistence, which successfully predicted MD results [8]. Also studied was sublimation of solids in nanopore with successful prediction by a simple thermodynamic model [9].

On the basis of the series of findings and models, an entire phase diagram of confined Lennard-Jones fluid, at least in slit-shaped nanopore, can now be predicted (Fig. 2) with no adjustable parameter. This presentation reviews first the above activities by the authors, then overviews the phase diagram for other geometries, and finally presents hot results for the adsorption-induced lattice structure transition of "flexible" nanoporous bodies (MOF: Metal-Organic Frameworks).

[1] Miyahara, Yoshioka, Okazaki, *J.Chem.Phys.*, 106, 8124 (1997). **[2]** Miyahara, Kanda, Yoshioka, Okazaki, *Langmuir*, 16, 4293 (2000). **[3]** Kanda, Miyahara, Higashitani, *Langmuir*, 16, 6064 (2000). **[4]** Kanda, Miyahara, Yoshioka, Okazaki, *Langmuir*, 16, 6622 (2000). **[5]** Miyahara and Gubbins, *J.Chem.Phys.*, 106, 2865 (1997). **[6]** Kanda, Miyahara, Higashitani, *Langmuir*, 16, 8529 (2000). **[7]** Miyahara, Kanda, Shibao, Higashitani, *J.Chem. Phys.*, 112, 9909 (2000). **[8]** Kanda, Miyahara, Higashitani, *J.Chem.Phys.,* 120, 6173 (2004). **[9]** Kanda and Miyahara, *J.Chem.Phys.*, 126, 054703 (2007). **[10]** Watanabe, Sugiyama, ,Miyahara, *Langmuir*, 24, 802 (2008).

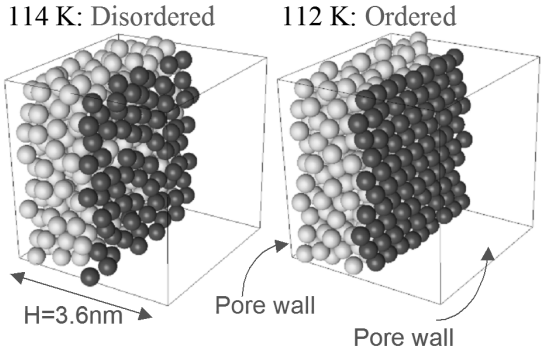

Fig. 1. Peculiar phase behavior of LJ-methane in carbon nanospace: Enhanced freezing even above the freezing point of bulk fluid (102K).

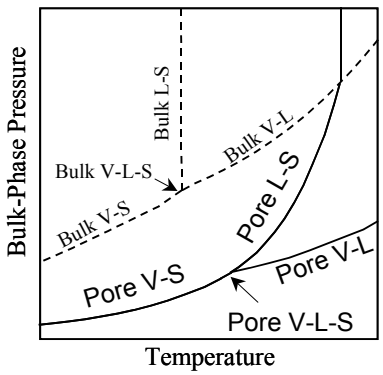

Fig.2 Schematic example of phase boundaries for LJ-methane in strongly attractive nanopore, superimposed on bulk-phase *p-T* diagram.

miyahara@cheme.kyoto-u.ac.jp

2A03

Antibacterial Effects of Carbon Nanotubes

Menachem Elimelech
Department of Chemical Engineering
Environmental Engineering Program
Yale University

Carbon nanotubes (CNTs) are some of most attractive nanomaterials due to their unusual physicochemical, mechanical, and electrical properties, as well as their broader range of potential applications. The increase in commercial interest and subsequent mass production will lead to a greater possibility for interactions of CNTs with human and the environment. Understanding the toxicology and environmental impacts of CNTs are therefore critical for the future application of these emerging nanomaterials.

Despite the general agreement about the potential toxicity of CNTs, a mechanistic explanation for CNT toxicity is still elusive. As an alternative to human cells, bacteria, especially those found in diverse environments, such as *E. coli*, can provide a particularly valuable model for exploring how single-celled organisms respond to environmental stressors such as exposure to CNTs.

Here, we present results of interaction of *E. coli* cells with single-walled carbon nanotubes (SWNTs) and multi-walled carbon nanotubes (MWNTs). We show that highly purified SWNTs exhibit strong antimicrobial activity. By using pristine SWNTs with a narrow diameter distribution, we demonstrate that cell membrane damage resulting from direct contact with SWNTs is the likely mechanism leading to bacterial cell death. We further demonstrate that the size (diameter) of CNTs is the key factor governing their antibacterial effects. Experiments with well-characterized SWNTs and MWNTs demonstrate that SWNTs are much more toxic to bacteria than MWNTs. Gene expression data shows that in the presence of both MWNTs and SWNTs, *E. coli* express high levels of stress-related gene products, with the quantity and magnitude of expression being much higher in the presence of SWNTs.

menachem.elimelech@yale.edu

2A04

Control of Morphology and Nanostructure of Carbon Cryogels

H. Tamon*
Department of Chemical Engineering, Kyoto University,
Katsura, Kyoto 615-8510

Carbon cryogels are prepared via sol-gel polycondensation of resorcinol with formaldehyde, freeze drying, and pyrolysis. The cryogels are unique materials with high surface areas and large mesopore volumes, being expected to be used as catalysts, adsorbents, electric double layer capacitors, and materials for chromatographic separation. Considering these usages, it is desirable for RF carbon gels to be tailor-made to have suitable shapes, which are easy to be applied to various purposes, such as cylinder, tablet, microsphere, and honeycombs. Here the methodologies for controlling morphology and nanostructure of carbon cryogels are introduced.

RF hydrogels were prepared by the sol–gel polycondensation of resorcinol with formaldehyde using sodium carbonate as a basic catalyst and distilled water as a diluent. Carbon cryogels were obtained by freeze drying of hydrogels and pyrolysis in an inert atmosphere. An inverse emulsion polymerization or a unidirectional freezing of hydrogels are also applied to the preparation of hydrogels to control their morphology.

Fig. 1 shows four morphologies of carbon cryogels. Monolithic carbon cryogels shown in Fig. 1 (a) were obtained by molding the hydrogels prior to drying. Fig. 1 (b) suggests that carbon cryogel microspheres were successfully prepared by an inverse emulsion polymerization of resorcinol with formaldehyde in cyclohexane, followed by freeze drying and pyrolysis in an inert atmosphere. From Fig. 1 (c), one can see that carbon cryogel microhoneycomb were prepared by pseudosteady state growth of ice crystals which occurs during the unidirectional freezing of freshly gelled RF hydrogels followed by freeze drying and pyrolysis. As for nanostructure of carbon cryogels, experimental results suggested that the synthesis conditions of hydrogels changed mesoporosity of carbon cryogels. It was experimentally verified that the mesoporosity can be controlled by using catalyst concentration of RF solutions.

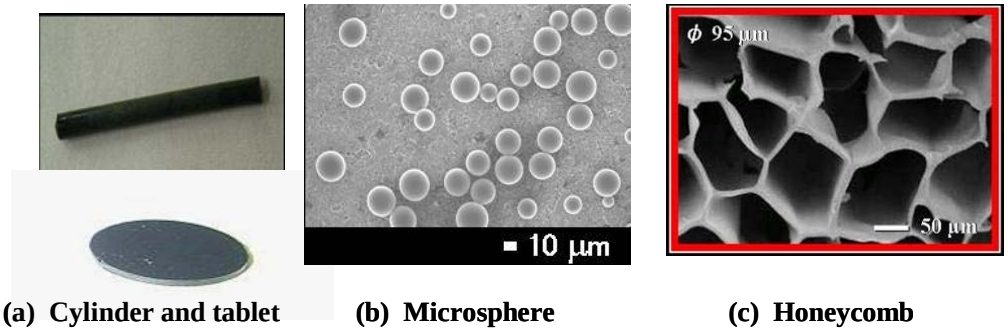

(a) Cylinder and tablet **(b) Microsphere** **(c) Honeycomb**

Fig. 1 Morphology of carbon cryogels.

*tamon@cheme.kyoto-u.ac.jp

2A05

Micro pore filling membranes and their unique performances ~from Bio-inspired materials to polymer electrolyte fuel cells~

T. Yamaguchi*

Chemical Resources Laboratory, Tokyo Institute of Technology

R1-17, 4259 Nagatsuta, Midori-ku, Yokohama 226-8503

Systematic membrane design is important to develop new generation membranes, for example, electrolyte membranes for fuel cells or bio-inspired membranes. Necessary functions are not only separation but also electrochemical reaction, molecular recognition and actuation. Those functions should be coordinated in the micro pores of membranes and the assembly to maximize a specific output. We should systematically design the multi functions in the membrane pores. To develop a high performance polymer electrolyte fuel cell (PEFC), a novel electrolyte membrane is needed. The pore filling type polyelectrolyte membranes are proposed. The membranes composed of porous matrix and filling polymer electrolyte, and the matrix showed swelling suppression effect and the filling polymer showed proton conductivity. The membrane showed high proton conductivity and low fuel crossover, and those performances can be controlled by changing each component. The pore filling membrane electrode assembly showed high fuel cell performances. Biomembrane-like systematic functions can be achieved by introducing molecular recognition hosts and stimuli responsive polymer in pores of a porous membrane. The pores rapidly open and close in response to specific ion signals. Grafted polymer composing of N-isopropylacrylamide (NIPAM) and benzo[18]crown-6 pendent copolymer was fixed onto the surface of the membrane pores. The membrane pores close when the membrane comes in contact with aqueous solution containing K^+, Sr^{2+}, Ba^{2+} or Pb^{2+}, but Na^+, Li^+ or Ca^{2+} ion did not affect the pore closure. The molecular recognition membranes can be utilized for membrane separation, micro reactors, drug delivery systems, tissue engineering etc.

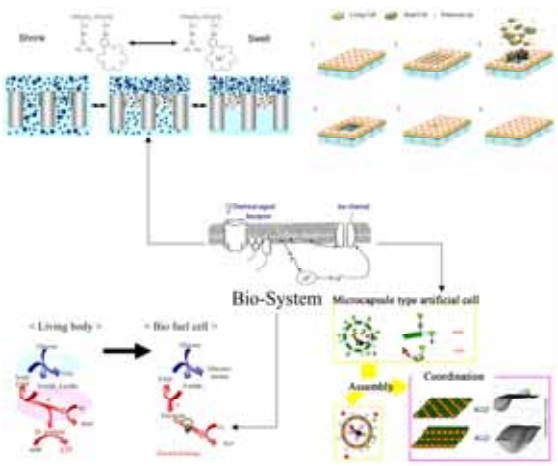

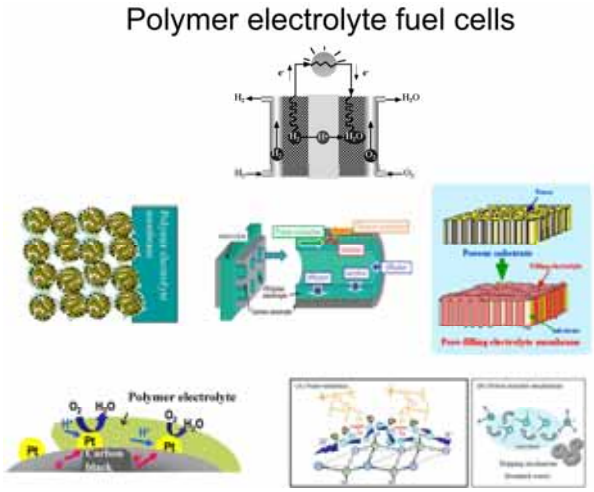

*yamag@res.titech.ac.jp

2A06

Gas permeation properties through ultra microporous inorganic membranes

T. Yoshioka*

Department of Chemical Engineering, Hiroshima University,

1-4-1 Kagamiyama, Higashi-Hiroshima, 739-8527, JAPAN

Membrane separation processes are known to be useful for energy saving in chemical industries. In particular, porous inorganic membranes have chemical and thermal stability, and they are expected to be used for precise separation processes of several gas molecular mixtures under severe conditions. In order to adequately design those membranes and to decide effective operation conditions, it is important to understand gas permeation and separation mechanisms in ultra-micropores on membranes from a point of microscopic view.

In a small pore on silica membranes that have high CO_2 permselectibity, the interaction energy between a permeant molecule and the pore wall affects gas permeation properties. A simple gas permeation model was proposed considering the effect of the attractive and repulsive pore wall potential field, which gave a deviation of the gas molecule concentration in a pore from the ambient gas phase. By the model, the experimental gas permeation properties could be successfully explained (Fig. 1)[1].

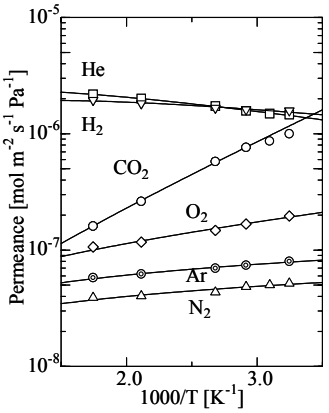

Fig. 1 Temperature dependencies of gas permeance for a silica membrane.

Effects of ultra microporous structure on gas permeation properties were investigated by preparing two types of small pores, silica network pores and inter-particle pores, on virtual silica membranes, and a boundary driven non-equilibrium molecular dynamics simulation method was used to conduct gas permeation simulations through those membrane models. The simulated permeation properties of several gases were in agreement with experimental data on actual ultra microporous silica membranes, indicating the qualitative validity of the microporous structure model composed of small openings in a silica network phase and larger inter-particle pores[2), 3)]. Transport properties of condensable gases were also studied using both the sol-gel derived microporous silica membranes and molecular dynamics simulations (Fig. 2)[4].

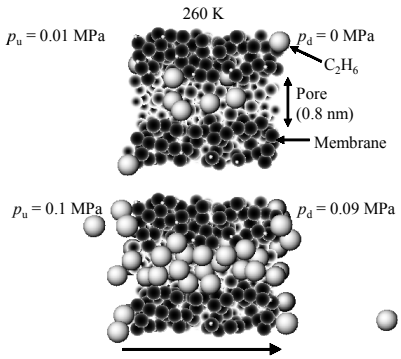

Fig. 2 Snapshots of a cross-sectional view of membranes and permeating C_2H_6 molecules at 0.05 and 0.095 MPa of mean pressure through a pore, 0.8 nm in diameter.

Further development of molecular simulation studies for ultra microporous inorganic membranes would bring about more precise predictions of gas permeation and separation performances.

1) T. Yoshioka et al., *AIChE J.*, **47** 2052 (2001), 2) T. Yoshioka. et al., *Mol. Phys.*, **102** 191 (2004), 3) T. Yoshioka et al., *J Membr. Sci.*, **293**, 81 (2007), 4) T. Yoshioka et al., *Sep. and Purif. Technol.*, **32** 231 (2003)

*tom@hiroshima-u.ac.jp

2A07

Reversible NO_x Sorption-Desorption on Pt/mixed oxides

Koichi Eguchi*, Shunkei Suzuki, Toshiaki Matsui, Ryuji Kikuchi
Department of Energy and Hydrocarbon Chemistry,
Graduate School of Engineering, Kyoto University,
Nishikyo-ku, Kyoto 615-8510, JAPAN

Catalytic deNOx for diesel engines is actively investigated by employing various types of deNO$_x$ catalyst and/or systems. NO$_x$ storage reduction (NSR) catalysts have been reported as the most advanced solution for the elimination of NO$_x$ in lean-burn engine emissions for gasoline based exhaust. We have reported that the NO$_x$ sorbents such as Pt-Li-TiO$_2$ system function as reversible NO$_x$ sorbents and the NO removal by them were not affected by the presence of CO$_2$. This removal action is initiated by oxidation of gaseous NOx species into nitrate ions on the solid. Then the sorbed NO$_x$ species can be released to the gas phase on reduction of the nitrated solid.

Sulfur-tolerant NO sorbents based on Pt/TiO$_2$ were developed by adding base oxide additives. The base oxide additives were effective in improving the NO sorption capacity of Pt/TiO$_2$ under both SO$_2$-free and SO$_2$-containing atmosphere. The NO sorption capacity of Pt-Li$_2$O/TiO$_2$ was unaffected under SO$_2$-containing atmosphere. TPD spectra of H$_2$S in H$_2$ after sorption reaction of 6h in SO$_2$-containing atmosphere showed that SO$_2$ stored on Pt-Li$_2$O/TiO$_2$ was released at the lowest temperature among the modified sorbents. In addition to weak basicity of lithium compared to the other additives, formation of Li$_2$TiO$_3$ over Pt-Li$_2$O/TiO$_2$ could lead to instability of the sulfates on Pt-Li$_2$O/TiO$_2$, giving rise to the desorption of sulfur-containing species at the lowest temperature. In situ FT-IR indicated formation of bulk-like sulfate was slow over Pt-Li$_2$O/TiO$_2$, which also contributed to the excellent SO$_2$-tolerance of Pt-Li$_2$O/TiO$_2$. Preparation of Pt-Li$_2$O/TiO$_2$ was investigated by using various TiO$_2$ sources. It was noted that the sorption capacity of NO$_x$ depended strongly on the kind of TiO$_2$ used for preparation of Pt-Li$_2$O/TiO$_2$ (PLT). The PLT catalysts prepared from metal alkoxide and from anatase TiO$_2$ (SSP-25) demonstrated high sorption capacities, as shown in Fig. 1. The sorption catalysts composed of Pt-Li$_2$O/TiO$_2$ were successfully tested for removal of NO$_x$ from diesel exhaust.

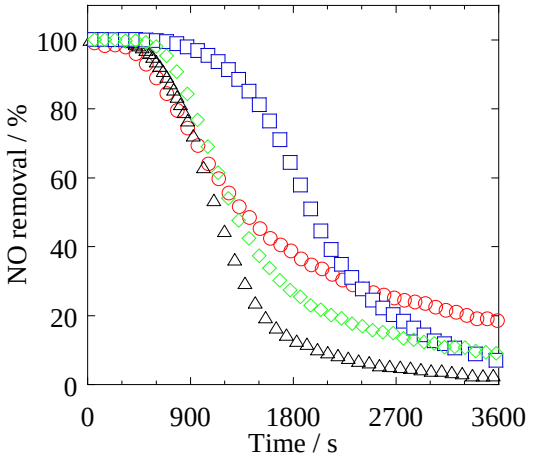

Fig.1 NO removal over 1wt.% Pt-10wt.%Li$_2$O/TiO$_2$. Sorption conditions: 800 ppm NO, 10 % O$_2$, He balance; T = 300ºC

Catalyst	BET surface area (m^2 / g)	NOx sorption ($\times 10^{-5}$ mol)
○PLT(alkoxide)	45	11.8
△PLT(P-25)	40	5.0
□PLT(SSP-25)	57	7.9
◇PLT(STR-100N)	53	6.4

* eguchi@scl.kyoto-u.ac.jp

2A08

Mesoporous silica-based composite materials as molecular selective photocatalysts for purification of water

K. Inumaru*

Graduate School of Engineering, Hiroshima University

1-4-1 Kagamiyama Higashi-Hiroshima, Hiroshima 739-8527

Since TiO_2 is well known as a versatile photocatalyst, many researchers have attempted to combine titanium oxide with mesoporous silicas by various methods such as simple impregnation, the sol-gel method and surface grafting. We have reported a novel type of composite material consisting of TiO_2 crystalline particles and organo-templated mesoporous silica: Highly active TiO_2 crystalline particles (P-25) were directly incorporated into mesoporous silica.[1] This is the first example, to our knowledge, in which oxide particles was directly embedded into mesoporous materials particles. This material shows molecular selective photocatalysis for decomposition of molecules such as 4-nonylphenol, an endocrine disrupter present in water. The TiO_2 content was able to reach more than 60 wt %.

Fig. 1 shows a schematic illustration of the structure of the nanocomposite. TiO_2 particles (20 – 30 nm in diameter) were embedded into mesoporous silica (pore diameter, 3 nm). The silica moiety had uniform mesopores and large pore volume similar to pure meosporous silica. TEM observations and other experiments revealed that, in the nanocomposite, crystalline TiO_2 particles were surrounded by mesoporous silica. Fig. 2 shows the photocatalytic activity for the decomposition of a mixed aqueous solution of several alkylphenols. A mechanical mixture of mesoporous silica and TiO_2 showed non-selective photocatalysis (Fig. 2b). On the other hand, as shown in Fig. 2a, the composite catalyst exhibited higher decomposition rates for 4-nonylphenol and 4-*n*-heptylphenol than for the other phenols. Of the alkylphenols tested here, molecules having a larger alkyl group were decomposed at a higher rate. These results demonstrated that composite catalyst showed highly active and molecular selective photocatalysis.

[1] K. Inumaru et al., *Chem. Commun.* (2005) 2131.

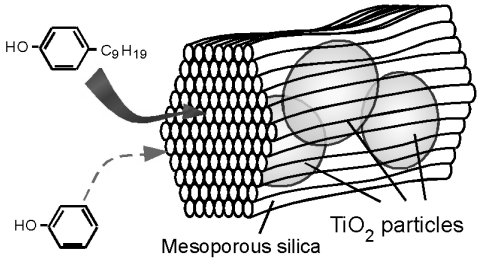

Fig. 1. Schematic illustration of the nano-composite photocatalyst.

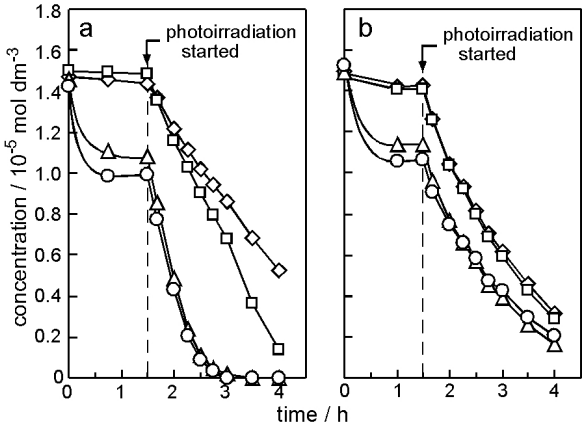

Fig. 2. Photocatalytic decomposition of alkylphenols by 30 mg nano-composite (TiO_2 60 wt%) (a), and by a mechanical mixture of TiO_2 (18 mg) and mesoporous silica (12 mg) (b). ○ , 4-nonylphenol; △ , 4-*n*-heptylphenol; □, 4-*n*-propylphenol; ◇; phenol.

*inumaru@hiroshima-u.ac.jp

2A09

Surfactant-Modified Zeolite and Its Application to Treatment of Oilfield Wastewaters

Robert S. Bowman*

Department of Earth and Environmental Science, New Mexico Institute of Mining and Technology

Socorro, New Mexico 87801, USA

Surfactant-modified zeolite (SMZ) is readily prepared by combining a cationic surfactant with naturally occurring zeolite minerals. The surfactant forms a stable bilayer on the surface, fundamentally altering the zeolite's interfacial properties. The SMZ is very inexpensive (~$500/tonne, $500/m^3), and capable of simultaneous sorption of cations, anions, and nonpolar organics from water.

We tested SMZ as a component of a system to remove dissolved organics, particularly benzene, toluene, ethylbenzene, and xylenes (BTEX), from oilfield wastewaters. Disposal of such waters typically represents about 10% of the cost of hydrocarbon production. We demonstrated in laboratory column experiments that BTEX-saturated SMZ is readily regenerated by air sparging. There was no loss in BTEX sorption capacity, and a minor decrease in hydraulic conductivity, after 50 sorption/regeneration cycles (Fig. 1). Based upon the laboratory results a pilot-scale treatment system was designed and tested at a commercial wastewater reinjection facility. The SMZ-based system was designed to treat up to 110 L of produced water per hour on a continuous basis by running two SMZ columns in series. The system performed as predicted based on laboratory results over repeated feed and regeneration cycles during the month-long operation. The BTEX-laden sparge gases were treated with a vapor-phase bioreactor system resulting in an emissions-free process.

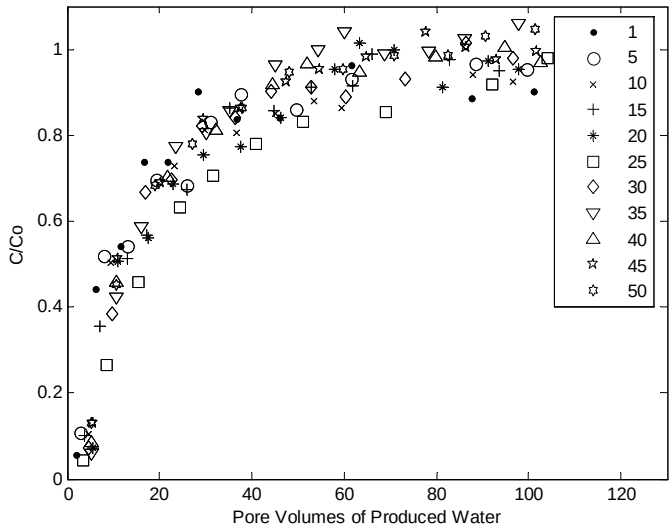

Fig. 1 Breakthrough curves for benzene transport through packed columns of SMZ. Sorption curves for every 5th sorption/regeneration cycle are shown.

*bowman@nmt.edu

2A11

Consideration about Bacterial Attachment as Soft Colloidal Particles

Hisao Morisaki

Graduate School of Science and Engineering, Ritsumeikan University

1-1-1 Noji-higashi, Kusatsu, Shiga 525-8577, Japan

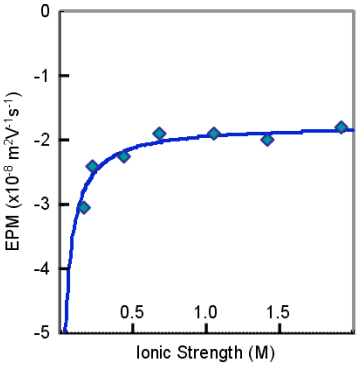

Fig. 1. EPM Change of a bacterial strain cells along with ionic strength.

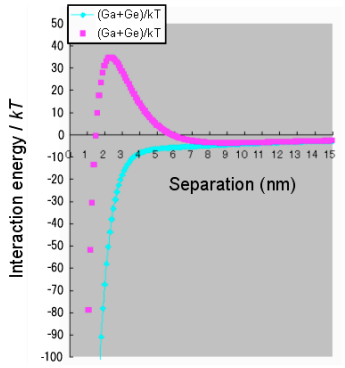

Fig. 2. Energy barrier between a bacterial cell and glass surface disappeared when polymers at the cell surfaces were taken into account.

Bacteria are organisms of colloidal dimension, carrying various kinds of polymers at their cell surfaces. The electrophoretic mobilities (EPM) of bacterial cells change along with increase in ionic strength of suspending medium as illusrtated in Fig. 1, approaching to a non-zero constant value due to the presence of polymers at the surfaces. The EPM change along with ionic strength can be analyzed by applying the Ohshima's theory for soft colloidal particles.

Calculation of interaction energy between *Vibrio alginolyticus* cells and glass surface differed greatly whether taking the presence of polymers at the cell surface into account or not. The energy barrier between the cells and the glass surface disappeared above a certain ionic strength for the bacterial cells when treated as soft colloidal particles (Fig. 2). In this case, the bacterial cells will hit the glass surface more frequently with increment in swimming velocity of the cells. This was quantitatively confirmed as shown in Fig. 3.

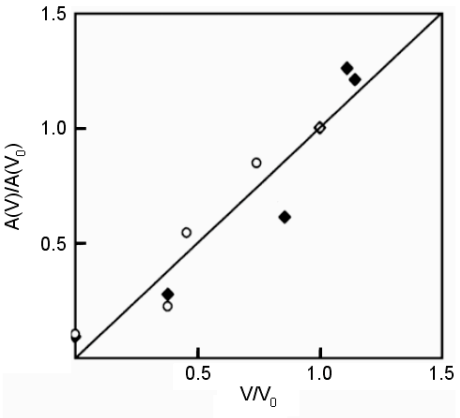

Fig. 3. Relationship between the ratio of swimming velocity of bacterial cell and the ratio of bacterial attachment rate.

At a low ionic strength a small energy barrier between bacterial cells and substrate surface seems to still remain. Further study taking a small energy barrier into account will be introduced and discussed.

2A12

Adhesion, uptake, and cytotoxicity of engineered particles for living cells

H. Shinto*, Y. Aso, J. Tsujimura, Y. Ohta, M. Ito, K. Higashitani
Department of Chemical Engineering, Kyoto University,
Katsura Campus, Nishikyo-ku, Kyoto 615-8510

In the last decade, nanomaterials (i.e., structures with characteristic dimensions of 1–100 nm) have been widely produced in the laboratories and industries throughout the world. Central components of the nanomaterials are engineered nanoparticles. Although the use of nanoparticles is considerably increasing, their potential adverse impacts on the biological systems (i.e., Nano-Risk) are not well understood.

In the present study, the interactions of micrometer- and nanometer-sized particles with living cells have been examined *in vitro* using Atomic-Force-Microscopy (AFM) and Confocal-Laser-Scanning-Microscopy (CLSM), in order to understand the effects of the particle size and the particle surface functionality on the particle–cell affinity and the cellular uptake. Also, the cytotoxicity of the nanoparticles was evaluated using the Trypan Blue assay.

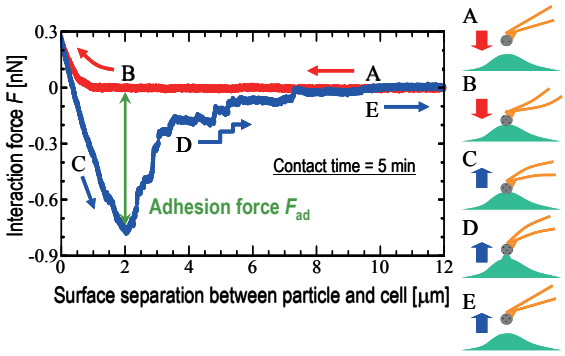

Fig. 1 Typical force–distance profile between a living mouse melanoma cell (B16F10) and a COOH-terminated polystyrene particle of 6.90-μm diameter.

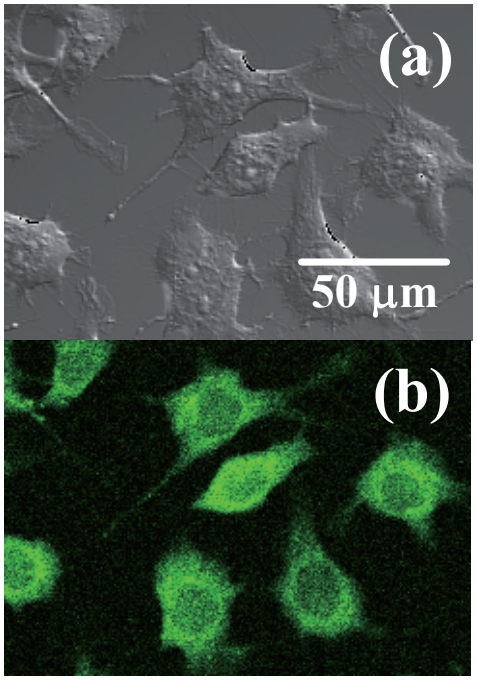

Fig. 2 Mouse melanoma cells (B16F10) after 180-min exposure to the culture medium including COOH-terminated polystyrene particles of 15-nm diameter at 0.080 % (v/v): (a) Differential interference contrast (DIC) image and (b) CLSM image near the basal membranes.

*shinto@cheme.kyoto-u.ac.jp

2A13

Algal assemblages on submerged reed stems and their influence on microbial activities

T. Ohtsuka[1*], D. Nakai[2], Y. Nakamura[1], H. Morisaki[3], I. Yoshinaga[2], I. Imai[2]

[1]*Lake Biwa Museum, Oroshimo 1091, Shiga 525-0001*

[2]*Faculty of Agriculture, Kyoto University, Kitashirakawa-oiwake-cho, Sakyo, Kyoto 606-8502*

[3]*Faculty of Science and Engineering. Ritsumeikan University,*
1-1-1 Noji-higashi, Kusatsu, Shiga 525-8577

The structure of epiphytic biofilms on submerged reed (*Phragmites australis*) stems is chiefly determined by algae, the dominant components of the biofilm. Algal assemblages therefore play a major role as an interface not only of biological activities themselves, but also through constructing a substrate for various microbial activities. We attempt to clarify the species composition and architecture of algal assemblages on submerged reed stems in Lake Biwa, and their effects on bacterial abundance and microbial activities, especially denitrification.

Among the algae composing the biofilm on submerged reed stems, diatoms are the richest in species number and often the most abundant in the degree of cover. We examined 42 diatom samples collected from reed stems in Lake Biwa and its satellite lakes in May and September 2003. In total 226 species including unidentified ones were observed. Diatoms of stalked (e. g., *Gomphonema*, *Cymbella*), tube-dwelling (e. g., *Encyonema*), rosette-forming (e. g., *Fragilaria*, *Eunotia*), and adnate (e. g., *Cocconeis*, *Achnanthidium*) attaching modes were dominant depending on samples. This marked variation of diatom species composition indicates large variations of biofilm architectures.

We examined secondary successions of algal assemblages on reed stems in terms of species composition and community architecture after wiping off the original biofilm. An experiment was conducted on the eastern shore of Lake Biwa's Southern Basin from 19 May to 17 July, 2007. At first, just before wiping biofilms off, a combination of *Gomphonema*, *Encyonema*, and *Fragilaria* standing among *Cocconeis* formed thick and highly porous biofilm architectures (Fig. 1). Ten days after wiping off these biofilms, tube-dwelling *Encyonema* became dominant and formed three-dimensional but gappy biofilm structures. Subsequently *Encyonema* were gradually replaced by adnate *Cocconeis*, and thus the biofilm became planar on the 31th day. Finally all diatoms decreased and cyanobacteria became dominant, submerged in abiotic foulings.

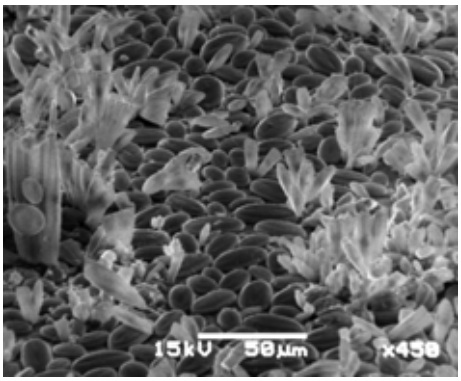

Fig. 1. SEM of the original biofilm.

Bacterial abundances are highly correlated with diatom cell density. This correlation suggests that the diatoms provided microhabitats to bacteria through forming three-dimensional biofilm architecture. Higher denitrifying potential just before wipe-off than those in later months also corresponded to the thick and highly porous biofilm architecture which can provide an aerobic-anaerobic interface.

*ohtsuka@lbm.go.jp

2A14

Factors affecting adhesion of *Staphylococcus epidermidis* cells on stainless steel surface

Melba Padua Ortega*, Tomoaki Hagiwara, Hisahiko Watanabe, and Takaharu Sakiyama
Department of Food Science and Technology, Tokyo University of Marine Science and Technology, Tokyo 108-8477, Japan

The initial adhesion of microbial cells on surfaces is considered as a significant stage in biofilm formation and could potentially lead to increased opportunity for contamination in food processing environments. Microbial adhesion on substrata is governed by complex interactions of microbiological, physical, chemical and material-related parameters. In this study, factors including initial concentration of cell suspension, suspending medium and surface roughness were considered. *Staphylococcus epidermidis* NBRC12993 cells suspended in peptone saline at prescribed concentrations were used to artificially contaminate stainless steel plates (SUS 304, 50x50mm) for 0.5 to 6 h at 25°C. The swab-vortex method was used to determine the number of adhered cells on the stainless steel surface. Results showed that within 0.5min of exposure, initial cell adhesion occurred at low levels, reached maximum levels after 2-3h and remained almost constant until 6h. The effect of suspending medium on initial adhesion was studied using phosphate buffered saline and physiological saline solutions. Cells suspended in peptone saline solution adhered in significantly greater numbers (P<0.05) relative to phosphate buffered saline and physiological saline. Finally, stainless steel plates of varying surface roughness (#100, Ra=1.37µm; #300, Ra=0.14µm; and #400, Ra=0.04µm) were immersed in 10^4 cfu/ml cell suspensions for 3h at 25°C to observe the effect of surface topography on cell adhesion. Significantly higher adhesion of cells was observed for surface with the lowest degree of polish (#100). To study the removability of the adhered cells, contaminated plates were washed with shear force application (2,000 rpm) using water. Only about 20 to 50% of the initially attached cells remained after the washing treatment.

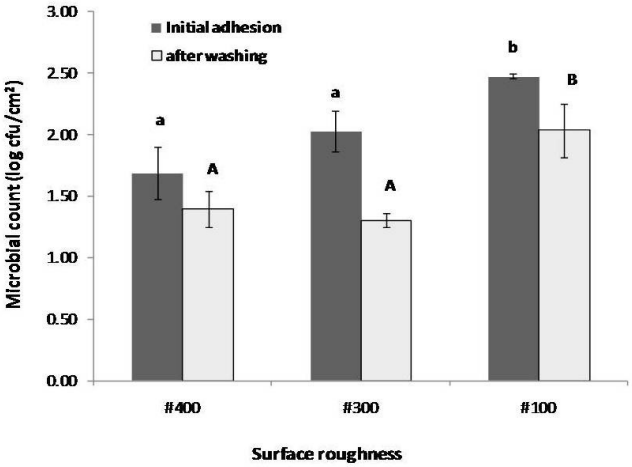

Figure 1. Adhesion of *Staphylococcus epidermidis* onto stainless steel of various surface roughness (Ra=0.04 – 1.37µm) before and after mechanical washing (2,000 rpm) with water.

*melba.ortega@gmail.com

2A15

Interactions of soil macromolecules and microbial DNA isolation

J. Z. He*

Department of Soil Environmental Science, Research Centre for Eco-environmental Sciences, Chinese Academy of Sciences, Beijing 100085, China

Soil is a complex, dynamic and living habitat for a large number of microrganisms. One gram of soil may contain 10^9 bacteria, 10^7 actinomycetes, 10^6 fungi, 10^4 algae and 10^5 protozoa. Soil solid phase is the assemblage of mineral particles, organic matters and organisms. Soil organisms participate in the genesis of the habitat and the formation of soil aggregates and structure. Microorganisms are negatively charged at neutral pH and tend to form complexes with those positively charged minerals such as iron and manganese oxides. Problems are aroused in line with the development of molecular soil microbiology which are greatly based on biomarkers (such as DNA and RNA) isolated from soil matrix. Owing to the complicated interactions among soil components and the biomarkers, it is hard to obtain high quality soil DNA for subsequent bio-molecular analyses. Soil components and also the bio-molecules can be dealt with as soil macromolecules. Clay minerals, clay oxides, humic substances, proteins (enzymes) and DNA/RNA are soil inorganic and organic macromolecules. Thus understanding the interaction mechanisms among soil macromolecules, developing separation technology of DNA/RNA and protein from soil matrix, are important pre-requisite for molecular microbiology. Based on the mechanisms of soil macromolecular interaction mechanisms, we developed a pre-lysis washing soil DNA extraction procedure which was successfully used for high organic matter soil DNA extraction and improved extraction effectiveness and purity by about 30%. A further improved method was successfully used for DNA extraction from soil iron-manganese nodules. The extracted DNA was successfully PCR amplified using bacterial universal primers, cloned and digested (Fig. 1).

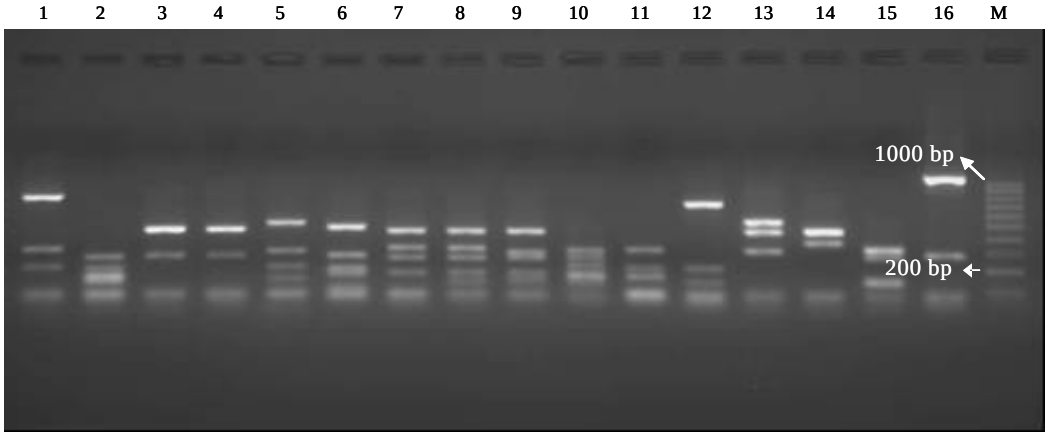

Fig.1. Restriction patterns of 16S rDNA of clones digested with *Hae* III from Wuhan iron-manganese nodule sample. No. 1-16: numbered clones. M: DNA marker.

*jzhe@rcees.ac.cn

2A16

The impact of cell surface properties on the stability of inoculated yeast strains in a biological system used for treating high-strength oil-containing wastewater

Wenzhou Lv[1,2], Yu Zhang[1], Min Yang[1]*

[1] *State Key Laboratory of Environmental Aquatic Chemistry, Research Center for Eco-Environmental Sciences, Chinese Academy of Sciences, Beijing 100085, China*

[2] *College of Architectural, Civil Engineering and the Environment, Ningbo University, Ningbo 315211, China*

Yeast technique used for treatment of oil-containing wastewater has received growing concern because of the superior capabilities of yeast in degrading high-strength oil. In previous study, ten yeast strains were applied to a Sequencing Batch Reactor (SBR) to treat high-strength oil-containing wastewater. In 30-day continuous wastewater treatment, COD and Oil removal rate achieved 86.8%-96.9% and above 99.5%, respectively under the influent conditions of the COD of 9000-23000 mg/L and Oil of 4500-16000 mg/L. However, loss of yeast biomass directly threatened the stability of system. In this study, the stability of inoculated yeast strains in biological system was investigated with PCR-DGGE and some measurements of cell surface properties for tracing yeast strains and understanding the impact factors of the system stability. The results of PCR-DGGE showed that G1 (*Candida lipolytica*), O2 (*Candida tropicalis*), and W1 (*Candida halophila*) tended to be surviving in the complex yeast system and became the predominant strains. After the three dominant strains and two non-dominant ones were individually cultured, the cell surface hydrophobicity, cell surface charge, flocculation, emulsification, and growth rate of each strain were compared. The results showed cell surface hydrophobicity of yeasts was one of the decisive factors for the selection of dominant populations by the complex yeast system for treating the high-strength oil-containing wastewater.

Table 1 Cell surface hydrophobicity of different yeast strains

Yeast strains	O5	G1	W1	O2	W2
Hydrophobicity (n-Hexadecane) %	6.6	95.1	23.1	87.7	10.5
Hydrophobicity（salad oil）%	0	97.1	3.4	66.1	0

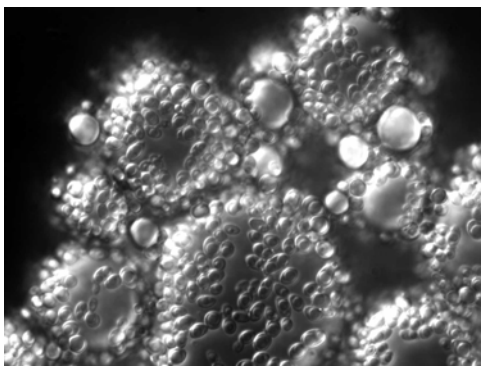

Fig. 1 *Candida lipolytica* cells' selective affinity for oil drops in oil-containing wastewater

* yangmin@mail.rcees.ac.cn

2A17

Biosorption of some heavy metals using microorganisms

T. Tsuruta[1]*, Y. Aiba[2], T. Hirajima[2], and K. Sasaki[2]

[1]*Department of Chemical Engineering on Biological Environment, Faculty of Engineering, Hachinohe Institute of Technology, 88-1 Aza-Ohbiraki, Oh-aza-myoh,Hachinohe, Aomori 031-8501*

[2]*Department of Earth Resources Engineering, Graduate school of Engineering, Kyushu University, 744 Motooka, Nishi-ku, Fukuoka, 819-0395*

The removal of radionuclide and toxic heavy metals from aqueous solutions, especially from contaminated sources, seems to be a significantly useful subject for environmental control and human health. In this regard, the biosorption of several heavy metals from the aqueous solution using various microorganisms has been investigated. Among the microorganisms tested, high uranium absorption ability was exhibited by certain gram-positive bacterial strains, notably *Arthrobacter nicotianae* IAM12342, *Bacillus subtilis* IAM1026, and *Micrococcus luteus* IAM1056 at pH 5.8. *A. nicotianae* cells which showed the best performance, could adsorb 698 mg uranyl ion (2.58 mmol) per gram dry wt. microorganism cells in 1 h. The amount of uranium absorbed by *A. nicotianae* cells was increased with increasing pH of the solution below pH 5. On the other hand, zeta-potential of the surface of *A. nicotianae* cells was decreased with increasing pH of the solution below pH 5. The dominant chemical species of uranium is UO_2^{2+} below pH4. Thus, the bond between positively charged uranyl ion and negatively charged *A. nicotianae* cells was increased with increasing pH of the solution below pH 5. Generally, the negative charge of gram-positive bacteria depends of the amount of phosphate groups in the teichoic acid polymers of the surface of the cells. The molar ratio of negatively charged $H_2PO_4^-$ increased with increasing pH of the solution below pH 4.5.

Additionally, the biosorption of gold using various microorganisms were also examined. The amounts of absorbed gold by the most of gram-negative bacteria were higher than those by the most of gram-positive bacteria. The effect of pH on the amount of absorbed gold and the zeta-potential of the surface of *Pseudomonas maltophilia* cells, which absorbed the highest amount of gold, will be also discussed.

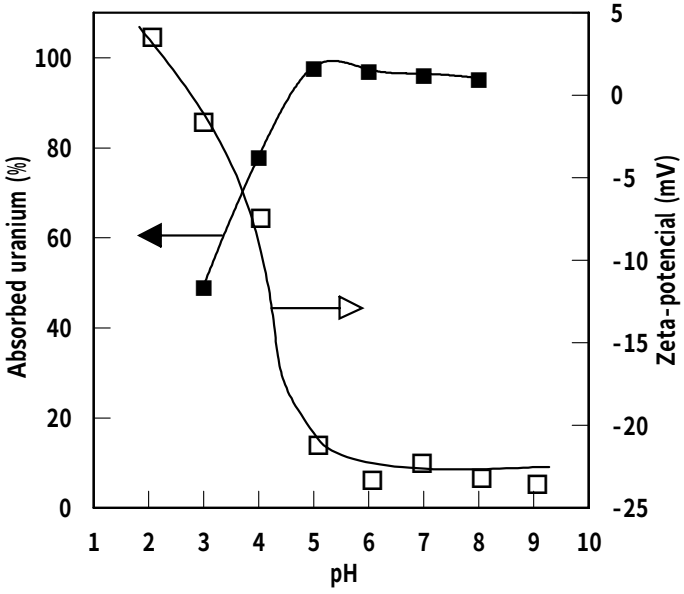

Fig.1 Effect of pH on the amount of uranium absorbed and zeta-potential of the surface of *A. nicotianae* cells.

*tsuruta@hi-tech.ac.jp

2A18

Determination of Copper and Cadmium Binding on Bacterial Cells by Chemical Modifications and Potentiometric Titration

Linchuan Fang, Peng Cai, Xingmin Rong, Wei Liang and Qiaoyun Huang*[1]

Key Laboratory of Subtropical Agriculture and Environment, Ministry of Agriculture
State Key Laboratory of Agricultural Microbiology, Huazhong Agricultural University, Wuhan 430070, China

Fourier transform infrared, potentiometric titration, chemical modification and metal sorption experiments were conducted to compare the behavior of Gram-positive *Bacillus thuringiensis* and Gram-negative *Escherichia coli* as sorbents of Cu^{2+} and Cd^{2+}. The FTIR spectra showed that the absorption band of γ (C=O) bond in –COOH at 1285 cm^{-1} shifted to 1294 and 1290 cm^{-1}, 1722 cm^{-1} shifted to 1731 cm^{-1} and 1727 cm^{-1} for Cu(II)- and Cd(II)-loaded *B. thuringiensis*. However, there were no changes for Cu(II)- and Cd(II)-loaded *E. coli*. The results indicate that carboxyl groups may play an important role in the binding Cd(II) and Cu(II) for *B. thuringiensis*, but not for *E. coli.* A three site non-electrostatic model provides an excellent fit to the titration curves for both *E. coli* and *B. thuringiensis* with the corresponding first pK_a values of 4.16±0.18 and 3.30±0.24 respectively, suggesting that *B. thuringiensis* contains more carboxyl groups than *E. coli* cell walls. Chemical modification and metal sorption experiments further conformed that carboxyl groups play a more important role in the binding Cd(II) and Cu(II) for *B. thuringiensis* than for *E. coli*, which could be attributed to the higher concentration of carboxyl sites on *B. thuringiensis* than *E. coli*. These studies could provide a better understanding of the geochemical behavior of Gram-positive and Gram-negative bacteria with heavy metals in aqueous and terrestrial environments.

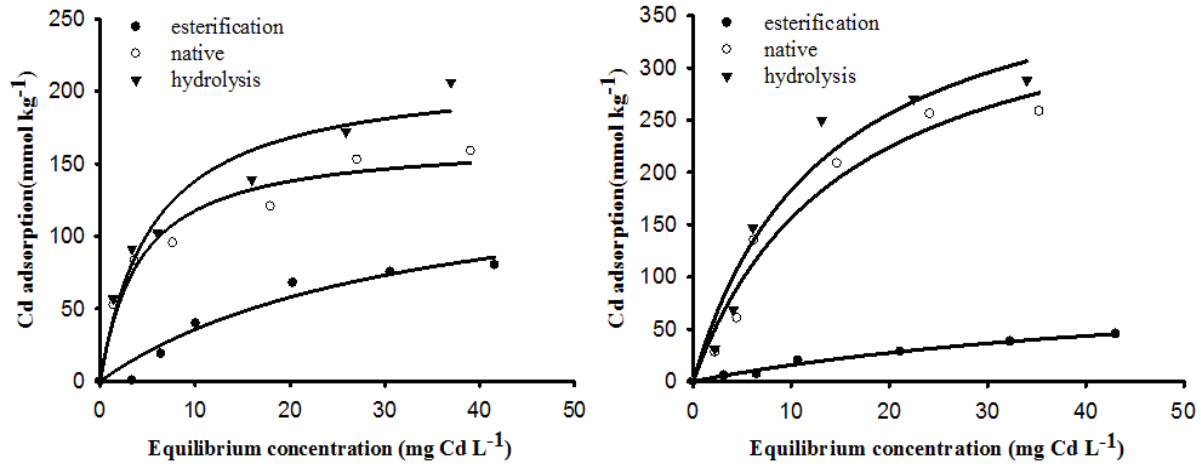

Fig.1 Langmuir isotherm of Cd uptake by *E. coli* (left) *and B. thuringiensis* (right)

[1] qyhuang@mail.hzau.edu.cn

2B11

The Direct Determination of Intermolecular Structure of Pollutants in Micropore Using *in situ* X-Ray Diffraction

T. Iiyama*, S. Ozeki
Faculty of Science, Shinshu University,
3-1-1 Asahi, Matsumoto, Nagano 390-8621

The importance of porous materials is increasing in an environmental field such as removal of toxic substances from emission gas and tap water. It is possible that the porous materials remove the pollutants without consuming the energy by the enhanced surface-molecule interaction. The intermolecular structure of molecules in limited spaces is helpful in understanding the removing mechanisms of pollutants using porous materials. The direct determination method for the intermolecular structure of adsorbed phase has strongly desired from the view point of catalytic, biological and adsorption science. However, the analysis method for adsorbed phases in the micropore is limited in molecular level, because the microporous space is surrounded by the solid. X-ray can penetrate various materials, so we can detect directly the structural information on adsorbed phase itself with the X-ray techniques. The information of intermolecular structure among adsorbed molecules can be obtained by in situ X-ray diffraction (XRD) measurements. In previous studies, Iiyama et al. showed that water molecules formed a solid like structure in the carbon micropore even at room temperature from radial distribution function analysis of XRD results [1]. Furthermore, the evidence for the formation of organized molecular assembly of water in carbon micropore was shown by using in situ small angle X-ray scattering (SAXS) [2].

We will report an elaborate method to determine directly intermolecular structure of adsorbed phase using XRD measurements and their reverse Monte-Carlo (RMC) analyse [3]. This method gives a direct image of adsorbed phase in the micropore, even though it is complicated adsorption system containing binary adsorbates. We tried to determine intermolecular structures of H_2O, CH_2Cl_2, $CHCl_3$ and these binary mixtures adsorbed on activated carbon fibers (ACFs) at room temperature. In H_2O/ACF adsorption system, the H_2O cluster formation was confirmed. The CH_2Cl_2 and $CHCl_3$ molecules form a chain-like structure. When $CHCl_3$ was added to the H_2O/ACF system, both H_2O and $CHCl_3$ molecules were mixed well in the micropore, associating with destruction of water structure. We will discuss in detail about these systems with snap shots of molecular arrangements of adsorbed molecules in the carbon micropore.

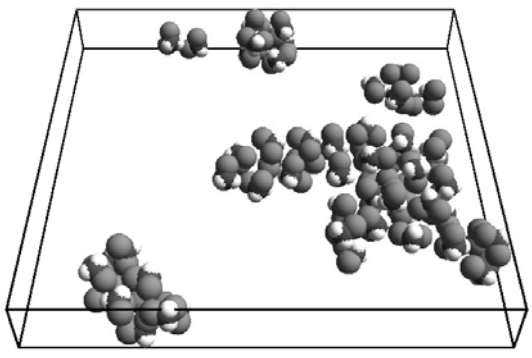

Fig. Snapshot of CH_2Cl_2 adsorbed in the 0.82 nm carbon micropore as obtain from RMC.

[1] *J. Phys. Chem.*, **99**, 10075 (1995). [2] *J. Coll. Surf. A*, **241**, 207-213 (2004). [3] *Adsorpt. Sci. Technol.* **24**, 815 (2006)

*tiiyama@shinshu-u.ac.jp

2B12

Speciation and Hydration of Mineral Surfaces Determined at the Molecular Level

M. Flörsheimer[1-3*], K. Kruse[1,3], R. Polly[1,3], B. Schimmelpfennig[1,3], R. Klenze[1,3], T. Fanghänel[2-4]

[1]*Institute for Nuclear Waste Disposal, Research Center Karlsruhe, Helmholtz-Platz 1, D-76344 Eggenstein-Leopoldshafen, Germany*

[2]*Institute of Physical Chemistry, University of Heidelberg, Im Neuenheimer Feld 252, D-69120 Heidelberg, Germany*

[3]*Virtual Institute Functional Properties of Aquatic Interfaces, Helmholtz-Platz 1, D-76344 Eggenstein-Leopoldshafen, Germany*

[4]*European Commission, Joint Research Centre, Institute for Transuranium Elements, Helmholtz-Platz 1, D-76344 Eggenstein-Leopoldshafen, Germany*

The determination of the exact chemical composition and geometric structure of the functional species at the mineral/electrolyte interfaces is crucial for the reliable transport modeling of pollutants and contaminants in the aquifer. Here we apply two independent techniques to the corundum (001)/water interface: quantum chemical calculations (ab initio and DFT) and the interface selective nonlinear optical technique of infrared sum frequency spectroscopy. The two methods allow us to determine the speciation of the functional groups and to observe their interaction with the adjacent water molecules.

From the bulk crystal structure, a single type of functional species is expected. We can distinguish, however, four aluminol species. They are all doubly coordinated and differ in their OH bond tilt angle. This geometric parameter turns out to be a crucial quantity for the mineral/water interaction. We determine the preferential polar order of the water molecules near the interface. In a broad range around the point of zero charge (pzc), this order is not controlled electrostatically but by hydrogen bonds. Flat oriented OH groups act preferentially as hydrogen bond acceptors and thus favor a water orientation with the net dipole moment pointing to the mineral surface. Steeper oriented OH species serve preferentially as donors thus favoring the opposite polar water orientation. The relative concentration of the OH species and thus the donor/acceptor ratio depend on the pH. When changing the pH in the region around the pzc, the net dipole of the water molecules flips due to a change of the hydrogen bonding network. Such insight in hydrophilic hydration is important for the determination of the energy for any ion or organic molecule bonding to the interface because the removal of water molecules and changes of the preferential water order contribute to the energy balance.

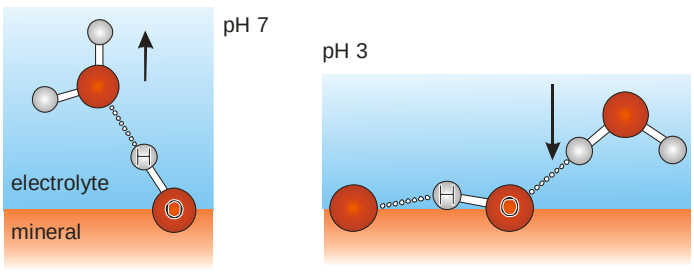

Fig.1 Simplified scheme of mineral/water interaction at corundum (001) surface. Aluminol species with different OH bond tilt angle are detected. The functional species' relative concentrations change with pH. Depending on its tilt, a species acts preferentially as hydrogen bond donor or acceptor.

*florshg@ine.fzk.de

2B13

CH_4 Storage and CO_2 Separation through Expansive Modulation of a Porous Coordination Polymer Sample

Atsushi Kondo,[1] Hiroshi Noguchi,[1] Hiroshi Kajiro,[2] Aya Tohdoh,[1] Yoshiyuki Hattori,[3] Wei-Chun Xu,[4] Mamoru Inoue,[2] Tsutomu Sugiura,[2] Kazuhiro Morita,[5] Hideki Tanaka,[6] Tomonori Ohba,[1] Katsumi Kaneko[1], Hirofumi Kanoh[1]*

[1]Graduate School of Science, Chiba University, Yayoi, Inage, Chiba 263-8522,Japan, [2]Nippon Steel Corporation, Shintomi, Futtsu, Chiba 293-8511, [3]Department of Chemistry, Faculty of Textile Science and Technology, Shinshu University, Ueda 386-8567, [4]Institute of Research and Innovation, Takada, Kashiwa, Chiba 277-0861, [5]Nippon Steel Chemical Co., Ltd., Chiyoda-Ku, Tokyo 101-0021, [6]Department of Chemical Engineering, Kyoto University, Kyoto 615-8510, Japan

Gaseous fuels such as CH_4 and H_2 are considered to be cleaner energy sources than fossil fuels. For the storage and transportation of these gases, compression in high-pressure containers or liquefaction by cooling is generally used. However, new systems that can store gases at moderate pressure and ambient temperature are in demand for the popularization of the clean-energy fuels. Although a gas adsorption system that uses appropriate adsorbents is one of the candidates for such a system, CH_4 and H_2 are classified as supercritical gases at ambient temperature, and it is intrinsically difficult to store them by physical adsorption because of their weak interaction with the adsorbents. Therefore, nanoporous materials such as carbon nanotubes, carbon nanohorns, and porous coordination polymers (PCPs) have currently attracted considerable interest because of their strong affinity to CH_4 and H_2. This affinity arises from a strong potential that is the result of the superposition of potentials from the nanopore surfaces. However, there is a serious disadvantage in using such nanoporous materials and traditional microporous materials (activated carbons and zeolites) that owing to their strong adsorptivity, the high energy is required for the recovery of the adsorbed gas from these materials. Consequently, a guiding principle that is different from the conventional nanoporous adsorption system is required for the development of materials to enable a large-amount adsorption/easy desorption. Such a “large-amount adsorption/easy desorption” is an ideal property for pressure swing adsorption and temperature swing adsorption systems, which are designed for the separation of “global warming gases” such as CH_4 or CO_2. The principle of these systems is selective adsorption and recovery at low pressure or high temperature. Therefore, a gas-releasing property is important in addition to selectivity and high adsorptivity.

We have previously reported a type of PCP, $[Cu(bpy)_2(BF_4)_2]_n$ (bpy = 4,4′-bipyridine), which is termed as a latent porous complex (LPC) [1]. This complex shows a specific response to gas pressure, known as a "gate phenomenon." Although this two-dimensional layered-type PCP contains no effective pores in the initial state, it undergoes a cooperative structural change through clathrate formation with gas molecules at the relatively high gas pressure condition and adsorbs a large amount of gases. When the gas pressure decreases, the adsorbed gases are easily recovered because of the reverse reaction of the clathrate formation. In this paper, we report the utilization of an LPC for practical applications such as CH_4 gas storage and CO_2 separation with more than 99% purity by a single process.

[1] A. Kondo *et al*., *Nano Lett.*, **2006**, 6, 2581.

*kanoh@pchem2.s.chiba-u.ac.jp

2B14

The Change of morphology and CO_2 adsorptivity of a Cu-MOF on Rehydration

Y. Cheng[1]*, A. Kondo[1], H. Noguchi[1], H. Kajiro[2], K. Urita[1], T. Ohba[1], H. Kanoh[1], and K. Kaneko[1]

[1]Graduate School of Science, Chiba University,

1-33 Yayoi, Inage, Chiba, 263-8522 Japan,

[2]Nippon Steel Corporation, Shintomi, Futtsu, Chiba, 293-8511, Japan.

Porous Metal-organic frameworks (MOFs) are attracting considerable attention owing much to their potential applications in environmentally friendly technologies for gas separation, recovery and storage. As to flexible frameworks, it is important to know how guest molecules affect a frame structure and thus their functionality. Here, we report the structure change of a Cu-MOF, $\{[Cu(bpy)(H_2O)_2(BF_4)_2](bpy)\}$(1), and its dehydrated form, $\{[Cu(bpy)_2(BF_4)_2]\}$(1a) upon rehydration and the resulting CO_2 adsorption adsorptivity.

After removal of water molecules, 1 changes to 1a, which shows unique CO_2 "gate adsorption". Reversible adsorption of water molecules on 1a was found through water adsorption, IR, in situ XRPD and TG studies. On the other hand, examination of CO_2 adsorptivity on rehydrated form, 2, shows an abrupt CO_2 uptake at nearly the same "gate pressure" as that of 1, but with isotherms slightly deformed, as shown in Fig.1. This is probably due to morphology change caused by partly deviation of the orientation of stacking structure during the rehydration process, which can be inferred from significant increase of intensity in certain reflection planes (Fig.2) and supported by the SEM photos.

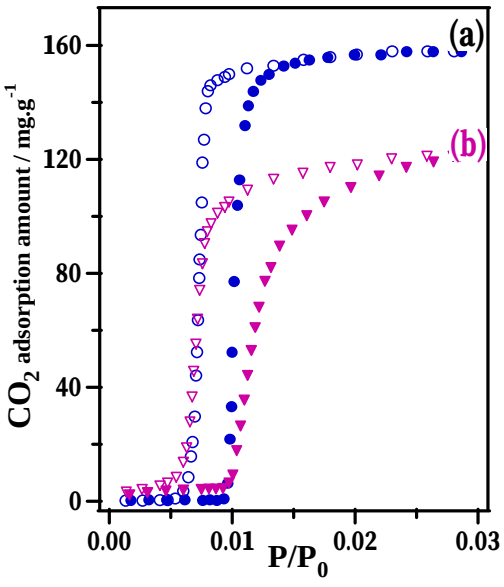

Fig.1 CO_2 adsorption isotherms at 273K for (a) 1 pretreated at 423K and (b) 2 pretreated at 423K

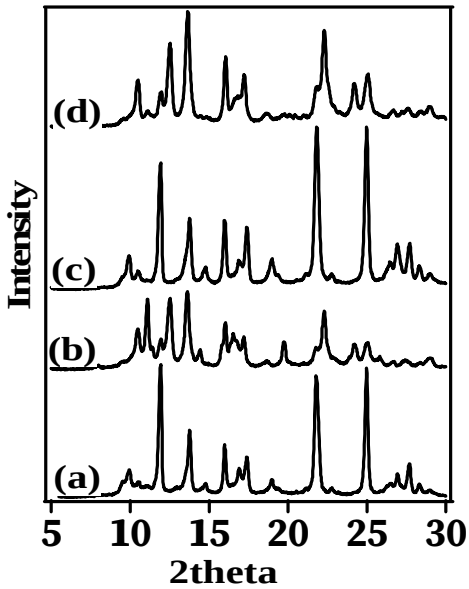

Fig.2 XRPD patterns of (a) 1, (b) 1a, (c) 2 and (d) 2a

*chengyan@pchem2.s.chiba-u.ac.jp.

2B15

Stripe Pattern Formation on Hydrophilic Surfaces by Convective Self-Assembly

S. Watanabe*, S. Mizuta, T. Yamamoto, and M. Miyahara
Department of Chemical Engineering, Kyoto University,
Katsura, Nishikyo, Kyoto 615-8510

A lot of efforts have been devoted to study the formation process and characteristics of colloidal crystals prepared with "bottom up" self-organization processes. A recent interest is in controlling particle positions to construct complex functional structures. In this study, we fabricate stripe-patterned particle layers by using the convective assembly method, and examine the effects of several factors on the periodicity of the stripe pattern to clarify the mechanism of the formation process.

Stripe-patterned layers spontaneously formed on a hydrophilic substrate from a suspension containing silica particles, an example of which is shown in Fig.1(a). White stripes are composed of close-packed particle arrays, as seen from Fig.1(b), and they form parallel to the liquid–substrate contact line. Dark gray bands indicate bare parts of the substrate where almost no particles are deposited.

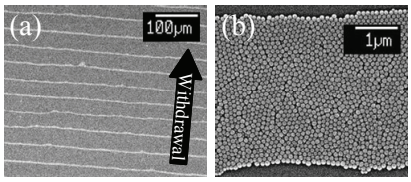

Fig.1 (a) A SEM image of a stripe-patterned layer. (b) A magnified image of a stripe.

The stripe width is found to be proportional to the particle volume fraction, ϕ. The stripe spacing, in contrast, does not depend on ϕ, but increases with the increase of the number of stacked layers comprising stripes. Furthermore, the stripe width and the spacing show a clear correlation. After having struggled with some possibilities such as the energy balance, force balance for the meniscus, and others, all of which went in vain, we have finally devised a new mechanism for the formation of stripe patterns on a hydrophilic surface (Fig. 2).

(i) The front edge of a meniscus is pinned to the tail end of a particulate film, width of which increases due to particle flux from underneath.

(ii) In the present condition, ϕ is so small that particles are not supplied enough to keep the growth, and accordingly the meniscus is elongated and curved to narrow the "path" of particle flux between the regions (A) and (B). The particle flux into (A) gets fewer, and in (B), on the other hand, the concentration gets higher.

(iii) The meniscus elongation stops at a certain limit, resulting in the formation of a stripe and spacing. Because (B) is in high concentration, the next stripe is ready to be formed stably.

In this manner, a negative feedback of the particle concentration around the regions (A) and (B) plays a key role in the stripe pattern formation. We demonstrate the quantitative validity of the proposed mechanism by comparing with experimental results.

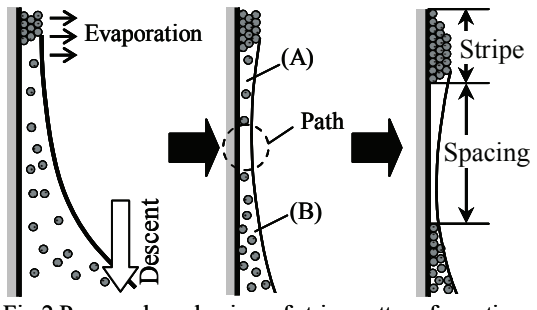

Fig.2 Proposed mechanism of stripe pattern formation.

Acknowledgment
This work was partly supported by Kyoto Prefecture Collaboration of Regional Entities for the Advancement of Technological Excellence, JST.

*nabe@cheme.kyoto-u.ac.jp

2B16

Ultrasound imaging of antibody-labeled microbubbles

K. Tsuchiya[1]*, K. Fujiwara[1], T. Konno[2], K. Itani[2], T. Ito[2], T. Matsuura[3], K. Ohkawa[4], K. Tsubone[1], K. Sakai[1], H. Sakai[1], M. Abe[1]

[1]Faculty of Science and Technology, Tokyo University of Science, 2641 Yamazaki, Noda, Chiba 278-8510, [2]Aloca Co. Ltd., 3-7-19 Imai, Ome-shi, Tokyo, 198-8577, [3]Department of Laboratory Medicine, The Jikei University School of Medicine, 3-25-8 Nishi-Shimbashi, Minato-ku, Tokyo 105-8461, [4]Department of Biochemistry, The Jikei University School of Medicine, 3-25-8 Nishi-Shimbashi, Minato-ku, Tokyo 105-8461

We report the preparation of micro/nano bubbles with an antibody (anti-CD147) for ultrasound contrast agents and the ultrasound imaging for the bubbles. Newly synthesized cycloamylose-modified surfactant and polymerizable cationic gemini surfactant were used to prepare "nanobubbles". Sulfur hexafluoride (SF_6) and 30% glycerin aqueous solution were respectively used as entrapped gas and solvent for the stabilization of bubbles. Nanobubbles (ca. 200 nm) of cycloamylose-modified surfactant were prepared by the irradiation of ultrasonic wave (20 kHz) and imaged by ultrasound. Monodispersed nanobubbles (ca. 600 nm) formed by polymerizable cationic gemini surfactant were obtained when SF_6 gas was pressed in the flow of the surfactant solution through a porous glass with the pore size of 70 nm.

Then an antibody (anti-CD147) which selectively adsorbs on tumor cells due to antigen-antibody reaction was labeled to microbubbles. Ultrasound imaging for the microbubbles labeled with anti-CD147 was tried using a Radial Flow Bioreactor (RFB). To create a three-dimensional model of liver organoid, a hydroxy apatite-fiber scaffold (AFS) column, was used, and a human liver tumor (FLC-7) was cultured in the column. The anti-CD147-labeled microbubbles were accumulated on the liver tumors, and clearly imaged by ultrasound for 10 min after injection to the RFB (Figure 1a). On the other hand, microbubbles formed by a commercial ultrasound contrast agent were not accumulated on the liver tumors (Figure 1b).

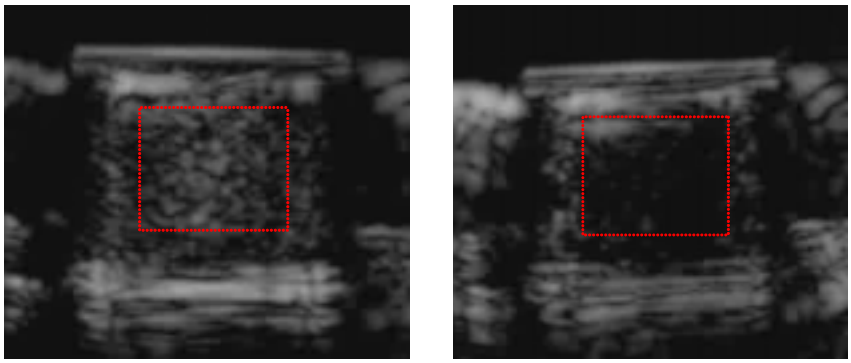

(a) anti-CD147 labeled microbubbles (b) commercial ultrasound contrast agent

Fig. 1 Ultrasound imaging using a three-dimensional model of liver tumors

*kjtsuchi@rs.noda.tus.ac.jp

2B17

Adsorption of Ionic and Non-ionic Surfactants on Shungite

A.V. Sineva*, A.M. Parfenova

Faculty of Chemistry M.V. Lomonosov Moscow State University,

Leninskie gory, 119991, Moscow, Russia

The adsorption ability of surfactants contaminating surface-water and ground-water, either ionic (sodium dodecylsulfate—SDS and cetyltrimethylammonium bromide—CTAB) or non-ionic (Triton X-100), on powders of non-activated and mechano-chemically activated shungite of the type III in comparison to the activated shungite of the type I [1], were investigated in the work presented. The surface tension of the solutions of surfactants was determined by the method of the maximum bubble pressure. Previous measuring dynamic surface tension both of water and of aqueous solutions of surfactants were determined for adsorption times up to 10 to 150 sec. The absence of dynamic surface tension as well as of minimum in the equilibrium surface tension versus concentration isotherms allows to conclude about surface-chemical purity in the surfactants studied. Adsorption isotherms of surfactants at the air/water and solid/water interfaces at varying time of adsorption process (from 2 h to 7 days) were obtained. The experimental data were fitted to the Langmuir equation and the Gibbs-Langmuir model and the following adsorption parameters were estimated for both the air/water and the solid/water interfaces: the adsorption maxima Γ_m and Γ^*_m, the adsorption activities k and k^*, a surfactant molecule cross-sectional area at the air/water interface, s_1, and the specific surface area of adsorbent, S_1. As shown in *Fig.*, the adsorption of CTAB on the activated type III shungite appeared to be about 10 times higher than those on the non-activated shungite as a result of the large specific surface area of shungite after activation (40.2 m^2/g; cp. 4.2 m^2/g for non-activated shungite). Adsorption of all surfactants on the activated type I shungite as well as its specific surface area were several times lower than those found for the activated type III shungite. The peculiarity of the type III shungite structure is known to be the existence of an penetrating network between two phases—carbon and silica, which are the main components of shungite rock and have a great surface area. As for S_1 of activated the types I and III shungite obtained, it has been shown that these values are in good agreement with the BET surface area values or lower than the BET area. The comparative thermodynamic characterization of adsorption and accompanying micellization of surfactants in water was implicated for the selection of adsorbents, which are efficient in the purification of sewage.

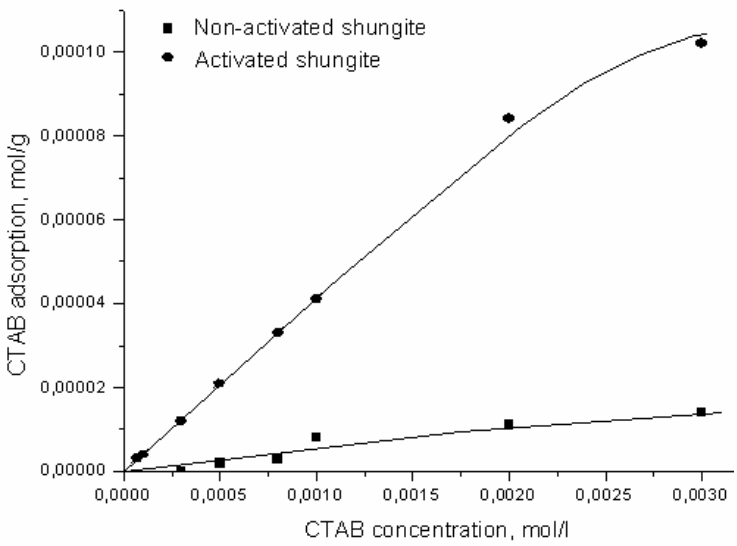

References

1. A.V. Sineva, A.M. Parfenova, A.A. Fedorova. Colloids and Surfaces A: Physicochem. Eng. Aspects. 306 (2007) 68-74.

* asineva@mail.ru

2B18

Adsorption of water and methanol on ZSM-5 zeolite

Ken-ichi Sawamura[1], Yasushi Sekine[1,2], Eiichi Kikuchi[1,2], Masahiko Matsukata[1,2*]

[1]*Department of Applied Chemistry, Waseda University*

3-4-1 Okubo, Shinjuku-ku, Tokyo 169-8555, Japan

[2]*Advanced Research Institute for Science and Engineering, Waseda University*

Zeolites, microporous aluminosilicate crystals, have widely been used as adsorbents, catalysts, and ion exchangers. Zeolites have superior physicochemical properties, such as molecular sieving and preferential adsorption, in addition to high thermal, chemical, and structural stability. Therefore, researchers have been motivated to apply in a variety of applications like membranes, microelectronics, and medical diagnosis. For these applications, adsorption properties are fundamental but essential.

In this study, we measured the amount of water and methanol loadings on ZSM-5 type of zeolite by means of tapered element oscillating microbalance [1] in the temperature range of 150-300^{o}C. Adsorption properties of ZSM-5 with different Si/Al ratios and kinds of exchanged cation were discussed. Since experimental data are not influenced by such factors as buoyancy and flow patterns, which are encountered with conventional gravimetric methods, experimental conditions can be varied over a wide range of temperature. Fig. 1 shows adsorption isotherms of water and methanol on Na^+-exchanged ZSM-5 with different Si/Al ratios at 250^{o}C. The amounts of water and methanol loadings significantly increased with a decrease in the Si/Al ratio. The lack of quick uptakes of water and methanol at low partial pressures with high silica ZSM-5 suggests a dominant role of Al (exchanged cation sites) in the adsorption of water and methanol. In addition, we compared the adsorption isotherms of water on Na^+-ZSM-5 (Si/Al = 12) and Na^+-free, H^+-ZSM-5 (Si/Al = 12). For instance, at 250^{o}C and 10 kPa of water, the water loading significantly decreased from 7.2 to 3.7 molecules per unit cell by exchanging Na^+ with H^+. On the other hand, at 423 K and 10 kPa of water, water loading exceeded 10 molecules u.c.$^{-1}$ on both Na^+-ZSM-5 and H^+-ZSM-5. These results indicate that the interaction of Na cation with molecules is dominant for the adsorption of polar molecules at higher temperature rather than van der Waals force between molecules and zeolite framework.

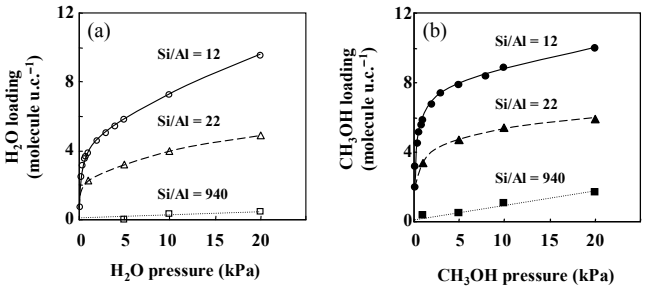

Fig. 1 Adsorption isotherms of Na^+-exchanged ZSM-5 for (a) water and (b) methanol at 250^{o}C.

Reference

[1] W. Zhu *et al*., Ind. Eng. Chem. Res. 37 (1998) 1934–1942.

*mmatsu@waseda.jp

2E11

Wastewater treatment: TiO_2 Photoassisted Degradation of the Binary Systems of Cationic/Anionic surfactants and their Components in Aqueous Dispersions

H. Hidaka[1]*, H. Honjo[1], T. Koike[1], T. Oyama[1], N. Serpone[2]

[1]*Frontier Research Center for the Global Environment Science, Meisei University, 2-1-1 Hodokubo, Hino, Tokyo 191-8506*

[2]*Dipartimento di Chimica Organica, Universita di Pavia, via Taramelli 10, Pavia 27100, Italia*

The plural component of different surfactants is commonly employed for practical application of detergent, shampoo, rinse and others. The aquatic contamination after using them is serious for wastewater treatment. Particularly, a cationic surfactant is accumulated at the bottom of rivers and seas without biodegradation over a period of several months or years. Therefore, the photocatalytic degradation of recalcitrant cationic (e.g. BDDAB*) /anionic (e.g. DoS**) mixed surfactants was investigated to reveal the oxidative pathways of their photomineralization. The adsorption behavior of the mixed surfactants on the TiO_2 surface is closely dependent upon the degradation rate. Since the TiO_2 catalyst exhibits a positive zeta-potential in acidic media, an anionic surfactant is preferentially adsorbed on the TiO_2 surface. The OH radicals species formed on the TiO_2 surface attacked first to an anionic one followed by hydroxylation, formation of organic acid intermediates and CO_2 evolution. Whereas, a cationic surfactant, which exists somewhat in bulk solution due to the electric repulsion, is slowly decomposed after definite time lag. The cmc value for system is remarkably lower than that of the individual pure system because of the formation of complex or the mixed micelle (Fig. 1). The cationic BDDAB surfactant was degraded more slowly than the anionic DoS from the temporal results of surface tension, TOC and CO_2 evolution (Fig. 2). The influence of co-habitation of two different types in the overall photodegradation of the mixed surfactant was assessed and the speculation model concerning adsorption behavior and the mineralization was proposed.

*BDDAB (benzyldimethyldodecyl ammonium bromide)

**DoS (sodium dodecyl sulfonate)

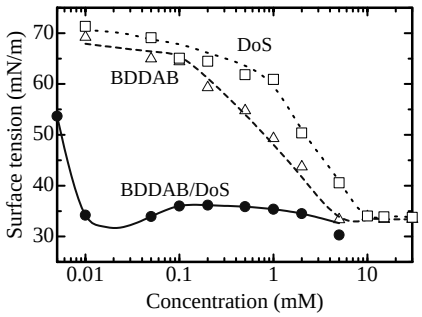

Fig.1 Surface tension for the mixed BDDAB/DoS concentration.

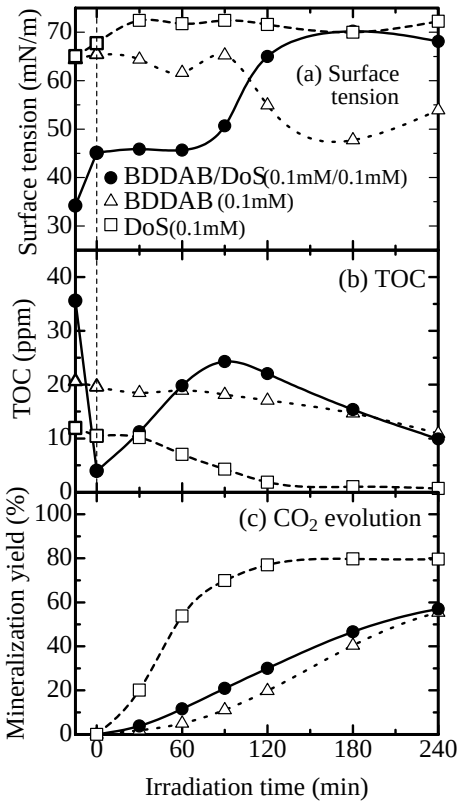

Fig.2 Temporal photodegradation for the mixed BDDAB/DoS surfactant.

*hidaka@epfc.meisei-u.ac.jp

2E12

Photoelectrocatalytic Degradation of Organic Contaminants at Novel Electrodes

Xu Zhao*, Huijuan Liu, Jiuhui Qu

State Key Laboratory of Environmental Aquatic Chemistry, Research Center for Eco-Environmental Sciences, Chinese Academy of Sciences, Beijing, 100085, China

Combined electro-oxidation and photocatalysis (CEP) has shown great potential in water treatment recently in comparison with individual electro-oxidation and photocatalysis. In the present work, $ZnWO_4$, Bi_2WO_6, and γ-Bi_2MoO_6 films were fabricated onto indium-tin oxide glass (ITO) and they are used as anode materials to degrade organic contaminants such as dyes and 4-chlorophene by combined electro-oxidation and photocatalysis at various bias potentials. These film materials showed high efficiency in degrading these organic contaminants. The applied bias potential below redox potential of target contaminants enhanced the photocatalytic degradation of these contaminants by promoting the separation and transfer of photogenerated holes and electrons. At the potential between redox potential and evolution oxygen potential, the degradation of target compounds was further enhanced, which is induced by direct electro-oxidation and photocatalysis. At the potential greater than evolution oxygen potential, indirect electro-oxidation of target compounds occurred with the largest synergetic effect (Fig. 1). The synergetic effect can also increase the mineralization degree of these target compounds. Based on the X-ray photoelectron spectra analysis of the surface of the electrode after electrochemical reaction, the electropolymerization occurred which blocked the electrode and slowed down the electro-oxidation of these target compounds. Active species generated via the photocatalytic process can activate the passivated electrode and promote the electro-oxidation of these target compounds. The O_2 electrochemically generated at the anode promoted the photocatalysis by capturing the photogenerated electrons and may induce the formation of H_2O_2. Thus, more active species could be formed through new reactive routines in CEP process. The stability of the electrodes in CEP process were confirmed. In general, these novel anode materials have a good performance for organics degradation in the combined process.

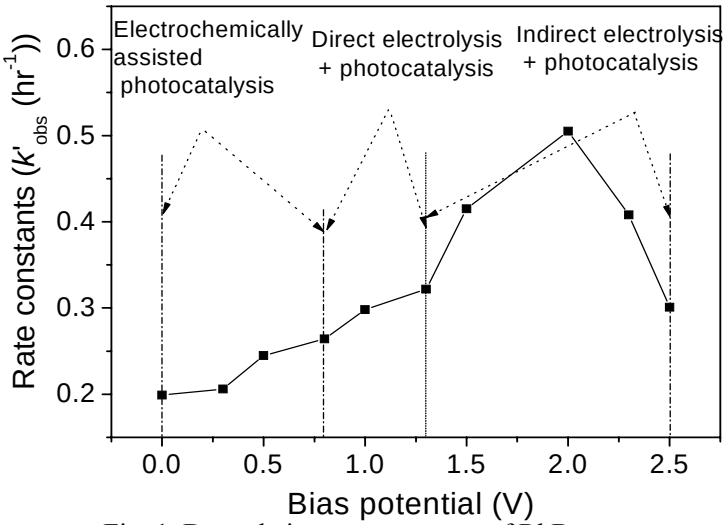

Fig. 1. Degradation rate constants of RhB versus applied bias potential under UV light irradiation

* Email: zhaoxu@rcees.ac.cn

2E13

Oxidation of trichloroethylene with persulfate in the presence iron oxide-coated sand

Chung-Lin Chuang [1], Ming-Chun Lu [2]*

[1] Department of Environmental Engineering and Science, Chia Nan University of Pharmacy and Science, Tainan, Taiwan

[2] Department of Environmental Resources Management, Chia Nan University of Pharmacy and Science, Tainan, Taiwan

In situ chemical oxidation (ISCO) involves the injection or application of an oxidant into the subsurface to transform organic contaminants into less toxic byproducts. An accelerated reaction using persulfate ($S_2O_8^{2-}$) to destroy trichloroethylene (TCE) can be achieved via chemical activation with ferrous ions to generate sulfate radicals ($SO_4^{\cdot-}$) (E^0 = 2.6V). In laboratory study, iron oxide-coated sand catalyzed persulfate oxidation of dissolved TCE was investigated in aqueous systems.

For the iron oxide-coated sand catalysis, 1g, 0.5g and 0.25 g of iron oxide-coated sands were added to conduct the oxidation experiment at 25 ^{0}C. Addition of iron oxide-coated sand accelerated the degradation of TCE by persulfate; the removal was 25%, 15% and 10%, respectively. During the reaction, ferrous ions were dissolved from the iron oxide surface in the rang of 0.08~0.25 mg/l. Under this concentration rage, the catalytic ability can be ignored according to the observation from the control experiment. Therefore, the major catalytic reaction came from the iron oxide surface. However, the dissolved ferrous ions were recrystalized on the iron oxide surface. The reaction pathway is proposed as below,

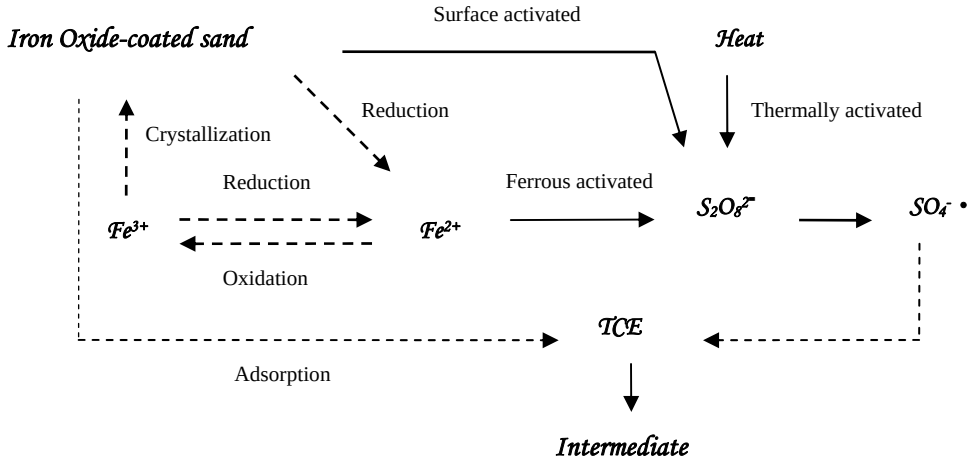

Fig.1 Possible pathway of iron oxide-coated sand catalyzing persulfate for the TCE oxidation.

*mmclu@mail.chna.edu.tw

2E14

Photocatalytic degradation of pathogenic bacteria with AgI/TiO_2 under visible light irradiation

Chun Hu*, Jian Guo, Jiuhui Qu, Xuexiang Hu

State Key Laboratory of Environmental Aquatic Chemistry, Research Center for Eco-Environmental Sciences, Chinese Academy of Sciences, Beijing, 100085, China

The photocatalytic disinfection of pathogenic bacteria in water was investigated systematically with AgI/TiO_2 under visible light (λ>420 nm) irradiation. The two catalysts were found to be highly effective in killing *Escherichia coli* and *Staphylococcus aureus*. The main active species on the surface of the catalysts were clarified by the studies of electron spin resonance and the effect of radical scavengers. The process of destruction of the cell wall and the cell membrane was verified by TEM, potassium ion leakage, lipid peroxidation and FTIR measurements. Some products from photocatalytic degradation of bacteria such as aldehydes, ketones, and carboxylic acids were identified by FTIR spectroscopy. These results suggested that the photocatalytic degradation of the cell structure caused the cell death. The electrostatic force interaction of the bacteria-catalyst significantly affected the efficiency of disinfection on the basis of the E. coli inactivation under different conditions.

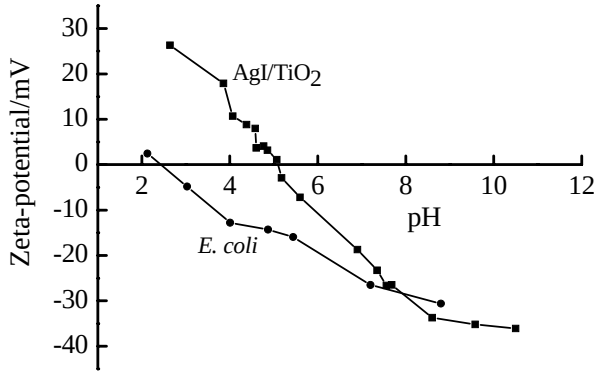

Fig. 1. Zeta potentials for a suspension of 1.0 g/L AgI/TiO_2 in the presence of KNO_3 (10^{-3} M).

*Email: huchun@rcees.ac.cn

2E15

K-doped Microporous Tectoaluminosilicate for Soot Combustion

M. Ogura*
Institute of Industrial Science, The University of Tokyo,
Komaba 4-6-1, Meguro, Tokyo 153-8505

A novel approach, phase transformation at the interface, is proposed for stabilization of potassium in catalytic system employed for combustion of carbonaceous soot matters emitted from diesel engine vehicles. Potassium is known as an active metal for carbon combustion but its mobility leads to its agglomeration and its volatility causes damage to honeycomb-type catalytic converter. The performances of amorphous silica-alumina and crystalline aluminosilicate zeolites are investigated as the support of potassium. Among the materials tested, sodalite, one of clathrate tectoaluminosilicate zeolites, showed the best performance and found to be a promising candidate, especially because of its unique repeatable catalytic activity even after repeated usage at higher temperatures. The better catalytic activity of sodalite compared with open microporous ZSM-5 or LTA-type conventional zeolites might be mainly due to the intimate contact of the catalytically active potassium sites with carbon. The inherent nature of tectoaluminosilicate to hold potassium strongly and stabilize it against high temperatures, and its stability under alkaline conditions generated by hydrated potassium ions under practical driving conditions, further vouch for its better activity. Apart from these experimental facts reported, phase transformation is found to occur at the interface of potassium and sodalite surface, which leads to the formation of further active phase.

*oguram@iis.u-tokyo.ac.jp

2E16

In-situ FT/IR Study on Dynamics of Stored Nitrates on Pt/Ba/MOx (M=Al, Zr, Si, Mg)

Yoshinori Saito,[1] Ken-ichi Shimizu,[1] Takeshi Nobukawa,[2] Naoto Miyoshi,[2] and Atsushi Satsuma[1*]

[1]*Graduate School of Engineering, Nagoya University, Nagoya 464-8603, Japan.*

[2]*Toyota Motor Corporation, Toyota-cho, Toyota, Aichi 471-8572, Japan.*

NOx storage-reduction (NSR) system is an effective technology to remove NOx from lean-burn gasoline and diesel engines. Catalyst for the NSR system is originally based on $Pt/Ba/Al_2O_3$. NOx is stored in Ba as nitrates during lean conditions, and the stored NOx is reduced on Pt by H_2, hydrocarbons, and CO in rich conditions for a short period. In this study, in order to clarify the effect of supports (SiO_2, Al_2O_3, ZrO_2, MgO) on the reaction steps under lean and rich conditions, a kinetic study of surface nitrates is carried out by means of in-situ FT/IR under reaction conditions.

In a flow of NO/O_2 mixture (lean condition), the absorption bands are observed at 1320, 1462, and 1540 cm^{-1}, which are assignable to nitrates on bidentate (1320 and 1540 cm^{-1}) and monodentate (1462 cm^{-1}) nitrates, respectively. When the flowing gas was switched to diluted H_2 (rich condition), the intensity of the bands steeply decreased due to consumption of nitrates by H_2, as shown in Fig. 1. The rates of storage and reduction of nitrates were estimated from the time course of the amount of stored nitrates. Under the lean conditions, the rate of nitrate storage was in the order of $MgO > Al_2O_3 \sim ZrO_2 > SiO_2$. Under the rich conditions, on the other hand, the rate of nitrate consumption was in the order of $Al_2O_3 > ZrO_2 > SiO_2 > MgO$, as shown in Fig. 2. Taking Pt dispersion into account, the reduction activity was compared as turnover frequency, i.e., the reduction rate per exposed Pt atom. The order of the turnover frequency was $SiO_2 > Al_2O_3 > ZrO_2 > MgO$. This trend was entirely opposite to the storage amount of nitrates, and in accordance with that of acid strength of the supports. The dependence of the rate of nitrates reduction on the oxidation state of supported Pt will be discussed.

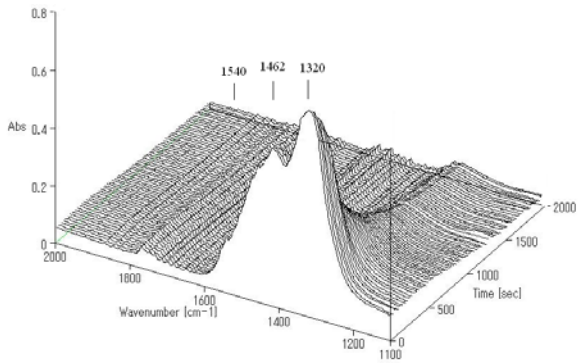

Fig. 1 In-situ FT/IR spectra of adsorbed species on $Pt/Ba/Al_2O_3$ in a flow of H_2 =0.2% at 573 K, after exposure to a flow of NO/O_2 = 200ppm/3%.

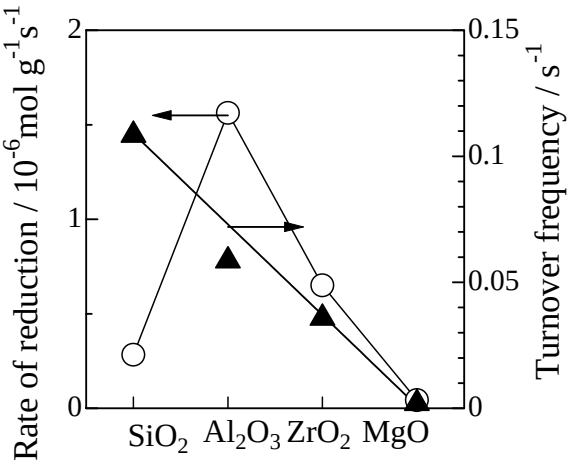

Fig. 2 Rate and turnover frequency of nitrate reduction in H_2 on supported Pt-Ba catalysts under the rich (H_2 =0.2%) conditions at 573 K.

* satsuma@apchem.nagoya-u.ac.jp

2E17

Role of Zeolite for Air Pollution Control

Takashiro Muroi*
Chemical Catalysts Group, N.E.Chemcat Corporation
2-4-1 Hamamatsu-cho, Minatoku, Tokyo, Japan 105-6124

1 . Zeolite as adsorbent

Diluted aromatics, VOC from painting and coating furnace are adsorbed and concentrated with ZSM-5 to reduce for catalytic abatement system. ETS-4 zeolite, modified with Sr can adsorb N_2 (3.6A) from methane (3.8A) which is commercialized as separation of N_2 before sending natural gas through pipeline. High pure N_2 as inert gas for production of semiconductor is introduced from the air by cryogenic. CO can not be removed because of similar boiling point to N_2. CO should be removed at low temperature before cryogenic. Pt-Al_2O_3 is affected by CO_2 and moisture in the room temperature and needs frequent regeneration. Pt-Al_2O_3 coated on 13X can be used long time.

2. Halogen compounds abatement

Pt-Al_2O_3 on Honeycomb catalysts are used widely for VOC abatement. Addition of Pt to SiO_2-B_2O_3-Al_2O_3 mixed with zeolite gives high activity of HC oxidation. Ethylene di-chloride (EDC) is difficult with Pt-Al_2O_3. NaMOR(SiO_2/Al_2O_3=16) is effective to decomposition of EDC.

$C_2H_4Cl_2 \rightarrow C_2H_3Cl + HCl$ And Pt-Al_2O_3 is high active for oxidation of halo-compounds. Then hybrid catalyst, mixed of NaMOR and Pt-Al_2O_3 is developed as abatement catalyst for EDC.

3. NOx abatement catalyst

NH_3 SCR for gas turbine off gas with V_2O_5-TiO_2 is difficult because of high NH_3 oxidation activity at high temperature. Fe- β zeolite does not produce NOx from NH_3 at high temperature.
N_2O produced nitric acid plant can be decomposed with zeolite catalysts, the order of activity is

Cu-ZSM-5=Co-Beta> Cu-Beta>Co-L＞Co-erionite＞Cu-Y＞Cu-L=Ni-ZSM-5>Mn-ZSM-5

Rh-ZSM-5, Ru-ZSM-5, Rh-Al_2O_3, Pd-ZSM-5 gives higher activity than Cu-ZSM-5.

4. Auto exhaust gas

β-zeolite absorbs HC at cold start and oxidize at warm condition. V_2O_5 is vaporized at high temperature on urea SCR system of Diesel engine exhaust gas. NOx can be reduced by OHC with zeolite. OHC can introduced from HC and ozone, generated with plasma. NOx is possible to reduce to NH_3 with CO, H_2 in rich burn atmosphere and adsorb with zeolite, then adsorbed NH_3 reduces NOx at lean burn atmosphere. Any reductive agent may be no need.

5. Expecting application

V_2O_5-TiO_2 cannot be used for NOx abatement of ship boat diesel exhaust gas abatement because of containing large amount of SOx. Fe- β zeolite or Cu- β zeolite does not produce $(NH_4)_2SO_4$ because of low oxidation activity of SO_2.
Direct decomposition of NOx catalyst is expecting to find.

*takashiro.muroi@ne-chemat.co.jp

2E18

Detoxification of organic pollutant by multi-functionalities of humic substances

M. Fukushima*

Division of Solid Waste, Resources and Geoenvironmental Engineering, Graduate School of Engineering Hokkaido University, Sapporo 060-8628, Japan

Humic substances (HSs), which widely distribute in aquatic and soil environments, have been known to be weak-acid polyelectrolytes that are produced via polycondensation of low-molecular-weight phenolic acids. They play important roles in fates and toxicity of ecotoxicants, such as heavy metal ions and pesticides: (i) metal complexing abilities by acidic functional groups; (ii) solubilization of PCBs, PAHs and PCDD/Fs; (iii) transformation of inorganic and/or organic chemicals by the redox activity in the quinone/hydroquinone redox couple. In this presentation, I would like to introduce the following two topics in my works with respect to the detoxification of pentachlorophenol (PCP) using the multi-functionalities of HSs.

(1) Enhanced photo-Fenton reactions by Fe(III)-HA complex [1]

The Fenton reactions have been known as the catalytic degradation of H_2O_2 by Fe(II), and this leads to the generation of hydroxyl radicals (HO·). The HO· can serve as an effective oxidant to degrade organic pollutants in aquatic environments. Photoirradiation of HA brought about the generation of H_2O_2, and photoreduction of Fe(III) to Fe(II) was enhanced in the presence of HA. Such the phenomena, including photoredox reactions of HA and iron, resulted in an enhanced photo-Fenton reaction, and the degradation characteristics of PCP were investigated.

(2) Effect of HSs on the biomimetic catalytic oxidation of PCP [2]

In soil environments, white-rot fungus produce oxidative enzymes such as ligninase and peroxidase, and these can degrade organic pollutants. Although HSs exist as soil organic matter, their effects on the enzymatic degradation of organic pollutants have not been elucidated. To elucidate the enzymatic reactions in soil environments, iron(III)-porphyrin catalysts (Fig. 1) that mimic the active center of the oxidative enzymes were examined. I investigated the effects of HSs on the degradation of PCP via the iron(III)-porphyrin catalytic systems. It was found that the addition of HSs with higher hydrophobicity resulted in an enhanced degradation of PCP. This reason can be attributed to the retardation of self-degradation of the catalyst, due to the formation of supramolecular between iron(III)-porphyrin and HA via the hydrophobic interaction.

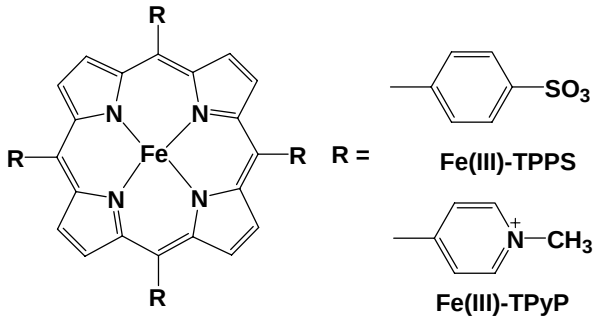

Fig. 1. Iron(III)-porphyrin catalysts

[1] M. Fukushima and K. Tatsumi, Environ. Sci. Technol. 35 (2001) 1771-1778.

[2] M. Fukushima, Y. Tanabe, K. Morimoto and K. Tatsumi, Biomacromolecules 8 (2007) 386-391.

*m-fukush@eng.hokudai.ac.jp

2F11

Removal mechanism of dilute As(V) or F(I) in wastewater using Fe(III) or Al(III) hydroxides co-precipitation method

C. Tokoro[1], Y. Yatsugi[2], D. Haraguchi[2]*, A. Otsuki[1], S. Owada[1] and H. Sasaki[1]

[1]*Faculty of Science and Engineering, Waseda University, Okubo 3-4-1, Shinjuku, Tokyo 169-8555*

[2] *Graduate School of Science and Engineering, Waseda University, Okubo 3-4-1, Shinjuku, Tokyo 169-8555*

The mechanism of co-precipitated phenomena of dilute As(V) or F(I) for Fe(III) or Al(III) hydroxides was investigated toward a quantitative modeling of the co-precipitation process between toxic elements and hydroxides. To discuss the mechanism of co-precipitation phenomena of As(V) co-precipitation for ferrihydrite, four experimental studies have been carried out: (i) adsorption isotherm measurement, (ii) zeta potential measurement, (iii) XRD analysis, and (iv) EXAFS analysis. The results of zeta potential and XRD measurement of As(V) co-precipitated ferrihydrite showed the mechanism of As(V)-ferrihydrite co-precipitation is predominantly simple adsorption of As(V) to the surface of ferrihydrite at low surface coverage (initial molar ratio of As/Fe < 0.5) and surface precipitation of As(V) at high surface coverage (initial molar ratio of As/Fe > 0.5). Moreover, the results of EXAFS analysis showed 65 % of As(V) co-precipitated ferrihydite is surface precipitation at As/Fe = 0.25 and more than 90 % is at As/Fe ≥ 0.5.

In the F(I) case, the adsorption isotherm of co-precipitated F(I) for aluminum hydroxide showed the BET-typed one at both pH5 and 7, which indicates the mechanism of F(I) co-precipitation for aluminum hydroxide is not only simple adsorption but also surface precipitation, as same as As(V) co-precipitation for ferrihydrite.

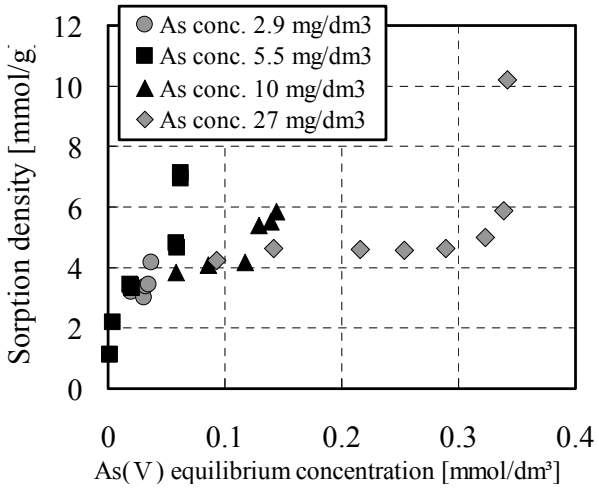

Fig. 1 Adsorption isotherms of As(V) for aluminum hydroxide at pH 5.

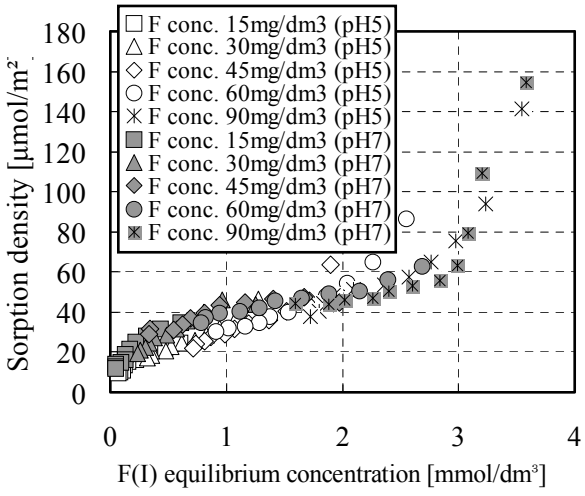

Fig. 2 Adsorption isotherms of F(I) for aluminum hydroxide at pH5 and 7.

*gilford-para525@suou.waseda.jp

2F12

SPECIATION OF ARSENIC IN TREATMENT OF GROUNDWATERS SPIKED WITH ARSENITE USING PERMEABLE REACTIVE MATERIALS

K. Sasaki[1,*], H. Nakano[1], W. Wilopo[1], T. Hirajima[1]
[1]*Faculty of Engineering, Kyushu University,*
744 Motooka, Fukuoka 819-0395

The potential for As removal from groundwaters using permeable reactive materials was evaluated by column experiments. The column materials, organic carbon and zero valence iron (ZVI), were exposed to the simulated groundwaters spiked with 30 mg L^{-1} As(III) to assess the potential for As removal. This high As(III) concentration was selected to ensure that there would be a sufficient mass of As-bearing reaction products available for mineralogical characterization. The experiment was conducted in an anaerobic chamber to replicate the anaerobic conditions that prevail in permeable reactive barrier systems. After loading 22 pore volumes of influent with upflow, the column effluent contained less than 0.001 mg L^{-1} As. After the column experiments were completed, the reactive materials were sampled in the anaerobic chamber and examined using scanning electron microscopy coupled with energy dispersion X-ray analysis (SEM-EDX), and X-ray photoelectron spectroscopy (XPS). The XPS results revealed that arsenic was immobilized as mainly arsenite and partly arsenate to ZVI granules. These observations suggest that the mechanism is explained not by reduction but by simple sorption. The results of geochemical calculation and SEM-EDX suggested that arsenite and arsenate were co-precipitated with mainly Fe(III)-bearing minerals and carbonates.

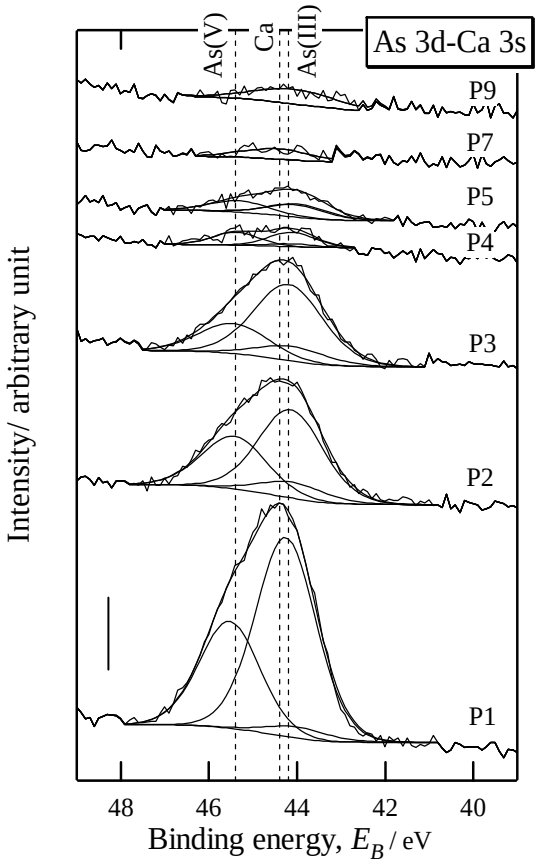

Figure 1 XPS spectra of As 3d-Ca 3s region for ZVI granules at each column level P1(bottom)～P9 (top). A vertical bar indicates 200 cps.

keikos@mine.kyushu-u.ac.jp

2F13

Use of orange waste and pectic acid gel for arsenic removal

B.K. Biswas*, J. Inoue, K. Inoue, H. Harada, K.Ohto, H. Kawakita

Department of Applied Chemistry, Saga University, Honjo 1, Saga 840 0027, Japan

Orange waste, an agricultural byproduct, saponified with $Ca(OH)_2$ and pectic acid crosslinked with formaldehyde, which are called saponified orange waste (SOW) and crosslinked pectic acid (CPA) gels, respectively, were further loaded with Zr(IV) to investigate feasible adsorption of arsenic from aquatic environment. Zr(IV)-loaded SOW gel strongly adsorbed As(V) at pH 2-6 while Zr(IV)-loaded CPA gel was effective only at very low pH (1.4-3). On the other hand, both gels adsorbed As(III) at pH 9-10. Adsorption capacity of Zr(IV)-loaded SOW gel for arsenate (88 mg/g) and arsenite (130 mg/g) was much higher than that of Zr(IV)-loaded CPA gel. Adsorption of arsenate onto both gels followed pseudo-second-order kinetics. Presence of common competing anions e.g. chloride, carbonate and sulfate did not interfere the adsorption of As(V) onto Zr(IV)-loaded SOW. But phosphate, possibly due to its similar chemistry, affected the arsenate adsorption. However, substitution of hydroxyl ligands and/or water molecules, coordinated with zirconium loaded onto the gel matrices, by arsenic anions was supposed to be the pertaining mechanism for adsorption. Both gels were tested for continuous-mode adsorption at laboratory scale by using a column set up. Zr(IV)-loaded SOW gel showed higher dynamic adsorption capacity for both arsenate and arsenite than Zr(IV)-loaded CPA gel. Sodium hydroxide was used to elute arsenate more than 95% from both gels. Such studies showed that cheap and abundant agricultural by-product (orange waste) could be successfully employed for the remediation of an aquatic environment polluted with arsenic.

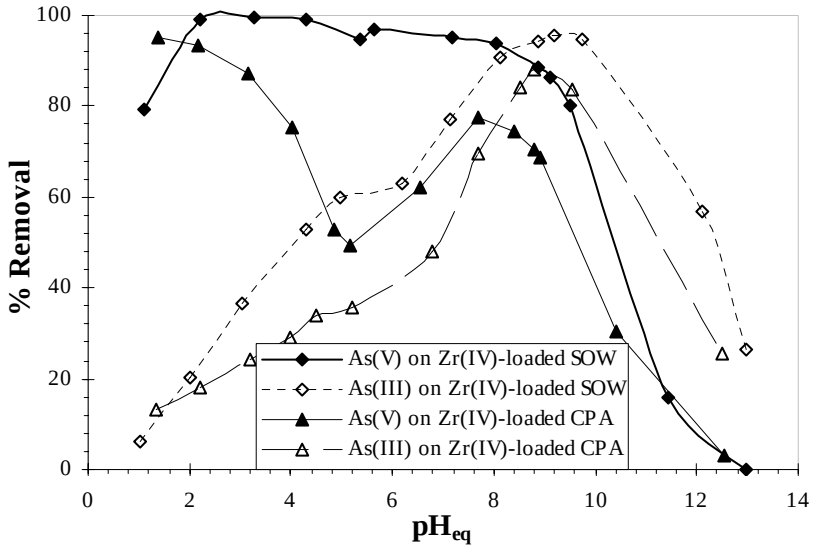

Fig. 1. Adsorption of As(V) and As(III) onto Zr(IV)-loaded SOW and CPA gels.

* 05641002@edu.cc.saga-u.ac.jp

2F14

Removal of Ammonia on Graphite Oxides

*M. Seredych and T.J. Bandosz**
Department of Chemistry, The City College of New York
New York, NY 100031, USA

)

Graphite oxide (GO) was synthesized from commercial graphite and modified by calcinations at 350°C. The samples were used as adsorbents of ammonia at dry and moist conditions. Their surface before and after exposure to ammonia was characterized using adsorption of nitrogen, XRD, SEM, FTIR, TA, CHN analysis, and potentiometric titration. The results showed that oxidation results in incorporation of significant amount of epoxy, phenolic and carboxylic groups which is directly manifested by a decrease in surface pH. The majority of latter is removed by calcinations. During this process the exfoliation of graphite occurs, resulting in formation of some micro- and mesporosity. The materials obtained have proven to be the excellent adsorbents of ammonia (Figure 1). The NH_3 reacts with carboxylic acids, is intercalated between layers, or dissolved in pores with adsorbed water. The mechanism depends on the conditions of experiments and surface features of the samples. The highest capacity is obtained on GO on which a significant amount of water is adsorbed, likely on functional groups. This helps in dissociation of carboxylic groups and their acid –base reactions with ammonia. Nevertheless, a significant amount of ammonia is intercalated between layers. Those two interactions are the strongest. When water is present in the challenge gas, the amount adsorbed decrease due to the competition between water and ammonia for active sties.

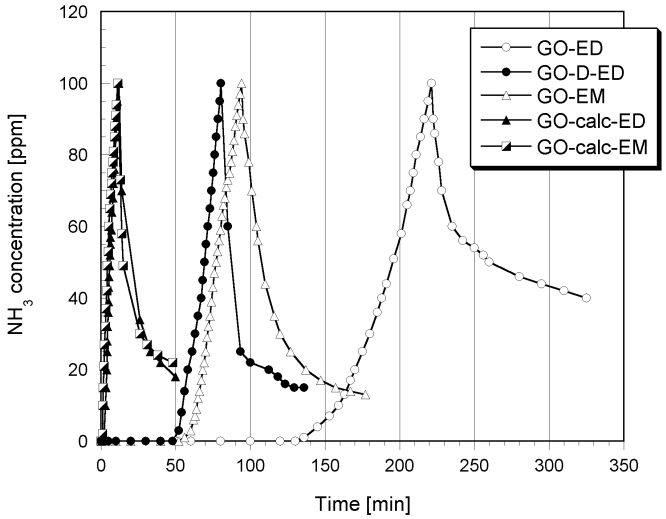

Fig. 1 Ammonia breakthrough curves on modified graphite oxides.

*tbandosz@ccny.cuny.edu

2F15

SURFACE PRECIPITATION MODELS FOR THE SORPTION OF HEAVY METALS ON CALCITE IN DRAINAGE FROM MINING DISTRICTS

O. Gaskova
Institute of Geology and Mineralogy SB RAS
Koptyug prosp. 3, Novosibirsk 630090, Russia

In many studies it has been clearly recognized that carbonate minerals are effective in removing divalent heavy metals (Cd, Cu, Pb, Zn) from solution with the mechanism of interaction found to be a combination between ion-exchange and precipitation on the carbonate surface. A number of investigations have recently examined the spectroscopic imaging and the thermodynamics of phase interfaces and they constitute a fundamental basis for understanding the complex relevant phenomena. But little research has focused on the computer thermodynamic simulation of the exact type of mechanisms affected the sorption of metal ions in natural and mine-related environments.

The Salair mine (West Siberia) has been working since the 1930's, and at present exploits and enriches gold- and silver-bearing barite-non-ferrous sulfide ore bodies. The major and minor components of surface waters, and the content of heavy metals (Cd, Cu, Pb, Zn and Fe) in suspended particles and bottom sediments in drainage streams from the mill tailings impoundment were determined earlier (Gaskova, Bortnikova, 2004). As a whole, the insignificant contribution of water release of toxic elements to the environment in the studied region is related to abundant limestones and dolomites providing effective pH neutralization.

As an example, as the water of Berezovy stream is slightly supersaturated with respect to the calcite and ferrihydrite, that indicate the tendency to precipitate these minerals, and undersaturated with respect to every phases of heavy metals (Wateq4F program), we could simulate the composition of ideal solid solution by Gibbs energy minimization computer code "HCh" of Yu. Shvarov (MSU). It is $Cd_{0,148}Cu_{1,23E\text{-}5}Pb_{0,0034}Zn_{0,137}Ca_{0,712}CO_3$ with $\Delta_fG^0_{298}$ = -240.99 kCal/mol. In case of equilibrated calcite suspensions, with no net calcite dissolution or precipitation that likely prevented metal incorporation into the lattice, the interfacial accumulation of sorbate was simulated using the ion exchange and surface complex formation (adsorption) models. The most uncertain question is which fraction of a total sorbent participates in surface sorption, and we treated it as a fitting parameter. Moreover, the surface precipitation model of (Zhu, 2002) for the most mobile element Zn was tested, where $\Delta_fG^0_{298}$ is -179.41 kCal/mol for $ZnCO_{3(sp)}$ that is different from the bulk $ZnCO_{3(s)}$ in concept.

The work was supported by the Russian Foundation for Basic Research (projects nos. 06-05-64528, 06-05-64166) and Integration Project 6.3. "Geochemistry of Environment and Mining Landscapes of Siberia and the Urals".

1. Gaskova O.L., Bortnikova S.B. Heavy metals mobility through the drainage system of disposed sulfide-bearing wastes. Proceedings of the IS on WRI-11, 2004, v. 2, p. 1509-1512.

*gaskova@uiggm.nsc.ru

2F16

Lead removal from a contaminated soil in shooting range by combining surface grinding and acid leaching

C. Tokoro[1], S. Owada[1], A. Otsuki[1], T. Shiozawa[2], and S. Yuki[2]*

[1]*Faculty of Science and Engineering, Waseda University, Okubo 3-4-1, Shinjuku, Tokyo 169-8555*

[2] *Graduate School of Science and Engineering, Waseda University, Okubo 3-4-1, Shinjuku, Tokyo 169-8555*

Effective environmental purification in soil washing must address not only toxic substance removal but also waste avoidance, reuse, and recovery. The objective of this study is to increase the efficiency of Pb leaching from a contaminated soil in shooing range by combining surface grinding and nitric acid leaching. We examined Pb leaching properties by nitric acid with or without surface grinding. Pb was leached from the contaminated soil at the pH of less than 4 and leaching rate to acid dosage was divided into 3 stages; (i) Pb was rapidly leached because of the desorption from the surface of soil particles and dissolution of minerals including Pb contents at the pH of 2-4, (ii) Pb was slowly leached because of only the dissolution of minerals at the pH of 1-2, and (iii) Pb leaching was saturated at the pH of less than 1. Many associated cations such as Na, K, Ca or Mg in the contaminated soil were leached before Pb leaching and determined the pH of leaching solution. The leaching properties of main cations such as Fe, Al or Si in the contaminated soil could be simulated by the chemical equilibrium calculation supposing about 1% of minerals dissolution.

Surface grinding using an intensive mixer increased the pH of leaching solution because of minerals amorphisation and increase of leaching amount of cations such as Al or Si. The amount of Pb leached was decreased after the surface grinding because of minerals amorphisation, which brought the high adsorption capacities on the surface of soil particles, at the pH of more than 1. However, the leaching efficiency was better after the surface grinding at the pH of less than 1 because Pb was no longer adsorbed to the surface at this pH and minerals dissolution containing Pb contents was advanced by the surface grinding.

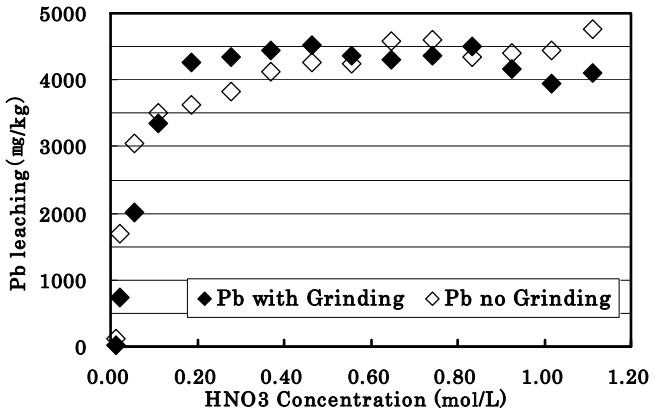

Fig.1 Pb leaching properties with or without surface grinding.

*you-say-sei@toki.waseda.jp

2F17

Removal of mercury ions from wastewaters by SBA-15 organosilicas

Mariusz Barczak*, Andrzej Dąbrowski, Stanisław Pikus
Faculty of Chemistry, Maria Curie-Sklodowska University,
Maria Curie-Sklodowska Sq. 3, 20-031 Lublin, POLAND

Ordered mesoporous organosilicas are very attractive materials due to their high surface areas, often extending 1000 m^2/g, large volumes of ordered mesopores and diverse morphology what makes them attractive potential catalysts and adsorbents. The SBA-15 materials are prepared by the sol-gel polycondensation of the silica source in the presence of large template molecules – block copolymers (see Fig. 1). Very important advantage of the sol-gel synthesis of SBA-15 is the possibility of introduction of the organic groups into the ordered structure during one-pot synthesis. Proper choice of organic functionalities introduced into the framework can result in creation of effective and selective sorbents for heavy metal ions.

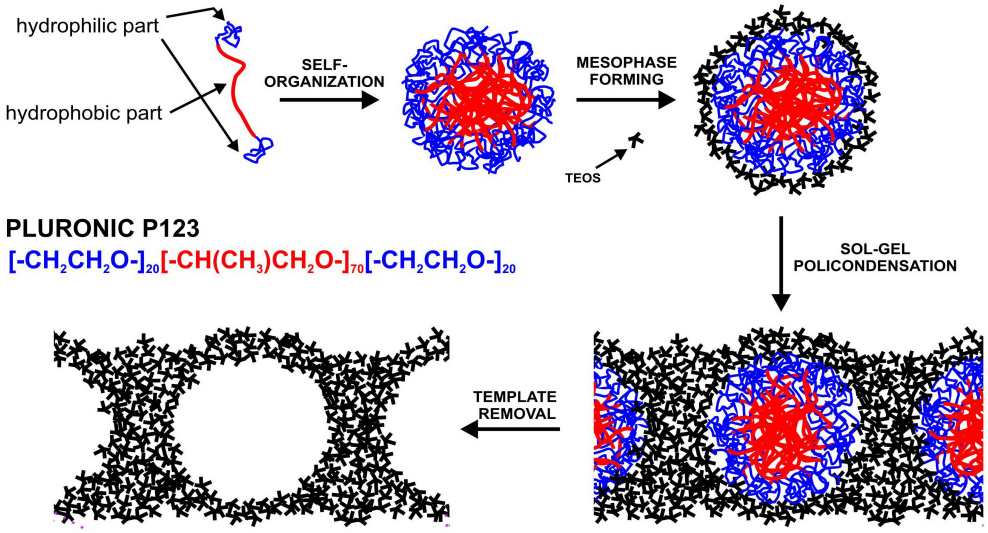

Fig. 1. Formation of the mesoporous structure of SBA-15

In this work SBA-15 materials were synthesized and characterized by FT-IR and Raman spectroscopy, powder X-ray diffraction, thermogravimetry, and nitrogen sorption measurements. The resulted materials exhibited well-ordered mesoporous structure, high values of surface area, large pore volumes and high contents of functionalities introduced during co-condensation of the proper monomers. Several materials have been tested as sorbents of Hg^{2+} ions from liquid phase. Observed static sorption capacities testify to great usefulness of these materials towards effective and selective removal of Hg^{2+} ions.

* mbarczak@hermes.umcs.lublin.pl

2F18

Purification of Heavy Metal Ions from Aqueous Solutions by Incorporation into DNA-Surfactant Complexes

Hiroomi Sakai, Anatoly A. Zinchenko*, Shizuaki Murata
Graduate School of Environmental Studies, Nagoya University,
Furo-cho, Chikusa-ku, Nagoya 464-8601

Heavy metal ions such as mercury, cadmium, lead, etc. are recognized to have adverse effects on environmental and human health; therefore, purification of the environment from heavy metals has attracted considerable attention. We propose a novel DNA-based method for purification of aqueous water solutions from heavy metal ions by two-step procedure: intercalation of water-dispersed metal ion into DNA double-helix and subsequent formation of polymer-colloid complexes between metal ion-bound DNA molecules and cationic surfactant such as CTAB (cetyltrimethylammonium bromide). Principle scheme of heavy metal removal on an example of mercury is shown on Figure 1. First, heavy metal ions form stable complexes with DNA nitrous bases (Figure 1, DNA-Hg complex). Formation of these complexes concentrates heavy metal ions inside DNA helix accompanying by changes in DNA secondary structure. Removal of DNA-Hg complex from aqueous solutions is a difficult task due to the colloidal stability of DNA polyelectrolyte in water. On the other hand, it is known that DNA forms polymer-colloid complexes interacting with cationic surfactants. The formation of such complexes (Figure 1, DNA-Hg-CTAB complex) causes DNA charge compactisation, hydrophobization, lost of DNA colloidal stability and subsequent precipitation of DNA complex from aqueous media. Removal of the complex from water media can be performed by centrifugation or filtration. The combined procedure shown on Figure 1 was used to remove mercury ions in concentration range from 0.02 ppm to 100 ppm from water phase with the efficiency over 90%. Further environmental advantage of the proposed method is a possibility to use inexpensive DNA from salmon milt, which is known to be a waste matter with potential environmental hazard, for heavy metal removal.

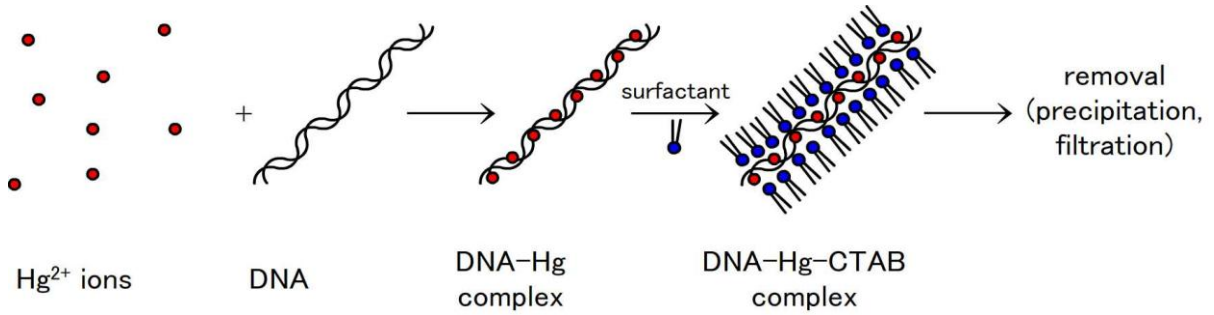

Figure 1. (a) Schematic representation of the method to remove heavy metal ions from aqueous solutions.

*zinchenko@urban.env.nagoya-u.ac.jp

3A01

Colloid Stability: Sixty Years after Verwey and Overbeek

Michal Borkovec
Department of Inorganic, Analytical, and Applied Chemistry, University of Geneva, Sciences II, 30, Quai Ernest-Ansermet, 1211 Geneva 4, Switzerland

Sixty years ago, Verwey and Overbeek published their influential book on colloid stability, expanding the earlier work of Derjaguin and Landau on the same topic. These views, currently known as DLVO theory, have revolutionalized our views on colloidal interactions and colloidal stability, and they are covered in all colloid science textbooks.

The initial success of the theory was mixed, however. While the theory explained certain trends in colloid stability with the counterion valency very well (i.e., Schulze-Hardy rule), there was concern from early on about the lack of particle size dependence in colloid stability predicted theoretically. In those times, however, neither well-defined colloidal particles nor sensitive experimental techniques were available, and firm conclusions were hard to reach. As the particles and techniques improved, evidence on serious quantitative disagreement with the theory started to accumulate, but clearly, nobody likes contradicting experts, well accepted by then.

With the availability of well-defined and monodisperse colloidal particles and non-invasive light scattering techniques, colloidal aggregation could be studied in unprecedented detail, both in the late and early stages. In the late stages, the fractal structure of the colloidal aggregates was evidenced. It was also realized, that comparison with the DLVO theory is only sensible in the early stages of aggregation, were the doublet formation dominate. Existing discrepancies could be indeed confirmed at high surface charge densities, while at lower charge densities good agreement with DLVO theory was found. Based on these results, a criterion for the validity of the DLVO theory can be formulated, which is equally in accord with direct force measurements. Nowadays, it is equally possible to analyze the stability of mixed binary colloidal systems, and distinguish between the eventually simultaneous occurring heteroaggregation and homoaggregation processes. For oppositely charged particles, heteroaggregation rate constants are in good agreement with DLVO theory too.

The observed discrepancies see to originate from surface charge heterogeneities on the nanometer scale, which induce additional attractive forces between the particles. Stability of colloidal particles in the presence of oppositely charged polyelectrolytes, which induce a charge reversal, corroborate this conclusion.

michal.borkovec@unige.ch

3A02

The state of interface and nearest layers of water and its influence on interparticle interaction

N. Mishchuk

Institute of Colloid and Water Chemistry of the National Academy of Sciences of Ukraine

pr. Vernadskogo, 42, Kyiv, Ukraine, 03680

Different technologies of water purification or mineral processing strongly depend on interparticle interaction. One of the problems actively discussed in the literature is the strong interaction between hydrophobic particles or between a hydrophobic particle and a bubble. This interaction is generally attributed to peculiarities of the hydrodynamic flow or cavitation of liquid in the vicinity of a hydrophobic surface and to hydrophobic forces, whose mechanism is not adequately explained as yet.

Several years ago the hypothesis was proposed for explaining the mechanism of long range hydrophobic forces, which implied an increase of attraction forces determined by nanosize bubbles present both in the near-surface layer of water and on the hydrophobic surface proper [1, 2].

Now a hypothesis regarding the impact of low water density near hydrophobic surfaces on the van der Waals and electrostatic interaction is offered. The theoretical model of Van der Waals forces under conditions of the variable density and, consequently, variable dielectric permittivity of water is developed. It is shown that the peculiar behaviour of water near hydrophobic interfaces increases the Van der Waals attraction. Simultaneously the theoretical model of an electric double layer under conditions of the variable properties of water near interface is developed. It is shown that reduction of the dielectric permittivity near interfaces determined by their hydrophobicity resulted in compression of double electrical layers and weakening of their overlapping. This, in its turn, results in reduction of the electrostatic repulsion of hydrophobic particles as compared with non-hydrophobic ones.

This enables us to make an interesting conclusion regarding the nature of the so-called hydrophobic forces. Since the DLFO forces are usually calculated on the basis of the bulk properties of water, the difference of such design forces and the forces calculated correctly with due regard for changes of water properties in the near-surface layer may turn to be that mystical hydrophobic force of attraction, which is usually postulated without any hint of proofs.

It should be also noted that the approach proposed must also introduce corrections to the DFLO forces for hydrophilic surfaces, near which a rise rather than a drop of the local dielectric permittivity should be observed. In this case, the sign of the difference of forces obtained on the basis of the bulk value of dielectric permittivity and on the basis of its locally modified values in the near-surface layer will be opposite to the sign of the difference of forces for hydrophobic surfaces, i.e., it will describe the repulsion rather than attraction.

1. N.A. Mishchuk, J. Ralston, D. Fornasiero, J.Colloid Interface Sci. 301 (2006)168.

2. N.A. Mishchuk, Colloids and Surfaces A 267 (2005) 139.

nataliya@mis.kiev.ua

3A03

Lubrication Forces in Squeeze Films

William Ducker* and Chris Honig
Department of Chemical and Biomolecular Engineering, University of Melbourne
Victoria 3010 Australia

When a particle approaches a flat surface at finite velocity, there is a repulsive lubrication force required to squeeze liquid from the thin film. There is an attractive force required to separate the particle from the plate. This force is important when considering the attachment of particles when the particles travel at high speed (> 1 μm/s). We will present accurate measurements of the force, separation, and velocity of silica particles approaching flat plates in sucrose solutions and in silicone oils. When we compare the measurements to Reynolds Lubrication Theory for squeeze films, we find excellent agreement at all speeds of approach for hydrophobic and hydrophilic solids. Our results are in disagreement with earlier work that found that it was necessary to invoke a slip length to fit the measured data to theory, which implied that the surface layers of liquid slipped past the solid. We find a zero slip length, or in other words, the no-slip boundary condition is obeyed, with nanometer precision. The causes of experimental disagreement are discussed, including the role of calibration of spring deflections and the effect of surface roughness. The difficulty of these force measurements means that they are a good test of our understanding of the colloid probe force measurement technique.

Christopher D. F. Honig, William A. Ducker* *Physical Review Letters*, **2007.** *98*, 028305.

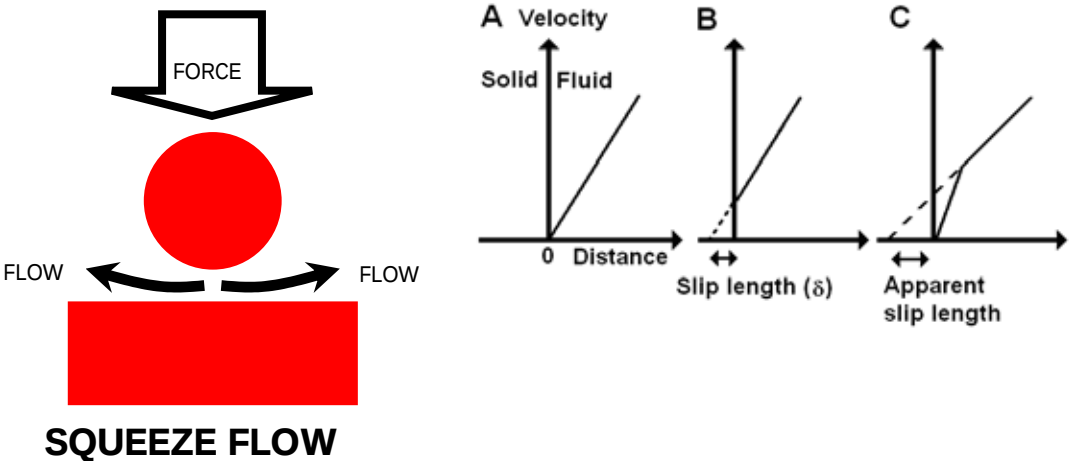

*wducker@unimelb.edu.au

3A04

Molecular-scale Structure on Surfaces and their Interaction, Adhesion and Friction in Solutions

Ko Higashitani
Department of Chemical Engineering, Kyoto University,
Katsura, Nishikyo-ku, Kyoto 615-8501 Japan

We conducted very carefully a series of AFM measurements of normal, adhesive and friction forces between completely-hydrophilic silica surfaces in various electrolyte solutions of normal and high pH's, and found that the adhesive and friction behaviors are classified into 4 cases, which are closely related with the microstructure of adsorbed ions on the silica surfaces in electrolyte solutions.

In the case of normal pH, the lubrication effect was observed by adding mono-valent cations, which was classified as Case A, although the degree of lubrication depends on the kind and concentration of cations. As for the divalent cations, the transition from Case A to Case B, in which the adhesion and friction became larger than those in water by adding cations, was found with increasing hydration enthalpy of cations. In the case of trivalent cations, the behavior was classified as Case B, and the anions also were found to play an important role.

In the case of high pH, the surfaces were hairy-like. It was found that (1) the relation of the friction vs. the loading force is non-linear, (2) whether the friction behavior is classified as Case C of non-linear lubrication or Case D, in which the friction becomes larger non-linearly than that in water by adding cations, depends on the adhesive property of adsorbed layers of cations on the hairy-like surfaces. The interesting relation of the friction vs. the scan rate in Case B and D was explained theoretically. The details will be given in the talk.

k_higa@cheme.kyoto-u.ac.jp

3A05

Polyelectrolytes at Solid-Liquid Interface Studied by Surface Forces Measurement

Kazue Kurihara*

Institute of Multidisciplinary Research for Advanced Materials (IMRAM), Tohoku University, Katahira, Aoba-ku, Sendai 980-8577, Japan

Elucidation of properties of polyelectrolytes is essential in developing technologies against the pollution. However, it is a challenging problem because polyelectrolytes exhibit interesting but complicated properties due to strong electrostatic interactions between ionized polymers and counterions. The surface forces measurement serves as a powerful tool for investigating polyelectrolytes at the solid-liquid interface. This paper reviews our studies on their adsorption on a charged surface and on polyelectrolyte brushes.

The adsorption of a negatively charged polyelectrolyte, poly(styrene sulfonate) (PSS), on a cationic monolayer of fuluorocarbon ammonium amphiphile has been found to be flat and stoichiometric at low concentrations of PSS, but the excess adsorption is possible at higher concentrations[1].

Two-dimensionally organized polyelectrolyte brushes have been used to simplify the complexities of polyelectrolyte solutions. The brush layers were prepared by the Langmuir-Blodgett deposition of amphiphiles bearing ionized poly(glutamic acid) (PLGA) or poly(lysine) (PLL) as a hydrophilic groups, and studied by surface forces measurement and FTIR spectroscopy with changing pH, salt concentration and polyelectrolyte chain density[2-5]. The surface forces measurement provides the effective layer thickness, the surface charge density, and the compressibility modulus of polyelectrolyte brush layers, whilst FTIR the density of ionized groups in the layers. Our results have indicated that the structure (thus compressibility) of the polyelectrolyte brushes is determined mainly by the osmotic pressure of counterions in the layers. We have also found the density dependent jump in the compressibility which can be accounted for in terms of change in the mode of counterion binding to polyelectrolytes.

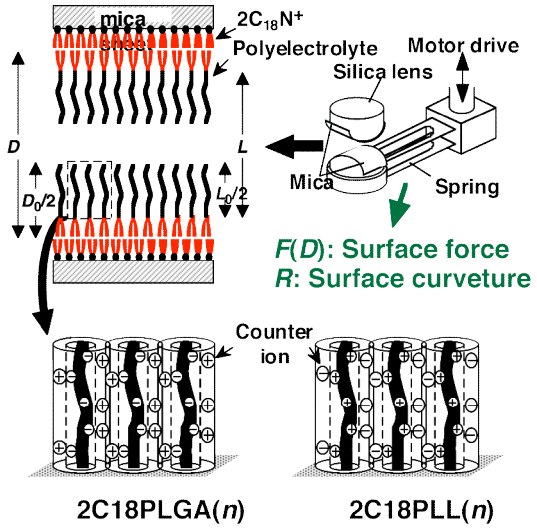

Fig. Schematic drawings of the measurement.

References:

(1) P. Berndt, K. Kurihara, T. Kunitake, *Langmuir*, **1992,** *8*, 2486-2490.
(2) S. Hayashi, T. Abe, N. Higashi, M. Niwa, K. Kurihara, *Langmuir*, **2002,** *18*, 3932-3944.
(3) T. Abe, N. Higashi, M. Niwa, K. Kurihara, *Langmuir*, **1999**, *15*, 7725-7731.
(4) S. Hayashi, T. Abe, N. Higashi, M. Niwa, K. Kurihara, *Mol. Cryst. Liq. Cryst.*, **2001**, *371*, 349-354.
(5) K. Kurihara, in "Handbook of Polyelectrolytes and Their Applications" (ed. By S. K. Tripathy, J. Kumar and H. S. nalwa), **2002**, *1*, 207-220.

*kurihata@tagen.tohoku.ac.jp

3A06

Bacterial adhesion and cell surface structure

K. Hori[1, 2]

[1]*Department of Materials Science and Engineering, Nagoya Institute of Technology, Gokiso-cho, Show-ku, Nagoya 466-8555, Japan*

[2]*PRESTO, JST, 4-1-8 Honcho Kawaguchi, Saitama 332-0012, Japan*

The adhesiveness of the toluene-degrading bacterium, *Acinetobacter* sp. Tol 5, is noteworthy so that inner walls of plastic tips and pipettes are coated with the cells at once by just sampling of them. We found two morphological types of bacterial nanofibers that have a function of connecting the Tol 5 cells to a substratum, an anchor-like fiber and a pili-like fiber. Contemporary electron microscopy techniques revealed that the former extends straight to the substratum without branching and tethers the cell body at its end from distances of several hundred nanometers, whereas the latter attaches to the substratum in multiple places, fixing the cell at much shorter distances.

We obtained a less-adhesive mutant, Tol 5 T1, which lost both types of nanofibers. Wild-type cells attained irreversible adhesion to polyurethane carriers within 30 s, while adhesion of T1 cells was still reversible at that time. While T1 showed decreased adhesion with decreasing ionic strength and did not adhere at all at 0.015 mM, adhesion of the wild type was fully independent of ionic strength (Fig. 1). This implies that WT cell adhesion via the long appendages does not follow the trends predicted by DLVO theory, whereas T1 cells, which lack these long appendages, adhere in a manner consistent with DLVO theory.

We revealed that in T1, the gene encoding a novel protein belonging to the autotransporter adhesin is disrupted and the expression level of type 1 pili descends. It was also reveled that the bald mutant T1 cells lack self-agglutinating property and adhere to hydrocarbon surfaces in a monolayer, which can be described by the Langmuir adsorption isotherm.

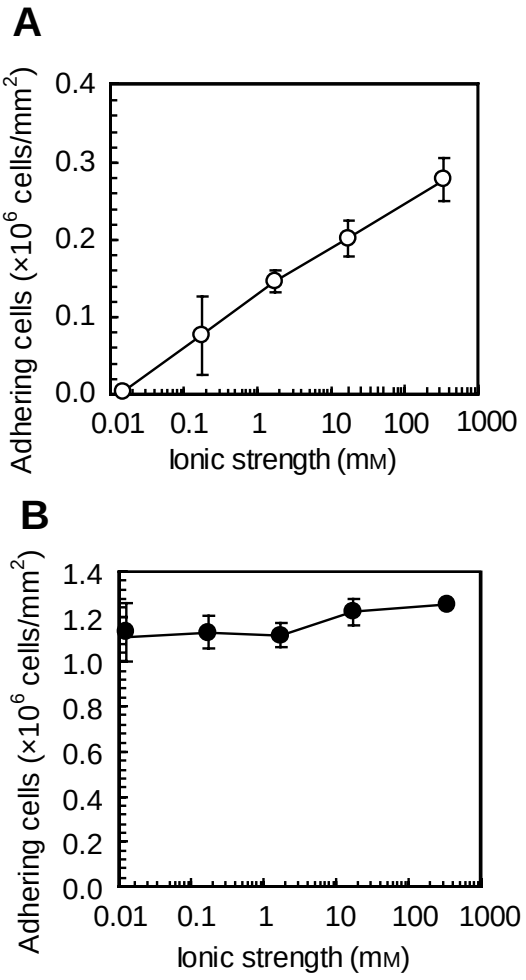

Fig. 1. Adhesion of T1 (A) and WT (B) of *Acinetobacter* sp. Tol 5 to the polyurethane carriers as a function of ionic strength.

hori.katsutoshi@nitech.ac.jp

3A07

Ion-sieve Adsorbents for Selective Removal of Minor Ions from Aqueous Solutions

K. Ooi*

National Institute of Advanced Industrial Science and Technology, Shikoku Center (AIST-Shikoku)
2217-14, Hayashi-cho, Takamatsu 761-0395

Hydrous metal oxides (HMeOs) generally have rigid structures with little swelling or shrinking upon immersion in aqueous solutions. Due to their rigid frameworks, some of them show ion-sieve properties, having a specific selectivity for particular ions or groups of ions depending on the pore size. They can be used as an adsorbent to separate minor hazardous ions from solutions containing major amount of similar ions. In this presentation, I introduce the preparation and properties of ion-sieve type HMeOs.

The cation-sieve HMeOs can be obtained by templating reaction using different kinds of cations as a template. A tunnel or layered metal oxide is prepared using template ions to direct its tunnel or layer dimension, subsequently the template ions are removed from the tunnel or interlayer space keeping the structure to obtain ion sieve HMeO. The HMeO obtained has atomic holes with a size depending on the templating ions used. It shows a remarkably high selectivity for the adsorption of ions that was used as templates (ion memory effect) when immersed in an aqueous solution. Structures and ion-sieve properties of cation-sieve type HMeOs are summarized in Fig. 1. They can be used to remove minor amount of alkali metal ion impurities from aqueous salt solutions.

The anion-sieve effect has been observed on NO_3^- exchange with layered double hydroxide (LDH).[1)] The interlayer distance of LDH varies depending on the kind of divalent metal and displaced trivalent metal atoms. A markedly high selectivity for NO_3^- is observed on Ni-Fe type LDH with a basal spacing of 0.81 nm. Since the thickness of brucite layer is 0.48 nm, the interlayer space of Ni-Fe type LDH is 0.33nm, which is suitable to fix the nitrate ions with ionic size of 0.33nm.

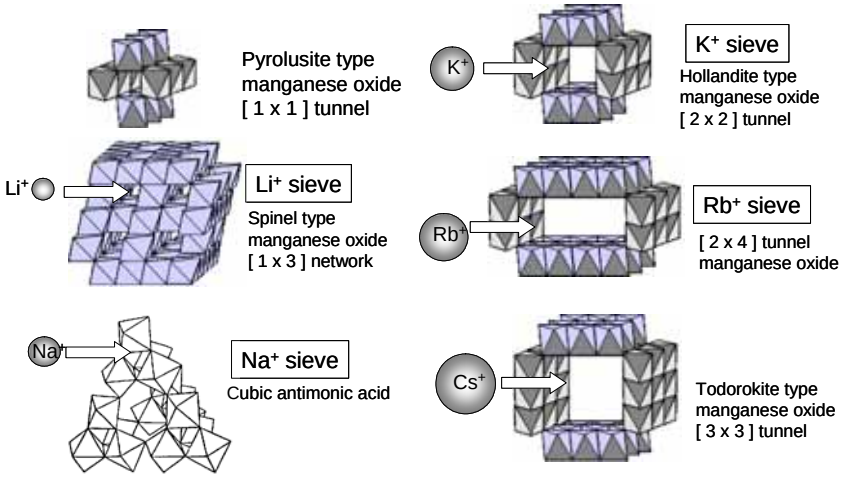

Figure 1 Structures of cation-sieve type hydrous metal oxides.

* k-ooi@aist.go.jp

3A08

Generation of the superoxide radical anion at biological interfaces and impact on iron acquisition by aquatic organisms

T. David Waite*, Andrew L. Rose, Shikha Garg and Manabu Fujii

School of Civil and Environmental Engineering
The University of New South Wales
Sydney. NSW 2052
Australia

Significant production of superoxide, a known reductant of both inorganic and organically-complexed iron(III), occurs in natural systems by both biotic and abiotic pathways. We have investigated the extracellular generation of superoxide by a range of phytoplankton and examined the role of superoxide in the acquisition of iron by these organisms. A generalized model for iron acquisition by aquatic organisms has been developed that includes three pathways of iron acquisition from organically complexed iron(III): non-dissociative reductive (NDR) uptake, dissociative reductive (DR) uptake and non-reductive dissociative (NRD) uptake (see Figure 1 below). The model is shown to be particularly useful in ascertaining the relative importance of these various iron uptake pathways as a function of solution parameters including concentration and iron-binding strength of the organic ligand and superoxide concentration.

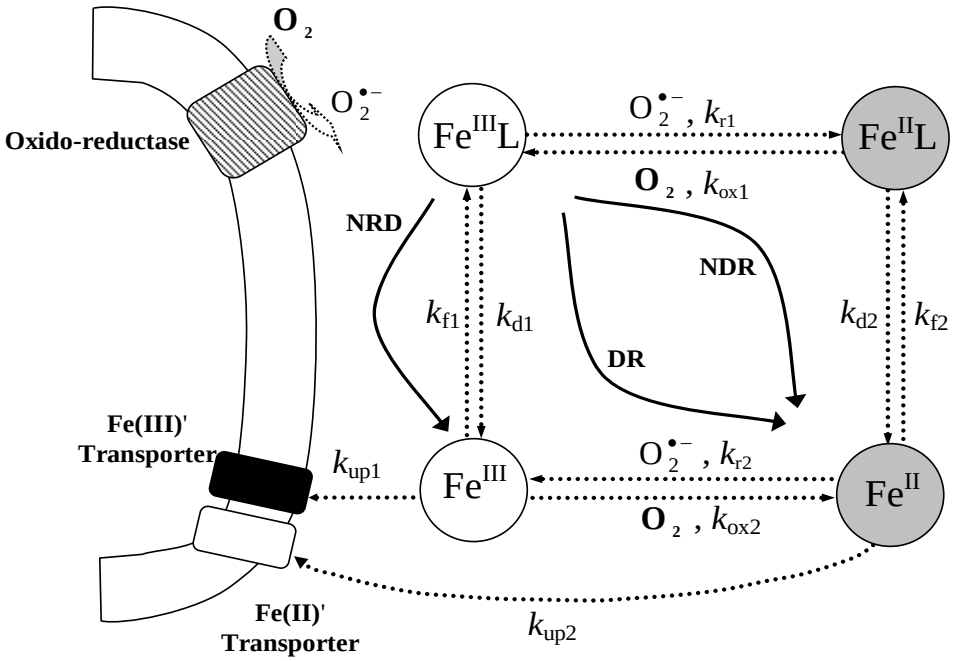

Figure 1. Model for iron uptake by aquatic organisms (after Garg et al., Journal of Phycology 43, 978–991 (2007)).

Corresponding author: Professor T. David Waite, d.waite@unsw.edu.au

3A11

The dissolution kinetics of humic acid particles

M. Brigante[1], G. Zanini[2], M. Avena[1]*

[1]*Departamento de Química, Universidad Nacional del Sur, Bahía Blanca, Argentina*

[2]*CERZOS (CONICET-UNS), Departamento de Agronomía, Universidad Nacional del Sur, Bahía Blanca, Argentina*

Humic acids (HA) are a very active fraction of the refractory organic matter in soils, sediments and natural waters. Their molecules can bind solid surfaces, metal ions and organic molecules such as pesticides or other contaminants. As a consequence of this binding HA can affect significantly the distribution and transport of contaminants in the environment. In fact, when HA molecules are in the dissolved state, they are rather mobile and can be transported by water flows (rivers, groundwaters), transporting with them the attached pollutants. On the contrary, when they are in the solid state forming part of the soil or sediment matrix, they are rather immobile, limiting the mobility of the attached pollutants.

A study of the dissolution kinetics of solid HA particles is presented here, and the ability of HA to become solubilized in aqueous media by different substances and conditions is evaluated. Thus, the effects on the dissolution rate of pH, temperature, concentration of inorganic and organic cations, organic acids and pesticides are investigated. The results show that the dissolution rate is strongly dependent on the pH of the aqueous solution; there is a 400-fold increase in the dissolution rate by increasing the pH from 4 to 11. Cations, either organic or inorganic, usually decrease the dissolution rate whereas organic acids and anionic pesticides increase that rate at constant pH. Dissolution appears to be controlled by sorption-desorption processes at the solid HA-water interface. These sorption-desorption processes are believed to modify the attractive forces that hold HA molecules together in the solid, modifying their rate of detachment from the surface.

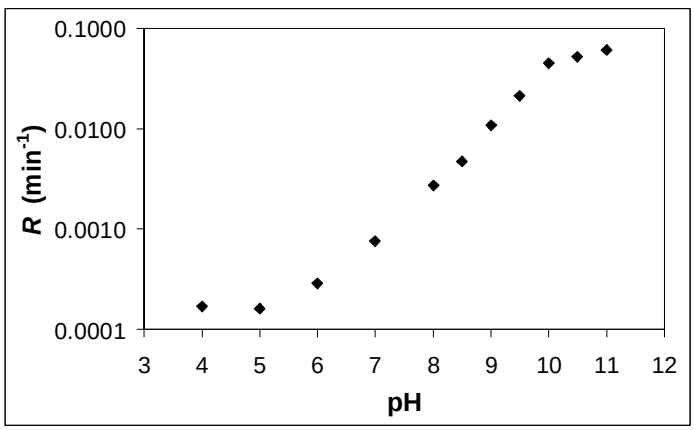

Fig. 1. Effect of pH on the dissolution rate (R) of solid HA particles

*mavena@uns.edu.ar

3A12

Particle-particle interaction in water treatment: Role of Coagulant Speciation and Hydrolysis Kinetic on NOM removal

Dongsheng Wang[1]*, Mingquan Yan[1,2], Jiuhui Qu[1], Christopher W.K. Chow[3]

[1]*SKLEAC ,Research Center for Eco-Envir. Sci., CAS, POB 2871, Beijing 100085, China*

[2] *Dept of Envir. Eng., Peking University, Beijing 100871, China*

[3] *CRC for Water Quality and Treatment, AWQC, SA Water, Private Mail Bag 3, South Australia 5108.*

The mechanism of natural organic matter (NOM) removal by $AlCl_3$ and polyaluminum chloride (PACl) was investigated through bench scale tests. The fraction distributions of NOM and residual Al after coagulation in solution, colloid, and sediment were analyzed as changes of coagulant dosage and pH. The influence of NOM, coagulant dose and pH on coagulation kinetics of $AlCl_3$ was investigated using photometric dispersion analyzer compared with PACl. Monomeric Al species (Al_a) shows high ability to satisfy some unsaturated coordinate bonds of NOM to facilitate particle and NOM removal, while most of flocs formed by Ala are small and not easily settleable. Medium polymerized Al species (Al_b) can destabilize particle and NOM efficiently, while some flocs formed by Al_b are not as large and precipitative as those formed by colloidal or solid Al species (Al_c). Al_c could adsorb and remove NOM efficiently. The removal of contaminant by species of Al_a, Al_b and Al_c follows mechanisms of complexation, neutralization and adsorption, respectively. Unlike preformed Al_b in PACl, in-situ formed Al_b can remove NOM and particle more efficiently via the mechanism of further hydrolysis and transfer into Al_c during coagulation. While the presence of NOM would reduce Al_b formed in-situ due to the complexation of NOM and Al_a.

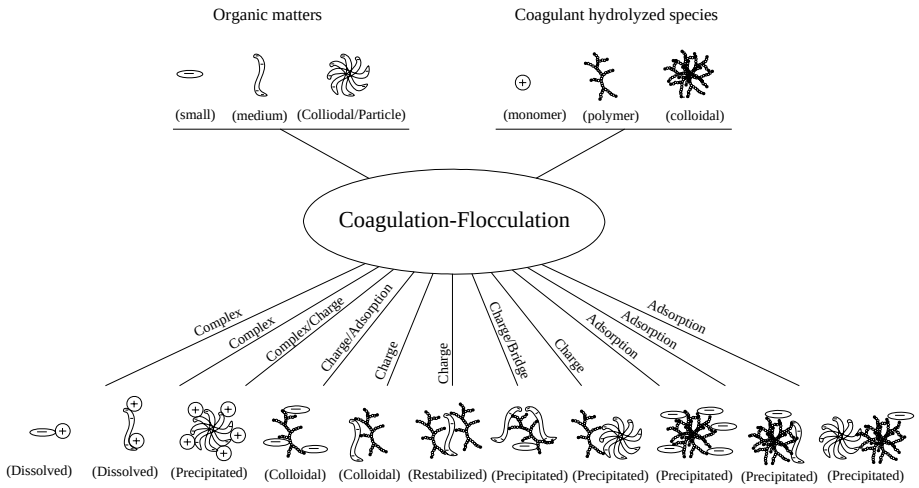

Fig. 1 Model of interaction of hydrolyzed coagulant species with organic matters..

*wgds@rcees.ac.cn

3A13

Evaluation of the electrostatic potential of a humic acid molecule by a fluorescence quenching technique

T. Saito[1]*, S. Nagasaki[2] and S. Tanaka[1]

[1]*Department of Quantum Engineering and Systems Science, School of Engineering, The University of Tokyo, 7-3-1 Hongo, Bunkyo-ku, Tokyo 113-8656, JAPAN*

[2]*Nuclear Professional School, School of Engineering, The University of Tokyo, 7-3-1 Hongo, Bunkyo-ku, Tokyo 113-8656, JAPAN*

Electrostatic interaction of natural organic materials (NOM) with toxic ions such as heavy metals and radionuclides is an important building block to develop a thermodynamic model for the binding of the ions to NOM. There are several models proposed to describe ion-NOM electrostatic interaction[1]. Considering the physical and chemical heterogeneity of NOM, it is not surprising that the different models can give reasonable descriptions with different (average) electrostatic potentials. In this study we employed the fluorescence quenching technique proposed by Green et al.[2], which enables us to evaluate an average electrostatic potential of NOM, for Aldrich humid acid (AHA) and compared the obtained potentials with the model calculations reported in ref. 1.

The quenchers used in this study are nitroxide radicals, 4-hydroxo-TEMPO (TEMPOL, Fig. 1 (a)) and 4-amino-TEMPO (TEMPAMINE, Fig. 1 (b)). The fluorescence of AHA in the presence of either of the quenchers with the increasing concentration was measured at different pH values and salt concentrations. Because of the structural similarity of the quenchers, their abilities to diminish the AHA fluorescence are assumed to be same except for their charges: positively charged TEMAPMINE can more strongly quench the fluorescence due to the electrostatic attraction. Thus, the ratio of the Stern-Volmer constants, which quantify the magnitude of the quenching, leads to the average electrostatic potential of AHA at a given condition.

In Figs. 1 (a) and (b) the fluorescence of AHA are shown at pH 4 and 0.1 M NaCl in the presence of TEMPAMINE and TEMPOL, respectively. As mentioned above, TEMPAMINE did quench the fluorescence of AHA more strongly than TEMPOL. The average potential calculated from the Stern-Volmer constants decreased as increasing pH and decreasing the salt concentration. Comparison with the model calculations suggested that the Donnan model, which is widely used in ion binding models to NOM, overestimated the negative potential of AHA.

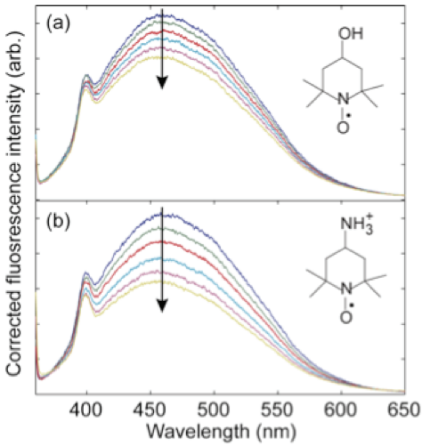

Fig. 1. Quenching of the AHA fluorescence by by (a) TEMPOL and (b) TEMPAMINE at pH 4 and 0.1 M NaCl.

Literature cited

1. Saito, T., et al., Colloid and Surf. A 265 (2005) 104.
2. Green, S. A., et al., Environ. Sci. Technol. 26 (1992) 294.

*takumi@flanker.q.t.u-tokyo.ac.jp

3A14

Acidic functionality of humic and fulvic acids isolated from deep aquifers

K. Kovács[1]*, A. Gáspár[2], Ph. Schmitt-Kopplin[2], E. Tombácz[1]

[1]*University of Szeged, Department of Colloid Chemistry,*
H-6720 Szeged, Aradi Vt. 1., Hungary

[2]*Helmholtz Zentrum München, German Research Center for Environmental Health,*
Institute of Ecological Chemistry,D-85764 Neuherberg, Ingolstädter Landstr. 1., Germany

The recent interest in thermal waters from deep aquifers tapped above 30 ºC seems to be increasing. The development of thermal spas and the exploitation of geothermal energy in Central Europe have been in the focus of the use of this natural resource recently. At the same time comprehensive research of thermal waters has not been achieved so this could be defined as an unexplored part of biogeosystems. These hot waters contain several mineral and organic components. The dissolved organic matter (DOM), such as humic substances (HS) is always present in all kind of groundwater. Organic matter in water is a complex mixture of both high and low molecular weight species, primarily organic acids that are relatively enriched in oxygen-containing functional groups. Isolation of functionally distinct fractions of the organic matter can determine fundamental chemical information about the biogenesis and environmental roles of these materials. Considering the composite character of HS and the difficulties of their isolation, HS fractions are operationally defined and classified into humic acid (HA) and fulvic acid (FA). The sampling of thermal waters was in the region of Szeged and Makó (Southeast Hungary). Hot groundwater samples were collected from wells tapped from different depths (993 – 2103 m) having temperature between 46 and 85 ºC in February 2006, January 2007. Isolation of DOM was in accordance with the procedure of International Humic Substance Society "Method for Preparation of IHSS Aquatic Humic and Fulvic Acids" available in the website (http://www.ihss.gatech.edu). This protocol is regarded and accepted by a large part of the scientific community as the reference method nowadays. The isolated and quantified HA and FA samples were characterized by several methods, among them the results of potentiometric acid-base titration and in part that of ESI-FTICR (electrospray ionization Fourier transform ion cyclotron resonance) mass spectrometry will be showed. The pH-dependent dissociation of humic and fulvic acids was determined from pH 3 to 10. The shape of proton binding curves is characteristic of HSs, and the amounts of acidic groups are in the range of standard and reference HA and FA samples of IHSS. The values of acidity of FA fractions (13-17 meq/g C) are greater than those of the HA samples (9-11 meq/g C). Molecule formulae obtained from high-resolution mass spectra and their relative abundances for oxygen containing compounds were calculated by using formula calculator software. Results showed that FA is more oxygenated shifting the maximum of relative abundances toward molecules with higher O content, and the most abundant compounds of HA and FA with from 5 to 7 and from 7 to 10 O atoms, respectively, depending on of samples.

*kkriszta@chem.u-szeged.hu

Utilization of Surfactant Binding for Characterization of Humic and Fulvic Acids

K. Hayakawa, M. Matsuda, Y. Muroi
Faculty of Science, Kagoshima University,
1-21-35 Korimoto, Kagoshima 890-0065

Humic substances have been utilized as soil improvement agent due to the nutritional and colloidal properties. They are recently recognized as a key material for redistribution of heavy metal ions in surface soil and hydrosphere because of the moderate solubility of the complex with metal ions. They are materials produced in the process of decaying plant and the properties are wide spreading depending on the source plant, places, age and so on. We pay attention on the amphiphilic property and expect to characterize them through the interaction with surfactant. Takisawa et al. proved the quantitative difference of hydrophobic property between humic and fulvic acids [1]. This paper concerns to the metal ion binding of humic acid investigated through surfactant binding with humic acid in the presence of metal ions and the fluorescence character of fulvic acid in the presence of surfactant.

The binding curves of surfactant ion decyltrimethylammonium bromide (C10TAB) by purified humic acid were determined in both the absence and presence of metal ions. The curves were analyzed by Langmuir equation and the two parameters, the binding constant K and capacity a of surfactant ions, were determined (Table 1). In the presence of metal ion, K decreases remarkably indicating a territorial binding of surfactant and metal ions. Only Zn ion remarkably interferes with surfactant binding. The decrease in a suggests the presence of irreversible binding site for metal ion in the presence of 1 mM metal ion.

Fulvic acid shows a complicated behavior of the fluorescence spectrum, which depends on the source and history of the sample. The spectral change of fulvic acid was measured in the presence of various surfactants and the fluorophore is predicted to be near ionic group of fluvic acid.

Table 1 Langmuir parameters of surfactant ion binding in the presence of metal ions.

	K / 1000	a / mmol g^{-1}	ΔG^0 / kJ mol^{-1}
$[M^{2+}]$	0.5 mM	0.5 mM	0.5 mM
None	600	3.43	-33.2
Cu	120	2.24	-29.2
Cd	130	2.83	-29.3
Zn	200	2.47	-30.4
Ca	120	3.49	-29.1
Pb	130	1.76	-29.5

[1] M. M. Yee, T. Miyajima, N. Takisawa, Colloids Surf. A, 272 (3), 182 (2006); 287, 68 (2006).

*khayak07@gmail.com

3A16

Binding of Surfactants to Polystyrene Sulfonate, Humic Substances and High-Humic Soil

Munehide Ishiguro[1]*, Luuk K. Koopal[2]

[1]*Graduate School of Environmental Science, Okayama University, Tsushima-naka, Okayama 700-8530 Japan*
[2] *Laboratory of Physical Chemistry and Colloid Science, Wageningen University, Dreijenplein 6, 6703 HB Wageningen, The Netherlands*

The binding of cationic surfactants to an anionic polymer, humic acids, fulvic acids and a high-humic soil is investigated. Fulvic acids, humic acids and the high-humic soil (non-allophanic volcanic ash soil) are natural anionic compounds with a complex structure. Sodium polystyrene sulfonate (SPSS) is a synthetic anionic polymer with a simple structure; it is a reference material for a better understanding of surfactant binding to the natural compounds. Alkylpyridinium chlorides with different carbon chain length are used as surfactants: C_{16}PC, C_{12}PC and C_{10}PC. The binding isotherms are obtained by using a surfactant-selective membrane electrode. The figure depicts the binding of the three surfactants to SPSS (double logarithmic plot). The longer the chain length is, the stronger is the binding to SPSS because of the increase of hydrophobic effect. The steep part of the isotherms indicates cooperative binding (surfactant aggregation). This is observed at 10^{-8}-10^{-7} M for C_{16}PC, at 10^{-6} to 10^{-5} M for C_{12}PC and at 10^{-5} to 10^{-4} M for C_{10}PC. For each alkylpyridinium chloride the binding isotherms at different salt concentrations have a common intersection point. The bound amounts at the intersection points are similar for the three surfactants and the value is also roughly the same as the isoelectric points that are measured with the Particle Charge Detector. The agreement between the common intersection points and the iso-electric points indicates that the alkyl pyridinium ions bind much stronger to the PSS poly-ion than the sodium ions.

For Humic acids the chain length effects are similar to those with SPSS, but the cooperative surfactant binding is weaker. C_{16}CP isotherms for humic acids also show an intersection point that matches the iso-electric point. The C_{12}PC binding to the humic acids is stronger than that to the fulvic acids.

The anionic surfactant, SDS, does not bind to humic acid at low salt concentration. On the other hand, anionic surfactants bind to the high-humic soil. The bound amount decreases significantly when the organic matter is removed in the soil. The anionic surfactant with a linear aliphatic chain binds stronger to the soil and shows a larger cooperativity than the anionic surfactant with a branched chain.

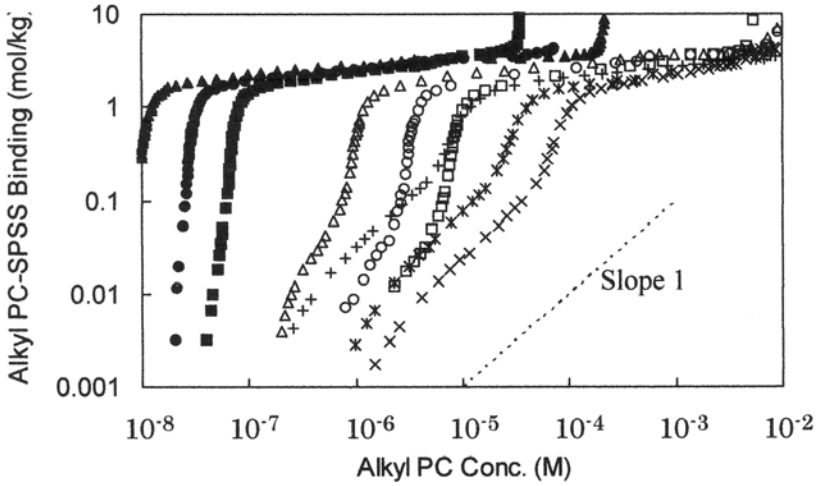

Fig. 1 Comparison of C_{16}, C_{12}, C_{10}PC-SPSS binding isotherms (log-log plot). 0.005 M NaCl; ▲C_{16}PC, △C_{12}PC, +C_{10}PC. 0.025 M NaCl; ●C_{16}PC, ○C_{12}PC, ∗C_{10}PC. 0.1 M NaCl; ■C_{16}PC, □C_{12}PC, ×C_{10}PC.

* ishi@cc.okayama-u.ac.jp

3A17

Interaction between humic substances and heavy metals as studied by two-dimensional correlation fluorescence spectroscopy

K. Nakashima*, S. Xing, and T. Miyajima

Department of Chemistry, Faculty of Science & Engineering, Saga University, 1 Honjo, Saga 840-8502, Japan

Humic substances play a crucial role in removal and/or migration of environmental pollutants in natural water, because some of the pollutants are effectively incorporated into the matrix of humic substances through hydrophobic interaction, electrostatic interaction, hydrogen bonding, and coordinate bonding. Therefore, a lot of works have been carried out to characterize humic substances by various techniques including fluorescence spectroscopy, IR spectroscopy, and chromatography. Among these techniques, fluorescence spectroscopy has attracted much attention because of its high sensitivity and selectivity [1]. However, it sometimes meets difficulty if the bands of different fluorophores are heavily overlapped. To overcome such a problem, we introduced two-dimensional (2D) correlation technique into fluorescence spectroscopy [2]. In this work, we tried to elucidate the interaction between humic substances and heavy metals by 2D correlation fluorescence spectroscopy. We studied two kinds of humic acids and two kinds of fulvic acids: Aldrich humic acid (AHA), Dando humic acid (DHA), Biwako fulvic acid (BFA), and Kuta fulvic acid (KFA). The heavy metals examined are Pb^{2+}, Cu^{2+}, and Fe^{3+}.

Figure 1 shows an example of fluorescence spectra of DHA in the presence and absence of Pb^{2+}. We note two prominent bands around 435 and 510 nm. It is interesting to know if these two bands are originated from the same or different fluorophores. The band around 510 nm seems to be quenched by Pb^{2+} more efficiently than that around 435 nm, implying that they can be assigned to different species. To confirm it, we carried out 2D correlation analysis. We obtained clear two peaks around (435nm, 510nm) and (510nm, 435nm) both in synchronous and asynchronous maps (data not shown). This fact indicates that the two bands are emitted from different fluorophores. By comparing the signs of the peaks in synchronous and asynchronous maps, it is also elucidated that the band around 510 nm is quenched earlier than the band around 435 nm.

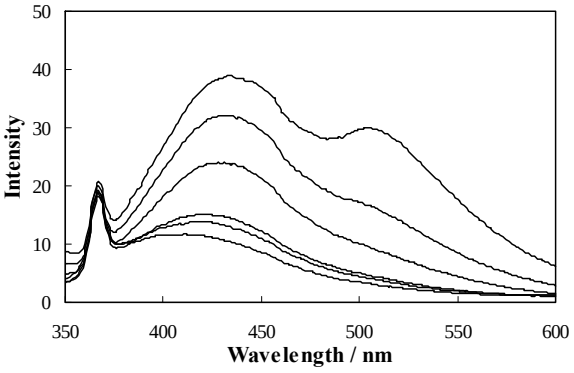

Fig. 1. Fluorescence spectra of DHA (10 ppm) in the absence and presence of Pb^{2+} ion (0, 20, 40, 60, 80, 100μM).

References: [1] P. G. Coble, S. A. Green, N. V. Blough, R. B. Gagosian, *Nature*, **1990**, *348*, 432.
[2] K. Nakashima, K. Yuda, Y. Ozaki, I. Noda, *Spectrochim. Acta, Part A*, **2004**, *60*, 1783.

*nakashik@cc.saga-u.ac.jp

3A18

Complexation of Am with size-fractionated soil humic acids

S. Nagao[1]*, M. Aoyama[2], A. Watanabe[3], T. Tanaka[4]

[1]*Faculty of Environmental Earth Science, Hokkaido University,*
N10W5, Kita-ku, Sapporo, Hokkaido 060-0810

[2]*Faculty of Agriculture and Life Science, Hirosaki University,*
1-1 Bunkyo-chou, Hirosaki, Aomori 036-8561

[3]*Graduate school of Bioagricultural Sciences, Nagoya University,*
Furou-cho, Chikusa-ku, Nagoya, Aichi 464-8601

[4]*Tokai Research and Development Center, Japan Atomic Energy Agency,*
2-4 Shirakata Shirane, Tokai, Naka, Ibaraki 319-1195

Humic substances (humic and fulvic acids) are ubiquitous in nature and have many beneficial effects on soils and aquatic environments. They play important role in geochemical behavior of trace elements such as actinides from fallout and local sources in aquatic environments. Therefore, characteristics of actinides bound to humic and fulvic acids can yield information on the geochemical role of humic substances in the migration of actinides. In this study, the association properties of Am with humic substances were studied on the basis of structural feature of humic substances. We separated two humic acids ('HA': fluorescence-poor and higher molecular size fraction, 'FL': fluorescence-rich and lower molecular size fraction) with different structural features from humic acids prepared from three types of soils (andisol, entisol and buried andisol) by Sephadex G-25. The association experiments were carried out in a medium of 0.01M $NaClO_4$ solution at a humus concentration of 10 mg/l and pH6-8. After finishing the association experiments, ultrafiltration was used to size-fractionate Am in the humus solutions. Figure 1 shows molecular size distribution of Am in the presence of size-fractionated HAs. The dominant size fractions of Am in the presence of 'HA' were 450nm-100k Da (48-53% for the andisol and entisol) and 100k-30k Da (60% for the buried andisol). On the other hand, 43-51% of Am was presented in the size of 30-10k Da in the 'FL' HA solutions from three soil types. These results indicate that characteristics of size-fractionated humic acids are related association properties with Am.

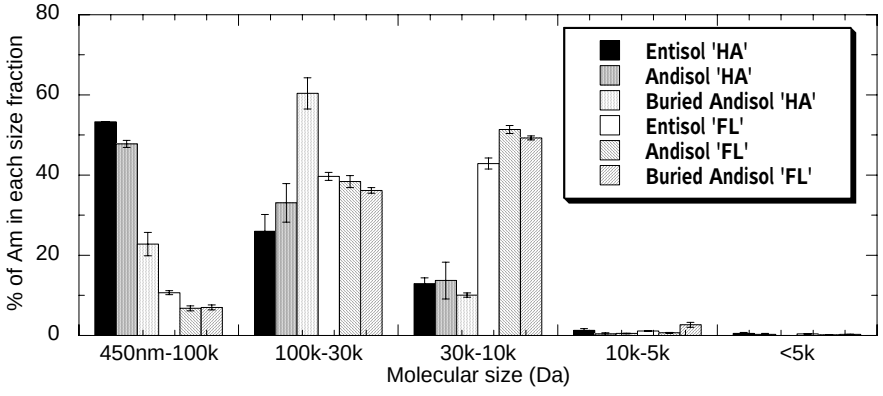

Fig. 1 Size distribution of Am in the presence of HAs.

*nagao@ees.hokudai.ac.jp

3B11

Distinct mechanisms of particle aggregation induced by alum and PACl: Floc structure and DLVO evaluation

Xiaohong Wu, Xiaopeng Ge*, Dongsheng Wang, Hongxiao Tang
State Key Lab of Environmental Aquatic Chemistry, RCEES,
Chinese Academy of Sciences, POB 2871, Beijing 100085, China

Interactions of silica microspheres were examined by light scattering in presence of alum and polymer aluminum chloride (PACl) with various OH/Al ratios. The coagulation and flocculation behaviors were investigated using different coagulant dosages at constant pH (6.5) and salt concentration (0.01mol/L). The size and structure of flocs were monitored with time. Based on the measurement of size distribution and zeta potential, charge neutralization was proposed to be the main coagulation mechanism for all the coagulants. Other flocculation mechanisms were also involved during aggregation process, depending on in situ formed or preformed hydrolyzing products. Precipitate patch and sweep flocculation were induced for alum, contrasted to polycation patch and bridging flocculation for PACl. The particle aggregation mechanisms were explained in terms of interaction forces based on simplified classical DLVO theory. It was demonstrated that PACl outperformed alum in particle agglomeration at lower concentration (1~2μmol/L), owing mainly to the considerable energy barrier reduction induced by high positive polycations. At high dosages of alum, amorphous precipitates with weak positive charge were responsible for cluster agglomeration. For all the coagulants, the secondary minimum in interaction energy was also found to influence particle aggregation.

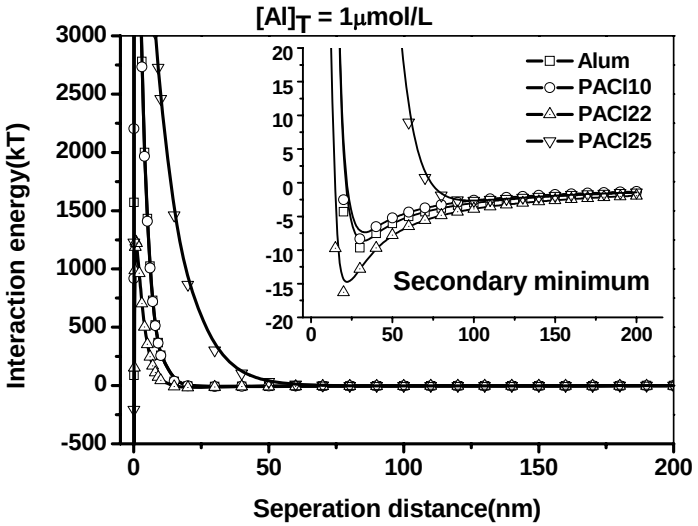

Fig. 1 The calculated interaction energy between silica particles induced by alum and PACl with various OH/Al ratios.

*xpge@rcees.ac.cn

3B12

Structures of tideland sediment flocs in Ariake sea

H. Kudoh[1], T. Miyajima[1]*, Y. Adachi[2],
[1]*Faculty of Science and engineering, Saga University,*
1Honjo, Saga 840-8502
[2] *Institute of Agricultural & Forest Eng, Tsukuba University,*
Tsukuba-shi, Ibaraki 305-8572

In recent years, environmental problems regarding Ariake sea such as decrease in living things and red tide has been reported. One possible reasoning for this environment deterioration is the decrease in sediment water permeability of tidal flat since seawater is the carrier of oxygen molecules to the bottom. In the sediment surface region, sediment flocs are always formed by aggregation/dispersion processes; it is expected that the nature of sediment flocs controls the sediment water permeability.

In order to understand the structures of the flocs we have measured the settling velocity of a single floc (V_f) and a floc diameter (D_f), and have calculated the fractal dimension (D) of the flocs. Two sampling points were chosen for comparison purposes, i.e., Higashiyoka tideland(relatively good environmental condition) and Iida tideland(worse condition with smell of rotten egg). For both cases, the settling velocity of the flocs increased with an increase of floc diameter by a power law as shown in Fig. 1. Even though they are scattered, by comparing the slopes of the plots of the two series, it is apparent that the slope of Iida is much steeper than Higashiyoka particularly in the region of D_f smaller than 0.1 mm, which indicates that the sediment flocs of Iida coast have a dense structure.

It can be concluded that by comparing with Higashiyoka the flocs of Iida coast have more dense structure and when the flocs accumulate on the sediment surface, the sediment water permeability will be highly restricted, which induces reductive condition at the bottom. This may activate the sulfate reducing bacteria to produce poisonous hydrogen sulfide.

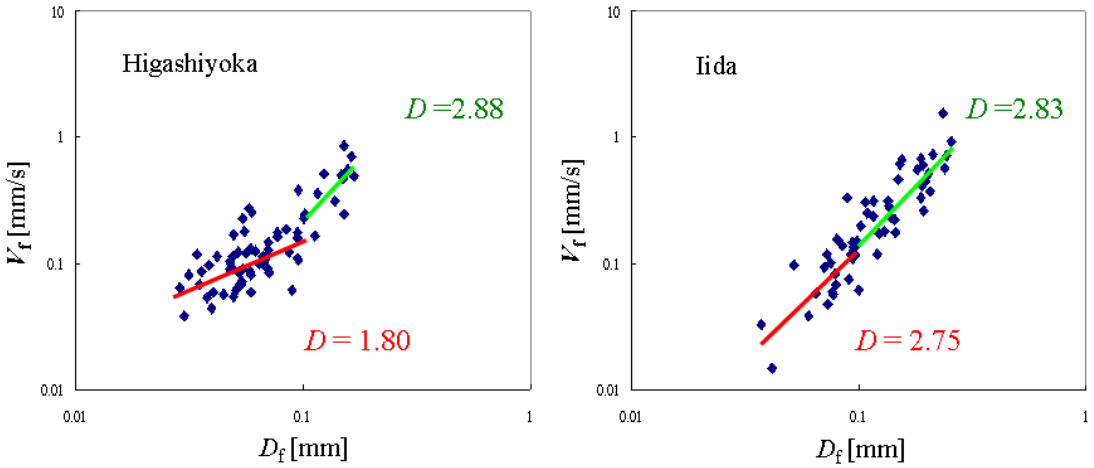

Fig. 1 Relationship between diameter of a single floc(D_f) and settling velocity(V_f). (October, 2007)

t-miyaji@ cc.saga-u.ac.jp

3B13

Coagulation behavior of Al_{13} aggregates

Jr-Lin Lin[1*], Ching-Ju M. Chin[2], Chihpin Huang[1], Jill R. Pan[3] and Dongsheng Wang[4]

[1]*Institute of Environmental Engineering, National Chiao-Tung University, Hsinchu, Taiwan*

[2]*Institute of Environmental Engineering, National Central University, Jungli, Taiwan*

[3]*Biotechnology Center, National Chunghsing University, Taichung, Taiwan*

[4]*SKLEAC, Res. Center for Eco-Envir. Sci., Chinese Academy of Sciences, Beijing, China.*

The coagulation behavior of Al_{13} aggregates formed in coagulation of kaolin was investigated by small angle static light scattering (SASLS), solid-state ^{27}Al NMR and tapping mode atomic force microscope (TM-AFM). A kaolin suspension was coagulated with PACl containing high content of Al_{13} polycation (PACl-Al_{13}). The results indicated that Al_{13} was predominant in destabilizing kaolin particles for PACl-Al_{13} coagulation even though at alkaline pH (pH 10). At such high pH, Al_{13} aggregates can be observed when the PACl-Al_{13} dosage was increased. In addition, the mechanism of PACl-Al_{13} coagulation at alkaline pH was dictated by dosage. When the dosage was insufficient, coagulation was caused by electrostatic patch, which leaded to compact aggregates with high fractal dimension (D_f). Interparticle bridging became dominant when the coagulant dosage approached the plateau of adsorption, which caused the more open aggregates with low D_f. However, the aggregates formed by interparticle bridging were easily broken during coagulation by mixing-induced shear. The in-situ AFM scanning in liquid system proved that the existence of linear Al_{13} aggregates composed of a chain of strongly curled Al_{13} in PACl-Al_{13} coagulation at a given high dosage under alkaline pH. Meanwhile, several curled Al_{13} clusters with various dimensions were observed.

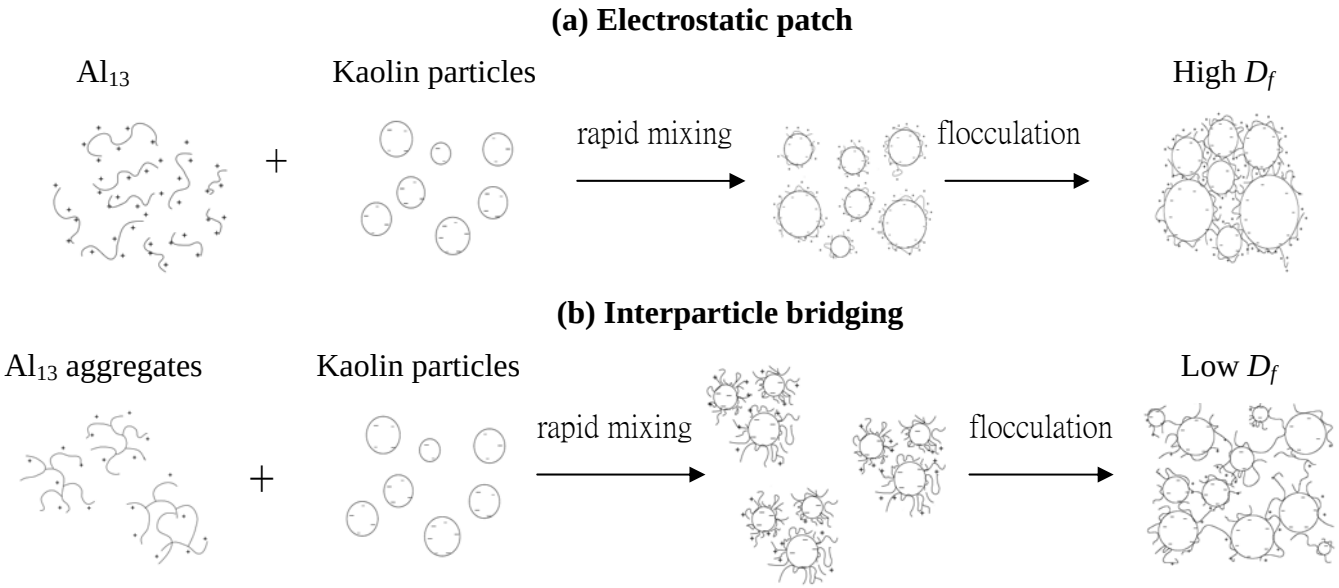

Fig.1 Schematic representation of the PACl-Al_{13} coagulation mechanism induced by Al_{13} and Al_{13} aggregates. (a) Electrostatic patch (b) Interparticle bridging

*speckzin.ev92g@nctu.edu.tw

3B14

Precipitation Flotation of Phosphate from Water

Warmadewanthi, Ching-Jung Chang, J. C. Liu*

Department of Chemical Engineering, National Taiwan University of Science and Technology

43 Keelung Road, Section 4, Taipei 106, Taiwan

The removal of phosphate from water was by precipitation flotation was examined. Calcium chloride ($CaCl_2$) was added to induce precipitates. Effects of both molar ratio ([Ca^{2+}]: [PO_4^{3-}]) and pH on precipitation were examined, and experimental results were compared with those from equilibrium modeling by PHREEQC. Molar ratio was the key parameter in determining the residual phosphate concentration, and hydroxyapatite ($Ca_5(PO_4)_3OH$) was found to be the dominant solid species. Dispersed air flotation was utilized for the removal of precipitates from water using various collectors. Kinetic experiments indicated that flotation reactions were completed within 5 minutes. Both anionic collector, sodium dodecylsulfate (SDS) and sodium oleate (NaOl), could become adsorbed onto solid surfaces via electrostatic force and facilitated the flotation removal of calcium phosphate precipitates. Cationic n-dodecyl ammonium chloride (DAC) could induce effective flotation removal of calcium phosphate precipitates as well since it can become adsorbed through specific interaction, while cetyltrimethyl ammonium bromide (CTAB) was not an effective collector. Effects of nitrogen flow rate and concentration of collector on flotation reactions were studied as well. The ionic strength and the presence of anions affected the removal efficiency of calcium phosphate precipitate. However, they can be overcome by increasing the concentration of collector.

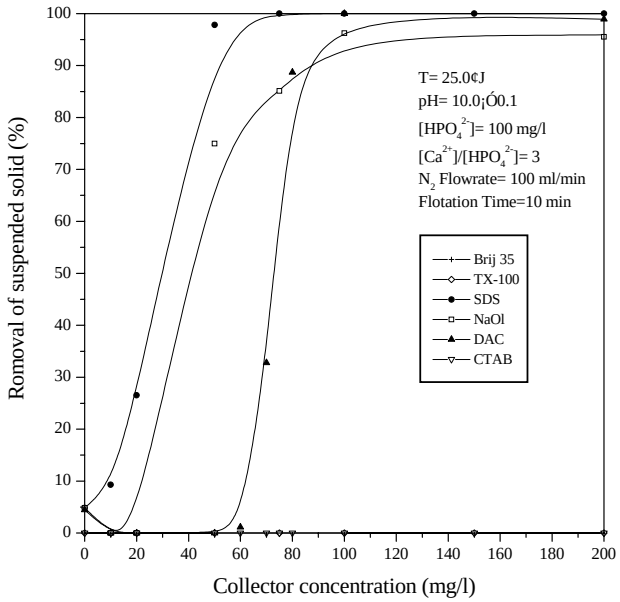

Fig 1. Removal of precipitates as affected by collector.

*liu@ch.ntust.edu.tw

3B15

Manufacturing Microcapsules for Controlled Release

Qingchun Yuan*, Richard A. Williams, Simon Biggs
Institute of Particle Science and Engineering,
School of Process, Environmental and Materials Engineering,
University of Leeds,
Clarendon Road, Leeds, LS2 9JT, United Kingdom

Microencapsulation has long been developed for controlled delivery/release of active components in food, pharmaceutical, personal care, home care, agrochemical and other functional products. Controlled release provides a means not only to increase the efficiency of active components, but also to reduce the amount required and further contamination of the active compounds in the application environment, caused by low efficiency of a large dose. So far, numerous physical and chemical techniques have been developed to encapsulate liquids or solids. Among them emulsification has been widely used as a template stage to generate discrete spherical particulates and control the particle size. To control the size and size distribution better, emulsification methods have developed from conventional ones using such as turbulent shear forces to a drop-by-drop production of membrane/microfluidic methods. However, the complexity of fluid systems can provide problems especially when larger droplets are desired and/or further processing is needed. We are currently exploring the combination of an advanced emulsification technique (cross-flow membrane emulsification) with the formulation of specific interface properties to achieve droplets with a desired larger size (20 – 50 μm) and narrow size distribution that are suitable for use as templates in microcapsule manufacture.

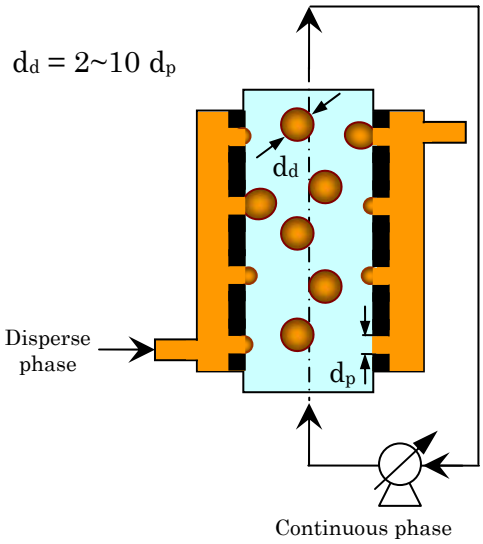

Figure 1 A concept diagram of crossflow membrane emulsification

*q.yuan@leeds.ac.uk

3B16

Effects of particle size and its distribution on size measurements of fine particles by means of interactive force apparatus

A. Otsuki[1]*, D. Gjergj[2], T. Fujita[2]

[1]*Department of Resources and Environmental Engineering, Waseda University, 3-4-1 Okubo, Shinjuku, Tokyo 169-8555*

[2]*Department of Geosystem Engineering, The University of Tokyo, 7-3-1 Hongo, Bunkyo, Tokyo 113-8656*

This paper describes the effects of particle size and its distribution on size measurements by means of interactive force apparatus. The apparatus was proposed for particle size measurement in our research group. The apparatus measures the interactive force between two plates, i.e. the gold-coated glass hemisphere and the brass flat plate, (which is fixed at the bottom of the sample cell). During the measurement, electric field is applied between the two plates, and thus dielectric particles are arranged toward the direction of electric field in the area between two plates. When the two plates are close to each other, two different forces (i.e. repulsive force and attractive force) alternately act on particles due to the structure change of the particles. The cycle of the repulsive and attractive forces is a primary size of particle or size of aggregate, which depends on the degree of agglomeration. The advantage of this apparatus is that size measurement using the apparatus is a direct measurement, not depending on the concentration and optical transparency of the solution. Moreover, the measurement can be conducted in both the aqueous solution and organic solvent. Other common apparatuses for size measurements using laser source (i.e., the dynamic light scattering and laser diffraction) are difficult to measure the size of particles in the solution of high particle concentration and/or low transparency accurately, due to multi-scattering of light in the sample solution or solvent. However, the appropriate experimental conditions for particle size measurement using the interactive force apparatus have not been fully determined. In the present study, (a) appropriate particle size range and (b) particle size distribution were determined by calculating (a) the forces acting on fine particles and (b) the potential energies of a cluster under the electric field (Fig. 1).

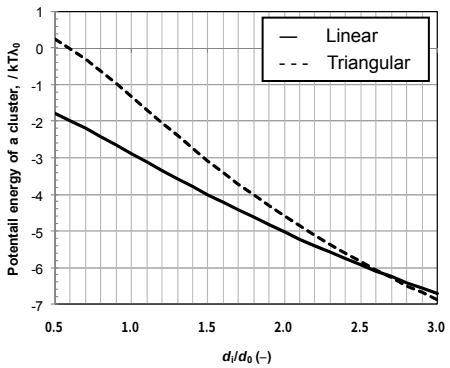

Fig. 1 Potential energies of linear and triangular formation as a function of particle diameter d_i / d_0.

*otsukiakira@aoni.waseda.jp

3E11

Preparation and characterization of a novel silica aerogel as adsorbent of toxic organic compounds

Sha Wei, Huijuan Liu*, Jiuhui Qu
SKLEAC, Research Center for Eco-Environmental Sciences, CAS,
POB 2871, Beijing 100085, China

The removal technology of toxic organic compounds from water has been paid much attention in recent years. Traditionally, adsorbents are porous materials with high specific surface area, large pore volume, well-developed pore distribution, and special pore surface chemistry. Silica aerogel, a unique material with wide application fields, has been more and more researched as adsorbent because of its high porosity (up to 99%) and easy surface modification. It shows high adsorption efficiency on different compounds from water. However, traditional preparation methods of silica aerogel involve the process of supercritical drying, which means a high cost and results in limited practical application.

A new ambient pressure drying (APD) technique, which overcoming the disadvantages of conventional supercritical aerogel processing, was used to produce silica aerogel in this study. The key steps of ADP are solvent exchange and surface modification. Main reaction of the surface modification is as follow:

$$(CH_3)_3\text{-Si-Cl} + \equiv\text{Si-OH} \rightarrow \equiv\text{Si-O-}(CH_3)_3 + \text{HCl}$$

So far, we prepared three silica aerogel adsorbents with different degrees of hydrophobicity using waterglass as precursors. Aerogel-A was dried silica aerogel whose surface had been modified by EtOH/TMCS/Hexane solution. Aerogel -B was obtained by calcining aerogel-A at 500°C for 30 min and aerogel -C was dried silica aerogel. Different analytical technologies, such as differential thermal analysis, elemental analysis, SEM, BET, FT-IR and contact angle measuring were utilized to obtain comprehensive structural properties of the silica aerogel adsorbents. Results showed that the properties of the three adsorbents were very different from each other.

Three different organic compounds selected to test the effectiveness of the novel adsorbents were rhodamine B, dieldrin, and toluene, which represented soluble, slightly soluble and insoluble organic compounds, respectively. Adsorption experiments results showed that, due to its high porosity and hydrophobic surface structure, aerogel A was highly effective in removing slightly soluble and insoluble matters from water. Nearly 90% of dieldrin was removed within 1 hour from water. The hydrophobic surface of aerogel A has a strong affinity for lipophilic dieldrin, and limited the water molecule to enter the inner structure. Aerogel A was totally soaked by toluene, and adsorbed 6.50 times toluene of its weight. However, when it came to the soluble sorbate like rhodamine B, the hydrophobic surface limited the thoroughly contact with the sorbate molecule, and therefore resulted in a slow adsorption process. Due to the hydrophobic surface, large surface area and pore volume, aerogel B showed a strong adsorption capacity on soluble sorbate, and removed 94% rhodamine B within one hour. The adsorption capacities of aerogel B on slightly soluble and insoluble organic matters in water were limited as the lipophilic methyl was burned away. Aerogel C, which had a hydrophilic surface and very compact space structure, showed almost no adsorption capacities on dieldrin and toluene, and a relatively fast, but small capacity on rhodamine B.

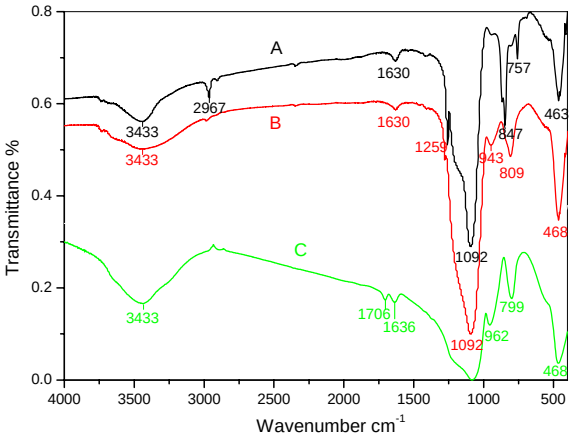

Fig.1 FTIR absorption spectra of the silica aerogel adsorbent A, B and C

*Email: hjliu@rcees.ac.cn

3E12

Hybrid Glass for Removal of Phenol in Wastewater

Zhang hai*, Pan Gaofeng and Kurumada Ken-ichi
Graduate School of Environment and Information Sciences,
Yokohama National University

By using sol-gel method, TPOZ/TEOS/TBP hybrid glass was successfully obtained. This type of hybrid glass is stable in the water and exhibits alkaline resistance. The hybrid glass contains TBP molecules which are the key functional parts to adsorb phenol molecules in water. Our measurements showed that TBP was immobilized in micropores in the glass matrix. As shown in Fig.1, the adsorption of phenol was rate-determined by the diffusion of phenol. This was shown by the difference only in the lapse of the time required for reaching the adsorption equilibrium. Phenol was adsorbed at the molar ratio of 1:1 to the incorporated TBP as indicated in the linearity of the adsorption isotherm shown in Fig.2.

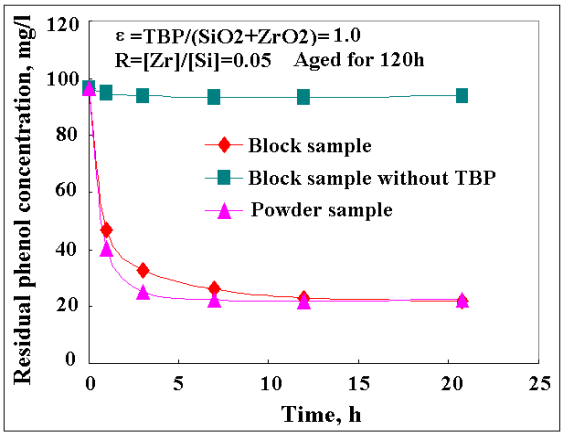

Fig.1 Example of time-dependence of the phenol adsorption behavior of the hybrid glass

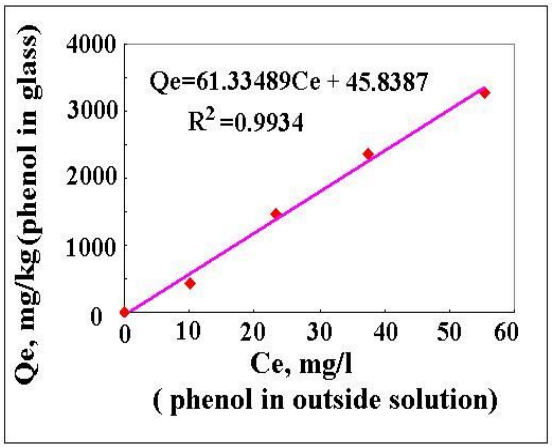

Fig.2 Example of adsorption isotherm obtained using the glass hybridized with TBP (Tributyl phosphate)

---

*d07hb902@ynu.ac.jp

3E13

Combined treatment of polishing wastewater and fluoride-containing wastewater from a semiconductor manufacturer

Mark Daniel Garrido de Luna, Warmadewanthi and J. C. Liu*

Department of Chemical Engineering, National Taiwan University of Science and Technology

43 Keelung Road, Section 4, Taipei 106, Taiwan

Collection and treatment of chemical mechanical polishing (CMP) wastewater and fluoride-containing wastewater in semiconductor manufacturers are conventionally separated. The combined treatment of these two streams of wastewater was studied. Polishing wastewater containing silica was mixed at different ratio with synthetic fluoride-containing (640 mg/L) wastewater. Calcium chloride ($CaCl_2$) was then added at neutral pH to induce calcium fluoride (CaF_2) precipitate. Fluoride removal efficiency increased from 96% to 99% when the mixing ratio (v/v) increased from 1:1 to 4:1 Scanning electronic microscopic (SEM) pictures and particle size analysis showed larger size of precipitates when at higher mixing ratio. It is proposed that fine silica present in polishing wastewater act as nuclei to enhance precipitation of CaF_2. The subsequent solid-liquid separation was very effective by the use of anionic flocculent, PAA. Results indicated that the combined treatment both polishing and fluoride-containing wastewater is feasible. Potential advantages include lower chemical dosage, better control, smaller footprint, and lower amount sludge.

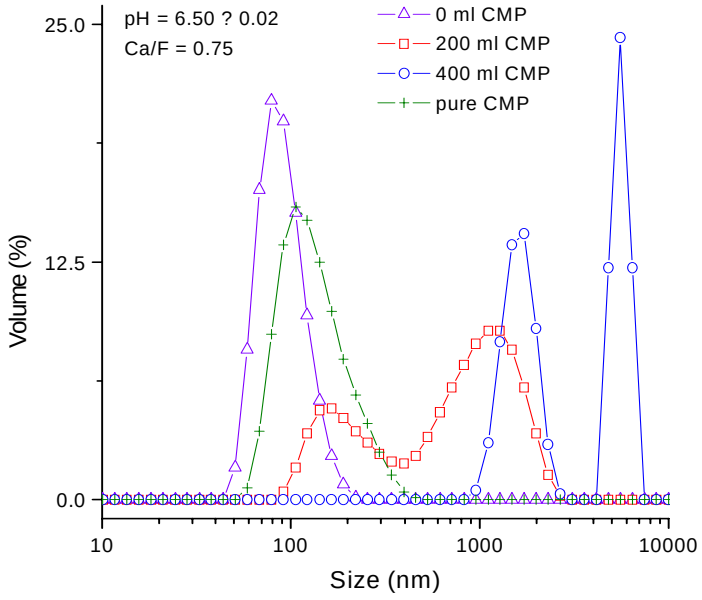

Fig 1. Size of precipitates as affected by mixing ratio.

*D9406801@mail.ntust.edu.tw

3E14

Essentials for Designing Recovering Materials of Oil in Water

H. Sakaguchi[1]*, A. Kawai[2]
[1]*Intermolecular Interaction Research Laboratory, Mol Labo Inc.,*
380-4 Takasaki, Tsukuba, Ibaraki 300-1245 Japan
[2]*Research Center for Compact Chemical Process, AIST,*
1-1-1 Higashi, Tsukuba, Ibaraki 305-8565 Japan

Water pollution by oil has become more and more severe problem for these decades. Mixed oil in water should be recovered, not be dispersed or diluted in water. Many kinds of oil recovering materials have been developed, but they are not efficient so far and not used widely. In this paper, fundamental factors for designing effective oil recovering materials are investigated all over again.
In order to adsorb small molecules effectively, large specific surface area of adsorbent is essential. In order to enlarge surface area, usually used adsorbents are composed of nanometer size pores. However, for the purpose of adsorbing oil in water, rather flat surface is desirable, because very large size oil droplets, compared with gas molecules, cannot reach into the inside of small pores. Therefore, simple flat plate or thin fiber is better.
Considering easy treatment after catching and gathering oil droplets, not nanometer or micrometer size, but millimeter or centimeter size adsorbents are better.
In order to catch and hold amounts of oil, not only adsorb one layer of oil directly contacted with adsorbent, adsorbed oil should be constructed and piled up like crystals. To do so, crystalline surface of the adsorbent is expected to be much more effective than amorphous one.
To catch oil, it's better for the surface of the adsorbent to be covered with oil-like radicals, alkyl chains.
To be well dispersed in water, it's better for the adsorbent to be amphiphilic than hydrophobic.
Mechanically tough and at the same time flexible adsorbent is desirable.
All these factors are considered, and one candidate was synthesized as shown in Figure one.
How to adopt essential considerations to practical adsorbents, advantage and disadvantage of the candidate, comparison with other examples, will be discussed.

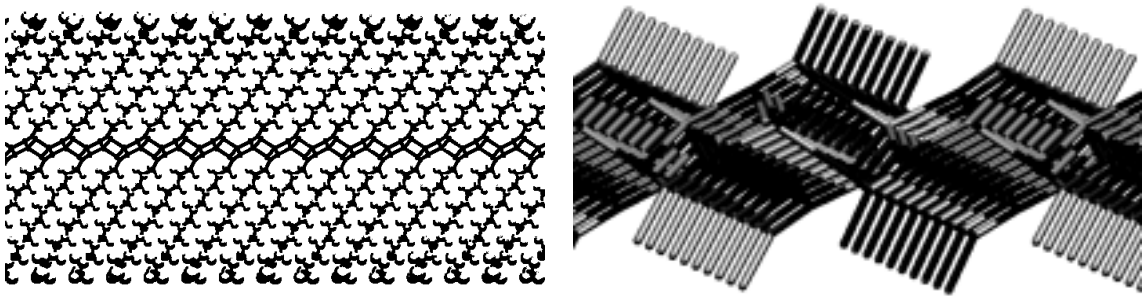

Fig. 1 Single crystal structure of Lithium Tetradecanoate clarified by X ray diffraction.
Left: On both sides of each flat ionic crystal part, alkyl chains are arranged regularly.
Right: Central ionic crystal part is constructed from COOLi.

*h-sakaguchi@mol-labo.jp

3E15

REMOVAL OF CHLORINATED HYDDROCARBONS BY NANOSCALE [Fe_3O_4]MgO

G.C.C.Yang*, S.W. Chan, T.C. Peng

Institute of Environmental Engineering, National Sun Yat-Sen University, Kaohsiung 80424, Taiwan

In this work nanoscale [Fe_3O_4]MgO was prepared, characterized, and tested for evaluating its capability as a novel destructive adsorbent in removing various chlorinated hydrocarbons in aqueous solutions. To this end, nanoscale MgO as the substrate was first synthesized by the sol-gel process. The prepared material was further calcined and then designated MgO-*S*. Further, Fe_3O_4 was synthesized using the reverse co-precipitation method to deposit on the surface of MgO-*S* forming the nanostructured *S*-[Fe_3O_4]MgO. The pattern of X-ray diffraction analysis has identified the co-existence of Fe_3O_4 and MgO for $S_{1/5}$-[Fe_3O_4]MgO (i.e., *S*-[Fe_3O_4]MgO with a molar ratio of Fe_3O_4/MgO = 1/5). The image of scanning electron microscopy (SEM) further showed that *S*-[Fe_3O_4]MgO was in a form of nanoscale Fe_3O_4 on the surface of MgO-*S*. The result of SEM-EDS (energy dispersive X-ray spectrometry) further verified the co-existence of O, Mg, and Fe elements. The isoelectric point of *S*-[Fe_3O_4]MgO was determined to be in the pH ranges of 8.0-9.1. Since $S_{1/5}$-[Fe_3O_4]MgO) had the greatest specific surface area (i.e., 116.69 m^2/g) among various metal oxide composites tested, it was selected as the model composite for the treatment of trichloroethylene (TCE), chlorobenzene (CB), and 4-chlorophenol (4-CP) in this study. The test results are shown in Fig. 1. Apparently, $S_{1/5}$-[Fe_3O_4]MgO performed differently with different chlorinated organic compounds in aqueous solutions. Based on a preliminary result of the daughter products analyzed by gas chromatography, $S_{1/5}$-[Fe_3O_4]MgO has demonstrated its capability of destructive adsorption towards chlorinated organic compounds in aqueous systems.

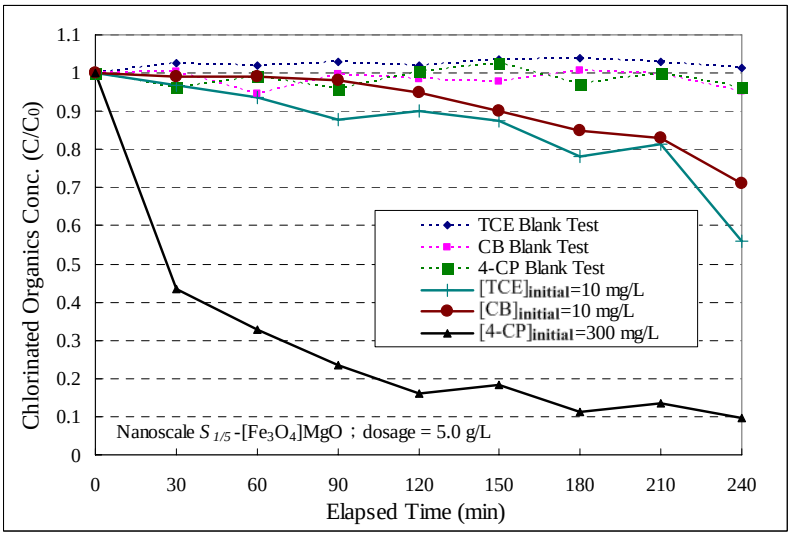

Fig. 1 Treatment of chlorinated organic compounds by $S_{1/5}$-[Fe_3O_4]MgO in aqueous solutions.

*gordon@mail.nsysu.edu.tw

3E16

Sensitive binding of bisphenol A in TiO_2 ultrathin films: a combination of molecular imprinting and host-guest interaction

S.-W. Lee*, N. Takahara, T. Kunitake

Graduate School of Environmental Engineering, The University of Kitakyushu

1-1 Hibikino, Kitakyushu 808-0135, Japan

Molecular recognition phenomena of host molecules have been extensively studied for various applications ranging from sensing to separations. Among others, cyclodextrins (CDs) that possess internal hydrophobic cavity and external hydrophilic surface in a molecule are widely employed in many industrial products, technologies, sensor developments and analytical chemistry. In order to achieve high sensitivity and selective detection for aromatic compounds, we combined in this study cyclodextrin hosts and imprinting effects in TiO_2 ultrathin layer. Bisphenol A (BPA), a known estrogenic compound that has activity even at lower concentrations less than 1 ppt, is used in the manufacture of polycarbonate plastics and epoxy resins. It is ubiquitous in the environment and found in many food and beverage containers, including baby bottles. In order to improve specificity and sensitivity to bisphenol A (BPA), the electrode surface was modified with a 2:1 complex of β-CD/BPA onto TiO_2 gel thin films, and then the BPA was removed by washing. The film formation and sensing ability of the BPA-imprinted TiO_2/2β-CD films were confirmed by quartz crystal microbalance (QCM) measurements. The electrode modification gave much high sensitivity for BPA than for other guest molecules and made it possible to detect the BPA selectively. The present method can be applied to a variety of aromatic compounds.

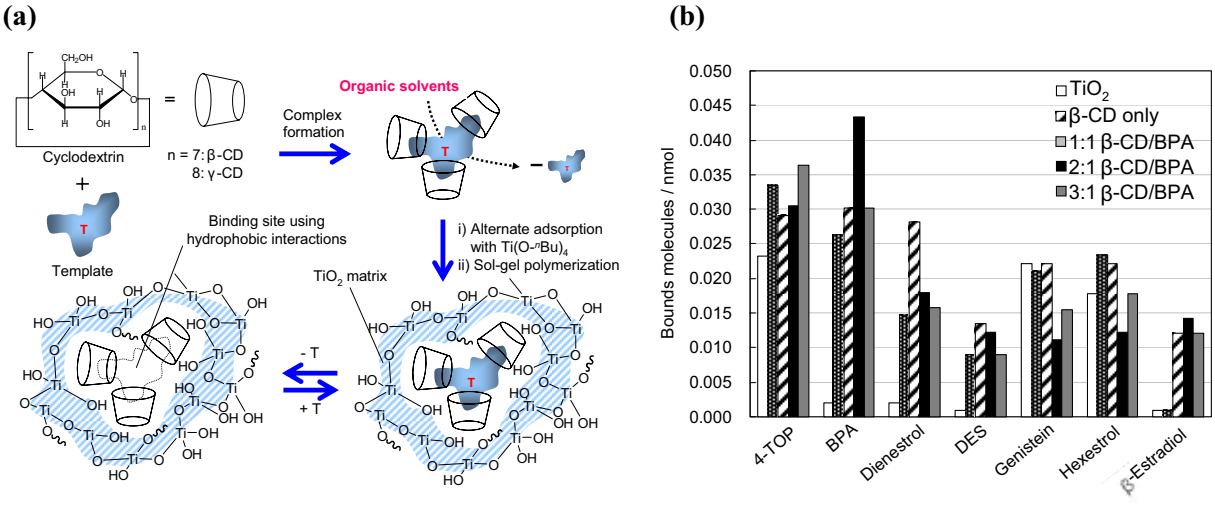

Fig. 1 Schematic illustration of the current imprinting method and comparison of guest binding on TiO_2 and TiO_2/β-CD complexed films.

*leesw@env.kitakyu-u.ac.jp

3E17

Synthesis of monodisperse carbon microspheres as adsorbents for detecting aqueous organic pollutants

Takuji Yamamoto[1], Young Han Kim[2], Takao Ohmori[1]*

[1]National Institute of Advanced Industrial Science and Technology,
1-1-1 Higashi, Tsukuba, Ibaraki 305-8565, Japan

[2]Department of Chemical Engineering, Dong-A University,
840 Hadan-Dong, Saha-gu, Pusan 604-714, Republic of Korea

Development of a simple and efficient system for monitoring a concentration of aqueous organic pollutants has been desired to control the quality of wastewater as well as natural water in rivers or lakes. A quartz crystal resonator (QCR) sensor coated with porous carbon adsorbents is expected to be useful for this purpose. The key is the synthesis of carbon with controlled and developed porous structure which is suitable for enabling rapid adsorption and desorption of organic pollutants. From this point of view, mesoporous carbon is one of the candidates for adsorbents. The authors previously applied mesoporous carbon microspheres to adsorbents of a QCR sensor for detecting aqueous organic pollutants and evaluated their performances[1]. In the previous study, the mesoporous carbon microspheres were prepared by the inverse emulsion polymerization of resorcinol with formaldehyde, followed by freeze-drying and carbonization in an inert atmosphere.

In the present study, synthesis of monodisperse carbon cryogel microspheres (MCC microspheres) is attempted through the membrane emulsification instead of the inverse emulsion polymerization. The effect of the concentration of surfactant used for the membrane emulsification on the porous structure of the MCC microspheres is studied to establish a method for controlling the mesoporosity (mesopore size, mesopore volume, and BET surface area) of the MCC microspheres. A QCR sensor was fabricated by coating a resonator with the obtained MCC microspheres, and the performance of the QCR sensor was evaluated by the on-line liquid phase adsorption experiments using reactive dyes (methylene blue and rhodamine-B) as model organic pollutants. Then, the performance of the QCR sensor was discussed with regard to the effect of the mesoporosity of the MCC microspheres.

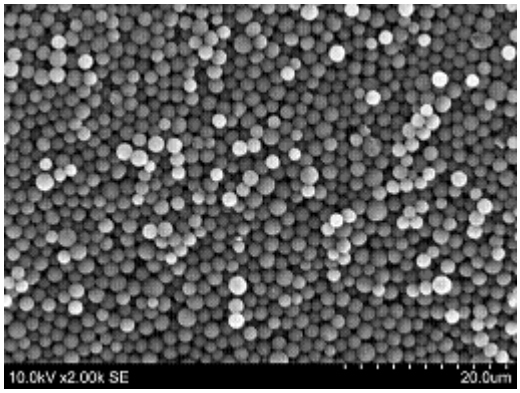

Fig. 1 Image of MCC microspheres.

*yamamoto-t@aist.go.jp

[Reference]

1. Young Min Park *et al.* , Sensors and Actuators B: Chemical, 125(2), 468-473 (2007).

3E18

Synthesis of Mesoporous Carbon Thin Films

S. Kataoka*, T. Yamamoto, A. Endo, M. Nakaiwa, T. Ohmori
National Institute of Advanced Industrial Science and Technology (AIST)
1-1-1 Higashi, Tsukuba, Ibaraki 305-8565, Japan

Porous carbon materials are employed for various applications because of their unique properties including chemical stability, thermal conductivity, and electroconductivity. Among many applications, these materials are used as a good adsorbent for malodorous and toxic volatile organic carbons (VOC). For the efficient uses of porous materials, the pore size control would be of great importance. Recently, the use of phenol resins structured with surfactant self-assembly has gained an increasing attention as a key to mesoporous carbon materials having uniform pore structures.

In our procedure, a precursor solution consisted of resorcinol (or phloroglucinol), surfactant, ethanol, sodium hydroxide, and water. Liquid thin films of the solution were formed on Silicon wafers by dip-coating and were exposed to formaldehyde vapor as a cross-linking agent at 50 ºC to obtain structured resins. Subsequently, the films were further hardened in an oven at 70 ºC for 12 h. The resin films were heated at 400 ºC in inert atmosphere for 4 h to remove the surfactant and to carbonize the resins.

The obtained mesoporous carbon films were observed with an atomic force microscope (AFM). Figures show AFM topographic images for the films made from resorcinol (Fig. a) and from phloroglucinol (Fig. b). The film made from resorcinol has C_3 symmetry with the pore diameter of ca. 9 nm. The film made from phloroglucinol has a less ordered structure, but has open pores with the similar diameter. In either case, the film has uniform open pores with a highly ordered structure. Furthermore, the films retain the ordered structure even after the carbonization at 800 ºC. We have demonstrated that the synthetic method using the structured phenol resins can provide the mesoporous carbon thin films with highly ordered pore structures.

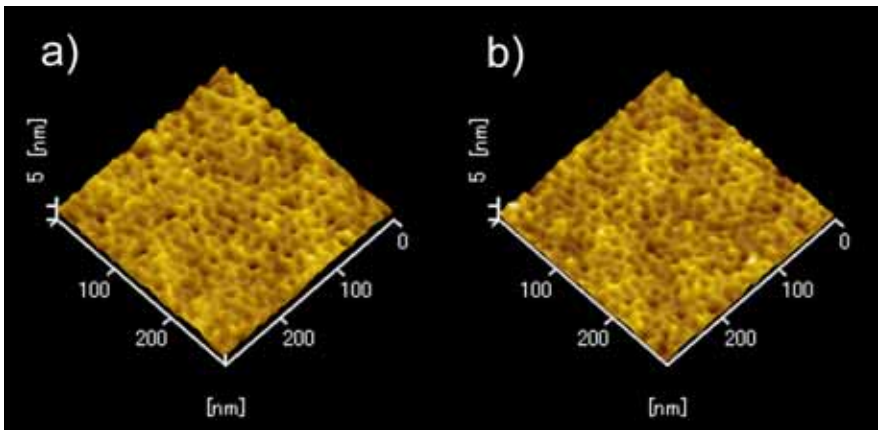

Fig. AFM images of mesoporous carbon films: a) resorcinol, b) phloroglucinol.

*s-kataoka@aist.go.jp

3F11

Evaluation of complete nitrate removal by Fe^0/CO_2, air/water lifted fluidized sand bed reactor, and air stripping in series

Chih-Hsiang Liao[1]*, Jin Anotai[2], Chalermchai Ruangchanikom[3]

[1]*Department of Environmental Resources Management, Chia Nan University of Pharmacy and Science, Tainan, TAIWAN.*

[2]*Department of Environmental Engineering, King Mongkut's University of Technology Thonburi, Bangkok, THAILAND.*

[3]*National Research Center for Environmental and Hazardous Waste Management, Chulalongkorn University, Bangkok, THAILAND.*

This study aimed to demonstrate the effectiveness of the integrated system consisting of zero-valent iron reduction, ferrous oxidation and pelletization, and ammonia stripping units for the removal of both nitrate and its by-products, ferrous and ammonia, as shown in Fig. 1. The results indicated that 70% of the 23 mg N/L of nitrate-spiked groundwater could be removed continually in the simulated first column reactor, with the influent feeding rate of 3 L/hr, Fe^0 dosage of 60 g, and CO_2 gas inflow of 200 mL/min. However, to maintain nitrate lower than 10 mg N/L as specified in the drinking water standard, supplement of 40 g of Fe^0 at every 27 hrs was required. In the second unit, the ferrous, resulting from the previous unit Fe^0 oxidation, was completely oxidized into ferric by using 5 L/min of air in a three-phase fluidized bed reactor, and the amount of greater than 75% was pelletized onto the sand surface. In the third unit, ammonium was the predominant nitrogen-containing specie as a result of nitrate reduction, noting that nitrite was not detected. After stripping with the air flow rate of 180 L/min and pH automatically controlled at 12, more than 80% of the generated ammonium was transferred to the atmosphere.

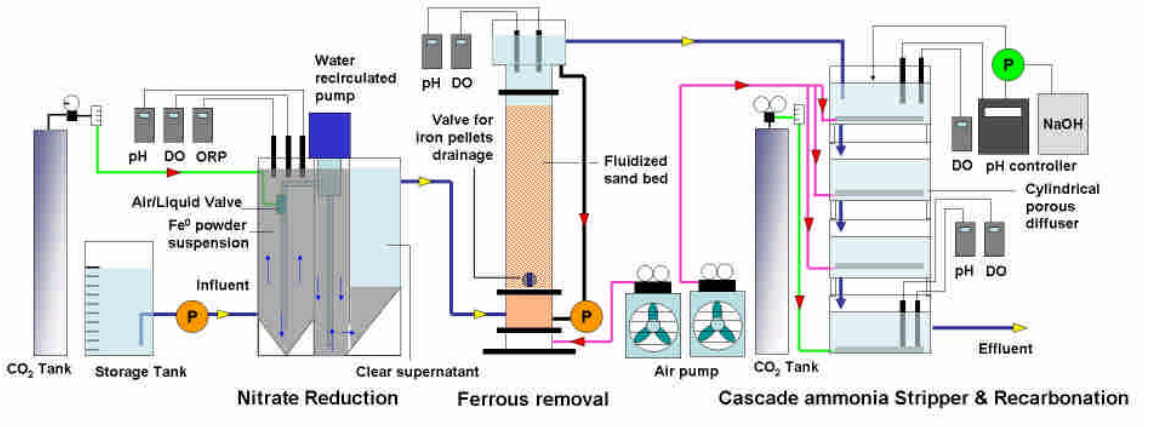

Fig. 1. Integrated system for complete nitrate removal: nitrate reduction, ferrous removal, ammonia stripping.

*chliao@mail.chna.edu.tw

3F12

Potentiality of Basic Slag for the Remediation of Soil Acidity and Changes in Exchangeable Cations in Acid Sulfate Soils under Various Moisture Regimes

A. H. M. Shamim[1, 3*], H. R. Khan[2] and T. Akae[1]

[1]*Department of Environmental Management Engineering, Faculty of Environmental Science & Technology, Okayama University, Okayama 700-8530, Japan*
[2]*Department of Soil, Water & Environment, Dhaka University, Dhaka-1000, Bangladesh*
[3]*School of Agriculture & Rural Development, Bangladesh Open University, Gazipur-1705.*

Severe acidifications in acid sulfate soils (ASSs) have occurred worldwide due to sulfuric acidity, which requires sustainable measures for their reclamation. Accordingly, an incubation study was conducted with the topsoil of two different ASSs (Cheringa and Badarkhali) to evaluate the effects of basic slag (BS: size <1 mm; pH 9.6; Ca 20.8 %; Mg 9.8 %, etc.) on the reduction of acidity and changes in exchangeable cations. It is noted that BS is a byproduct of steel industry in Bangladesh and can be collected almost free of charge. These soils received BS at the rate of 0 (T_0), 11 (T_1), 22 (T_2) and 33 (T_3) t ha^{-1} under various moisture regimes (saturated condition M_1, i.e. 100 % moisture, wetting-drying cycles of 50 and 100 % moisture M_2, and moisture at field condition M_3, i.e. 50 %). The impacts of these treatments on some selected parameters in these soils were studied within180 days of incubation. The application of BS was found to be increased the pH of soils from 3.6 to 5.1 for Cheringa; 3.9 to 5.2 for Badarkhali soils at the end of incubation. These increments were more striking with the highest doses of BS under saturated moisture conditions in both the soils. The ECe of the soils had not much influenced by the application of BS regardless of time. The treatments exerted significant ($p \leq 0.05$) effects on exchangeable cations in different periods of incubation. The striking changes were recorded for the rate of increments of Ca^{2+} and Mg^{2+}, which were about 2-3 times higher for Ca and more than 2 times higher for Mg^{2+} compared with the control after 180 days of incubation. These results suggest that the application of BS not only increased the Ca^{2+} to the higher amount than that of the increment of Mg^{2+} in the soils but also improved one of the important criteria of Ca^{2+} and Mg^{2+} ratio in the soils (Fig. 1).

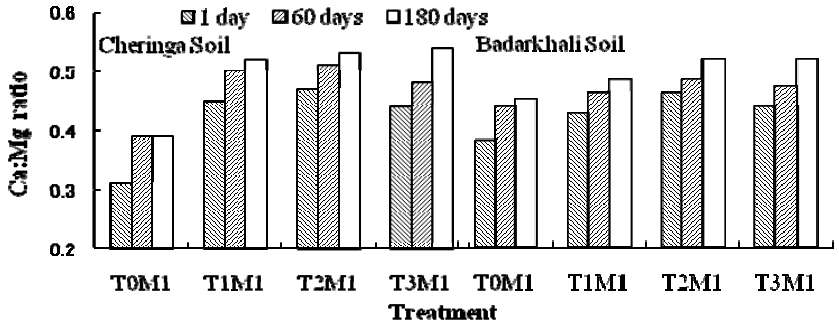

Fig. 1 Effects of basic slag, moisture regimes and incubation times on Ca:Mg ratio in acid sulfate soils.

*abulhasnats@yahoo.com

3F13

Assessment, Purification and Phytoremediation Strategies for the Pollution Arising from Lead, Zinc and Cadmium Released through Industrial Effluents

H. R. Khan* and S. A. Lipi

Department of Soil, Water and Environment, University of Dhaka, Dhaka 1000, Bangladesh.

Pollution by heavy metals and toxic substances released from industrial effluents is a serious problem. Accordingly, phytoremediation and purification of industrial effluents were considered for this study. The color, pH, EC, total dissolved solids (TDS), dissolved oxygen (DO), chemical oxygen demand (COD), total hardness, chloride, CO_3, HCO_3, alkalinity, Cu, Cd, Pb, Mn, Zn, and Cr contents in the effluents discharged from Hazaribagh tannery and Tejgaon textile industries in Dhaka were determined. These effluents had no significant ($p \leq 0.05$) effects on soil pH but exerted significantly positive effects on the CEC of the soil. The TDS of the effluents were also high but it decreased by alum [$K_2SO_4\,Al_2\,(SO_4)_3\,24\,H_2O$] treatment. The DO of the effluents was low and the COD was high leading to a serious threat for aquatic lives. The concentrations of Cd, Pb, Zn Mn and Cr were high. Filtration through rapid sand-gravity-filter and coagulation of effluents by alum decreased the concentrations of Cr and Pb below the permissible limits. The treated effluents were used for the production of vegetables (Grey, Red and Green spinaches) grown in a non-polluted soil under pot experiments. Application of treated effluents was found to have significant ($p \leq 0.05$) positive effects on the biomass production of the vegetables. Green spinach was found to be assimilated the highest amounts of Pb, Zn and Cd in shoots compared with Grey and Red spinaches grown under the treated effluents of tannery industries. But the Red spinach was recorded for the highest uptake of Pb, Zn and Cd in the roots compared with the roots of Green and Grey spinaches grown under the treated effluents of textile industries.

The present study revealed that the natural sand-gravity-filter and alum treatments were found to be effective not only for the remediation of polluted effluents but also improved the growth of vegetables. The use of natural filter and/or alum treatment should be practiced for the remediation of pollution of industrial effluents before discharging from industries.

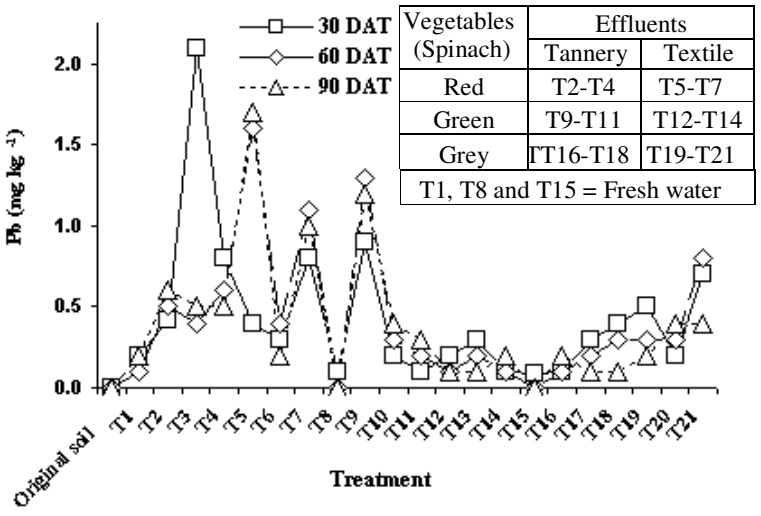

Vegetables (Spinach)	Effluents	
	Tannery	Textile
Red	T2-T4	T5-T7
Green	T9-T11	T12-T14
Grey	IT16-T18	T19-T21
T1, T8 and T15 = Fresh water		

Fig. 1 Content of Pd in soil at different sampling times (DAT = days after transplantation of vegetables)

*duharun@yahoo.com

3F14

Thermodynamic and kinetic processes at coal interface for CO_2 geological storage

D. Charrière[1, 2], Z. Pokryszka[1], P. Behra[2]*
[1]INERIS – Institut National de l'Environnement Industriel et des Risques
BP2 – 60550 Verneuil-en-Halatte – France
[2]Université de Toulouse – Laboratoire de Chimie Agro-Industrielle – UMR1010 INRA/INPT-ENSIACET – 118, route de Narbonne – 31077 Toulouse Cedex 4 – France

Currently, the geological storage of CO_2 is heavily studied around the world in order to limit global warming due to the greenhouse effect. The atmospheric CO_2, which has been steadily increasing for more than a century, is assumed to be in a large part responsible of this warming. Nowadays, various options have been considering to store CO_2 in an underground environment for periods covering several centuries. Among the options, one is to inject it in unexploited coal seams. The objective of our work is to characterise the interactions between CO_2 and coal interfaces from two French coal seams. This will contribute to identify the most adapted coal basin which could be used for storing CO_2 in France.

To study the feasibility of CO_2 storage in coal seams, experiments of adsorption were performed using gravimetric technique with a magnetic suspension balance for monitoring the kinetics and capacity of sorption. Adsorption experiments of CO_2 and CH_4 were carried out at conditions of pressure and temperature close to the underground sites and/or in the presence of moisture. The experiments were carried out for three different sample sizes at a pressure ranging from 0.1 to 5 MPa and temperatures ranging from 298 to 318 K.

From our results, the sorption kinetics of gases onto coals depends on several parameters, including:

- grain size: for increasing size, the sorption kinetics becomes slower (fig. 1) but the adsorption capacity remains constant;
- temperature: for increasing temperature, the sorption equilibrium is reached much faster but the adsorption capacity becoming lower;
- gas nature: in our experimental studied conditions, equilibrium is reached faster for CO_2 sorption than for CH_4 sorption, while the adsorption capacity of CO_2 is higher than for the one of CH_4;
- moisture: for wet coals, the kinetic rate of both gases is reduced by a factor of 2 to 3 depending on the moisture content compared to initial tests on dried coals. Moreover, the humidity is a parameter that negatively influences the gas adsorption capacity.

During this experimental study, we showed that the gas sorption at coal interfaces is due to a set of complex mechanisms involving a transfer diffusion through macropores and micropores followed by adsorption onto the sites at coal surfaces. The sorption kinetics can be modelled by a bidisperse model, considering both macropores and micropores. This model seems better suited of the gas diffusion into the coal than a single pore size model.

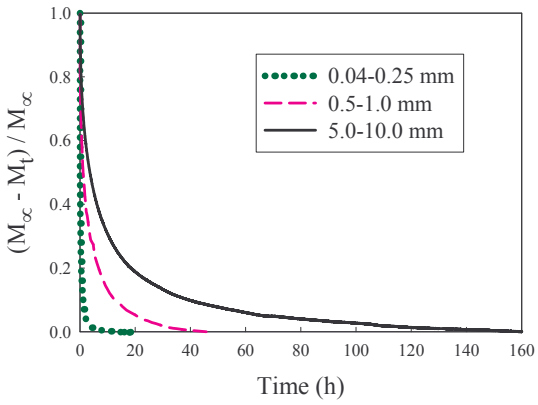

Fig. 1: Sorption kinetics of CO_2 for different grain size fractions of dried coal of Lorrain basin (France) (temperature: 298 K, pressure at equilibrium: ~ 0,1 Mpa, coal mass: 3 g, M_∞ mass of adsorbed CO_2 at equilibrium (g) and M_t mass of adsorbed CO_2 at time t (g))

*delphine.charriere@ineris.fr

3F15

Nanofoaming in silica glass matrix by instantaneous heating

K. Kurumada*, H. Okubo, K. Egusa
School of Environment & Information Sciences, School of Mechanical Engineering,
Yokohama National University, Yokohama 240-8501, JPN

Instantaneous heating of sol-gel derived silica glass was revealed to cause nanofoaming in silica glass matrix as shown in Figure 1. Since the foaming occurred at the same time with the instantaneous hardening of the silica glass matrix due to the rapid polycondensation, the mutual coalescence of the nanoscale cell was effectively hindered. The required conditions for the foaming to be induced were surveyed by various trials of preparation conditions. The formation of the nanofoam was checked by transmission electron microscopy (TEM) and measurement of apparent density by helium densitometer. The following results were obtained through the present study :

(1) Radiation is effective for foaming due to the rapidity which prevents the nanofoam cells from undergoing the mutual coalescence.

(2) The foam was formed as a result of “ballooning” by the gaseous moiety generated at the moment of the instantaneous heating.

(3) The ballooning behavior occurred when the silica matrix was sufficiently densified in its mechanical properties to prevent the gaseous molecules from going out of the matrix due to the higher inner pressure.

(4) The scarce adsorption of nitrogen demonstrated the closed-porosity type structure of the nanofoam. The complete absence of micropores (< 2nm) was indispensable for keeping the ballooning gas inside the silica glass matrix.

(5) Carbon moieties was indicated to be responsible for the occurrence of the nanofoaming because rinsing the sample with water prior to the calcinations lead to entire absence of the nanofoamed structure.

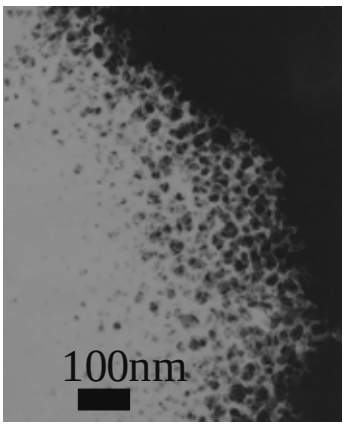

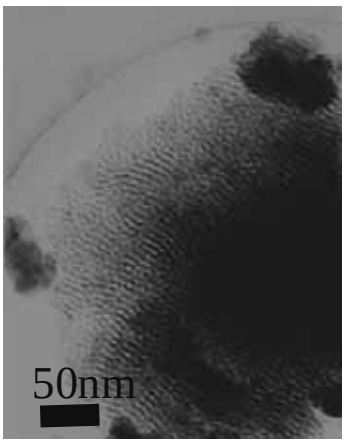

Figure1 (left) Silica nanoform with closed-porosity type structure
(right) Open-porosity type sample prepared by templating method with block copolymer

(6) Smaller organic groups were indicated to be favorable for the nanofoaming because they easily gasify on the instantaneous radiation heating.

(7) Relatively larger organic groups tend to lead to obvious residue of carbon as seen from the black outside appearnce.

*kurumada@ynu.ac.jp

3F16 Optimum conditions for hybridization of epoxy resin and silica

T.Umetsubo*, T.Hayakawa, K Kurumada
Department of Environment and Information Science, Yokohama National University
79-7 Tokiwadai, Hodogaya-Ku, Yokohama, Kanagawa 240-8501, Japn

As lead-free solder has prevailed, reduction in the coefficient of thermal expansion(CTE) has been desired because lead-free solder is less resistant to shear strain. For this purpose, hybridization of epoxy resin and silica is expected to be effective because silica has a significantly smaller CTE than epoxy resin. Since silica cannot be covalently bonded to epoxy in a direct manner, the hybridization needs to be carried out by mixing the sols of these moieties. Here, the problem is that the curing condition of silica is very different from that of epoxy resin. As a result of that, silica segregates during the curing process. As measures to this complication, we examined the following two methods.

1. Addition of mediating solvent for retarding polycondensation of silica.

As a result of trials with various mediating solvent, acetonylacetone was found to be the most effective in retarding the polycondensation of silica. The possible reasons for this effectiveness are as follows;

(1) The vapor pressure of acetonylacetone is relatively low. Its boiling point is as high as approximately 200℃. Therefore, it remains in the mixture of the sols of epoxy and silica even under heating at 150℃ where the curing is actually carried out.

(2) The acetyl group in acetonylacetone has hydrogen bondings with hydroxyl groups. Therefore, silanol moiety is blocked from the mutual polycondensation due to intermediation by acetonylacetone.

Our curing experiments showed that acetonylacetone actually retards the polycondensation of silica moiety. Nevertheless, the addition of acetonylacetone itself could not prevent the segregation of silica from epoxy resin.

2. Partial phenylation of silica.

In the present work, we used phenyl triethoxy silane (PTES) as the silica source. In the present case, the silica moiety was partially modified by a phenyl group covalently bonded to the central silicon atom. The curing temperature of partially phenylated silica is approximately 170℃, which is close to that of epoxy resin. On the whole, the partial phenylation was significantly effective to obtain the hybridized state. In the present case, mediating solvent species with lower boiling points were favourable for the formation of uniform hybrid. Addition of mediating solvents with relatively higher boiling point resulted in phase separation between a silica-rich and epoxy-rich phase. This is probably because the gradual progress of the polymerization of epoxy resin and polycondensation of silica in the presence of the mediating solvent leads to segregation due to the remaining mobility. On the other hand, in the case where acetone was used as the mediating solvent, the primarily proceeding polycondensation of partially phenylated silica and the rapid evaporation of acetone result in a rapid structural arrest followed by the formation of the uniformly hybridized state.

*d07hb006@ynu.ac.jp

3F17

Surfactant- and reducer-free metal nanoparticle synthesis in aqueous solutions: Particle size, shape and colloidal stability

Toshio Sakai[1]*, Hiroto Enomoto[2], Hideki Sakai[2], Masahiko Abe[2]

[1]*Fiber-Nanotech Young Researcher Empowerment Center, Shinshu University, 4-17-1 Wakasato, Nagano, Nagano 380-8553*

[2]*Faculty of Science and Technology, Tokyo University of Science, 2641 Yamazaki, Noda, Chiba 278-8510*

Metal nanoparticles are attracting significant attention because of their unique properties such as size- and shape-dependent optical, magnetic, electronic and catalytic properties. An important and challenging task for metal nanoparticle synthesis is the development of simple and versatile methods for the preparation of nanoparticles in a size or shape-selected and –controlled manner. In addition, utilization of non-toxic chemicals, environmentally benign solvents, and renewable materials are emerging issues that merit important consideration in a nanomaterial synthetic strategy. In this work, we examined metal nanoparticles synthesis from metal ions in aqueous solutions in the absence of any stabilizing or capping agents (surfactants) and reducing agents (reducers). The surfactant- and reducer-free metal nanoparticle synthesis matches with economical and/or environmental requirements since material use is minimized. Furthermore, simplified system (surfactant- and reducer-free conditions) should manifest the essential mechanism of the metal nanoparticle-size, -shape and –colloidal stability control. At the same time, this should provide better insight of surfactant (stabilizing agents or capping agents) utilization. We used the high-frequency (950 kHz) ultrasound for metal ion reduction to prepare metal nanoparticles in aqueous solutions. In particular, we examined the effects of ultrasound frequency, irradiation time, metal ion concentration, additional salts, pH and temperature on the size, shape and colloidal stability of gold nanoparticles ultrasonically prepared in the surfactant-free aqueous solutions. We found that those factors affect the size, shape and colloidal stability of gold nanoparticles ultrasonically prepared even in the surfactant-free conditions. For example, spherical (polyhedral) gold nanoparticles with diameter of 20-40 nm formed from a 0.1 mM $AuCl_4^-$ aqueous solution above 50 ˚C while hexagonal and triangular plates coexist with polyhedral particles below 40 ˚C (Figure 1).

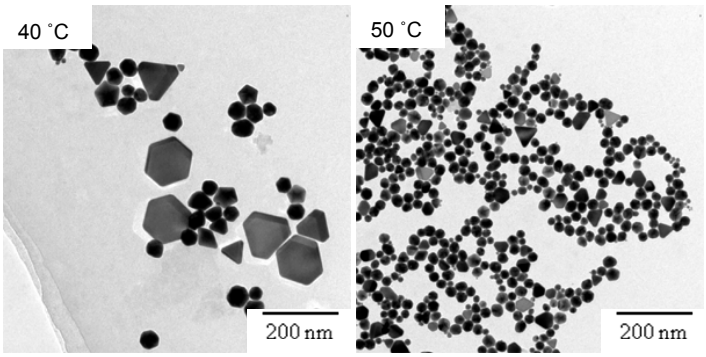

Figure 1. TEM images of gold nanoparticles formed from 0.1 mM $AuCl_4^-$ aqueous solutions at 40 ˚C (left-hand side image) and at 50 ˚C (right-hand side image) using 950 kHz ultrasounds for 8 min.

*tsakai@shinshu-u.ac.jp

3F18

Å-scale droplets of extractant in glass matrix

Y. Kamimura*, K. Kurumada, P. Gaofeng

Department of Environment and Information Science, Yokohama National University,

79-7 Tokiwadai, Hodogaya-Ku, Yokohama, Kanagawa 240-8501, JPN

TBP (tributyl phosphate) is an organic species that can be used extractant of phenol from wastewater. In this study, liquid TBP was directly incorporated in silica glass by sol-gel method. The results of differential thermal analysis (DTA) and thermo gravimetric analysis (TGA) shown in Fig.1 indicated that the whole TBP was completely and stably immobilized in the glass matrix without any leakage or evaporation. FT-IR results showed that TBP was immobilized intact in its molecular structure. The leakage of TBP was observed by immersing the TBP incorporated glass in aqueous phase. This result indicates that TBP were entrapped as droplets. As shown in Fig.2, increasing the incorporated amount of TBP leads to a gradual decrease in the Vickers hardness. Remarkably, the Vickers hardness could be measured even when TBP occupied approximately 69vol.% in the glass. Therefore, the minimal siloxane bondings were firmly formed to maintain the rigid glass matrix. WAXS results shown in Fig.3 revealed that the intercalation of TBP molecules caused a slight increasing in the average distance of adjoining Si atoms. This result suggests that TBP forms angstrom-size droplets and they were stably entrapped in rigid siloxane bondings.

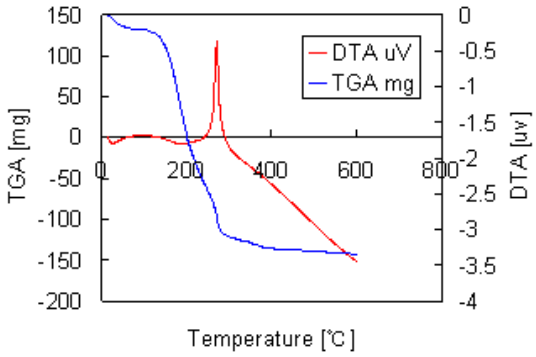

Fig.1 DTA/TGA results of TBP incorporated glass (ε=1).

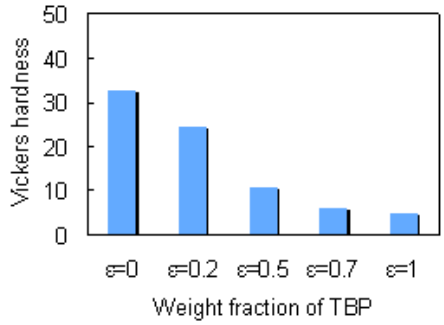

Fig.2 Vickers hardness of TBP incorporated glass.

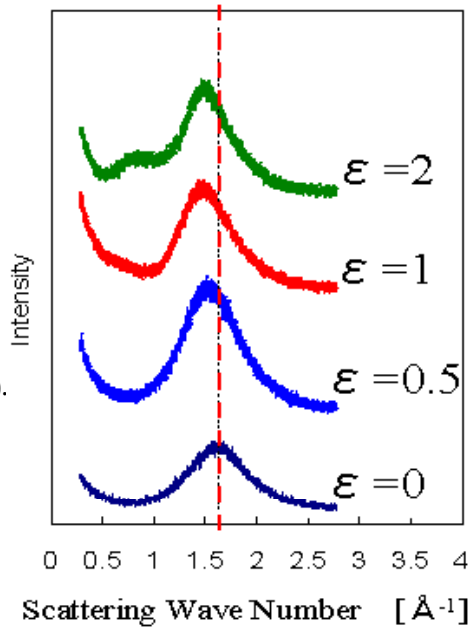

Fig.3 WAXS profiles of glass incorporated with various weight fractions of TBP. The red dashed line is a guide of the peak position of typical silica glass.

*d06tb001@ynu.ac.jp

4A01

Electrokinetic Boundary Condition Compatible with the Onsager Reciprocal Relation in the Thin Double Layer Approximation

M. Doi

Graduate School of Engineering, Department of Applied Physics, University of Tokyo, 7-3-1, Hongo, Bunkyo-ku, Tokyo, Japan 113-8656

The boundary condition which has been used in the conventional electrokinetic calculation in thin double layer approximation has a flaw that it does not give the Onsager reciprocal relation for the sedimentation of charged particle. We propose a new boundary condition which satisfies the local reciprocal relation of Onsager, and guarantees the reciprocal relation for macroscopic transport phenomena. We derive a general mobility matrix for the motion of charged particle of arbitrary shape and charge distribution under the action of external force, torque and electric field. We then calculate the mobility matrix explicitly for homogeneously charged spherical particle, and discuss the effect of surface slippage and the surface conductivity.

doi@rheo.t.u-tokyo.ac.jp

4A02

Direct Numerical Simulations for Electrokinetics of Colloids

R. Yamamoto*[1,2], S. Yamamori[1], Y. Nakayama[3], and K. Kim[4]

[1]*Department of Chemical Engineering, Kyoto University, Japan*
[2]*CREST Japan Science and Technology Agency, Japan*
[3]*Department of Chemical Engineering, Kyushu University, Japan*
[4]*Institute for Molecular Science, Japan*

We have developed a unique method for direct numerical simulations (DNS) of dense colloidal dispersions [1]. This method enables us to compute the time evolutions of colloidal particles, ions, and host fluids simultaneously by solving Newton, advection-diffusion, and Navier-Stokes equations so that the electro-hydrodynamic couplings can be fully taken into account. The electrophoretic mobilities of charged spherical particles are calculated in several situations. The comparisons with approximation theories show quantitative agreements for dilute dispersions without any empirical parameters; however, our simulation predicts notable deviations in the case of dense dispersions [2].

Recently, there observed experimentally the formation of string-like objects made of charged colloidal particles, similar to a "pearl chain" if external AC electric fields are applied. We have used our numerical method to investigate the mechanisms of this phenomena.

We calculated the force acting between a pair of particles fixed at a constant distance r with and without external AC fields. Distributions of ions become anisotropic under electric fields as schematically in Figure 1. This leads to an occurrence of anisotropic dipole-dipole type interactions which can be a possible mechanism for the pearl chain formation. The following equations [2] are solved simultaneously to examine this scenario.

i) The Navier–Stokes equation for fluid motions:

$$\rho(\partial_t + \vec{v}\cdot\nabla)\vec{v} = -\nabla p + \eta\nabla^2\vec{v} - \rho_e\nabla(\Psi + \Psi_{ex}) + \phi\vec{f_p}, \tag{1}$$

with incompressible condition $\nabla\cdot\vec{v} = 0$.

ii) The Newton's and Euler's equations of motions for colloid motions:

$$\dot{\vec{R}}_i = \vec{V}_i, \quad M_p\dot{\vec{V}}_i = \vec{F}_i^H + \vec{F}_i^c, \quad \boldsymbol{I}_p\cdot\dot{\vec{\Omega}}_i = \vec{N}_i^H. \tag{2}$$

iii) Advection-diffusion equation for ionic densities:

$$\partial_t C_\alpha^* = -\nabla\cdot C_\alpha^*\vec{v} + f_\alpha^{-1}\nabla\cdot((\boldsymbol{I} - \vec{n}\vec{n})\cdot C_\alpha^*\nabla\mu_\alpha). \tag{3}$$

Surprisingly good agreements were obtained between our numerical results and experiments. We thus conclude that the present scenario is correct.

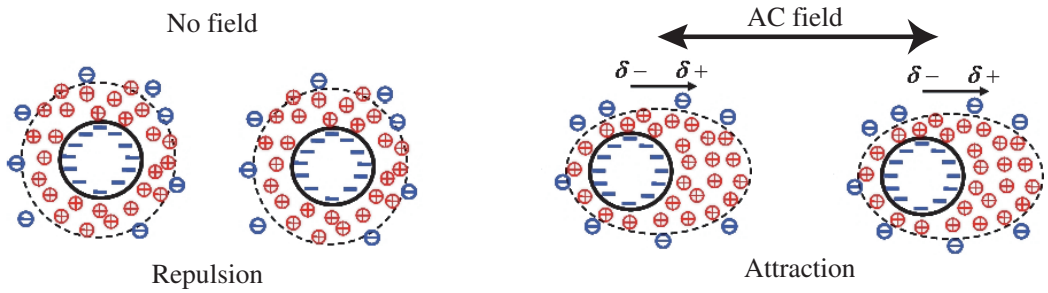

Figure 1: Attraction between likely charged colloidal particles under AC electric field.

REFERENCES

1. KAPSEL Homepage, http://www-tph.cheme.kyoto-u.ac.jp/kapsel/
2. Kim, K., Nakayama., Y, and Yamamoto, R., *Phys. Rev. Lett.* **96**, 208306, (2006).

4A03

Monitoring the electrochemical reactivity of pyrite/humics/electrolyte solution interface by electrokinetics of the second kind

Jérôme F.L. Duval
Laboratory Environment and Mineral Processing, CNRS, Nancy-University,
15 avenue du Charmois, B.P. 40, 54501 Vandoeuvre-lès-Nancy cedex, France

The electrokinetic features of electron-conducting substrates, as measured in a conventional thin-layer cell, strongly depend on the extent of bipolar faradaic depolarisation of the interface formed with the adjacent electrolytic solution. Streaming potential versus applied pressure data obtained for metallic substrates must generally be interpreted on the basis of a modified Helmholtz-Smoluchowski equation corrected by an electronic conduction term – non linear with respect to the measured lateral potential and applied pressure gradient – that stems from the bipolar electrodic behavior of the metallic surface. In the first part of the presentation, a general background for the physical operators that govern such electrokinetic phenomenon of the second kind will be presented both from a theoretical and experimental point of view. In the second part of the talk, a concrete environmental application of this process in relation with acide mine drainage remediation will be commented. For that purpose, streaming potential measurements performed in KNO_3 solutions on porous plugs made of electron-conducting grains of pyrite (FeS_2) covered by humic acids will be presented. For zero coverage, the extensive bipolar electronic conduction taking place in the plug leads to the complete extinction of the streaming potential over the entire range of applied pressure examined. For low to intermediate coverage, the local electron-transfer kinetics on the covered regions of the plug becomes more sluggish. The overall bipolar electronic conduction is then diminished which leads to an increase in the streaming potential with a non-linear dependence on the pressure. For significant coverage, a linear response is observed which basically reflects the interfacial double layer properties of the humics surface layer. A tractable, semi-analytical model is presented that reproduces the electrokinetic peculiarities of the complex and composite system FeS_2/humics investigated. The study demonstrates that the streaming potential technique is a fast and valuable tool for establishing how well the electron transfer kinetics at a partially or completely depolarised bare electron-conducting substrate/electrolyte solution interface is either promoted (catalysis) or blocked (passivation) by the presence of a discontinuous surface layer, as desired *e.g.* for monitoring the electrochemical reactivity of mineral sulphurs responsible for the acidification of soils.

jerome.duval@ensg.inpl-nancy.fr

4A04

Permeation and diffusion through nanoporous inorganic membranes

Toshinori Tsuru
Department of Chemical Engineering, Hiroshima University
1-4-1 Kagami-yama, Higashi-Hirohsima 739-3527

1.Introduction

The transport mechanism though nanofiltration membranes, which have pore sizes in the range of 1-2 nm, is not yet clear, although several mechanisms for gaseous permeation including the viscous flow, Knudsen flow, surface diffusion, and molecular sieving, have been proposed. The present paper will introduce the permeation and diffusion in liquid phase thorough nanoporous membranes.

2. Permeation of solvents though nanopores[1,2)]

Silica/zirconia (SZ; Si/ Zr molar ratio = 9/1) membranes having pore sizes in the range of 1- 5 nm were prepared by the sol-gel process. Organic/ inorganic hybrid membranes were developed by modifying the surface of the silica-zirconia porous membranes via a gas-phase reaction with trimethylchlorosilane (TMCS). As sown in Fig., the transport mechanism of pure solvents through the unmodified membranes does not obey the viscous flow mechanism, since the volumetric permeabilities multiplied by the viscosity, $L_p\mu$, which should be constant in the case of the viscous-flow mechanism, increased with temperature. On the other hand, SZ membranes modified with TMCS showed a relatively constant $L_p\mu$ for nonpolar solvents (hexane and toluene) as well as polar solvents (methanol and ethanol), suggesting that the viscous flow mechanism holds for porous membranes in which the pore diameter is several nms.

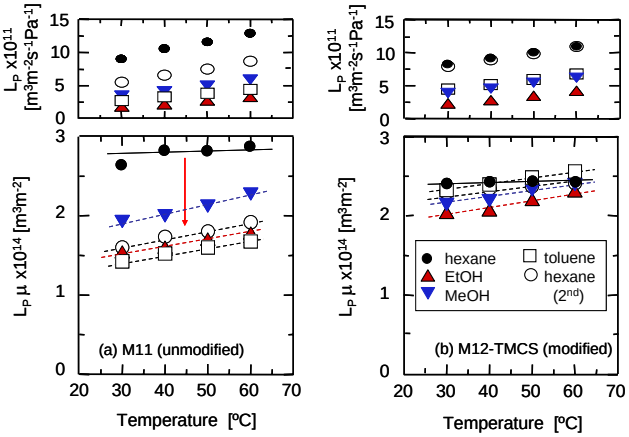

Fig. 1 Temperature dependency of solvent permeability, L_p, and $L_p\mu$, multiplied by solvent viscosity, μ, for (a) SiO_2-ZrO_2, and (b) methylated SiO_2-ZrO_2 membranes (pore size: 3 nm)

3. Diffusion of solutes though nanopores[3)]

Reverse osmosis of alcohols (hexanol, octanol, decanol) and alkanes (hexane, decane, tetradecane) in ethanol solutions over the temperature range from 25 to 60 °C. Rejection increased with the applied pressure, for both alcohol and alkane solutes. However, the rejection of alcohols were found to decrease with temperature, while that for alkanes remained nearly constant. The separation characteristics were examined for the following membrane parameters: solvent permeability, L_p, reflection coefficient, σ, and solute permeability, P, based on the Spiegler-Kedem equation.

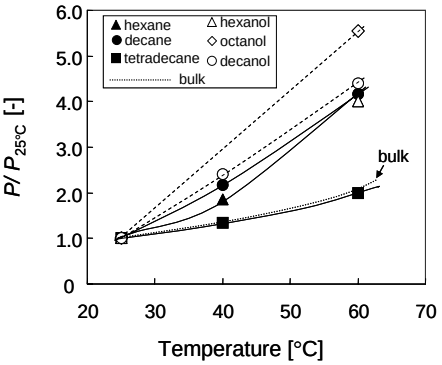

Fig. 2 Effect of temperature on permeabilities, P, normalized at 25 °C, for alcohols and alkane in ethanol solutions (pore size 1nm).

The viscosity of solutions and the diffusivity of alkanes and alcohol solutes in nano-sized pores were found to show a larger temperature dependency than in bulk. The diffusivity of alkane solutes showed the same temperature dependency as the viscosity of ethanol in nano-sized pores, while the diffusivity of alcohol solutes showed a larger temperature dependency than the viscosity of ethanol, probably because of a larger interaction between alcohol solutes and the hydrophilic surface of silica-zirconia membranes.

References 1) T. Tsuru, T. Sudou, S. Kawahara, T. Yoshioka, M. Asaeda, *J. Colloid & Interface Sci.*, 228 (2000) 292-296; 2) T. Tsuru, H. Kondo, T. Yoshioka, M. Asaeda, *AIChE J.*, 50 (2004) 1080-1087; 3) T. Tsuru, M. Miyawaki, T. Yoshioka, M. Asaeda, *AIChE J.*, 52 (2006) 522-531

tsuru@hiroshima-u.ac.jp

4A05

TRANSPORT PHENOMENA ACROSS MEMBRANES IN SOLUTION

A. TANIOKA*

Tokyo Institute of Technology, Graduate School of Science and Engineering

Department of Organic and Polymeric Materials,

2-12-1 Ookayama Meguro-ku , Tokyo 152-8552, Japan

Membranes are still to be comprehensive research subjects in the field of physical chemistry, chemical engineering, polymer chemistry, food chemistry, pharmacology, biology, and physiology, for instance. At the early stages in this field, ion-exchange membranes were preferentially researched because of the interesting electrokinetic phenomena which occurs during the electrolyte transport through the membranes. Moreover the precise investigation of electrokinetic phenomena on ion-exchange membranes, neutral porous membranes and reverse osmosis membranes were applied for dialysis, ultra- and micro-filtration and water purification in various solutions, for instance.

Various transport equations across membranes were derived from membrane model-independent relationships such as non-equilibrium thermodynamics and model-dependent ones such as the solution-diffusion model, the fine-porous membrane model, and TMS model relationships and their modifications. A complete phenomenological characterization of transport across synthetic membranes makes possible the classification of these membranes regarding their hydrodynamic, osmotic, and salt permeabilities as well as their reflection coefficients. Under this point of view, a comparison of different synthetic membranes by appropriate phenomenological transport parameters renders possible, in addition, the elucidation of the transport mechanisms of solute and solvent and their correlation with the membrane structure characterized by properties such as the porosity, water content and structure, fixed-charge density, free volume, solubility and adsorption behavior, etc. A deeper knowledge of the transport mechanisms of solute and solvent and their correlation with the membrane structure and features might enable one to artificial membrane for specific applications. Such information can be obtained if the listing of phenomenological transport parameters is complemented by exhaustive considerations of membrane models and i investigations of the membrane structure.

It is important to point out that the phenomenological transport relationships do not yield any deeper insight into the physical and physicochemical origin of distinct transport processes. The relationships, however, can give the guidelines for the design of corresponding experiments and their evaluation. There are no objections against the use of Ohm’s or Fick’s law although they do not give any information about the physical fundamentals of the electrical resistance or diffusion, for instance. However, a systematic analysis of corresponding experimental data would be made difficult without these phenomenological relationships.

*atanioka@o.cc.titech.ac.jp

4A06

Effective viscosity of a suspension of soft particles

H. Ohshima
Faculty of Pharmaceutical Science, Tokyo University of Science,
2641 Yamazaki, Noda, Chiba 278-8510, Japan

A theory for the primary electroviscous effect in a dilute suspension of soft particles (i.e., particles coated with an ion-penetrable surface layer of polyelectrolytes) in an electrolyte solution is presented.[1)] The general expression for the effective viscosity η_s of the suspension and the primary electroviscous coefficient p, which is further expressed in terms of a function L, is given. On the basis of the general expressions, we derive approximate analytic expressions for η_s and p, which are applicable when the density of the fixed charges distributed within the surface layer is low. Further we obtain a simple approximate analytic expression (without involving numerical integrations) for p applicable for most practical cases. It is found that the function L exhibits a minimum when plotted as a function of κa (κ is the Debye-Hückel parameter and a is the particle core radius), unlike the case of a suspension of hard particles, in which case L decreases as κa increases, exhibiting no minimum. The presence of a minimum for the case of a suspension of soft particles is due to the fact that L is proportional to $1/\kappa^2$ at small κa and to κ^2 at large ka. Because of the presence of this minimum, the difference in L between soft and hard particles becomes very large for large κa.

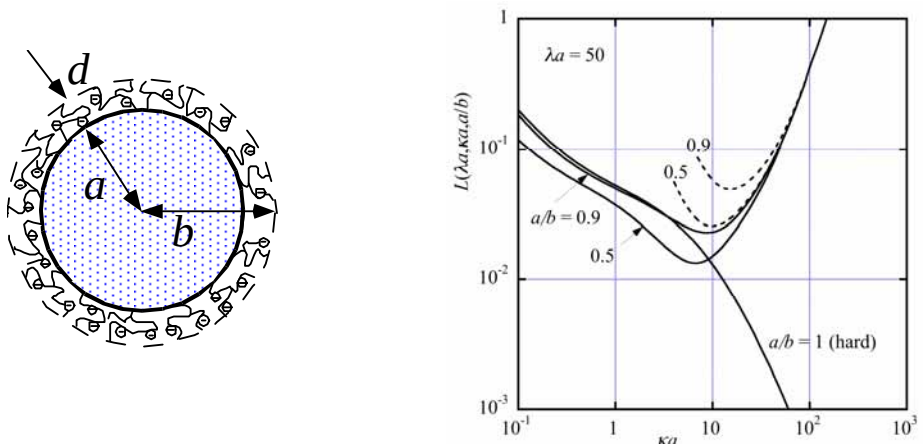

Fig. 1. A soft particle (left) and the function $L(\kappa a, \lambda a, a/b)$ for a suspension of soft particles as a function of κa for a/b = 0.5 and 0.9 at λa =50 (where $1/\lambda$ is the softness parameter and b is the sum of a and the thickness d of the polyelectrolyte layer). The solid lines represent exact results and the dotted lines approximate results. The curve for a/b=1 corresponds to a suspension of spherical hard particles.

Ref. 1, Ohshima, H., *Langmuir*, in press.

ohshima@rs.noda.tus.ac.jp

4A07

Fractal Materials and Their Functional Properties

K. Tsujii*

Nanotechnology Research Center, Research Institute for Electronic Science, Hokkaido University, (CRIS Building) N-21, W-10, Kita-ku, Sapporo 001-0021, Japan

Fractal is a mathematical (geometrical) concept, and has been used for long time as a measure of complexity in the fields of physics, chemistry, industrial technologies, and so on. But the fractal concept has been found by the present speaker and his coworkers to be also a powerful tool to develop some functional materials. In this presentation the following topics on fractal materials will be given.

1) Super water- and oil-repellent fractal surfaces

A super water-repellent surface has been obtained by utilizing the very large surface area of the fractal structure. Fig.1 (a) shows a water droplet on a super water-repellent fractal surface made of alkylketene dimer (AKD; a kind of wax). The contact angle of this droplet is 174°. However, the contact angle of water on a flat surface of the same material is 109° as shown in Fig.1 (b). One can see the great effect of the surface roughness of fractal structure.

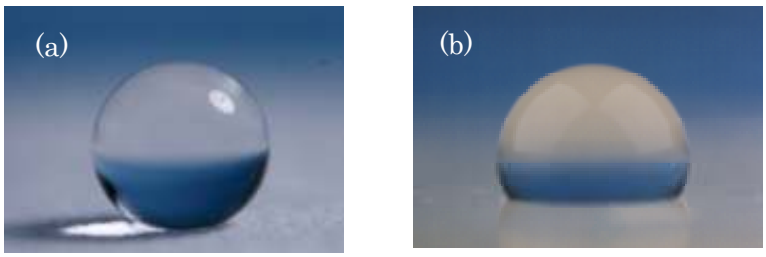

Fig.1 A water droplet on a super water-repellent AKD surface (a) and on a flat one (b).

Even super oil-repellent surfaces can be synthesized by making the surface fractal. A droplet of rape seed oil shows the contact angle of 150°, and rolls around without attachment on this super oil-repellent surface. Durable super water- and oil-repellent surfaces have been also made.

2) Creation of a fractal body

A fractal body having a smaller fractal dimension than 3 ($2 < D < 3$) should be the material of zero volume and infinitely large surface area (in pure mathematical sense).We have recently succeeded in making a fractal body utilizing the fine particles of AKD with fractal surface structure as templates. The densely packed fractal AKD particles were molded with a tetramethylorthosilicate solution, and the solution was solidified by sol-gel reaction followed by calcinations process. The cross-sectional fractal dimension of the fractal body was determined to be 1.87 ± 0.03 in ca. three decades of pore size distribution and volume fraction was 0.15. This unique novel material may hopefully show some unique functional properties in future.

tsujik@es.hokudai.ac.jp or tsujik@gc4.so-net.ne.jp

4A08

Antifouling surfaces obtained by adsorption of complex coacervate core micelles

Arie de Keizer*

Lab. of Physical Chemistry and Colloid Science, Wageningen University,

Dreijenplein 6, 6703 HB Wageningen, The Netherlands

Adsorption of proteins or adhesion of bacteria is strongly suppressed by coating surfaces with a brush layer of neutral water soluble polymers. Usually polymer brushes are prepared by grafting the neutral polymer covalently to the surface or by adsorption of a block copolymer with a water soluble block and an adsorbing block. A new method is to create a brush layer by adsorption of complex coacervate core micelles (C3M's) onto the surface.

C3M's are polymeric micelles formed upon mixing a polyelectrolyte and a block copolymer with an oppositely charged polyelectrolyte block and a water soluble neutral block due to co-assembly driven by electrostatic attraction. The micellar core consists of a complex coacervate of the oppositely charged polyelectrolytes and the corona consists of a layer of neutral water soluble brushes. The radius of the micelles is typically 20 and 30 nm whereas the aggregation number typically ranges between 10 and 100. At a critical ionic strength (between 0.1. and 2 M depending on the system) the micelles fall apart due to the decrease of the Coulombic attraction between the oppositely charged blocks. Two types of brushes were studied: polyethylene oxide and polyacrylamide.

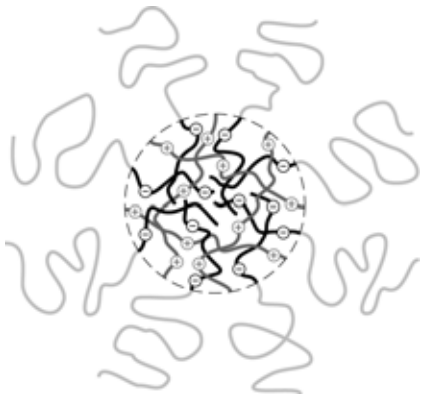

Fig. 1 Complex coacervate core micel

Adsorption of C3M's has been studied on hydrophilic (silica) as well as hydrophobic surfaces (polystyrene, cross-linked 1,2-polybutadiene). The formation of the C3M layer has been observed in situ by fixed angle optical reflectometry with a stagnation point flow cell on model surfaces (silicon wafer with a spin-coated organic layer or a silica layer formed by oxidation). It is interesting that the C3M's readily adsorb on all kinds of surfaces, independent of charge or wettability, although the structure of the C3M layer may be different.

Protein resistance has been studied for four proteins: lysozyme, bovine serum albumin, β-lactoglobulin, and fibrinogen. Protein adsorption is strongly reduced, but the reduction depends on the kind of protein and the nature of the C3M's. An advantage of C3M brush layers is that they can be formed in a reversible process, enabling surface regeneration after longer periods. Preliminary experiments of bacterial adhesion to some surfaces have also been carried out. C3M's can be potentially used in several antifouling applications, but our focus is mainly on nano- and ultrafiltration membranes used for drinking water preparation.

*arie.dekeizer@wur.nl

4A09

Sugar-Based Gemini Surfactants

Kenichi Sakai

Department of Pure and Applied Chemistry, Faculty of Science and Technology,
Tokyo University of Science, 2641 Yamazaki, Noda, Chiba 278-8510, JAPAN

Gemini surfactants, consisting of two monomeric surfactants linked with a spacer, have been synthesized with a view to developing 'next-generation' high-quality surfactants. When compared with a conventional monomeric surfactant, the corresponding gemini surfactants generally present e.g. (i) a significantly lower critical micelle concentration (cmc), (ii) a lower surface tension recorded at the cmc and (iii) a greater ability in increasing viscosity of the diluted aqueous solution. Indeed, a structural transformation from spherical micelles to vesicles is observed even in a diluted aqueous solution of gemini surfactants. Although the synthetic process of gemini surfactants is generally more complicated than that of monomeric ones (and thereby, the synthetic costs are still problematic), these physicochemical properties of gemini surfactants may reduce the total consumption of substances in chemical products. Therefore, gemini surfactants themselves are deemed to be an environment-friendly material.

From the standpoint of human health and ecology, sugar-based nonionic surfactants are also an important and possible alternative over conventional surfactants. With a combination of these concepts, we recently developed novel sugar-based gemini surfactants and studied the physico-chemical properties in aqueous media. As expected, the surface tension measured at the cmc is observed to be significantly lower than that of the corresponding monomeric surfactants. This suggests that the gemini surfactants are able to form a closely packed monolayer film at the air/aqueous solution interface. This finding should be useful in developing high quality surfactants in a field of detergents and other consumer products. Indeed, the cryogenic electron microscopy clearly confirms the formation of worm-like micelles.

The adsorption of sugar-based monomeric and gemini surfactants at the silica/aqueous solution interface has also been characterized. The resultant soft-contact atomic force microscopy data suggest that the structural transformation of the adsorbed layer occurs with an increase in the surfactant concentration. At the concentration above the cmc, the monomeric surfactants form either worm-like surface micelles or a patchy bilayer whereas the gemini surfactants only form a patchy bilayer. It is now required to study the adsorption at solid/aqueous solution interfaces with a view to developing fabrication of environmental surface coatings, which is also important in cosmetics and hair care applications.

E-mail: k-sakai@rs.noda.tus.ac.jp

4A11

High-rate Ion-transportable Nanoporous Carbons as a High Performance Electric Double-layer Capacitor Material

I. Moriguchi,* H. Yamada

Department of Applied Chemistry, Faculty of Engineering, Nagasaki University, 1-14 Bunkyo-machi, Nagasaki 852-85210

Porous carbons are important materials for adsorbents, catalysts, electrode materials, and so on. Although there are many porous carbons such as activated carbons, the development of template synthesis in the field of carbon materials is significant from the viewpoint of yielding a porous carbon with a specific pore size range because the conventional carbons possess broad pore size distributions from micropore to macropore range. Recently, there has been intensive interest in a development of electric and electrochemical energy storage devices. The nanoporous carbon materials with appropriate pore size range are also useful for high performance energy storage devices such as electric double-layer capacitors (EDLCs) and Li-ion secondary batteries. In case of EDLCs, the specific electric double-layer capacitance is theoretically proportional to the specific surface area, but the proportionality is not always observed because micropores developed in the high surface area carbons such as activated carbons cannot be accessible easily to electrolyte. Optimization of nanoporous structure so as to enable electrolyte ions to transport smoothly is necessary for developing a high performance EDLC electrode.

Here we will focus on a fabrication of nanoporous carbons via some template processes using a silica opal and an organic-inorganic hybrid source. The correlation between the nanoporous structure and EDLC property will be discussed. As a representative example, Figure 1 shows rate-dependent electric double-layer capacitances of porous carbons in *aq*. H_2SO_4. The high specific capacity above 150 F g^{-1} was maintained upto the high rate of 100 mV s^{-1} for a porous carbon with 16 nm mesopores (Carbon A), while a mesoporous carbon with a pore size of 2-4 nm (Carbon B) showed a low capacitance and a steep decrease in the capacity with increasing the rate irrespective to higher specific surface area. This means that the electrolyte resistance in pores becomes larger in smaller mesopores, and the resistance increases with increasing the charge-discharge rate.

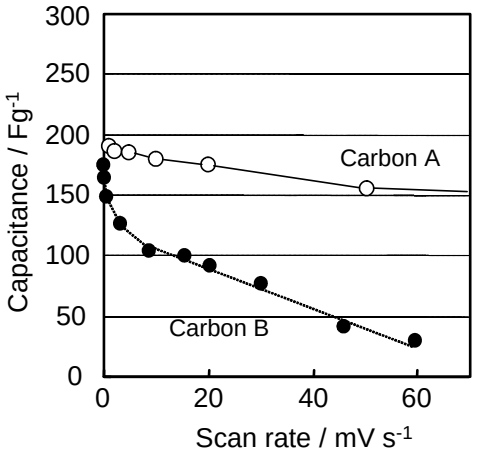

Figure 1. Scan rate-dependent electric double layer capacitances of porous carbons in 2 M *aq*. H_2SO_4. The pore size and specific surface area of these carbons are 16 nm and 1358 m^2g^{-1} for Carbon A and 2-4 nm and 1540 m^2g^{-1} for Carbon B, respectively.

*mrgch@nagasaki-u.ac.jp

4A12

Controlling Solute Transport Process in Soils using Dual-Characteristics of Soil Pore System.

Y. Mori[1]* , N. Higashi[2]

[1] *Faculty of Life and Environmental. Science, Shimane University, 1060 Nishikawatsu, Matue, 690-8504,Japan.*

[2] *Research Institute of Kyushu University Forest, Kyusyu University, 394 Tsubakuro, Sasaguri, Fukuoka, 811-2415, Japan.*

Soils were notorious of its heterogeneity and macropores conduct the solution by bypassing the surrounding soils and sometimes waste the fertilizer or remediation medicines. It would be beneficial in agriculture or environmental engineering field, if solute transport in soils were controlled with relatively simple techniques. In this study, solute transport process was controlled using dual-characteristics of soil pore system, namely convection/dispersion were controlled by changing the structure-dependent flow regime. Undisturbed soil samples and soil samples with/without artificial small macropores (diameter=1mm) were prepared and solute transport experiments (Fig.1) were conducted where variety of break through curves (BTC) was obtained by changing flow rate (from 1 to 0.1 of saturated conductivity) and saturation (saturation to –30cmH_2O). The results for undisturbed soil showed that BTC has gradually changed from bi-modal distribution to normal distribution with the suction changes from saturation to only –30cm. The results for artificial macropore system showed that totally different BTCs were obtained with small suction differences, namely saturation and –30cm (Fig.2). At saturation, BTC showed bi-modal distribution which is typical for soils with macropores. At slight unsaturated condition of –30cmH_2O, however, BTC showed normal distribution which is quite similar to repacked soil column. These results suggest that effective use of fertilizer or remediation medicines were possible with relatively simple and inexpensive technique, even there was macropores.

* yasushim@life.shimane-u.ac.jp

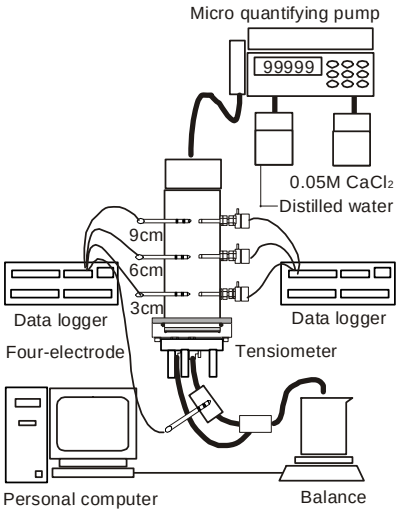

Fig.1 Experimental Setup

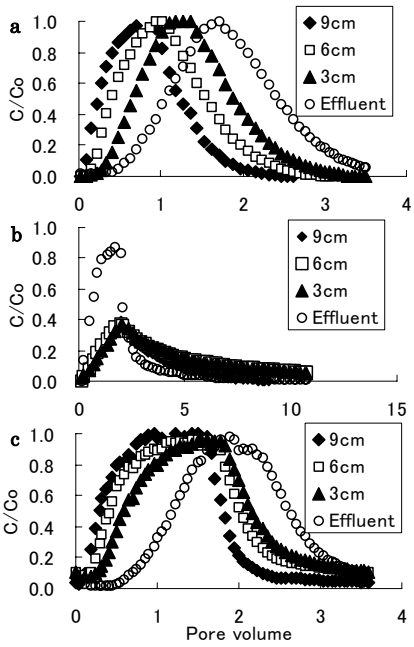

Fig. 2. Breakthrough curve for soils: a. repacked saturated soil; b. saturated soil, cylindrical macropore inside; and c. unsaturated soil, cylindrical macropore inside.

4A13

Diffusion in nanometer-sized pores studied by single microparticle injection and absorption microspectroscopy

K. Nakatani

Department of Chemistry, Graduate School of Pure and Applied Sciences, University of Tsukuba, 1-1-1 Tennoudai, Tsukuba, Ibaraki 305-8571

Mass transfer processes of a solute in a porous microparticle such as separation materials and soils are governed by external mass transfer between the microparticle and the surrounding solution, diffusion in the pores of the microparticle, adsorption at the pore walls, and so forth. We developed microcapillary manipulation and absorption microspectroscopy technique [1]. Using the technique, mass transfer rates of a solute between a single porous microparticle and solution could be directly observed and the intraparticle diffusion was kinetically analyzed. In this study, the diffusion in nanometer-sized pores of microparticles is discussed in terms of pore and surface diffusion.

A single porous microparticle with particle diameter of 20~150 μm was injected into a solution using microcapillary manipulation and a sorption or release rate for the single microparticle was measured by absorption microspectroscopy (Fig. 1). External mass transfer is efficient because of steady-state spherical diffusion in a single microparticle system, and adsorption/desorption rates are generally fast. Therefore, the mass transfer rate can be frequently analyzed as intraparticle diffusion. For phenol blue (PB) in octadecylsilyl (ODS)-silica gel (pore diameter (d_p) = 12 nm) and rhodamine 6G in silica gel (d_p = 3~30 nm), the observed diffusion coefficient (D_o) of the solute in the single microparticle was directly proportional to 1/(1+R) (R, distribution ratio of the solute between the microparticle and solution), indicating that D_o can be analyzed on the basis of the pore and surface diffusion model and the rate-determining step is the pore diffusion (diffusion in a solution phase of pores) [2,3]. For PB in a dibutyrylchitin microsphere, on the other hand, D_o was independent of R, suggesting that the diffusion is limited by the surface diffusion (diffusion along the surface of the pore walls) [4]. We consider that the single microparticle measurement technique can be sufficiently applied to mechanistic analyses of mass transfer processes in porous microparticle systems.

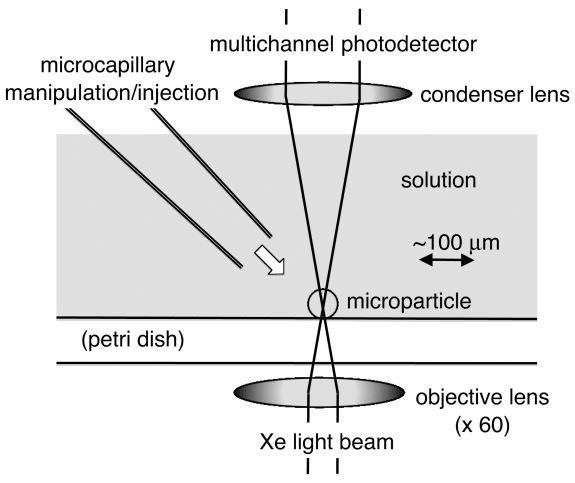

Fig. 1. Microcapillary manipulation-absorption microspectroscopy technique

[1] K. Nakatani and T. Sekine, *Langmuir*, 16, 9256 (2000). [2] K. Nakatani and H. Kakizaki, *Anal. Sci.*, 19, 1211 (2003). [3] T. Sekine and K. Nakatani, *Chem. Lett.*, 600 (2004). [4] K. Nakatani, Y. Kobayashi and A. Haga, *Anal. Sci.*, in press.

nakatani@chem.tsukuba.ac.jp

4A14

Adsorption of phenoxyacetates on colloids of a humus-rich Andosol

S. Hiradate*, H. Murano, A. Furubayashi, T. Otani
National Institute for Agro-Environmental Sciences (NIAES),
3-1-3 Kan-nondai, Tsukuba, Ibaraki 305-8604, Japan

Two phenoxyacetates having herbicidal activity, 2-(2,4-Dichloro-3-methylphenoxy)propanoic acid (DMPA) and 2,4-dichlorophenoxyacetic acid (2,4-D), were subjected to investigate the adsorption mechanisms on the surface horizon of a humus-rich Andosol. The soil sample was chemically treated to sequentially remove soil organic matter (SOM), active metal oxides, and free metal oxides, and the amount of phenoxyacetates adsorbed was compared at equilibrium pH range of 4 to 7. The amount of phenoxyacetates adsorbed increased by the removal of SOM and decreased by the removal of active and free metal oxides, suggesting that SOM was not the major adsorbent but active and free metal oxides were the important soil components on phenoxyacetate adsorption in the Andosol. The amount of phenoxyacetates adsorbed increased with decreasing equilibrium pH value. Therefore, it was concluded that the predominant mechanism of phenoxyacetate adsorption on the Andosol is a ligand exchange reaction, in which an active surface hydroxyl group on Al and/or Fe oxides is replaced by a carboxylic group of phenoxyacetates. Although a humic acid purified from the Andosol did not adsorb phenoxyacetates, the presence of the humic acid increased phenoxyacetate adsorption on Al and Fe by inhibiting the hydrolysis and polymerization of Al and Fe, resulting in the preservation of available adsorption sites on these metals. Therefore, metals complexed with SOM could be the major phenoxyacetate adsorbent in the humus-rich Andosol (Fig. 1).

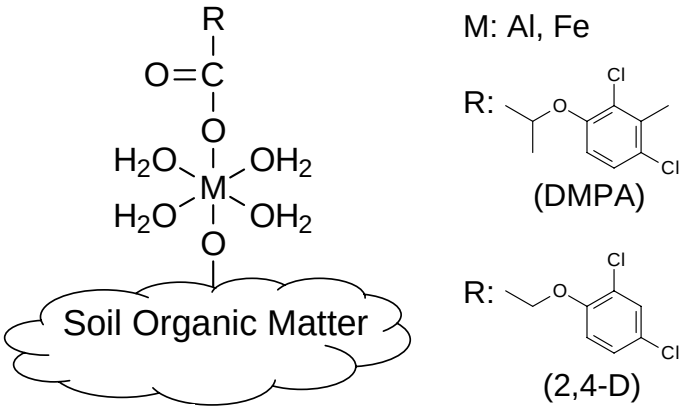

Fig. 1. A schematic representation of phenoxyacetate adsorption on a humus-rich Andosol. A metal complexed with soil organic matter adsorbs phenoxyacetates by forming a strong coordination bond between the metal and a carboxylic group on phenoxyacetates (a ligand exchange reaction between active surface hydroxyl on metal and carboxylic group on phenoxyacetates).

References:
Hiradate *et al., J. Environ. Qual.*, **36**, 101-109 (2007).
Murano *et al., J. Agric. Food Chem.*, **56**, 1350-1357 (2008).

*hiradate@affrc.go.jp

4A15

Interaction of a small molecule with polyisoprene surface studied by molecular simulations

M. Fukuda

Material Science Laboratory, Hyogo University of Teacher Education,

942-1 Shimokume, Kato, Hyogo 673-1494

The interaction of a small molecule on a polymer melt surface has been studied by molecular simulations. The melt surface structure of *cis*-1,4-polyisoprene (*cis*-PI) was constructed using a molecular dynamics simulation. The system contained 20 polymer chains and a total of 30,000 carbon atoms. The excess chemical potential and enthalpy terms (average interaction energy between the gas molecule and the polymer) were obtained for a methane molecule using a test-particle-insertion method with excluded volume map sampling as a function of the position from the inside to the surface. The thickness of the *cis*-PI surface estimated by the density change was 1.3 nm at 373 K. The excess chemical potential of CH_4 showed minimum and a negative value only at the surface just beyond the position with half of the inside density. These results showed the intrinsic properties of the polymer surface which accommodates gas molecules due to adsorption. The thermodynamics based on the interaction between a small molecule and polymer melt surface were totally understood by the present simulations.

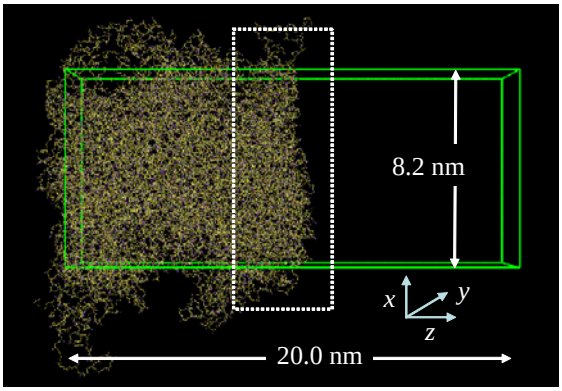

Fig 1. A snapshot of melt *cis*-PI membrane at 373 K. The cell-edge lengths of the *x*, *y*, and *z*-axes are 8.17 nm, 8.22 nm, and 20.0 nm, respectively. The white dotted box (from *z*=8.0 nm to 12 nm) indicates the area in which thermodynamic analyses in this study were carried out

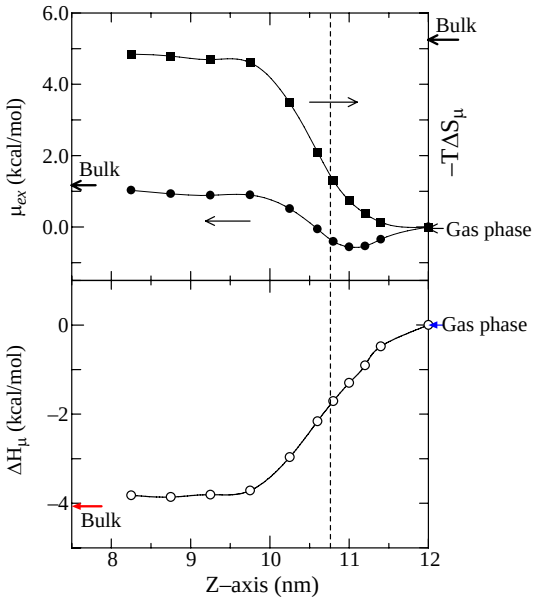

Fig 2. The profiles of three thermodynamic parameters for CH_4 on the surface of *cis*-PI membrane at 373 K. The values obtained independently by the bulk *cis*-PI are also indicated by the thick arrows.

*mifukuda@hyogo-u.ac.jp

4A16

Dynamic metal sorption by charged polysaccharides

Elise Rotureau[1*], Jérôme Duval[2], Herman P. van Leeuwen[1]

[1] *Laboratory of Physical Chemistry and Colloid Science, Wageningen University, The Netherlands*

[2] *Laboratoire Environnement et Mineralurgie, Nancy Université, France*

The general framework of this project is to understand the dynamic metal speciation in colloidal dispersion by taking into consideration the particles nature and permeability. In this study, we examine more particularly the properties of complexation of a permeable gel-like polysaccharide so called "soft particle". This colloidal ligand studied is a functionalised carboxymethyldextran (CMD) which has been previously characterised in terms of its electrostatic, hydrodynamic and conformational properties as function of pH and ionic strength. The investigation of dynamic aspects is performed by means of the electrochemical technique of stripping chronopotentiometry (SCP). The measured response (or characteristic time, τ^*) reflects the flux properties (limiting diffusive or kinetic fluxes) of metallic species towards a macroelectrode and allows the determination of their stability constants and lability features in aqueous solution. This study reveals a time-dependence of the metal ion complexation that was not observed in the case of hard-particle complexing agents as carboxylated latex nanospheres. The decrease of the SCP signal with time after addition of the ligand to the metal solution identifies strong differences in the dynamic nature (lability) of the successive metal complexes formed. Apparently, the formation of 1:2 complexes requires a slow conformational reorganisation of the macromolecule that probably becomes the limiting step in the multidentate complexation reaction. Metal release experiments have revealed also the capacity of the polyelectrolyte to immobilize metal ions at long time range. The mechanisms underlying metal-colloid interactions will greatly improve our understanding of the impact of dynamic speciation and bioavailability of metal ions on the fate in natural waters.

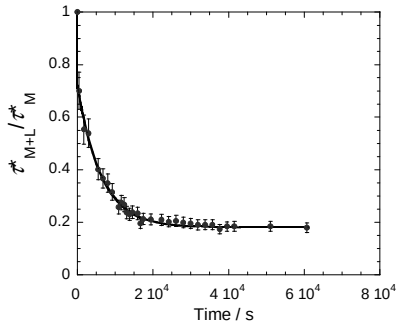

Normalized characteristic time as the function of time in case of the complexation between CMD and Pb at pH= 6 and I =100 mM

* elise.rotureau@wur.nl

4A17

Fouling monitoring during Microfitration of surface water and humic acid suspension by streaming potential measurement

Kazuho Nakamura[1]*, Shohei Fukada[2] and Kanji Matsumoto[1]
[1]*Dept. of Chemical Engineering, Yokohama National University,*
79-5 Tokiwadai Hodogaya-ku, Yokohama, Kanagawa 240-8501
[2]*JFE Engineering*

The fouling properties of PVDF hollow fiber Microfilration membrane during the filtration of surface water(Doshi river, Nishiya water plant, Yokohama) or model suspension(Kaolin and Humic acid) were studied with the dead-end filtration equipment with backwashing and streaming potential measurement systems. The change in fouling status during the filtration was monitored by the filtration resistance R_f , the filtration resistance at the backwashing R_b, and streaming potential. By comparing R_f with R_b the fouling resistance could be classified into the internal fouling, which means the standard blocking, and the external fouling, which means the cake formation, and in the filtration of both the surface water and the model suspension it was shown that the fouling was the internal fouling in the early stage of filtration followed by the external fouling. The zeta potential, which was estimated by the streaming potential measurement, was changed during filtration depending on the change in the fouling status. Fig.1 shows the change in the filtration resistance and zeta potential during the filtration of the model suspension(Kaolin 100mg/L and Humic acid 5mg/L).

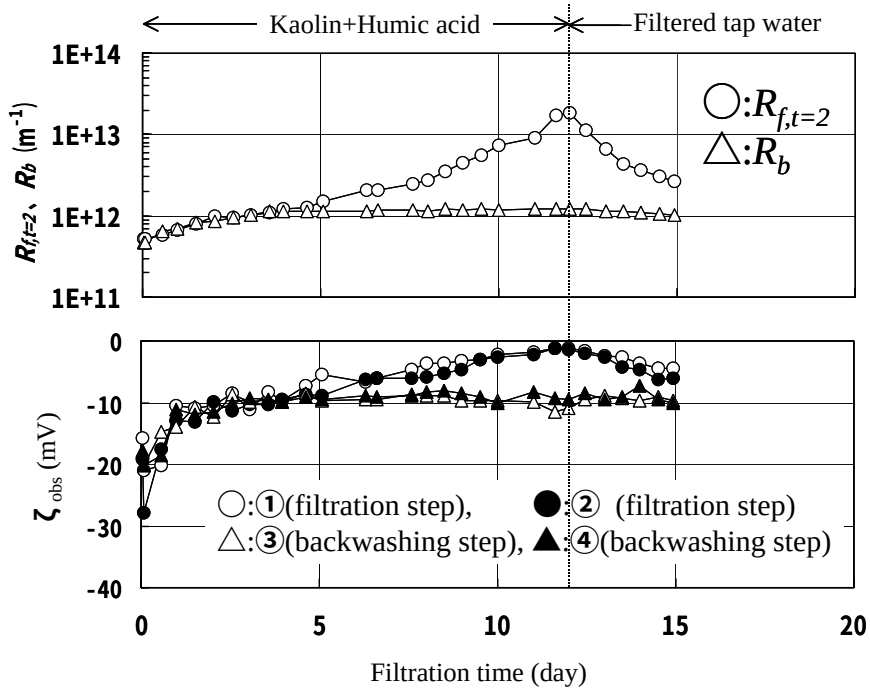

Fig. 1 Change in the filtration resistance and zeta potential during the filtration of the model suspension(Kaolin 100mg/L and Humic acid 5mg/L).

* naka1@ynu.ac.jp

4B11

Studies on matrix diffusion of colloid in a fractured medium

M. Takahashi*[1], D. Kawasaki[1], T. Saito[1], I. Shimizu,[2] S. Nagasaki[1], S. Tanaka[1]

[1]*Graduate School of Engineering, The University of Tokyo, 7-3-1, Hongo, Bunkyo-ku, Tokyo 113-8656*

[2]*Institute of Earth and Planetary Science, The University of Tokyo, 7-3-1, Hongo, Tokyo 113-0033*

Mineral and organic colloids present in geological environments can influence radionuclide transport. Colloid transport is different from solute transport because of its particle size and high surface charge density. It is generally assumed that the sizes of the colloid particles are larger than the pore sizes of the rock matrix and colloid particles cannot diffuse into the matrix. However, our preliminary measurement of the pore size distributions of *Makabe* granite indicated the presence of greater pores, into which typical natural colloids may diffuse. The objective of this study is to investigate the possibility of the matrix diffusion of colloids into rock matrix.

Granite blocks, immersed in fluorescent latex particle dispersions (0.028 μm and 0.10 μm in diameter) at pH 10 and the ionic strength of 0.01 M, were observed by confocal laser scanning microscopy (CLSM). By scanning the focal point, the depth profile of fluorescence intensity of the latex particles can be observed (Fig. 1). It was observed in Fig. 1(b) that the latex particles had diffused into the pores of the matrix.

Under different conditions of ionic strength and flow velocity, latex particle dispersions were injected into a flow channel created with the granite. The breakthrough curves of the latex in the channel were obtained (Fig. 2). At a flow velocity of 8.3×10^{-5} m/sec, the concentration (C) at the plateau of the breakthrough curve was lower than the concentration of injected latex particles (C_0), suggesting the diffusion of the latex into matrix. Compared with model calculation results, this result also implies the possibility of latex particles being captured in the pores of the matrix.

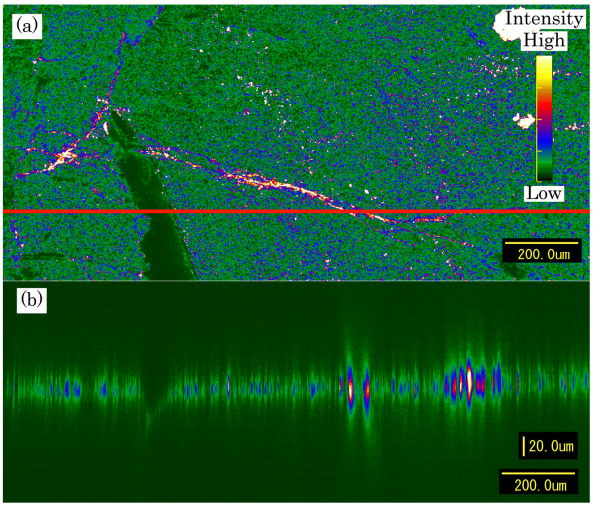

Fig. 1 Fluorescence images of granite immersed in latex dispersion; (a) surface and (b) depth profiles.

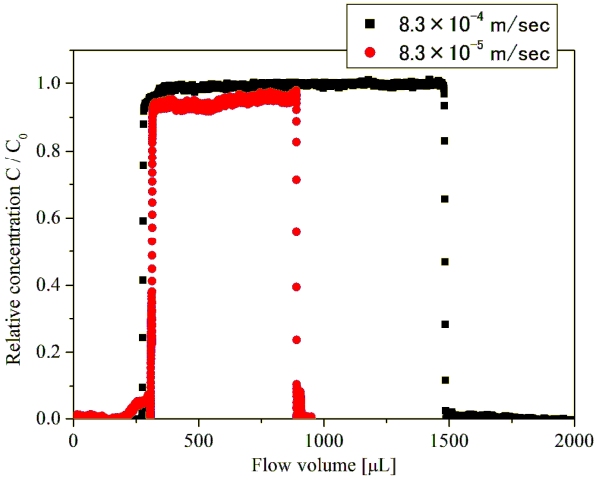

Fig. 2 The breakthrough curves of the latex particles at two flow velocities.

*takahashi@flanker.q.t.u-tokyo.ac.jp

4B12

Physical speciation of mobile trace elements by natural colloids

P. Le Coustumer[1]*, B. Eloifi[1], F. Huneau[1], F.v.d. Kammer[2] **&** M. Baalousha[3]

[1] *Earth & Sea UFR, Bordeaux1 University, B.18 Av. Facultés, 33405 Talence*

[2] *Nanogeosciences Division, Vienna, Althanstrasse 14, A-1090 Wien, Austria*

[3] *Department of Environmental Health, University of Birmingham, Birmingham, B15 2TT, United Kingdom*

Recent developments allow the scientific community to study natural colloids such humic acids and their interactions with mobile trace elements (MTE). Our approach is based on dynamic fractionation of colloids. Our analytical set is composed of an asymmetrical flow-field flow fractionation (AsFlFFF) coupled with UV-FLD light detectors, MALLS detector and ICPMS which allow us to study the metal content in separate colloid size fractions from the nm up to µm with a sub ppm sensitivity. About one ml is collected on a copper grid for HRTEM/X-EDS analysis. Several samples issued from two French major rivers (l'Adour et la Loire) has been analyzed. Our results put in evidence that MTE are carried and trapped selectively by different fractions. There is a clear evidence about the affinity of MTE with the size and the morphology of the sample. For example the couple Fe-Mn is a primary sorbents to trap some MTE, especially when they are in colloidal form. We propose to introduce the concept of physical speciation to understand complex mechanisms operating at the solid/water interface of natural systems.

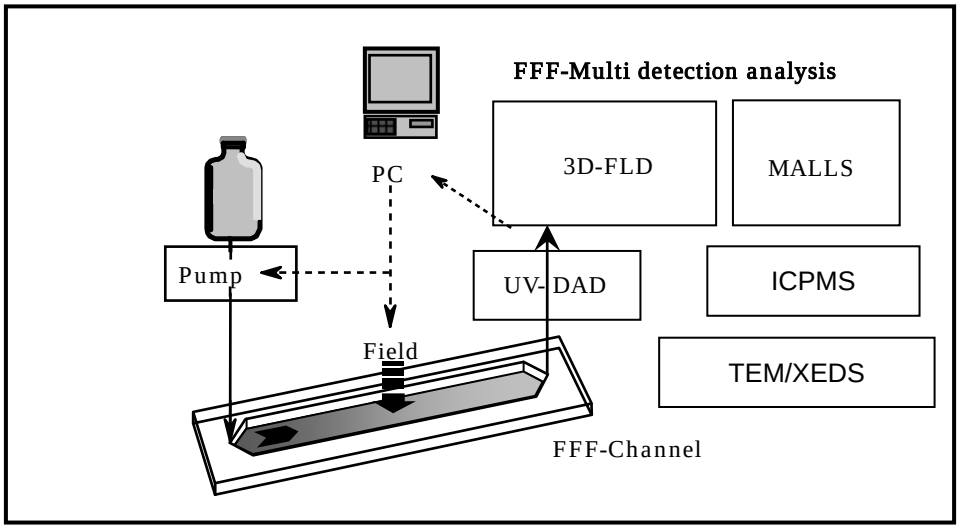

. Fig.1 Analytical set used .

* plc@lnet.fr

4B13

Transport und deposition of *Pseudomonas fluorescens* in porous media: Role of the cell concentration and morphology

E. Klumpp*
Agrosphere Institute, Research Centre Juelich,
52425 Juelich, Germany

A study was conducted to understand the role of cell concentration and morphology in the transport and deposition behaviour of *Pseudomonas fluorescens* with and without substrate addition. Therefore a series of column experiments with cell concentrations from 10^7 to 10^9 cells /mL was performed in quartz sand packing under saturated conditions at flow velocities 0.07 and 0.14 cm/min, respectively. For comparison experiments with microspheres were also conducted. The effluent concentrations and the retained particle concentrations were determined by fluorescent microscopy. For the transport of *Pseudomonas fluorescens* without substrate addition two consecutive breakthrough curves were detected at various input concentrations and both flow velocities which was attributed to the different breakthrough behaviour of rod and coccoid shaped cells of *Pseudomonas fluorescens*. Furthermore, a lower input concentration of *Pseudomonas fluorescens* tended to a lower relative effluent concentration. Generally, the spatial distribution of retained colloids in the column revealed a non exponential retention profile. Transport experiments with substrate addition and lower input concentration tended to a higher relative effluent concentration. In general, the substrate addition led to more bacteria being retained in column and the percentage of rod- and coccoid shaped bacteria in the retention profile significantly changed depending on the input concentration.

*e.klumpp@fz-juelich.de

4B14

Development of Two-Region, Three-Site Model for Bacterial Transport in Saturated Porous Media

Y. Shimojo[1]*, Y. Inoue[2] and A. Katayama[2]
[1]*Department of Civil Engineering, Nagoya University, Furo-cho, Chikusa-ku, Nagoya 464-8603, Japan*
[2]*EcoTopia Science Institute, Nagoya University, Furo-cho, Chikusa-ku, Nagoya 464-8603, Japan*

Many researchers have proposed various types of bacterial transport models. We have applied Two-region bacterial transport model that considered the first-order kinetic attachment of bacteria to a solid-phase; however, it could not reproduce the retarded transport observed in the early stage of breakthrough curve. In this study, a novel Two-Region, Three-Site model, assuming that a linear equilibrium attachment and a first-order kinetic attachment of bacteria to solid-phase occur simultaneously on the different sites, was developed. The model was verified by applying to the results of one-dimensional column experiments with variable parameters of flow rate, average particle size of porous media and surface hydrophobicity of bacteria. For the model verification, four bacterial species (*Escherichia coli* K12, *Pseudomonas putida* NBRC16141, *Rhodococcus rhodochrous* NBRC16069 and *Sphingomonas paucimobilis* EPA505) with different surface hydrophobicity were used for column experiments. The results showed that the simulation had a good agreement with the experimental data under almost all the experimental conditions. On the other hand, at the later stage of breakthrough curve in some cases, a disagreement was found when the bacterial concentration began to decrease with time. It was considered that this phenomenon occurred when the bacteria in the liquid-phase attached with the bacteria which had been already attached on the solid surface. In the Two-Region, Three-Site model, it was assumed that porous media were a clean bed condition and the attachment and detachment rate were constant all through the transport. It was suggested that this model should be modified to reflect the volume of bacteria attached on the solid surface into the attachment rate coefficient.

*inoue@esi.nagoya-u.ac.jp

4B15

A New Paradigm for Colloid and Colloid-Facilitated Transport and Retention in Porous Media

Scott A. Bradford[1]*, Saeed Torkzaban[2], Feike Leij[2], Nobuo Toride[3], Jiri Simunek[2], and Martinus Th. van Genuchten[1]

[1]*USDA, ARS, US Salinity Laboratory, Riverside, CA*

[2]*Department of Environmental Science, University of California Riverside, CA*

[3]*Faculty of Bioresources, Mie University, Japan*

Colloid and colloid-facilitated transport in porous media has traditionally been assumed to be controlled by chemical interactions between the colloids and the solid-water and air-water interfaces. The influence of pore space geometry, interface configuration, and system hydrodynamics in classical colloid retention models has largely been neglected. Recent experimental and theoretical work, however, has demonstrated that these factors can also play important roles in colloid retention under unfavorable attachment conditions. In particular, hydrodynamic forces can funnel weakly associated colloids to grain-grain contacts and air-water-solid triple points, as well as to hydrodynamically isolated low velocity (eddy) regions. The extent to which colloid mass transfer and retention will occur to/in these locations is a function of the balance of adhesive, diffusion, and hydrodynamic forces. One consequence of enhanced colloid retention in low velocity regions is that the colloid retention profile may not be exponential with depth. Pore- and column-scale experimental evidence that support this conceptual model for colloid retention is summarized. Furthermore, colloid and colloid-facilitated transport models that account for enhanced colloid retention in low velocity regions are demonstrated and discussed.

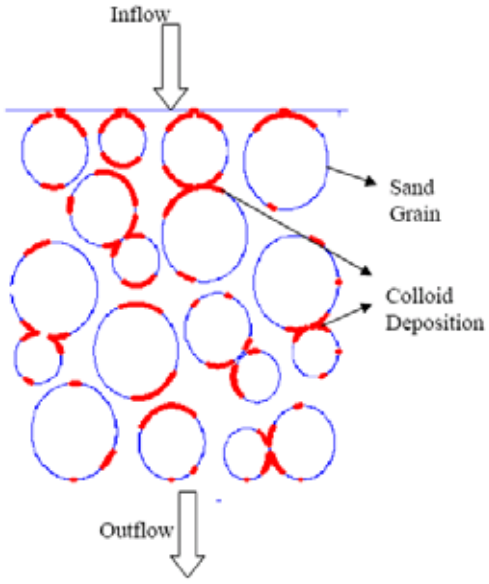

*sbradford@ussl.ars.usda.gov

4B16

A CTRW Approach to Column Adsorption Tests

Y. Kamio, K. Tabata, and Y. Hatano*
Graduate School of Systems and Information Engineering,
University of Tsukuba,
1-1-1 Tennodai, Tsukuba, Ibaraki 305-8573

Solute transport in geologic media is important for the environmental risk assessment. Both in the field tests and in the lab-scale tests, the concentration profiles of solute show a significant difference from the solutions of the advection-dispersion equation (ADE) as shown in Fig.1. We propose a new model, the Continuous Time Random Walk (CTRW) approach to reproduce the concentration profiles. The significance of the CTRW model is that, the model assume a very wide-range distribution of the velocities in the pores. The probability density function of the velocity is assumed to be in the form of the power-law, $\psi(v) \sim v^{\alpha}$. This function has a diverging variance and a diverging mean value when $0 < \alpha < 2$. When both the variance and the mean diverges, the concentration profiles show a very different behavior from those of ADE. The CTRW approach has begun to be accepted in the society of subsurface hydrology for recent years. However, the application of CTRW is limited to the solutes that are not adsorbed by the geologic media. Studies of adsorbing solutes are still lacking.

In the present study, we performed a series of column tests with adsorbed material. We used the solution of heavy metal and tested it with the column filled with *Toyoura* standard sand. We found that CTRW model can reproduce the concentration profiles in the cases of the adsorbing systems.

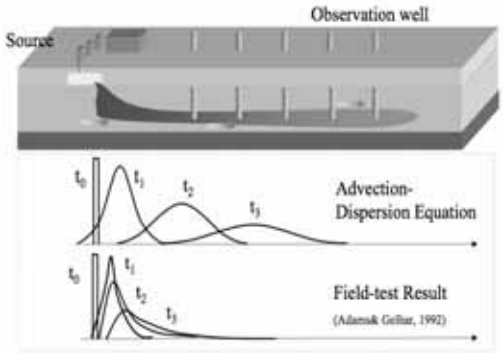

Fig. 1: Comparison between the calculated result with the Advection-Dispersion Equation (ADE) and the field observations of *Adams and Gelhar* (1992). In the field-test result, the concentration profiles have long-tails and their peaks look relatively immobile.

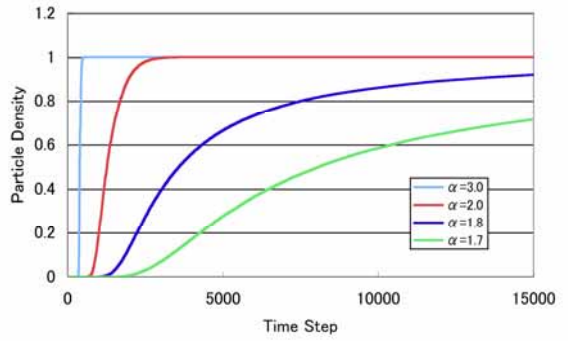

Fig. 2: Simulational results of CTRW. The time dependence of the concentration is shown. Note that the concentration profiles depend on the parameter alpha.

*hatano@risk.tsukuba.ac.jp

4B17

Quantification of heterogeneous colloid retention on the granite surface under varying chemical conditions

U. Alonso[1]*, T. Missana[1], A. Patelli[2], D. Ceccato[3], N. Albarran[1], M. García-Gutiérrez[1], T. Lopez - Torrubia[1], V. Rigato[3]

[1] *CIEMAT, Environmental Department, Avda. Complutense, 22, 28040 Madrid, Spain*

[2] *CIVEN, Via delle Industrie 9, 30175 Venezia-Marghera, Italy*

[3] *INFN, Laboratori Nazionali di Legnaro, Viale dell' Università 2, 35020 Legnaro-Padova, Italy*

The impact of colloids on the radionuclide migration in a high-level radioactive waste repository emplaced in a granite massif is still unclear, because of the mechanisms that lead to colloid retention are not very well understood nor quantified.

Colloid surface retention was studied here by contacting gold colloid suspensions to two types of granite, in order to evaluate the effects of the physical and chemical heterogeneities exhibited by the different granite minerals. The μPIXE (micro-Particle Induced X-Ray Emission) technique was used to quantify in areas of 4 mm^2 the colloid retention on the different minerals in the near surface region (several μm). The two granites showed different specific mineral porosities, being quartz minerals non-porous in one case. The effect of the colloid to mineral pore sizes on the retention was accounted for by using gold colloids of different sizes (from 2 to 100 nm). The effect of the heterogeneous electrostatic colloid /mineral interaction was evaluated by varying the pH conditions. Gold colloids are negatively charged almost over the whole pH range and at alkaline conditions the whole granite surface is also negatively charged (*unfavourable case*), but some granite minerals are positively charged at neutral-acidic conditions (*favourable case*).

μPIXE quantification of the colloid surface presence revealed higher colloid retention on preferential areas when favorable electrostatic interaction existed (Figure 1). Also in the unfavorable case colloids were retained at the surface but with a fairly homogenous distribution. However, this distribution seemed to be related to higher porosity areas or to physical defects (roughness, grain boundaries), as suggested by AFM measurements. The relevance of the main colloid retention mechanisms is discussed.

This work has been partially supported by EU within the FUNMIG project and the EURONS action and the Spanish Ministry of Education and Science under the grant CGL2005-01482/BTE (PROMICOL).

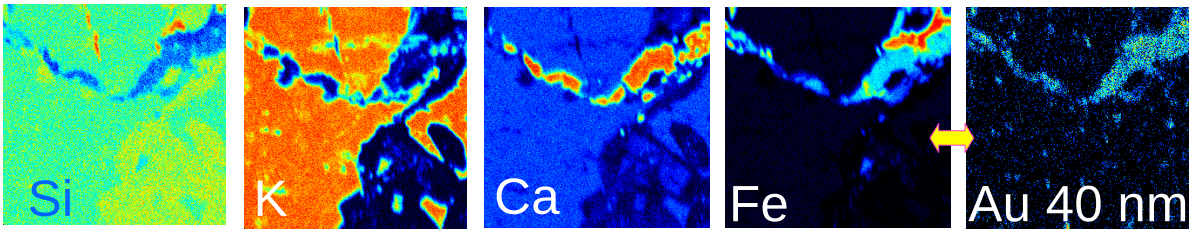

Fig. 1 μPIXE maps of a 2*2 mm^2 granite area after contact to 40 nm Au colloids at pH 5.5.

*ursula.alonso@ciemat.es

4E11

Investigation of the adsorption of cationic proteins on smectite clays

M. Szekeres[1]*, T. Körtvélyesi[2], I. Dékány[1], E. Tombácz[1], R. Schoonheydt[3]

[1]*Department of Colloid Chemistry, University of Szeged, H-6720 Szeged, Aradi vt. 1., Hungary,*

[2]*Department of Physical Chemistry, University of Szeged, H-6720 Szeged, Rerrich B. tér 1., Hungary,*

[3]*Centrum voor Oppervlaktechemie en Katalyse, Department Microbiele en Molekulaire Systemen, KU Leuven, Kasteelpark Arenberg 23, 3001 Leuven, Belgium*

Soil enzyme activity is widely investigated due to its importance in soil fertility. However, much less studies are devoted to the investigation of the colloidal behavior of the enzymes in soils. The adsorption of the enzymes on soil particle surfaces, for example, is responsible for the enhanced enzyme activity and enhanced enzyme durability in the environment. Thus, a clear understanding of the adsorption mechanism is necessary to shed light on enzyme functioning in various soil environments.

In the present paper we study several aspects of the multi-component process of the enzyme adsorption on soil surfaces. We have chosen model enzymes lysozyme (14300 Da) and papain (23305 Da) having permanent positive charges in the pH range 5 to 9, and model soil clays Na-montmorillonte and Na-saponite, which are negatively charged in the same pH-range. The model systems allowed us to study the effect of the charge density on both the enzymes and soil particles, with special attention to the effect of the relative amount of the pH-dependent charges on the edges of clay particles.

The adsorption isotherms were determined by the batch method. The smaller molecular weight lysozyme shows a high-affinity isotherm, while that of larger molecular weight papain is of Langmuir-type with well expressed linear increase in the low concentration range and a plateau at high concentrations. An electrostatic potential was measured by means of Particle Charge Detector (Mütek). Charge reversal was observed at protein surface concentrations considerably lower than the maximum adsorbed amounts found in the adsorption isotherms. To model the charge reversal, we have considered the effect of the edge charges of the clay minerals, as well. Potentiometric acid-base titrations were performed on the proteins to find their effective charge density. The experimental titrations revealed an excess free acid content of proteins, supposedly as buffers, to stabilize the commercial products. The commercial samples were purified by using ion-exchange resins: cationic and anionic in sequence. The experimentally determined effective charge vs. pH curves for the purified proteins coincided well with model titration curves. The model calculations involve Poisson-Boltzmann distribution, Monte Carlo simulation and MD calculation methods. The structure of the protein-clay complexes was investigated by means of XRD. We observed shifts in the basal plane distances of the clay minerals due to protein adsorption, revealing the formation of multilamellar intercalation complexes.

In conclusion, we present a model description of the possible mechanism of protein adsorption, taking into account the charge heterogeneity of clays and proteins, hydration effects and partial conformational freedom of the globular enzyme proteins.

* szekeres@chem.u-szeged.hu

4E12

Complexation reactions of inorganic anions on layered double hydroxide surfaces

K. Morimoto*, T. Sato, T. Yoneda
Graduate School of Engineering, Hokkaido University,
N13, N8, Kita-ku, Sapporo 060-6839, Japan

Layered double hydroxides (LDH) are well known as anionic clays since those have anion-exchange properties. Recently LDH have received considerable attention because of their extremely high anion-exchange capacities. However, in previous researches, the involved adsorption mechanisms have not yet been fully elucidated specifically surface complexation reactions.

To examine the adsorption mechanisms of anions onto LDH, this study has focused on surface complexation reactions on LDH surfaces. The environmentally important inorganic anions were used as the adsorbates in the experiments. In order to distinguish inner-sphere complexes from outer-sphere complexes of these anions, zeta potential measurements and spectroscopic analyses were performed.

Figure 1 shows the change in zeta potential as a function of the amount of anion adsorption. In the case of nitrate and chloride ions adsorption, these zeta potential remains almost constant at 30 mV. On the other hand, in the case of phosphate ions adsorption, there is a considerable decrease in zeta potential. These results indicate that nitrate and chloride ions inspired simply adsorption by an anion-exchange reaction. In contrast, phosphate ions formed inner-sphere complexes by a ligand-substitution reaction on LDH surfaces. This was also supported by infrared absorption spectrometry.

Figure 2 shows zeta potential of the anion adsorbed LDH as a function of pH. The point of zero charge (PZC) of phosphate adsorbed LDH were completely different from that of the original LDH or nitrate and chloride adsorbed LDH. The formation of inner-sphere complexes on LDH surfaces are therefore expected to change the physico-chemical properties of LDH such as long-term stability and resistance against pH change.

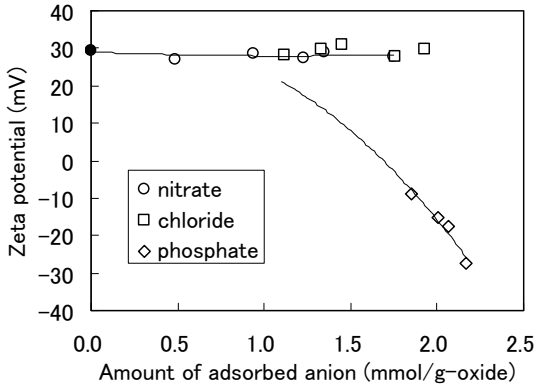

Fig. 1 Zeta potential of LDH with different anions.

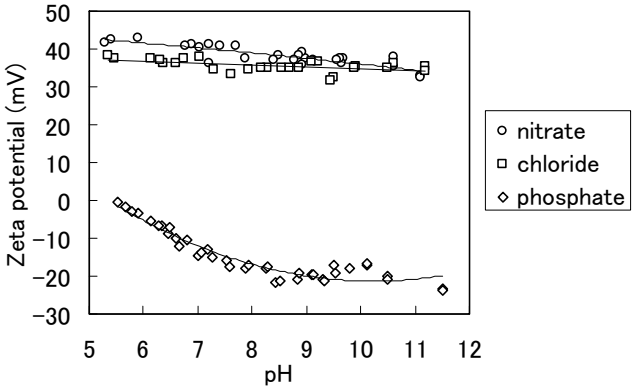

Fig. 2 Change in zeta potential of LDH with different anions as function of pH.

*morimo@eng.hokudai.ac.jp

4E13

^{137}Cs adsorption on soil clays blocked by hydroxy-Al polymers in acidic forest soils of southwestern Japan

A. Nakao[1]*, S. Funakawa[1], T. Kosaki[2]

[1]*Graduate school of Agriculture, Kyoto University, Kitashirakawa-oiwake, Sakyo-ku, Kyoto, 606-8502, Japan*

[2]*Graduate school of Environmental Science Studies, Kyoto University, Yoshida-honmachi, Sakyo-ku, Kyoto, 606-8501, Japan*

Adsorption of cesium-137 (^{137}Cs), a long-lived radionuclide ($T_{1/2}$ = 30.2 y), on soil components should be elucidated to predict its dynamics in the polluted soil ecosystems. Illitic mineral, a major micro-size 2:1 phyllosilicate in soil, has a selective adsorption site for ^{137}Cs in inner parts of the interlayers. The amount of the ^{137}Cs selective site in the illitic mineral, referred to as frayed edge site, is known to control the ^{137}Cs transfer from soil to plant. However, the ^{137}Cs adsorption on the frayed edge site may be blocked by the hydroxy-Al polymers irreversibly adsorbed in the interlayers in acidic soils with pH less than about 5.0. Before and after the artificial extraction of hydroxy-Al polymers, the amounts of ^{137}Cs adsorbed on micro-size soil particles (i.e. soil clays) separated from soils with pH(H_2O) 3.4-4.4 were measured using radiocesium interception potential (RIP) methodology to clarify the blockage effect of hydroxy-Al polymers on ^{137}Cs adsorption in acidic soils of southwestern Japan. The amounts of hydroxy-Al polymers extracted from the soil clays positively correlated with soil pH, indicating larger proportion of hydroxy-Al polymers had been released as soils are acidified. After the extraction of the hydroxy-Al polymers, the amount of ^{137}Cs adsorbed largely increased for the clays from soils with relatively high pH in the present study (4.0-4.4), whereas such increase was not observed in the clays from soils with very low pH (<4.0) (Fig. 1). Thus, the blockage effect of hydroxy-Al polymers on ^{137}Cs adsorption on frayed edge site was notable in soils with pH ranging 4.0-4.4, which was depleted in soils with very low pH (<4.0) by the release of hydroxy-Al polymers from the interlayers in southwestern Japan.

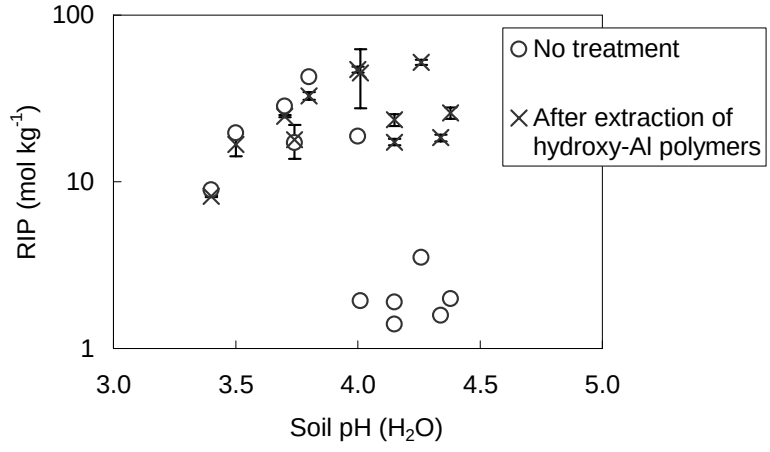

Fig. 1 Radiocesium Interception Potential (RIP) before and after the extraction of hydroxy-Al polymers from micro-size soil particles as a function of soil pH (H_2O). Bars indicate standard error (SE). Small bars are hidden behind symbols.

*na_4_ka@kais.kyoto-u.ac.jp

4E14

Surface charge heterogeneity of 1:1 and 2:1 type clay particles in aqueous suspension

Etelka Tombácz*, Márta Szekeres
Department of Colloid Chemistry, University of Szeged, Aradi Vt.1. H-6720 Szeged, Hungary

The lamellar clay particles have patch-wise surface heterogeneity. pH-dependent charges develop on the surface hydroxyls mainly at edges besides the permanent negative charges on silica basal plane due to isomorphic substitutions. Electric double layers (edl) with either constant charge density on tetrahedral faces (silica basal planes) or constant potential at constant pH on edges and octahedral faces (hydroxyl-terminated planes) form on patches. The local electrostatic field is determined by the crystal structure of clay particles, and influenced by the pH and dissolved electrolytes.

Suspensions of Na-montmorillonite and Na-kaolinite as typical examples for 2:1 and 1:1 type clay particles were investigated by means of acid-base titration, electrophoretic mobility, coagulation kinetics and rheological measurements. Oppositely charged surface parts on both types of clay particles are only below the pH~6.5 assigned to the point of zero charge (PZC) of edge sites of montmorillonite and the pH~6-6.5, considered as point of zero net proton charge (PZNPC) of kaolinite particles, therefore patch-wise charge heterogeneity exists under acidic conditions. Electrophoretic mobility measurements, however, showed negative values for both clays over the whole range of pH proving the dominance of permanent charges, and only certain decrease in absolute values, much larger for kaolinite was observed with decreasing pH below pH~6. Coagulation kinetic measurements at different pHs provided undisputable proofs for heterocoagulation of clay particles. In montmorillonite suspensions, edge-to-face heterocoagulation occurs above NaCl concentration 25-26 mmol l^{-1} at pH~4, where the hidden electric double layer of positively charged edge region has emerged, while only ~1 mmol l^{-1} NaCl can induce it in kaolinite suspensions due to the substantial difference in particle geometry. The electrolyte tolerance of both clay suspensions increased with increasing pH, pH ~6-6.5 range was sensitive, and even a sudden change occurred above pH~6 in kaolinite. There was practically no difference in the critical coagulation concentration of kaolinite and montmorillonite (c.c.c.~100 mmol l^{-1} NaCl) measured in alkaline region, where homocoagulation of negatively charged lamellae takes place. Rheological measurements showed shear thinning flow character and small thixotropy of suspensions at and above pH~6.7 proving the existence of repulsive interaction between uniformly charged particles in 0.01 M NaCl for both clays. The appearance of antithixotropy, the sudden increase in yield values, and also the formation of viscoelastic systems only at and below pH~6 verify the network formation due to attraction between oppositely charged parts of kaolinite particles. Under similar conditions the montmorillonite gels were thixotropic with significant elastic response.

References

E. Tombácz, M. Szekeres, Applied Clay Science, 27, 75-94. 2004. and 34, 105-124, 2006.

* tombacz@chem.u-szeged.hu

4E15

Arsenate Adsorption on an Fe-Ce Bimetal Oxide Adsorbent: Role of Surface Properties and Surface Complexation

Yu Zhang[1*], Xiaomin Dou[1, 2], Min Yang[1*], Hong He[1]

[1] *State Key Laboratory of Environmental Aquatic Chemistry, Research Center for Eco-Environmental Sciences, Chinese Academy of Sciences, P.O. Box 2871, Beijing 100085, China.*

[2] *College of Environmental Science & Engineering, Beijing Forestry University. No.35, Tsinghua East Road, Beijing, 100083, China.*

An Fe-Ce bimetal adsorbent (CFA) was investigated with X-ray powder diffraction (XRD), transmission electron micrograph (TEM), transmission Fourier transform infrared spectra (FTIR), X-ray photoelectron spectroscopy (XPS), EXAFS, and surface complexation model for a better understanding of the effect of surface properties and adsorption reactions on arsenate (As(V)) adsorption. In the adsorption test, CFA showed a significantly higher As(V) adsorption capacity than some other arsenate adsorbents reported recently. Combined with the results of XRD and TEM characterization, it was assumed the formation of a solid solution structure of Fe-Ce. The results of adsorption tests on CFA at different As(V) concentrations indicated that both the integral area of the As-O band at 824 cm^{-1} and the As(V) adsorption capacity increased almost linearly with the decrease of the integral area of M-OH bands at 1126 cm^{-1}, proving that the adsorption of As(V) by CFA is mainly realized through the mechanism of quantitative ligand exchange. A further EXAFS analysis of As(V) adsorbed CFA samples in combination with XPS characterization, suggested that the mainly reacted active sites were Fe-OH groups on CFA surface, and monodentate mononuclear and bidentate binuclear inner-sphere complex species coexisted on the adsorbed CFA surfaces. Adsorption envelope data fitted by 1-pk CD MUSIC with a TPM model revealed that $FeOAsO_3H^{1.5-}$ and $Fe_2O_2AsO_2^{2-}$ coexisted at the CFA surface, among which $FeOAsO_3H^{1.5-}$ was inferred to be dominant at relative low pH value, while species $Fe_2O_2AsO_2^{2-}$ was abundant at relative high pH value. With the surface loading increasing, the abundance of $FeOAsO_3H^{1.5-}$ also showed an increasing trend.

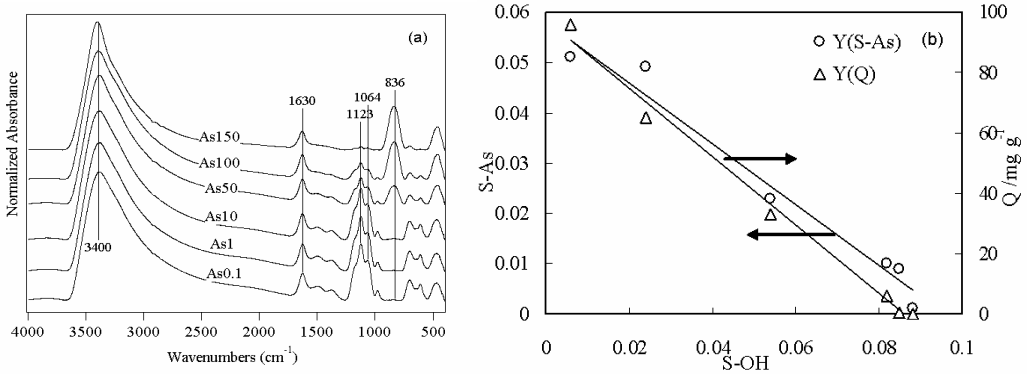

Figure 1. (a) The FTIR spectra of adsorbed species after As(V) adsorption on CFA. 0.1, 1.0, 10, 50, 100 and 150 mg L^{-1} As(V) solution (As0.1, As1, As10, As50, As100, As150), 20℃, 24h and pH 5.0; (b) Linear plots of integral area of As-O bands (S-As) and As(V) adsorption capacity (Q) vs integral area of M-OH band (S- OH) in FTIR spectra for Fe-Ce08. Linear equation for Y(S-As): Y=-0.6069X+0.0581, R^2 = 0.9697; For Y(Q): Y=-0.61132.1X+97.414, R^2 = 0.9905.

*zhangyu@rcees.ac.cn

4E16

Effect of electrolyte on adsorption/desorption of Cu^{2+} on Mn oxide

Wen-Feng Tan [1]* Fan Liu [1] Yuan-Peng Wang [1] Luuk Koopal [2]

1 College of Resources and Environment, Huazhong Agricultural University, Wuhan 430070, P.R. China

2 Laboratory of Physical Chemistry and Colloid Science, Wageningen University, Dreijenplein 6, 6703 HB Wageningen, The Netherlands

Oxides are the active and important components in soils and sediments. They are generally in fine particle and attached to surface of soil clay as a cutan or coating. Therefore, they play an important role in controlling some chemical reactions of soil interface, then will affect heavy metal's plant-availability and their transformation in soils and sediments. At the common pH in natural environment, Fe and Al oxides possess positive charge. The adsorption amount of heavy metals on Fe and Al oxides increased and their desorption percentage decreased with increasing ionic strength [1,2]. However, Mn oxide is lower point of zero charge (PZC) and negative charge in natural environment. It is unclear that the characteristics of adsorption-desorption on Mn oxides. This paper studied the influences of electrolyte (KNO_3, KCl) concentration on Cu^{2+} adsorption and desorption on synthetic birnessite. The PZC and specific surface area (SSA) of birnessite is 2.5 and 75 m^2/g, respectively. The pH of birnessite in suspended solution increased slightly with increasing electrolyte concentration, but the changed value in KCl solution is higher than that in KNO_3 solution at same concentration. The amount of Cu^{2+} absorbed on birnessite decreases gradually with the increasing ionic strength. However, the desorption percentage of Cu^{2+} absorbed on birnessite surface increases when increasing electrolyte (KNO_3, KCl) concentration. Furthermore, the desorption percentage of Cu^{2+} with KCl solution is higher than that in KNO_3 solution. These results are different from the adsorption/desorption of Fe and Al oxides.

Reference

1 Daihua Zou, Xueyuan Li, and Fenglin Xu. *Chinese Science Bulletin*. 1996, 41: 421-425.
2 Daihua Zou, Fenglin Xu, Yuanyan Dong, and Xueyuan Li. *Chinese Science Bulletin*. 1996, 41: 1483-1487.

E-mail: tanwf@mail.hzau.edu.cn

4E17

SORPTION OF BORIC ACID ON MAGNESIUM OXIDE IN PERMEABLE REACTIVE BARRIERS

K. Sasaki[1], H. Takamori[1]*, H. Yoshizaka[1], T. Hirajima[1]
[1]*Faculty of Engineering, Kyushu University,*
744 Motooka, Fukuoka 819-0395

Magnesium oxide has a high zero potential of charge in natural oxides, resulting in being favorable to remove anionic contaminants in natural waters. Magnesium oxide was effective sorbent for boric acid with the following Freundlich type of sorption isotherm:

$$\log (Q/\text{mmol kg}^{-1}) = 1.92 + 0.784 \log (C_e/\text{mmol dm}^{-3}) \quad (\text{at } 25^{\circ}\text{C})$$

Additionally magnesium oxide is well known as Louis base, easily reacts with H_2O to form magnesium hydroxide. The XRD patterns for the residues after sorption of boric acid to magnesium oxide showed that larger amounts of boric acid were sorbed, more remarkable broadening was observed at 101 plane of the crystal of $Mg(OH)_2$. The mechanism of boric acid removal is expected by not only simple sorption of $B(OH)_4^-$ to magnesium hydroxide but also formation of surface complexes such as -Mg-O-$B(OH)_3$ during the process in the formation of magnesium hydroxide from magnesium oxide. Surface complexation of boric acid with magnesium hydroxide was also investigated using X-ray photoelectron spectroscopy (XPS). Analysis of binding energies of B 1s and Mg 2p regions, revealed that there are two types of B components, probably assigned to $B(OH)_4^-$ and -Mg-O-$B(OH)_3$, and two types of Mg components, assigned to -Mg-O-$B(OH)_3$ and $Mg(OH)_2$ (Fig. 1). Performance of reactivity and permeability in the permeable reactive barrier column containing agglomerated magnesium oxide for removal of boric acid in simulated groundwaters was monitored.

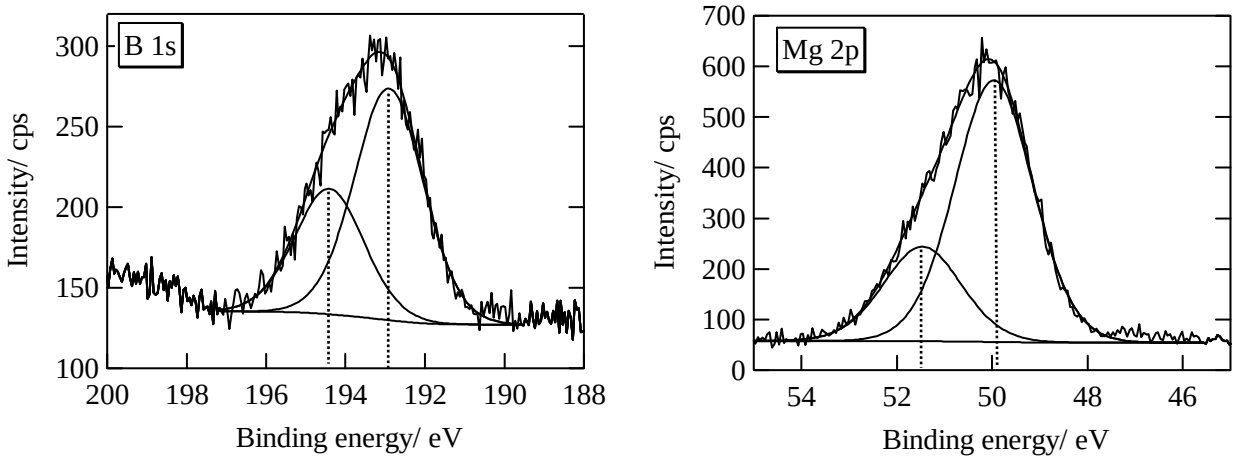

Figure 1 XP-spectrum of B 1s (left) and Mg 2p (right) for the residue after sorption equilibrium of boric acid to magnesium oxide.

*h-takamori@mine.kyushu-u.ac.jp

4F11

SORPTION AND BIODEGRADATION OF NATURAL ESTROGENS IN SEDIMENT MUD CORES

Reni Desmiarti[1]*, Fusheng Li[2], Chihiro Yoshimura[2], and Yutaka Suzuki[3]

[1]*Graduate School of Engineering, Gifu University,*
1-1 Yanagido, Gifu 501-1193, Japan
[2]*Department of Civil Engineering, Gifu University,*
1-1 Yanagido, Gifu 501-1193, Japan
[3]*Water Environment Research Group, Public Works Research Institute,*
Tsukuba, Ibaraki 305-8516, Japan

The presences of natural estrogens such as 17β-estradiol (E2), estrone (E1) and estriol (E3) in the environment and their adverse effects have been documented. We designed four sediment cores (two aerobic ones and two anaerobic ones) consisted of 30 cm of undisturbed sediment and 60 cm of overlying water collected from two sites within a natural reservoir for investigating the behavior of E2 and its byproduct E1 in the sediment cores. Besides, the effect of easily biodegradable organic substrates on the behavior of E2 and its byproduct of E1 was also assessed. The experimental results were analyzed using a mass balance model that considers the mechanisms of sorption and biodegradation. In aerobic cores, the trend of sorption of E2 onto the sediment phase decreased with increasing glucose concentrations and the biodegradation rate constants of E2 decreased. The sorption rate constant of E2 (K_d k_b) fell in the ranges of 0.0045–0.0166 h^{-1} and 0.0025–0.0046 l $gsediment^{-1}$ h^{-1}, and the biodegradation rate constant (k_{E2}) fell in the ranges of 0.249–0.352 h^{-1} and 0.181–0.215 h^{-1} for aerobic and anaerobic cores, respectively. The presence of glucose was capable of lowering the sorption rate and the biodegradation rates of E2 especially under aerobic condition.

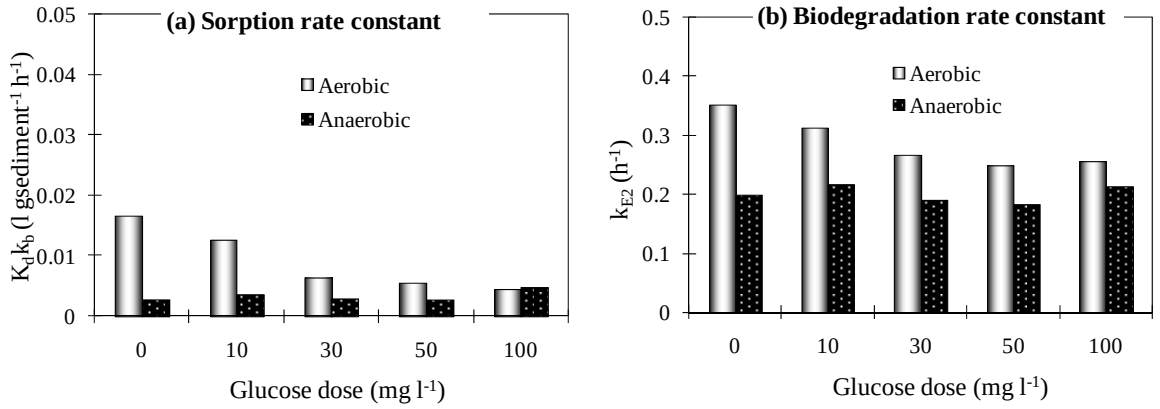

Figure. Comparison of the sorption rate constant (a) and the biodegradation rate constant of E2 (b) under different glucose concentrations in sediment mud cores operated under aerobic and anaerobic conditions.

* *desmiarti@yahoo.com*

4F12

THE EFFICIENT PURIFICATION OF OIL-CONTAMINATED SOIL BY SURFACTANT

S. Aidarova*, A. Babayev, A. Sharipova, A. Makhambetova
Innovation Laboratory of Petroindustrial and Colloid chemistry,
Kazakh-British Technical University,
Tole bi 59, 050000 Almaty, Kazakhstan

The development of technologies on oil recovery and oil producing are accompanied by increasing of the oil pollution and waste volumes, which causes the rise of the ecological threat, decreasing of the economical areas and reducing of the ground fertility and human health change for the worse. The intensification of activity of oil mining and oil refinery as economy branches leads to the situation when the existing technologies of liquidation of hydrocarbon (oil) soiling does not supply the required volumes, rates and purification efficiency of natural, industrial and economic objects from oil contamination. They are not enough efficient and expensive and can not correspond to the modern ecological requirements. The modern ecological situation dictates a necessity of new technology entering in oil recovery and refinery enterprises to provide the decreasing of waste and to make the processes simple, cheap and safety.

Nowadays, a number of mechanical, biological and physical-chemical methods are used for soil purification from oil. The mechanical and biological methods are not so efficient for solving this problem.

The aim of work done is usage of the water-organic solutions of surfactants for soil purification from oil contamination. This physical- chemical method is based on selective wetting and adsorption phenomena application.

The organic-water solutions of decylpiridinium chloride (DPC), olein acid and hexane were used. The hexane-water, (hexane:olein acid)-water, hexane-water solutions of DPC in various ratios have been prepared. The concentrations of surfactants were 10^{-3} and 10^{-2} M.

The main procedure is based on the washing of polluted ground by different cleaning mixtures. The efficiency of soil purification and rate of oil extraction were calculated on the difference of masses before and after the pollution.

The obtained results allows to conclude that the soil purification from oil and the oil extraction degree are most efficient when the hexane-water solution of DPC (10^{-2} M) is used. At the ratio of these components equaled 9:1 the extraction degree is 76.7%. The efficient oil extraction from polluted soil can be achieved when the surfactants concentration is close to the critical ones of micelles formation.

*s.aidarova@kbtu.kz

4F13

In situ Washing by Sedimentation Method of Organics-Contaminated Sandy Soil

BUDIANTA Wawan*, SALIM Chris, HINODE Hirofumi, and OHTA Hideki

Department of International Development Engineering, Tokyo Institute of Technology, 2-12-1 Ookayama, Meguro-Ku, Tokyo 152-8550, Japan

We propose a new method of *in situ* soil remediation called *in situ* washing by sedimentation (IWS), accomplished by injecting a high air-pressure into a mixture of saturated water-sandy soil at a certain depth (D) and hydraulically separating the soil particles based on their particle size and density (Fig.1). This physical separation exploits the distribution of contaminant in the soil by physically separating a selected contaminant-rich fraction. For the *in situ* application, the physical separation by sedimentation and on-site water wash treatment happen as an integrated process and it is important to isolate the ground site to protect the leakage of the aqueous solution used. The advantage of IWS that the washing and separation processes take place simultaneously during the remediation process, quick, effective and cheap since there are no costs for excavation of contaminated soil from the site.

The laboratory study on the effect of soil-water ratio of IWS was investigated. The soil-water ratio required by the soil-water column in order to obtain an appropriate separation on IWS was at least 1:2 by volume. It is necessary to fix casing in the ground surface to protect water solution used as illustrated in Fig.1. The suitability of IWS for Polycyclic Aromatic Hydrocarbon (PAH) remediation, such as Napthalene, Phenantrene and Pyrene, were examined by batch sedimentation column experiment. The laboratory experiment was effective to produce a distinct size separation of the contaminated soil into the coarse and fine fractions, as well as the wash water, indicating that a significant reduction in Napthalene, Phenantrene and Pyrene level (90%) may be achieved.

In IWS, by sedimentation, the coarse fraction was easily recovered by settling in the order of seconds to few minutes. However, the fine particles remained in suspension for a longer period. We performed an initial screening of the settling and coagulation to reduce the amount of suspended solids. The addition of alum as coagulant to the washing solution during the sedimentation process has produced some benefit to reduce suspended solid generated in our experiment.

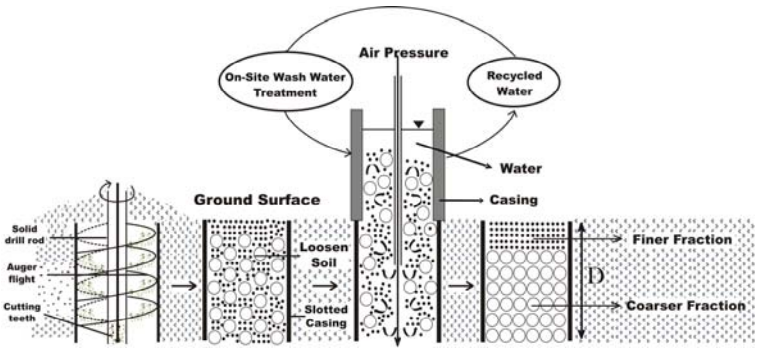

Fig 1. *In situ* Washing by Sedimentation Method (IWS)

*budianta.w.aa@m.titech.ac.jp (Wawan Budianta)

4F14

Sorption of Anions and Formation of Minerals at Naturally-occurring Hyperalkaline Condition

Sohtaro Anraku, Kazuya Morimoto, Tsutomu Sato* and Tetsuro Yoneda
Laboratory of Environmental Geology, Graduate School of Engineering, Hokkaido University, Sapporo, Japan

The extensive use of cement is envisaged in geological repositories of waste for encapsulation, backfilling, and grouting purposes. However, degradation of the cement materials in the repositories can produce a high pore fluid pH initially ranging from pH 13.0-13.5 (Atkinson, 1985). The long-term safety assessment of radioactive waste disposal should also take into account resultant anionic species in radioactive waste (i.e. $^{99}TcO_4^-$ and $^{129}I^-$). These anionic species, however, poorly adsorb to common minerals at the hyperalikaline condition and the alternative mechanism should be expected at such hyperalkaline conditions. In this context, this study focused on the sorption behavior of anions such as CO_3^{2-}, $H_3SiO_4^-$, I^- and formation of their host minerals at naturally-occurring hyperalkaline springs in the Oman ophiolite to learn the sorption mechanism of anions from natural processes.

All water samples were filtered (0.2 μm PTFE filter) at the time of collection and were split into acidified and raw fractions for the appropriate chemical analyses. The precipitates were identified by XRD and supplied to extraction experiment to identify the mineral fraction dominated the each anion uptake. The spring water is characteristically hyperalkaline (pH = 11.0-11.4), reducing (Eh = -557-18.9 mV), low-Mg, Si and CO_3^{2-}, and high Ca, while the surface water is moderately alkaline (pH = 8.87-9.02), oxidizing (Eh = 207-262 mV), high Mg and HCO^{3-}. Aragonite was dominant phase in the observed precipitates at the mixing points of the springs and surface water. However, when the hyperalkaline springs was comparatively rich in Al, hydrotalcite (Mg-Al hydroxides) and calcite were also observed as accessory minerals. During formation of the minerals at the mixing points, HCO_3^- in the surface water was fixed as carbonate minerals such as aragonite and calcite. $H_3SiO_4^-$ in the surface water was fixed into interlayers and surface of hydrotalcite. Iodine in the springs and surface water was mainly fixed in aragonite (see Table). This result was consistent with the results reported by Kitano and Okumura (1973) for F, Cl and Br.

*tomsato@eng.hokudai.ac.jp

Table Constituent minerals and iodine concentrations in the precipitates

Sample	Constituent minerals			Iodine conc. μmol-I/kg-precip.
	Hydrotalcite	Aragonite	Calcite	
Bath-P1	○	○	○	2.85
Bath-P2	○	○	○	2.56
Bath-P3	○	○		2.00
Bath-P4		○		7.12
Bath-P5		○		4.33
Faydh1-P1	○	○		1.27
Faydh1-P2	○	○		1.50
Faydh1-P3		○		8.19
Faydh2-P1	○	○	○	3.60
Faydh2-P2		○		9.05
Faydh3-P1	○	○	○	1.99
Faydh3-P2		○		6.79
Faydh4-P1	○	○	○	0.92
Faydh4-P2		○		2.39

4F15

The Role of Divalent Fatty Acids Soaps at Soil Particle Interfaces in Controlling Wetting Kinetics of Water Repellent Soils

Graber*[1], E.R., Tagger[1,2], S., and Wallach[2], R.
[1]Institute of Soil, Water and Environmental Sciences, The Volcani Center, ARO, POB 6, Bet Dagan, 50250, Israel; [2]Department of Soil and Water, The Faculty of Agricultural, Food and Environmental Sciences, The Hebrew University of Jerusalem, Rehovot, 76100, Israel

Soil water repellency, defined as the situation whereby the soil does not wet spontaneously when water is applied to its surface, has been reported in soils around the world. Water repellent soils exhibit time-dependent wetting behavior, which to now has eluded a detailed physical-chemical understanding. The purpose of this paper is to explore the role of fatty acids, and in particular, of divalent salts of fatty acids, in soil water repellency, with the goal of explaining time-dependent wetting behavior and many hitherto unexplained features of repellent soils.

Soils have many positively charged mineral surfaces that can interact with the headgroups of dissociated fatty acids via lattice cations, and negatively charged surfaces that can interact via divalent cation bridges. Such fatty acid divalent metal salts can lead to hydrophobicity when adsorbed in sufficient numbers to form a close-packed monolayer with perpendicular or nearly perpendicular chains facing outward from particle surfaces. The rate of reorientation of the adsorbed molecules will determine the persistence of repellency when the soil is in contact with water. To test this model, we examined the effect of mono- and divalent cations at different pHs on repellency persistence (as measured by drop penetration time; DPT) of water repellent and wettable soils. Repellency persistence increased at elevated pH in the presence of Ca^{2+} but not Na^{+} (Fig. 1), increased at high cation concentrations, and decreased at elevated temperature. These results are consistent with the behavior of monolayers of fatty acid divalent salts adsorbed on solid substrates, but not with other hydrophobic film-forming compounds such as long chain alkanes, long chain compounds with polar functional groups other than carboxylic acids, or hydrophobins. Abundant long chain fatty acids, capable of forming very well-oriented layers, were identified in the test soils and in many other repellent soils.

Conditions required for development of soil water repellency include: (i) organization of fatty acid divalent salt molecules into a close-packed layer with hydrophobic tails perpendicular to soil particle surfaces; (ii) slow rate of reorientation of those molecules in contact with water; and (iii) low abundances of easily-hydrated hydrophilic moieties in the surface film. The extent of repellency persistence will be substantially affected by small differences in these conditions, and the absence of any one of them will render a soil wettable. Email: ergraber@volcani.agri.gov.il

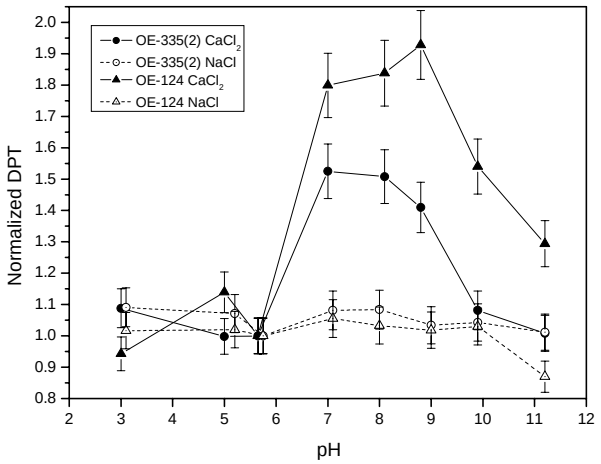

Figure 1. Normalized drop penetration time (DPT) of $CaCl_2$ and NaCl solutions versus pH on two soils (OE-335 and OE-124). The addition of NaCl at all pH levels had little or no effect on DPT, while in the $CaCl_2$ system, DPT is significantly increased at pH 7 and above, reaching maximal values in the pH range of 7 to 9.

4F16

Characterizing Soil Water Repellency Properties by Soil Organic Carbon Content, Soil Texture and Sieved-size Fractions

A.K. Karunarathna[1*], Ken Kawamoto[1], Per Moldrup[2], Toshiko Komatsu[1], L.W. de Jonge[3]

[1]*Graduate School of Science and Engineering, Saitama University, 255 Shimo-okubo, Sakura-ku, Saitama 338-8570 Japan.*

[2]*Environmental Engineering Section, Dep. of Biotechnology Chemistry and Env. Engineering, Aalborg University, Sohngaardsholmsvej 57, DK-9000 Aalborg Denmark.*

[3]*Dep. of Agroecology and Environment, University of Aarthus, P.O. Box 50, DK-8830 Tjele Denmark*

Soil water repellency (WR) is a significant problem worldwide effecting natural and agricultural ecosystems, with important environmental consequences, for which proximate causes are poorly understood. The emergence of WR of a particular soil primarily depends on the water content of the soil at which WR is assessed, and the intensity of WR may determine by other factors such as quantity and quality of soil organic carbon (SOC), soil texture and structure. In order to discuss the relationship between SOC and WR, we investigated soils from diverse origins; grasslands and mixed forests (Danish soils) of Denmark, and forest flows in Japan (Fukushima Volcanic ash, Aichi Cypress forest and Aichi Brown forest). The WR of soils were determined by Molarity of Ethanol Droplet (MED) test for water contents at 0.02 m^3 m^{-3} intervals starting from air dried water content to highest water content at which WR disappears. The SOC contents were determined by a C-N autoanalyzer. The degree of WR decreased greatly with increase of sampled depths, while the smaller fraction of sieved soil showed higher degree of WR than larger. Moreover, the uppermost soil layers and smaller fractions of sieved soils had higher SOC content. For a comprehensive comparison, the total area below the $S_{WR(\theta)}$ (N m^{-1}) against water content, ɵ (m^3 m^{-3}) curve was calculated for each soil, and plotted against SOC percentage. The relationship between $S_{WR(\theta)}$ and SOC was best described by a linear regression as illustrated in fig. 1, resulting a simple expression for WR. The deviation of $S_{WR(\theta)}$ for different soils at same water content may be caused by different qualities of SOC and soil texture.

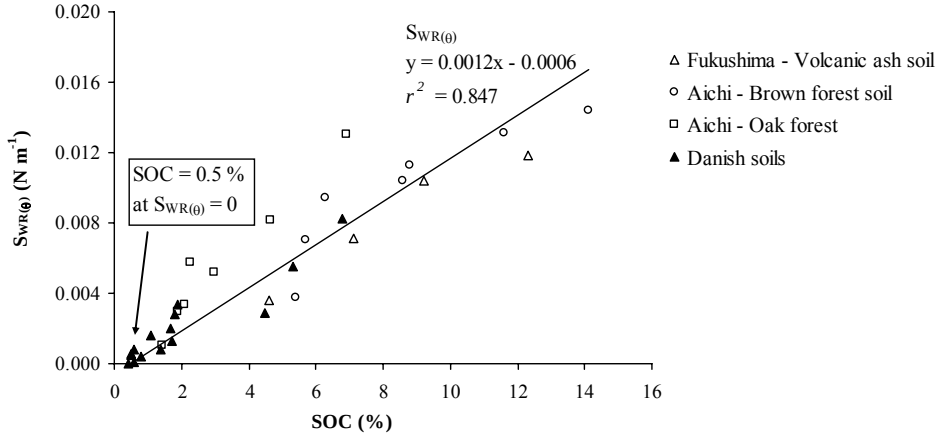

Fig. 1 Relationship between SOC content and area below the soil water repellency curve ($S_{WR(\theta)}$).

*anujica@yahoo.com

4F17

A new methodology for measuring continuous soil air content using sound resonance

K. Fukada[1]* , S. Kawashima[1] , K. Nakamura[1]
[1]*Graduate School of Agriculture, Kyoto University*
Kitashirakawa Oiwake-cho, Sakyo-ku, Kyoto 606-8502

Soil air which is connected to the atmosphere constitutes an interface between the soil and the atmosphere and contributes to the gas exchanges. The connectivity of soil air to the atmosphere has not been evaluated, however. We made the experiment to evaluate the connectivity of soil air to the atmosphere using the acoustic wave. The experimental apparatus shown in Figure 1 consists of cylindrical sampler of 5cm inside diameter, and vinyl pipes of 2.5cm inside diameter and 25, 50, 100 cm lengths. The pipe is equipped with speaker and microphone on its side to detect the resonance frequency. The Soma silica sand of 0.6 mm mean diameter was used. The water content of sand was adjusted to nine levels and they were packed in samplers. The samples were dried in oven to determine the air content after the acoustic experiment, and we examined the relations between the air content in sample and the resonance frequencies. Figure 2 shows the relation between the wave length calculated by resonance frequency and the air content in soil sample. Both axes are normalized by the length and the cross section area of the resonance pipe. The values for the longer pipes are on the straight line derived from the theory on the standing waves. The wave length of resonance frequency is linearly related with the air content in the soil sample. This figure also shows that the values for the 25cm pipe are scattered widely. The deviations of them from the straight line are larger as the air content is smaller. This deviation may be the effect of the entrapped air that disconnected to the atmosphere and did not oscillate. The acoustic wave is a possible way to estimate the continuous air content in soil.

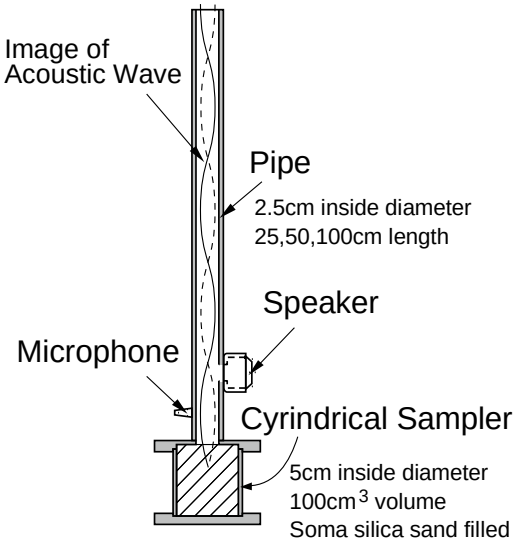

Figure 1 Experimental apparatus

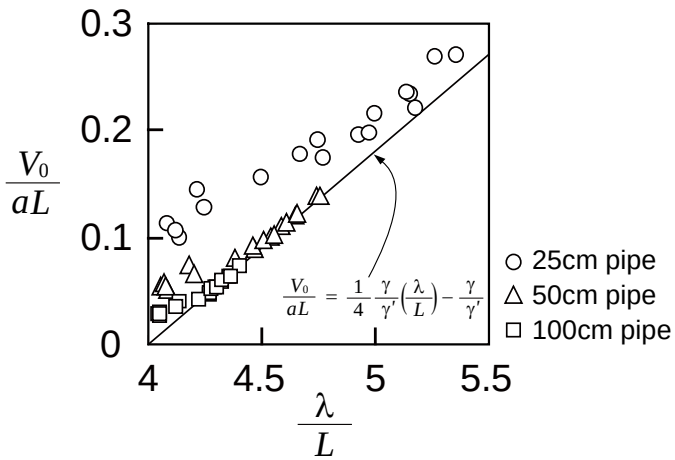

Figure 2 Relation between wave length λ and soil air content V_0. a and L is the cross section and the length of the pipe, respectively. γ and γ' is the ratio of specific heat at constant pressure to specific heat at constant volume for the air in sampler and in the pipe, respectively. We chose γ=1.0 and γ'=1.4.

*kfuka@kais.kyoto-u.ac.jp

Poster Presentations
Abstracts

P001

Sedimentation and Electrophoresis of Porous Colloids

Y. Uchida*, Y. Adachi, K. Aoki

Graduate School of Life and Environmental Sciences, University of Tsukuba,

Tennodai 1-1-1, Tsukuba-shi, Ibaraki, 305-8572, Japan

Sedimentation and electrophoresis of porous materials; colloidal floc and colloidal particles covered with adsorbing polyelectrolytes, are visited to examine the characteristic length scales of transport phenomena. The simultaneous measurement of floc structure and the settling velocity revealed that the size of floc is dominative in the determination of Stokes drag, while the permeability is determined by the large pore in flocs. However, if the floc is placed in the electric field, outside fluid can easily penetrate into the floc by means of electro osmosis. In this regime, the characteristic length scale of hydrodynamic drag is Debye length. In the case of electrophoresis of latex particle covered with adsorbing polyelectrolyte, the characteristic length scale of permeability was estimated mostly same as the distance between charged segments.

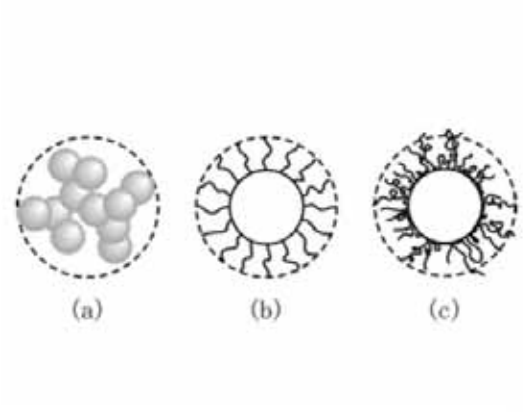

Fig.1 Porous colloids. (a)colloidal floc, (b)colloidal particle with grafted polymer, (c)colloidal particle with adsorbed polymer.

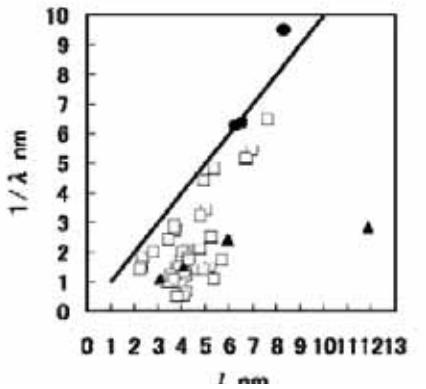

Fig.2 Distance between the charged segments of surface charge layer vs. the length of permeability. (●) adsorbed polyelectrolyte layer[1], (▲) temperature sensitive hydrogel layer[2], (□) surface layer of microorganism[3-6].

References

1. K. Aoki, Y. Adachi, *J. Colloid and Interface Sci.*, **300**(2006)69.
2. K. Makino, S. Yamamoto, K. Fujimoto, H. Kawaguchi, H. Ohshima, *J. Colloid Interface Sci.,* 166(1994)251.
3. R. Sonohara, N. Muramatsu, H. Ohshima, T. Kondo, *Biophys. Chem.*, **55**(1995)273.
4. S. Tsuneda, H. Aikawa, H. Hayashi, A. Hirata, *J. Colloid Interface Sci.*, **279**(2004)410.
5. H. Morisaki, S. Nagai, H. Ohshima, E. Ikemoto, K. Kogure, *Microbiol.*, **145**(1999)2797.
6. V.V. Rodríguez, H.J. Busscher, W. Norde, H.C. van der Mei, *Electrophoresis*, **23**(2002)2007.

* s0721333@ipe.tsukuba.ac.jp

P002

New extractive substances for extraction of boric acid from industrial sewage

Beissembaeva M.R.*[1], Sydykbaeva S.[2], Kalabaeva M.K.[3], Tanasheva M.R.[4]

[1]*Chemical Faculty, Kazakh National University,*

95A, Karasai batyr, Almaty, Kazakhstan

[2]*Chemical Faculty, Kazakh National University,*

95A, Karasai batyr, Almaty, Kazakhstan

[3]*Chemical Faculty, Kazakh National University,*

95A, Karasai batyr, Almaty, Kazakhstan

[4]*Chemical Faculty, Kazakh National University,*

95A, Karasai batyr, Almaty, Kazakhstan

Kazakhstan has powerful mineral raw material reserves of boron ores and, despite the fact that the part of the raw material which is easily available and rich in boron has been considerably depleted, our country ranks among the first ten countries of the world by the resources of natural borates. This provides favorable preconditions for increasing the strength of the country's economy. However, boron raw material of Indersk deposit is distinguished by a low content of boron and practically unstudied mineralogical composition, this making the use of the known technologies ineffective.

The work deals with general regularities of phase distribution, solubility, composition of borates in multicomponent systems containing boric acid, water and organic solvent.

Crystallization regions of earlier unstudied borates of sodium, lithium, zinc ($NaB_2O_8 \cdot 5H_2O$, $LiB_5O_8 \cdot 5H_2O$, $Zn_2B_2O_{11} \cdot 7H_2O$, NaB_5O_{28}) depending on temperature have been stated. Using solubility diagrams of the studied systems, it is possible to determine separate regions of $LiB_5O_8 \cdot 5H_2O$ for accelerated synthesis of sodium, lithium pentaborates, zinc hexaborate and sodium nonaborate on the basis of three-component system with boric acid.

When using a synergic mixture SAS – diluent, DBBA – diluent, the distribution factor of boric acid was shown to increase 2-3 times.

We have carried out investigations on extraction of boron and gypsum from natural ores of Indersk deposit using a technical mixture of monocarbonic acid – alcohol production waste. It is shown that the used extracting agent selectively extracts boron and maximum extraction degree reaches 98.7 %. It is stated that under optimum conditions (the mixing time of 30 minutes, the ratio of solid and liquid phases being equal to 1:100, temperature 60^oC, pH = 4.0-4.3), boron passes quantitatively into the extractant phase, and gypsum and other ionic impurities are not extracted. The coefficient of separation of boron from gypsum has high values (β=500-600).

Sodium and lithium pentaborates, zinc hexaborates and ammonium tetraborates were synthesized on the basis of the obtained extracts under the established optimum conditions. To identify the synthesized compounds, IR investigations and X-ray phase analysis were carried out.

As a result of the carried out experimental investigations, a principal technological scheme of ammonium borates was proposed. The technological regime of the process was grounded.

---

asomarov@yandex.ru

P003

Dynamic interaction between oppositely charged vesicles

D. Saeki[1,2]*, S. Sugiura[2], T. Baba[2], T. Kanamori[2], S. Sato[1], S. Mukataka[1], S. Ichikawa[1]

[1]*Graduate School of Life and Environmental Sciences, University of Tsukuba, 1-1-1 Tennodai, Tsukuba, Ibaraki 305-8572*

[2]*Research Center of Advanced Bionics, National Institute of Advanced Industrial Science and Technology (AIST), Central 5th, 1-1-1 Higashi, Tsukuba, Ibaraki 305-8565*

A vesicle consists of lipid bilayer membrane and internal water phase, and has been studied as a model of cell membrane. Fusion of cell membranes while retaining membrane continuity occurs in vivo, but the mechanism is not as yet fully understood. Positively charged vesicles interact electrostatically with negatively charged membranes, and fuse under certain conditions. Therefore, charged vesicles are useful for studying the fusion mechanism.

In this study, we investigated dynamic interactions between oppositely charged small unilamellar vesicles using positively charged vesicles containing 1,2-dioleoyl-3-trimethylammonium-propane (DOTAP) or 3ß-[N-(N',N'-dimethylaminoethane)-carbamoyl] cholesterol (DC-Chol) and negatively charged vesicles containing L-α-phosphatidyl-DL-glycerol (PG). Aggregation, lipid bilayer mixing, contents mixing and contents leakage were systematically examined using optical density measurements, fluorescence resonance energy transfer assays, fluorescence quenching assays, light-scattering analyses, and freeze-fracture transmission electron microscopy. The oppositely charged vesicles aggregated immediately (Fig. 1, Fig. 2(A)(B)). The vesicle aggregates disaggregated spontaneously after several minutes (Fig. 2(C)). Lipid mixing was observed, but there was no mixing of the contents. The surface potential of the disaggregated vesicles was neutralized. From these results, we infer that the lipids in the external monolayers were exchanged between the oppositely charged vesicles while the internal monolayers remained intact. The two types of cationic lipids used exhibited different speeds of disaggregation (Fig. 1).

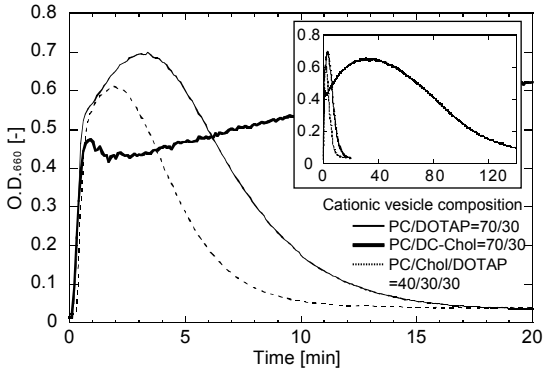

Fig. 1. Changes in optical density with time. PC/PG (70/30 molar ratio) vesicles were mixed with PC/DOTAP (70/30) vesicles (solid line), PC/DC-Chol (70/30) vesicles (bold line) or PC/cholesterol/DOTAP (40/30/30) vesicles (dashed line).

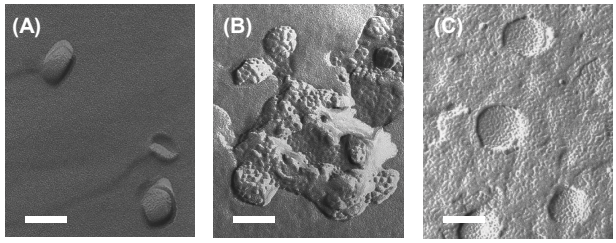

Fig. 2. Freeze fracture TEM micrographs for the interaction between PC/DOTAP (70/30) vesicles and PC/PG (70/30) vesicles. (A) PC/DOTAP vesicles before mixing. (B) Vesicles at 1 min after mixing. (C) Vesicles at 60 min after mixing. Scale bar shows 100 nm.

*dsk.saeki@aist.go.jp

P004

Adsorbing Materials Designed for Remediation of Oil-Polluted Water

A. Kawai[1]*, H. Sakaguchi[2]
[1] *Research Center for Compact Chemical Process, AIST,*
1-1-1 Higashi, Tsukuba, Ibaraki 305-8565 Japan
[2] *Intermolecular Interaction Research Laboratory, Mol Labo Inc.,*
380-4 Takasaki, Tsukuba, Ibaraki 300-1245 Japan

Water pollutions by oil; run out of industrial waste water into rivers, leakage from tanker into sea, and many other cases, have become more and more severe problems for these decades. Many kinds of oil recovering materials and ways have been developed, but they are not so efficient or useful so far. In this paper, some newly designed oil recovering materials, simple aliphatic linear crystalline polymers, are introduced, and are compared with already existing and known absorbing materials.

Original synthesized crystalline polymer was completely dissolved in much amounts of organic solvent at high temperature, and was cooled down gradually to room temperature. Dissolved polymer could be precipitated in two shapes, minute particles and thin and long fibers. In each case, original crystalline structure was maintained after precipitation. SEM photos of these polymers are shown in Figure 1. Both types of crystalline polymer precipitates could catch much amount of aliphatic hydrocarbons in water.

Minute particles of amorphous polymer, the same type of aliphatic polymer as crystalline one, were prepared in the same manner. However, these amorphous polymer particles could catch only small amount of aliphatic hydrocarbons in water. Decisive point of the difference, effective or non-effective as adsorbent, is crystalline or amorphous.

Compared with already reported sodium carboxylate and lithium carboxylate fiber crystals (IAP2002, 2004, 2006), crystalline polymer adsorbents are mechanically more tough and flexible, do not dissolve in water at all, are not dispersed in water well. How to use as practical adsorbents, advantage and disadvantage of the crystalline polymers, comparison with other examples, will be discussed.

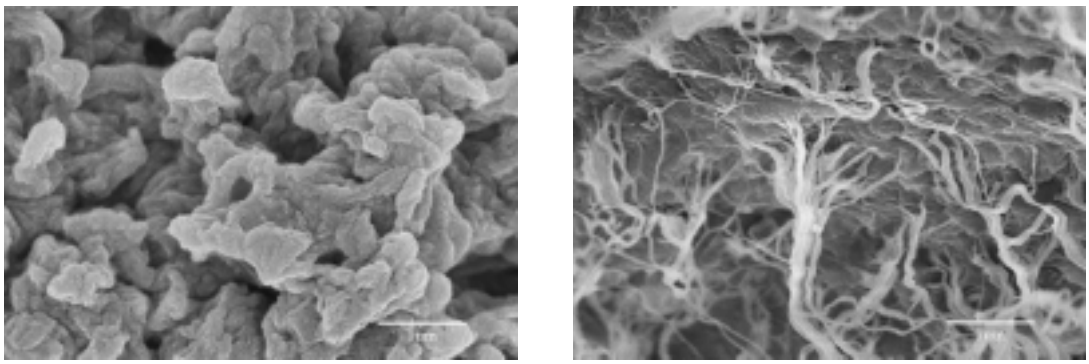

Fig. 1 SEM photos of aliphatic linear polymer for adsorbent of oil in Water.
Left: Minute particles of polymer crystal Right: Fiber crystal of linear polymer

*akiko-kawai@aist.go.jp

P005

Effects of charge density of polyelectrolyte chain on the flocculation of polystyrene latex particles

Y. Adachi* T. Hara, K. Aoki,
Graduate School of Life and Environmental Sciences, University of Tsukuba,
1-1-1 Tennodai, Tsukuba, Ibaraki, 305-8572, Japan

Effects of charge density of polyelectrolyte chain used as colloidal flocculants on the adsorption behavior on to colloidal surface and subsequent bridging flocculation were investigated as a function of ionic strength. The flocculation experiments were designed in order to elucidate the unfolding behavior of polyelectrolyte chain attached onto bare surface. In the Brownian flocculation, i.e., flocculation induced without mixing, charge neutralization is the dominant mechanism to induce flocculation. However, flocculation in the flow field, i.e., flocculation induced with fluid mixing, protruding polymer from the colloidal surface will bring about the formation of bridge between colliding particles. It was demonstrated that the effect of difference in charge density of polyelectrolyte chain and ionic strength is more pronounced in the presence of mixing flow. The sharp transition from unstable bridging state to stable state is confirmed with high charged chain in low ionic strength.

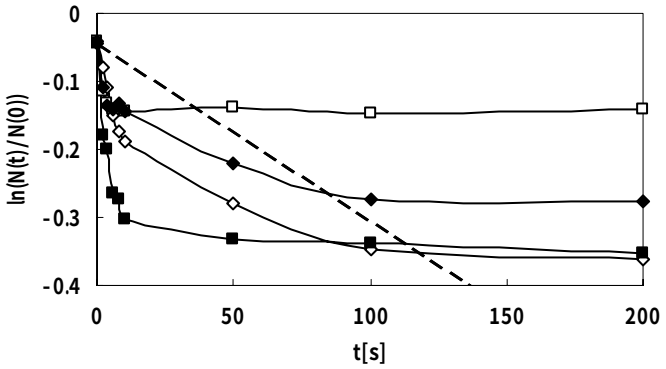

Fig.1 ln($N(t)/N(0)$) vs. t, for flocculation with polyelectrolyte.
Here, $N(t)$ is number concentration of polystyrene latex particles at time (t)
Charge density (τ) of polyelectrolyte and ionic strength (I):
(□) $\tau = 1$, $I = 1.0\times10^{-4}$ [mol/l], (■) $\tau = 1$, $I = 1.0\times10^{-2}$ [mol/l],
(◇) $\tau = 0.04$, $I = 1.0\times10^{-4}$ [mol/l], (◆) $\tau = 0.04$, $I = 1.0\times10^{-2}$ [mol/l].
The dashed line indicates salt-induced coagulation.

* yas@sakura.cc.tsukuba ac.jp

P006

Diffusion of pesticide in nanometer-sized pores of ODS-silica gel by single microparticle injection and absorption microspectroscopy

K. Chikama[1]*, K. Nakatani[2]

[1]*Analysis Research Department, Chemical Research Laboratories, Nissan Chemical Industries, Ltd., 722-1 Tsuboi, Funabashi, Chiba, Japan, 274-8507*

[2]*Department of Chemistry, Graduate School of Pure and Applied Sciences, University of Tsukuba, 1-1-1 Tennoudai, Tsukuba, Ibaraki, Japan, 305-8571*

The studies of the mass transfer processes of a pesticide in a porous microparticle are very important for environmental, analytical and physical chemistry. In this study, the sorption/desorption processes of a pesticide between a single ODS-silica gel microparticle and water were kinetically analyzed using a single microparticle measurement technique. The results are discussed in terms of the diffusion and adsorption/desorption processes in the nanometer-sized pores of the microparticle [1].

A single ODS-silica gel microparticle (particle diameter (d) of 20-50 μm, pore diameter of 12 nm) was injected into an aqueous quinoclamine (ACNQ) or prodiamine (PD) solution by microcapillary manipulation and the sorption rate for the single microparticle was measured using absorption microspectroscopy [2] (Fig. 1). After the sorption equilibrium, the single microparticle was injected into a solution without the pesticide and the desorption rate was measured. In an ODS-silica gel/water system, adsorption of an organic solute on ODS and silanolate groups of the pore walls can be observed. ACNQ is a neutral species at pH ~ 6 so that the pesticide was adsorbed on the ODS groups. The sorption and desorption rates of ACNQ could be analyzed by the intraparticle diffusion model. The intraparticle diffusion coefficient (D_p) for the sorption was in good agreement with that for the desorption. The D_p was analyzed on the basis of the pore and surface diffusion model and contribution of the pore diffusion was much larger than that of the surface diffusion. On the other hand, since PD is a cation at pH ~ 7, the pesticide was adsorbed on the ODS and silanolate groups. The adsorption of the PD is so strong that the desorption of PD from the silanolate groups was extremely slow compared with that from the ODS groups.

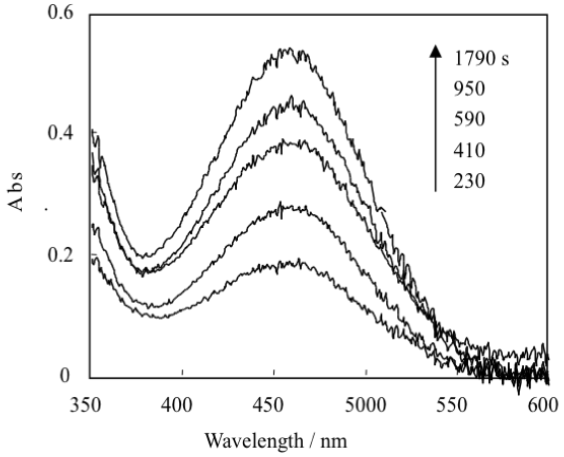

Fig. 1 Time dependence of absorption spectrum of ACNQ sorbed into a single ODS-silica gel (d = 46 μm, $[ACNQ]_w$ = 30 μM)

(1) K. Chikama et al., *Colloids Surf. A: Physicochem. Eng. Aspects*, 315, 250 (2008).
(2) K. Nakatani and T. Sekine, *Langmuir*, 16, 9256 (2000).

*chikamak@nissanchem.co.jp

P007

THE $A1_2O_3$ NANOFILMS THICKNESS EFFECT ON THE DEPENDENCE OF CONTACT ANGLES

N. Jadagayeva[1]*, S. Aidarova[1], E. Gribanova[2]
[1]*Kazakh-British technical University,*
Tole bi 59, 050000 Almaty, Kazakhstan
[2]*St.Petersburg State University, .Petersburg, Russia*

Using the method of molecular layering the samples with 1-12 layers of Al_2O_3 at the surface of glass plates and also the samples with 1 - 3 layers of alumina at the powder of the same glass were received. Investigation of a dependence of contact angle on solution pH (HCI, KOH in bidestilled water) ($\theta = f(pH)$) using microphotography of sitting drops and also of points of zero charge using the method of potentiometric titration and specific surface on methylene blue adsorption were done for these samples. The amount of Al_2O_3 at the surface of glass powder was also determined All the ($\theta = f(pH)$) dependences obtained were polyextremal (spectrolike). The position an expressiveness of θ maxima had regular dependence on the number of alumina lasers.

The ($\theta = f(pH)$) dependence measured for initial glass was similar to that for quartz surface measured earlier [l]. Carrying out just one cycle of molecular layering of Al_2O_3 significantly changed the wettability of the surface of the investigated glass. This fact confirms the "monolayer effecf" opened earlier and is in agreement with the results of quantity detemination of alumina piled up at the surface. The PZCh values, measured for received powders (pH = 4,6; 4,8 and 5,0 for one, two and three layers of Al_2O_3 respectively) show significant displacement in more basic region as compared to initial glass (pH = 2,5 – 3,0).

In the process of subsequent layering the next tendency of the changing of average level of contact angle with the layer number. The total level of contact angles have tendency to the raising, the increases of contact angle taking place from 1 to 3 layers, from 6 to 8 and from 9 to ll layers the tendency is repeating. From 3 to 4, from 8 to 9 and from 11 to 12 the decreasing of contact angles occurs.

At comparison of ($\theta = f(pH)$) dependences for different numbers of Al_2O_3 layers it was found also that for 1-7 layers the total level of contact angles is higher in acid medium and for 8-12 1ayer in base one. This evidently shows the regular changing of acid - base properties of the surface in the process of Al_2O_3 structure formation. At the comparison of the dependences obtained for 1-7 and 8-12 layers it can also be concluded that θ maximum at pH=6,0 which can be regarded as one of the most character maxima for the balk Al_2O_3 is well shown only for large layer number (10 and 12).

[l].E.V.Gribanova, L.I.Molchanova and others, Kolloid.Zh.(RU) 1983. Vol.45. P.316-320

*n.jadagaeva@kbtu.kz

P008

Interface processes of carbonyl sulfide on atmospheric particles

Y. Liu*, H. He

Research Center for Eco-Environmental Sciences, Chinese Academy of Sciences, Beijing, China 100085

Carbonyl sulfide (OCS) is the most abundant sulfur containing compound in the atmosphere. The source and sink of carbonyl sulfide in the troposphere is related to the source of stratospheric sulfate aerosols and the global sulfur cycles. Modeling studies have shown that atmospheric particles often acting as a sink for certain species. In this study, the interface processes of carbonyl sulfide on mineral oxides were investigated using a Knudsen cell flow reactor and an *in situ* diffuse reflectance infrared Fourier transform spectroscopy (DRIFTS). It was found that besides adsorption process, hydrolysis of OCS and succeeding oxidation of intermediate products readily takes place on mineral oxides. Gaseous CO_2 and H_2S were identified with DRIFTS and mass spectroscopy. The key intermediate of hydrolysis, thiocarbonate ($HSCO_2^-$), was observed on some mineral oxides. Surface sulfite and sulfate were also identified with infrared spectroscopy. The uptake coefficients and adsorption capacities of OCS on mineral oxides were determined on the basis of Knudsen cell signal. The global flux of OCS due to heterogeneous processes on mineral dust was estimated at 0.13-0.29 $Tg \cdot yr^{-1}$, which is comparable to the annual flux of OCS for the reaction with •OH. Our results indicate that heterogeneous reactions of OCS on mineral dust should be considered into its global sinks. This also shows that the role of heterogeneous reactions in the environmental chemistry cycles of long-life trace gases needs to be investigated detailedly.

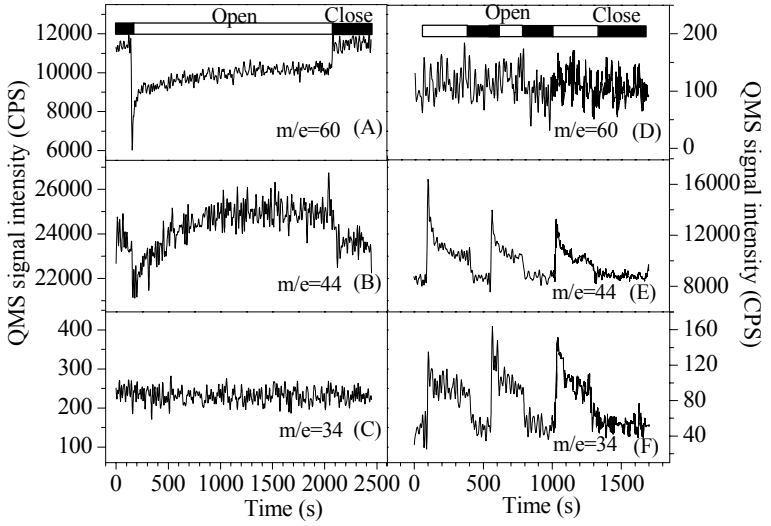

Fig. 1 The typical heterogeneous process profile of OCS on α-Al_2O_3 at 300 K (left side) and the *in situ* desorption of surface species in the end of uptake (right side).

* 5115065@rcees.ac.cn

P009

Effect of humic acid on radiocesium sorption in illite

N. K. Ishikawa*, S. Uchida, K. Tagami

Office of Biospheric Assessment for Waste Disposal, National Institute of Radiological Sciences, 4-9-1 Anagawa, Inage, Chiba 263-8555

Radiocesium isotopes (^{134,135,137}Cs) are contaminants that can be released from nuclear facilities. Knowledge of the behavior of Cs in the soil environment is important in assessing potential crop uptake. Among the soil components, clay minerals play important roles in Cs sorption. Moreover, sorption of Cs varies among the clay minerals. For example, illite has not only ion exchange sites but also special sites (Frayed edge sites; FES) which show high sorption selectivity for Cs^+, K^+ and NH_4^+. In addition, soil organic matter (SOM) can bind to clay minerals and block direct sorption of Cs on sorption sites in clay minerals. However, effects of SOM on Cs sorption in clay minerals have not yet been clarified. In this study, Cs sorption on mixtures of illite and humic acid, which is a component of SOM, was determined.

Batch sorption test was carried out using ^{137}Cs as a tracer with 100-mg mixtures of illite and HA. The solid/liquid ratio was kept at 100 mg/10 mL. Initial Cs concentration ranged from 8×10^{-5} to 0.8 mg/L. After the batch sorption test, sequential extraction methods were carried out using 0.05M $CaCl_2$, for determination of water soluble and/or weakly sorbed Cs fraction, and 0.16M $Na_4P_2O_7$ for determination of the organic matter bound Cs fraction. The amount of Cs remaining after $Na_4P_2O_7$ extraction was considered to be the fixed Cs fraction.

The sorption isotherms of variety of illite-HA mixtures are shown in Fig.1. These isotherms were applied to Freundlich isotherm given as follows,

$$q = K \cdot C^a$$

where K and a are constants. At 100% HA samples, the a value of the isotherm was 0.99. This result could be suggested that Cs sorption in HA is almost independent on Cs concentration in the solution. In addition, the a values decrease with increasing illite contents and the a value at 100% illite samples was 0.87. This result could be indicated that Cs sorption in illite depended on Cs concentration in solutions. Further discussion will be presented in the presentation.

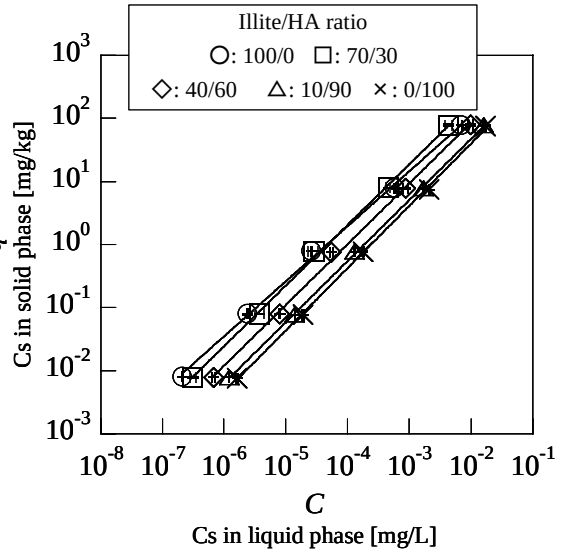

Fig. 1 Sorption isotherms of Cs on illite-HA mixtures

Acknowledgment: This work has been partially supported by the Agency for Natural Resources and Energy, the Ministry of Economy, Trade and Industry (METI), Japan.

*nao@nirs.go.jp

P010

Could iron oxide particles generated at the steel/bentonite interface move along the compacted bentonite barrier in a Deep Geological Repository for High Level Nuclear Wastes?

E. Torres[1], A.L. Morales[2], M.J. Turrero[1], P.L.Martín[1], A.Escribano[1], U.Alonso[1]*

[1]*CIEMAT, Division of Engineered and Geological Barriers,*
Avda. Complutense 22, Madrid, 28040

[2]*College of Physics, Universidad de Antioquia,*
67-53-108 Sede de Investigación Universitaria, Medellín, 1226

The multibarrier system for the isolation of High Level Nuclear Wastes (HLNW) includes the concept of spent fuel encapsulated in canisters of carbon steel. The Engineered Barrier System (EBS) is completed with a bentonite and a concrete layer. The repository is placed in a geological host formation: granite or argillaceous formation, depending on the concept chosen by each country.

The movement of iron oxide particles could favour the mobility of radionuclides and their ingress in the biosphere, as radionuclides could get sorbed onto the corrosion products and move along the bentonite barrier. It has already been reported the migration of corrosion products in compacted bentonite. During this work, several tests were realized under different conditions. In all cases, it has been observed the occurrence of iron oxides along bentonite blocks. Techniques such as Transmission Electron Microscopy, Mössbauer Spectroscopy and N_2-BET measures indicate that small-size particles (nanometers or even smaller) can be found in areas distant from the bentonite/steel interface. This fact could confirm the feasibility of the movement of iron oxide particle along the compacted bentonite barrier.

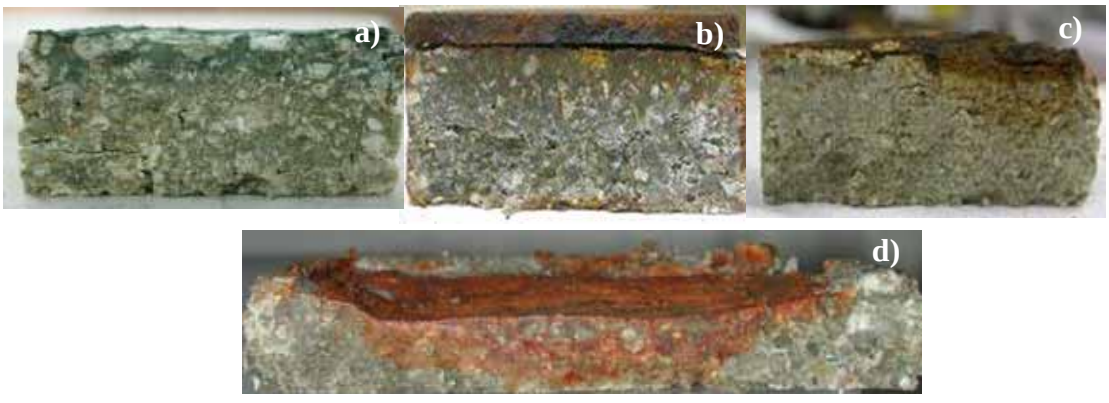

Fig. 1 Transversal cuts of compacted bentonite blocks after the tests: anoxic conditions: a)100ºC, b)50ºC, c)25ºC; d) room conditions

*elena.torres@ciemat.es

P011

Effect of ionic strength on deposition kinetics of humic acid through columns packed with glass beads

Y. Yamashita[1]*, T. Tanaka[2], Y.Adachi[1]

[1]*Graduate Scholl of Life and Environmental Sciences, University of Tsukuba, 1-1-1 Tennodai, Tsukuba, Ibaraki, 305-0005, Japan*

[2] *Nuclear Safety Research Center, Japan Atomic Energy Agency, 2-4 Shirane Shirakata, Tokai, Naka, Ibaraki 319-1195, Japan*

Transport behavior of humic acid was studied from the aspects of colloidal stability. Deposition kinetics of purified Aldrich humic acid was investigated over a wide range of monovalent (0.1 to 2.0 M NaCl) and divalent (0.001 to 0.05 M $CaCl_2$) electrolyte concentrations at pH 3.0 by using packed-bed technique. Spherical glass beads with diameters of 0.2-mm were utilized as model collectors. Breakthrough curves of humic acid were measured with UV-VIS spectrophotometer. The values of C/C_0 (C and C_0 are the effluent and influent concentrations of humic acid, respectively) decreased with increasing electrolyte concentrations. Experimental collision efficiencies were determined from measured single collector efficiencies. The results are presented as stability curves, which is the logarithm of the collision efficiency as a function of the logarithm of salt concentration (Fig. 1). Stability curves of humic acid obviously showed favorable (fast) and unfavorable (slow) regimes and critical deposition concentration (CDC) in the presence of both electrolytes. As a consequence, it is indicated that transport behavior of humic acid is primarily controlled by electrostatic interaction between humic acids and collectors.

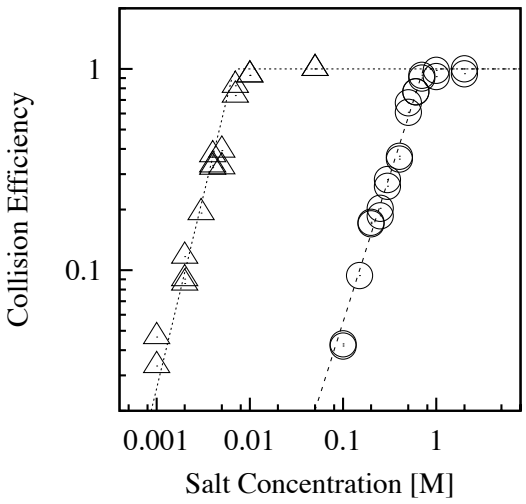

Fig. 1. Calculated collision efficiency of humic acid through the columns packed with glass beads as a function of NaCl (○) or $CaCl_2$ (△) concentrations. Doted lines are extrapolated from favorable and unfavorable regimes as used eye guide.

*nabla826@hotmail.com

P012

The effects of humic acid adsorption on the deposition behavior of kaolinite particles in the sand column.

K. Shiratori*, Y. Yamashita, Y. Adachi
Graduate School of Life and Environmental Sciences, Tsukuba University
1-1-1 Tennodai, Tsukuba, Ibaraki 305-8572, Japan

Effect of adsorption of humic acid on the surface charge property of kaolinite and its deposition behavior onto the sand surface was studied by column experiments as a function of pH at constant ionic strength (10^{-3}M). The amount of adsorption of humic acid onto kaolinite particle increases with the decrease of solution pH. Adsorption of humic acid was detected by the shift in electrophoretic mobility. The magnitude of this shift was larger at lower pH corresponding to the increment of adsorption amount of humic acid. The initial deposition rate of kaolinite coated by humic acid was smaller than that value of pure kaolinite for all pH range. The data of electrophoresis implies that the ripening takes place in the condition with small electrostatic repulsion and the blocking (observed at pH 10.80 in Fig.1 (b)) takes place with large electrostatic repulsion and possible steric repulsion humic acid.

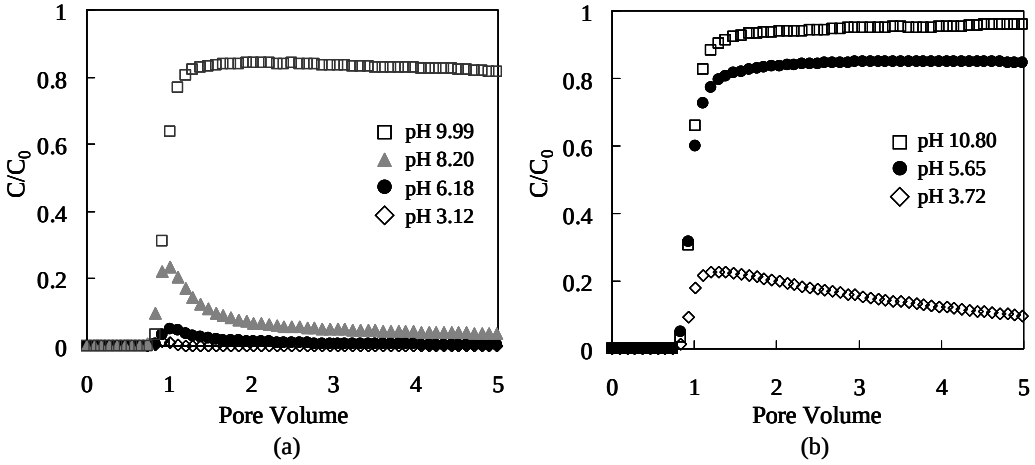

Fig.1 Breakthrough curves of column experiments.
(a) Pure kaolinite. (b) Humic acid coated kaolinite.

s0621245@ipe.tsukuba.ac.jp

P013

Oxidative degradation of 2,4,6-trichlorophenol by an Iron (III)-porphyrin-Humic Acid Supermolecular Catalyst

S. Shigematsu* and M. Fukushima

Division of solid Waste, Resources and Geoenvrionmental Engineering, Graduate School of Enginnering, Hokkaido University, Sapporo 060-8628

Tetrakis (4-hydroxyphenyl) porphine iron (III) ($FeTPP(OH)_4$) is known as one of biomimetic catalysts, which mimic the active center of oxidative enzymes from wood-rot fungus. This catalyst is effective in the degradation of chlorophenols. However, $FeTPP(OH)_4$ is inactivated in the presence of peroxide, such as $KHSO_5$, because of its self-degradation. To suppress the self-degradation of the catalyst and to enhance the catalytic activity, $FeTPP(OH)_4$ was bond to humic substances (HSs) via the formaldehyde polycondensation. In general, polyphenol compounds, formed by the formaldehyde polycondensation in the presence of base catalyst, is called “Resol”. First, the self-degradation rate of the synthesized catalysts was analyzed by a stopped-flow spectroscopy, showing that the self-degradation of $FeTPP(OH)_4$ was retarded by formation of resol (Fig.1). Second, to evaluate the catalytic activity of resol catalysts, oxidation characteristics of 2,4,6-trichlorophenol (TrCP) were observed, in terms of percent degradation, dechlorination, and mineralization to CO_2. Percents degradation of TrCP for resol catalysts were 10% larger than that for $FeTPP(OH)_4$ alone and dechlorination was also enhanced in the presence of resol catalysts. As shown in Fig.2, the percent CO_2 conversion was significantly increased in resol catalysts (17-18% for resol, 4% for $FeTPP(OH)_4$). These results show that formation of resol is effective in the retardation of self-degradation of $FeTPP(OH)_4$ and an enhanced catalytic activity.

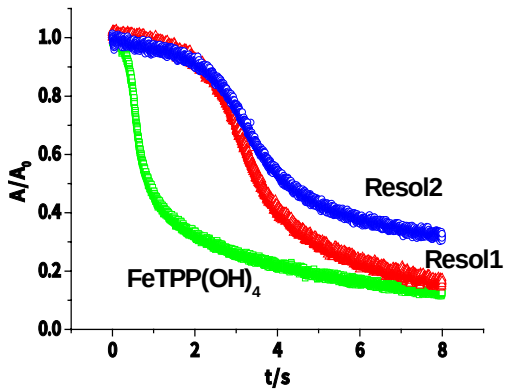

Fig1. Kinetic curves of self-degradation of $FeTPP(OH)_4$ and its Resols (pH3)

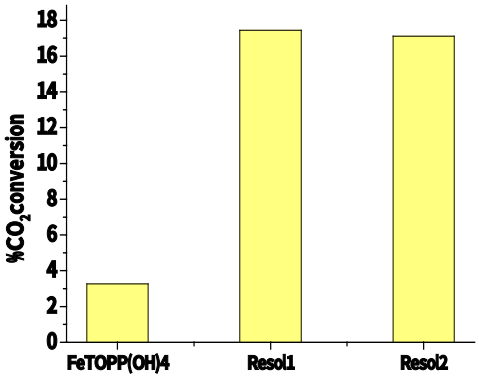

Fig2. Mineralization to CO_2 as result of oxidation by $FeTPP(OH)_4$ and its Resols.

*t040584k@ec.hokudai.ac.jp

P014

Cadmium solidification on clay mineral and Fe oxide using Magnesium Oxide

S. Oishi*[1], R. Takamatsu[2], I. Kitazawa[2] and K. Tanaka[2]

[1]*Graduate School of Veterinary Medicine and Animal Science, Kitasato University,*
35-1 Higashi 23 bancho, Towada, Aomori 034-8628, JAPAN

[2]*School of Veterinary Medicine, Kitasato University,*
35-1 Higashi 23 bancho, Towada, Aomori 034-8628, JAPAN

Magnesium Oxide (MgO) is useful to immobilize heavy metals in contaminated soil as a promising method for soil remediation. There are many advantages for MgO: magnesium oxide has low cost, minimal environmental impact, low stability, and reaching a maximum pH of 10. Pyrophyllite and goethite which Cd sorbed on were applied instead of Cd polluted soil. Batch desorption experiments using EDTA in replenishment method were carried out to evaluate the effectiveness of MgO treatment for Cd sorption on pyrophyllite and goethite.

Under MgO addition, Cd was sorbed on pyrophyllite and goethite. Cd desorption behavior in samples are shown in Fig. 1. The results of Cd desorption in the non-additional MgO samples are also illustrated for comparison. Amounts of desorption in the samples with MgO decrease compared with those without MgO. Inhibition of Cd desorption in the samples indicated the solidification of Cd was caused by using MgO. Magnesium (Mg) dissolution from MgO was obtained and concerned with the stabilization of Cd. Therefore, we suggested that Cd became less soluble by Mg-Cd compound formation (Cd surface precipitate including Mg). While the Cd desorption in goethite sample was lower than pyrophyllite sample at the beginning of washing, both amounts of these samples coincided at the latter washing. Cd solidification mechanism was affected by the sorbent.

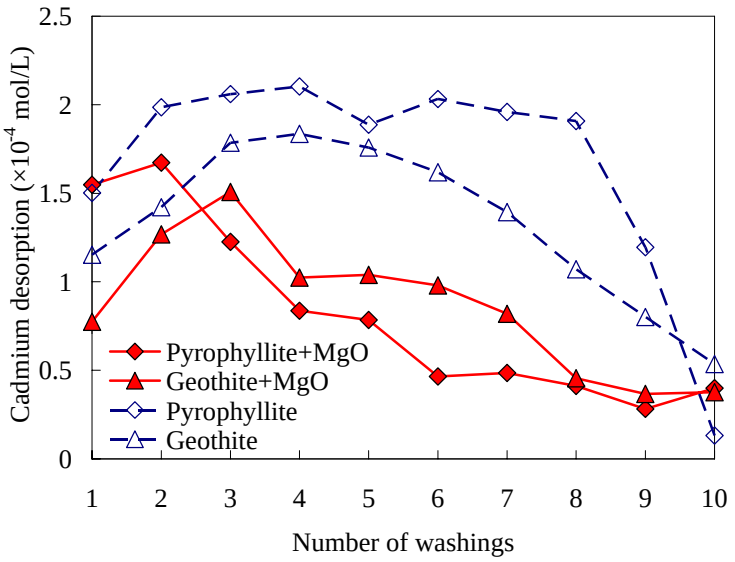

Fig.1. Behavior of Cd desorption in the samples which Cd was sorbed with MgO. Amonts of Cd desorption are shown in pyrophyllite sample (◆) and goethite sample (▲) added MgO. The results in the pyrophyllite (◇) and goethite (△) without MgO are also illustrated for comparison.and

*takamats@vmas.kitasato-u.ac.jp

P015

Interfacial and precipitation reactions between soil colloids and water-soluble materials eluted from compost

K. Funaba[1], K. Kakisaka[1], K. Otsuki[1], M. Nanzyo[1]*
[1]*Graduate school of Agricultural Science, Tohoku University,*
1-1 Tsutsumidori-Amamiyamachi, Aobaku, Sendai, 981-8555, Japan

In order to avoid N and P loading to environment, recent manure composting is carried out under a roof. Organic and inorganic water-soluble materials are stored in the compost and the compost shows a high electric conductivity (EC). When the compost is applied to agricultural soils, several reactions take place between the water-soluble materials and soil colloids. We examined these reactions and estimated factors affecting the water-percolation in a lowland soil using a soil column overlain by cattle manure compost (CMC). The results showed that with watering the column, a large amount of dissolved organic matter (OM) and K^+ were released from CMC and they reduced water-percolation in the soil (Fig. 1). The K^+ from CMC incorporated in the soil replaced Ca^{2+} at the exchange site in the soil. The Ca^{2+} reacted with the dissolved OM to precipitate and the precipitate clogged capillary pores in soil. Due to precipitation of Ca-OM complex, EC values of the solution in the soil were relatively low, K^+ saturation at the soil colloid surface increased and swelling of the K^+-clay might also have involved in reducing water-percolation in the soil. Although many bubbles were present in the soil column, the abundance of the bubbles appeared to be similar between soil columns with and without CMC. Other changes in soil with CMC were increases in labile P, OM and CEC. In contrast to the lowland soil, reduction of water-percolation was not significant in the soil column in which an Ap horizon soil of nonallophanic Andisol was filled. Due to its high preference to Ca^{2+}, exchange of Ca^{2+} with K^+ in the nonallophanic Andisol was less than that in the lowland soil.

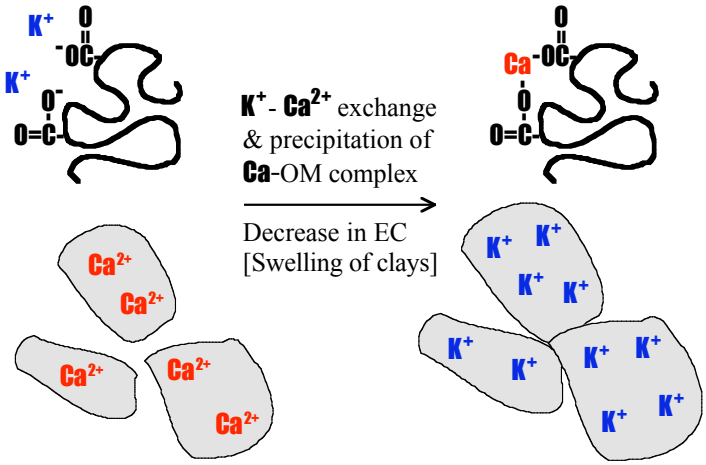

Fig. 1. Suggested mechanisms related to reduction of water-percolation in a lowland soil overlain by cattle manure compost.

*nanzyo@bios.tohoku.ac.jp

P016

Effects of bound water on the measurement of solid-phase permittivity for volcanic soils

T. Miyamoto[1]*, K. Kameyama[1]

[1] *National Institute for Rural Engineering, National Agriculture and Food Research Organization, 2-1-6 Kannondai, Tsukuba, Ibaraki 305-8609*

Volcanic soils have a unique aggregate structure and large volumes of bound water. Therefore, the effects of bound water on measurements of solid-phase permittivity need to be evaluated for volcanic soils even though bound water is often assumed similar to ice with much lower permittivity than free water. The effective permittivities (ε_{eff}) for both air-dried and oven-dried samples were measured when immersed in fluids with different permittivities. Moreover, the ε_{eff} was calculated from the permittivities of ice (ε=3.2) and free water (ε=80.4) by using a dielectric mixing model. When the permittivity of water was assumed 80.4, the calculated ε_{eff} values agreed well with the measured ε_{eff} for air-dried soil. Contrarily, when the permittivity value of water was assumed 3.2, the calculated ε_{eff} values were underestimated when compared to the measured ε_{eff} for the air-dried soil (Fig. 1). The ε_{eff} values calculated by ε = 3.2 correspond well with the measured ε_{eff} for oven-dried soils. These results suggest that the permittivity of water in air-dried soils is similar to free water rather than ice. Therefore, the amount of bound water causes an overestimation in the solid-phase permittivity if air-dried soils with large specific surface areas are examined.

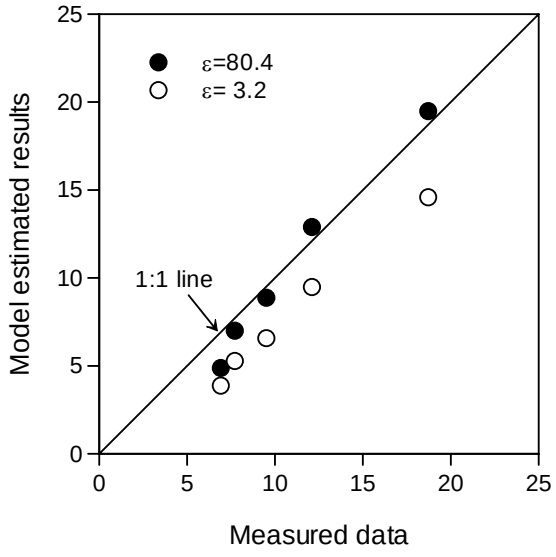

Fig. 1. Comparisons between measured effective permittivities and values estimated by the dielectric mixing model.

*teruhito@affrc.go.jp

P017

Effect of an allophone-imogolite on the formation humic-like compounds from catechol and glycine.

A. Miura[1]*, M. Fukushima[1], M. Sasaki[2], K. Izumo[1]

[1]*Division of Solid Waste, Resources and Geoenvironmental Engineering Graduate School of Engineering, HokkaidoUniversity, Sapporo, 060-8628*

[2]*National Institute of Advanced Industrial Science and Technology, 2-17-2-1Tsukisam-Higashi, Toyohira-ku, Sapporo, 062-8517*

A ligno-protein theory is known to be one of possible pathways for the genesis of humic substances (HSs). This indicates that phenolic compounds from wood lignin can bind to amino acids from biota via the nucleophilic reaction. Such the formation of HSs is mainly due to biological processes. However, influences of abiotic processes, such as catalytic reactions on clay minerals, have not been studied. Clay minerals can serve as solid acid catalyst that can enhance the nucleophilic reactions. In the present study, the influences of clay minerals on the formation of humic-like substances from phenolic compounds and amino acids were investigated, in terms of reaction products. In this works, catechol (CT) and glycine (Gly) were used as models for phenol compounds and amino acids, respectively. The clay mineral used was Kanuma soil (allophone-imogolite), and the mixture of CT and Gly was prepared as a control. First the amounts of humic-like substances formed were compared using an E_{600} value that represents the absorptivity at 600nm. After a two-week reaction period, E_{600} values in the presence of Kanuma soil was significantly higher than that in the absence of clay mineral (CT+Gly) (Fig.1). This suggests that the presence of such clay minerals results in enhancing the formation of humic-like substance. The formed humic-like compounds were analyzed by FT-IR, pyrolysis-GC/MS and solid state CP-MAS ^{13}C NMR (Fig.2) spectroscopies. There results indicate that nitrogen atom in Gly can bind to aromatic carbons in CT, and this leads to the formation of anilino compounds and imines.

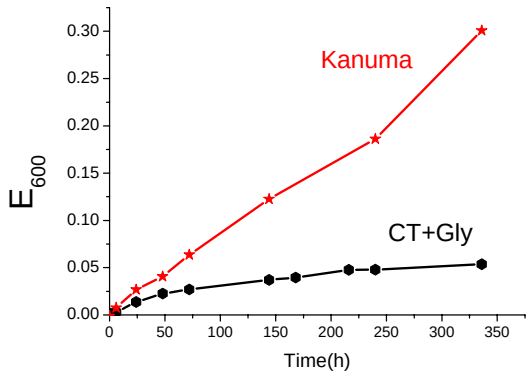

Fig.1 Variation in E_{600} values

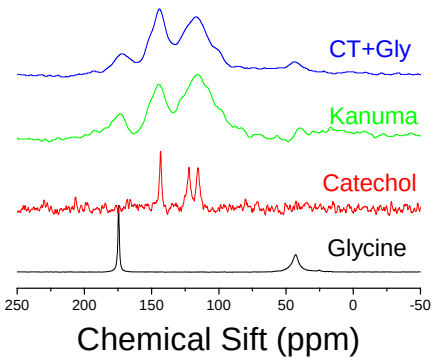

Fig.2 Solid state CP-MAS ^{13}C NMR spectrum

m-fukush@eng.hokudai.ac.jp

P018

Effect of humic acid on the water repellency of imogolite membrane

M. Kumagai*, Y. Watanabe, Y. Adachi
Graduate School of Life and Environmental Science, University of Tsukuba,
1-1-1 Tennoudai , Tsukuba, Ibaraki 305-8573, Japan

In the present study, we fabricated imogolite membrane from pure suspension of imogolite. Imogolite sample was purified from natural soil located at the upper portion of pumice layer at Kitakami Iwate prefecture in Japan, according to the method of [1)]Yoshinaga and Aomine. The membrane was fabricated on a hydrophilic filter paper.

Using fabricated membrane, the contact angle of water droplet on the membrane was measured as a function of the concentration of humic acid when the membrane was fabricated. In order to clarify the effect of ionic strength, the measurement of contact angle was carried out for distilled water and 2.0M NaCl solution at pH 4.81.

The obtained result indicated that contact angle increases with increase of humic acid and demonstrates the plateau (Fig.1). It is considered that the surface free energy of the membrane decreased by adsorption on the surface of membrane of humic acid. The increase of contact angle with increase in concentration of humic acid had a threshold. The contact angle with 2M NaCl solution was larger than that with distilled water.

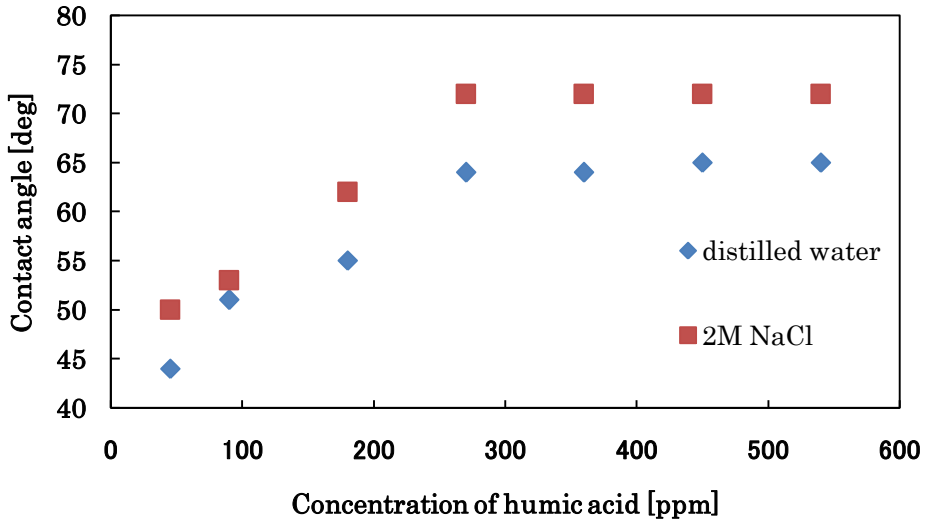

Fig.1 Contact Angle plotted against the concentration of humic acid for different solutions.

REFERENCE

[1)]Yishinaga. N and Aomine. S (1962 a) SoilSci. Plant Nutr. (Tokyo), 8(2), 6-13

*ybgsp681@yahoo.co.jp

P019

Anion-exchange property of the functional charcoal prepared from plant wastes

T.Takahashi[1], R.Yokoyama[2], S.Hayashi[2] and T.Iwata[2]*

[1]*Shizuoka Prefectual Research Institute of Agriculture and Forestry, 678-1Tomioka, Iwata, Shizuoka 438-0803*

[2]*Okayama Laboratory, Nisshoku Corporation, 5325-2 Haga, Okayama 701-1221*

The functional charcoal we developed has high NO_3^--N adsorption ability. It is prepared from wood waste by dipping in $CaCl_2$ solution, carbonizing at proper temperature and acid treatment. In this study, various plant wastes such as coffee grounds, soybean sauce refuse, tofu refuse, bagasse, apple juice refuse and hinoki bark were investigated as raw materials. NO_3^--N adsorption abilities of samples washed with water or treated with HCl are shown in Fig.1. When coffee grounds were used as a raw material, the highest adsorption amounts were obtained, 17.8 mg/g for washed samples and 19.5 mg/g for acid-treated samples, respectively. Moreover, NO_3^--N adsorption ability of each sample treated with HCl was higher than that washed with water. NO_3^--N adsorption abilities of the samples except for coffee grounds were enhanced by a factor of approximately 1.5 to 2 by acid treatment. Furthermore, the charcoal from coffee grounds shows high adsorption ability against fluoride anion, but extremely low adsorption against sulfuric and phosphoric anions. It is experimentally-confirmed that the adsorption is anion-exchange with chloride anion as shown in Fig.2. The NO_3^--N adsorbed with the functional charcoal can be effectively used by plants as fertilizer. It is suggested that the functional charcoal with NO_3^--N adsorption ability can contribute to nitrogen cycle by purifying NO_3^--N pollution and promoting the growth of plant.

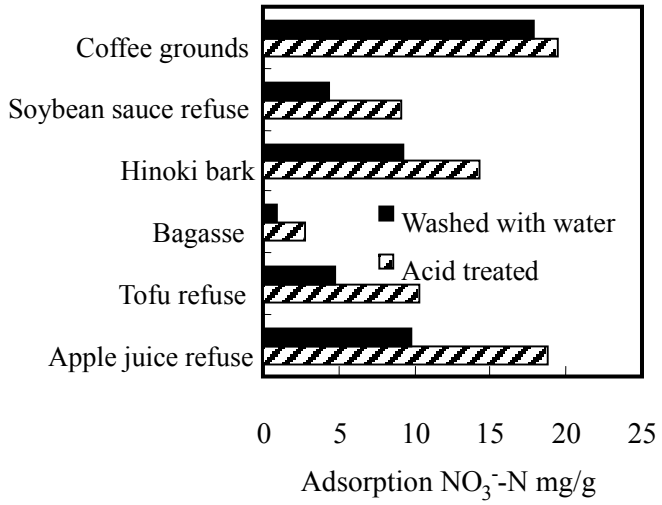

Fig.1 NO_3^--N adsorption when using various plant wastes as raw materials.

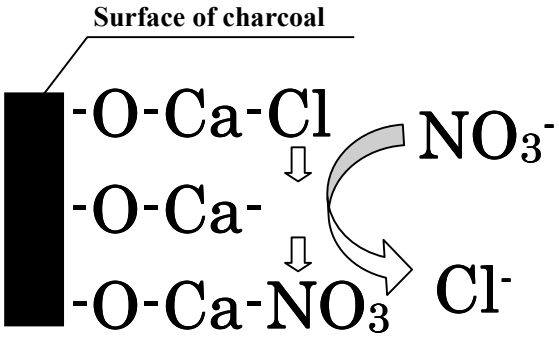

Fig.2 Anion exchange of the functional charcoal.

*okayama-re@nihon-shokusei.co.jp

P020

Chemical fractionation and behavior of Zn, Cu and Mn in upland fields after long-term application of pig farm manure

K. Asada[1]*, M. Kato[1], T. Nishimura[2]

[1]*Graduate School of Agriculture, Tokyo University of Agriculture and Technology, 3-5-8 Saiwaicho, Fuchu, Tokyo 183-8509 Japan*

[2] *Graduate School of Agricultural and Life Sciences, University of Tokyo, 1-1-1 Yayoi, Bunkyoku, Tokyo 113-8657 Japan*

Heavy metal contamination in agricultural fields by excessive and continuous application of livestock manure has become evident. The application of pig farm manure (PFM) not only results in the accumulation of heavy metals in the plow layer, but also enhances transfer of heavy metals toward deeper layers. Soils were sampled at fields under chemical fertilizer (CHF, 360 kg-N ha^{-1} $year^{-1}$), 53 Mg-PFM ha^{-1} $year^{-1}$ (SM, 360 kg-N ha^{-1} $year^{-1}$) and 160 Mg-PFM ha^{-1} $year^{-1}$ (TM, 1080 kg-N ha^{-1} $year^{-1}$) application during 13 years. We examined the adsorption characteristics of Zn, Cu and Mn by six-step sequential extraction procedure. Also, adsorption isotherms of Zn in the soils applied chemical fertilizer and PFM were determined.

Adsorption isotherm of Zn was fitted with Freundlich isotherm. Distribution coefficients for adsorption isotherms of Zn, K_F(dm^3 kg^{-1}), increased as the amount of applied PFM increased as follow Fig. 1. Greater K_F suggests higher Zn adsorption capacity of the soil in the plow layer.

Metal-organic-complex-bound (Me-Org), exchangeable-with-CH_3CO_2Na (NaOAc) and water soluble-exchangeable (EXCH) Zn fractions of soils from 0-60cm deep layers under the TM and SM were significantly greater than those under the CHF. On the other hand, H_2O_2-extractable-organically-bound (H_2O_2-Org) fractions of the same layers were less than those under the CHF. Outer-sphere complex form with organic matter can not retain Zn strongly. Following to PFM decomposition, Me-Org, heavy metals associated with humic acid and fulvic acid in the soil, and H_2O_2-Org, heavy metals associated with persistent organic matter (ex. soil organic matter taken up by soil organisms) changed to be more mobile, EXCH and NaOAc extractable forms.

Even though adsorption capacity of Zn may increase with PFM application, the greater amount of mobile Zn is likely to be moved downward by water percolation and moved laterally by surface water runoff after excessive and continuous application of PFM to the soil over a long time.

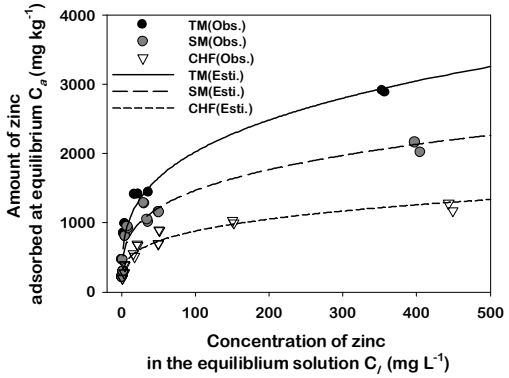

Fig.1 Adsorption isotherms of Zn in the plow layer

*50005951034@st.tuat.ac.jp

P021

^{13}C PST/MAS and CP/MAS NMR for estimation of biodegradation properties of environmental organic matters at hydrated and desiccated states

A. Suetsugu[1]*, K. Asakura[2], T. Miyazaki[3], K. Hori[4]

[1]*Arid Land Research Center, Tottori University, 1390 Hamasaka, Tottori 680-0001*

[2]*Catalysis Research Center, Hokkaido University, 10 N21W Kita-ku, Sapporo, Hokkaido 001-0021*

[3]*Graduate School of Agricultural and Life Sciences,*
The University of Tokyo, 1-1-1 Yayoi, Bunkyo-ku, Tokyo 113-8657

[4]*Graduate School of Engineering, Nagoya Institute of Technology,*
Gokisho-cho, Showa-ku, Nagoya, Aichi 466-8555

For a precise estimation of the fate of organic matters (OMs) in the environment, the stability of macromolecular structures of the OMs and its relation to the surface hydration properties should be understood. In the present study, the biodegradation properties of environmental OMs (a sewage sludge and a peat) under a wet (-30 J/kg water potential; the optimum moisture for aerobic biodegradation) and an extremely dry (-100 kJ/kg water potential) conditions were investigated by 70-days laboratory incubation. Incubated samples were subjected to chemical analysis and molecular mobility analysis at hydrated (D_2O-added) and desiccated states. Chemical composition and molecular mobility of the OMs were estimated by the ^{13}C pulse saturation transfer/magic angle spinning (PST/MAS) and the cross polarization transfer (CP)/MAS nuclear magnetic resonance spectroscopy (NMR). The results suggested that an experience of aerobic condition made the hydrophobic aromatics in the peat to be irreversibly mobile. The increase in molecular mobility was explained by fragmentation and surface exposure of polymerized aromatics. However, the mobilized aromatics performed still more resistance to further biodegradation compared to the mobile aliphatics in the OMs. In the sewage sludge, some of the fragmented (poly)saccharide structures in the incubated sewage sludge could be re-stabilized by hydrogen bonding upon hydration.

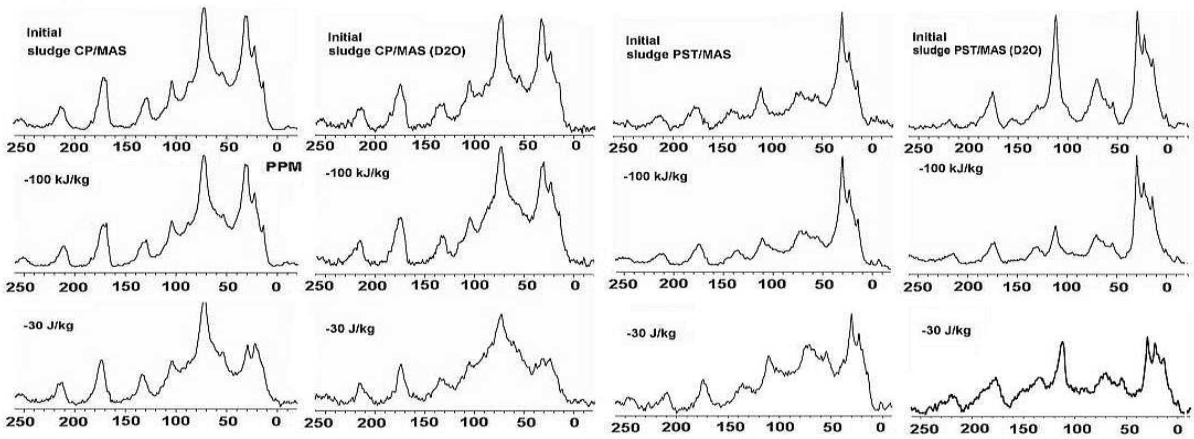

Fig. 1 Example of NMR spectra of environmental organic matter (sludge sample)

*suetsugu@alrc.tottori-u.ac.jp

P022

Removal of Phenol from Aqueous Solution using Hydrogel Media

G.F. Pan*, K. Kurumada

Graduate School of Environment and Information Sciences, Yokohama National University,
79-1 Tokiwadai, Hodogaya-ku, Yokohama 240-8501

Following our preceding results of fabricating phenol-adsorbing hydrogel, we aimed to prepare a gel adsorbent for removal of phenol from its aqueous solution. As a practical requirement, the gel adsorbent needs to be durable in repeated uses in adsorption and desorption. In our previous works, we succeeded in fabricating N-isopropylacrylamide (NIPAM) hydrogel incorporated with tributyl phosphate (TBP). This hybrid gel showed a potential adsorption ability to phenol dissolved in water. In this work, we succeeded in sealing the above hybrid gel completely with poly (vinyl alcohol) (PVA) thin layer coating by repeated freezing and thawing. The coated hybrid gel was remarkably improved in its mechanical durability. In the performance of adsorption of phenol, the PVA thin layer coating hardly hindered the mass transfer of phenol. The mechanical durability was sufficiently improved for both adsorption of phenol in aqueous solution and desorption (stripping) of the adsorbed phenol by immersing the adsorbent gel in sodium hydroxide solution (Fig. 1). The cycle of the adsorption and desorption could be repeated without loss of the phenol adsorbing ability.

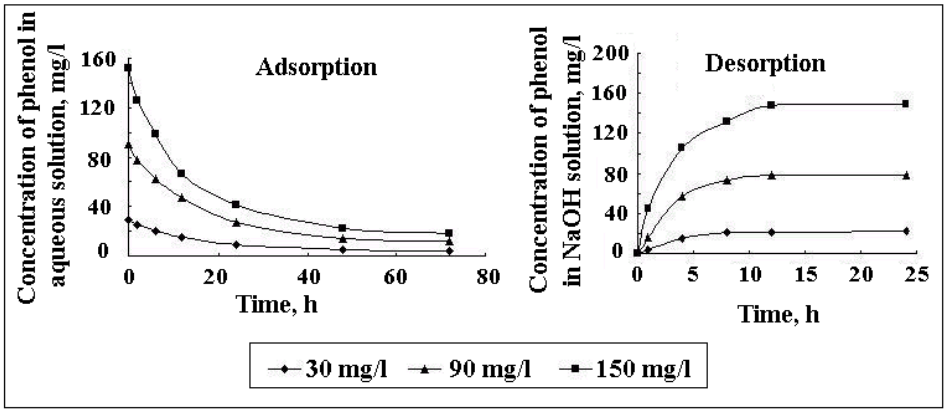

Fig.1 Phenol adsorption in aqueous solution using the reinforced hybrid gel as adsorbent and desorption of phenol adsorbed using 0.1 M sodium hydroxide solution at 25℃

---

*d06tb902@ynu.ac.jp

P023

Power law tailing in removal of pollutants from water to gas: a invasion percolation and random walk model study

Takuya Kawanishi*, Dastagir Muhammad Rehan, Hironori Sugiyama
Graduate school of Natural Science and Technology, Kanazawa University, Kakuma-machi, Kanazawa 920-1192

Power law tailings are often seen in removal of pollutants from soil or ground water. Present knowledge tells us that power law can occur due to Freundlich type adsorption, distribution of diffusion rate in micropores. In addition, we propose a hypothesis that the power law can be caused by the distribution of diffusion distance of pollutants in water phase, in the groundwater and soil remediation technologies involving the mass transfer between water and gas phases, such as vapor extraction and air sparging.

In order to prove this, we constructed a model for removal of solute in water by diffusion to gas based on the invasion percolation and random walk. In a simple cubic bond lattice, invasion percolation is performed, assuming that the invading phase is gas and remaining phase is water. After gas and water configuration was calculated by the process of invasion percolation, a particle was placed at the center of each water filled throat, and the gas and water interface was set as absorbing ends. Then diffusion process was calculated with random walk method.

The removal rate of the particles from the lattice filled with water and the top and bottom face are set as zero concentration or absorbing, we got the slope in double-log plot of -0.5, this was in good accordance with the theory. The power law behavior can be seen at the gaseous saturation of up to near the percolation threshold, and the absolute value of the slope in the double log plot increased from 0.5 at gas saturation 0 to about 1.0 near the threshold. Thus, we have got the power law tailings with exponent other than -0.5 in diffusion in water network invaded by gas phase. The effect of the shape of gas and water interface on the exponent will be investigated as one of the future work.

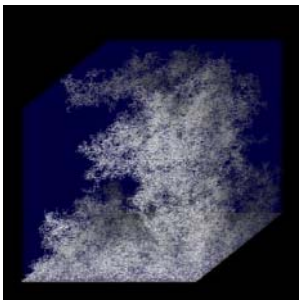

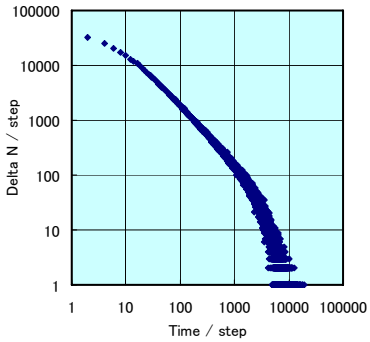

Fig. 1 (a) Example of gas and water configuration. (b) Power law tailing.

*kawanisi@t.kanazawa-u.ac.jp

P024

Adsorption of Basic Dye and Reactive Dye by Kaolin Coated with Chitosan

Soydoa Vinitnantharat* and Sonthirat Klankrong
Division of Environmental Technology
School of Energy, Environment and Materials
King Mongkut's University of Technology Thonburi
Prachauthit road, Thungkru, Bangmod, Bangkok 10140

This study aims to investigate the adsorption capacity for the removal of cationic dye of basic red 14 (BR14) and anionic dye of reactive red 141 (RR141) by kaolin coated with chitosan and compare to uncoated kaolin. The chitosan flakes 90% deacetylated was homogenized in acetic acid by varying the chitosan:acetic acid ratio of 0.5:1, 1:1 and 1.5:1 to make chitosan gel solutions. Each solution was used to coat on kaolin with the kaolin:chitosan ratio of 5:1. Results from scanning electron microscope revealed that chitosan could coated on kaolin and the amount of chitosan increased as the ratio of chitosan increased (Figure 1). In addition, the pore volume and pore size of coated adsorbent increase as the ratio of chitosan increased. The FTIR-spectrum shows the difference peaks between common kaolin and chitosan coated kaolin. The chitosan coated kaolin has got amino group from chitosan. The values of pH of solution (pH_{sol}) and pH of zero point of charge (pH_{zpc}) were around 7 for both of coated and uncoated kaolin. Investigation of adsorption capacity using adsorption isotherm revealed adsorption of dyes followed both Langmuir and Freundlich adsorption models. Uncoated kaolin could increased adsorption capacity for the removal of BR14, whereas the chitosan coated kaolin gave maximum adsorption capacity for the removal of RR141. This due to the amino functional group could enhance the adsorption of negative charge of RR141. Results also showed that the highest adsorption capacity of coated and uncoated kaolin occurred at pH of 9 and 5 for the removal of BR14and RR141, respectively. Results from desorption studies revealed that uncoated kaolin could desorbed reactive dye easier than coated kaolin, whereas the chitosan coated kaolin could desorbed BR14easier than uncoated kaolin as shown in Figure 2. Hence, chitosan coated kaolin can be used for post treatment of textile wastewater.

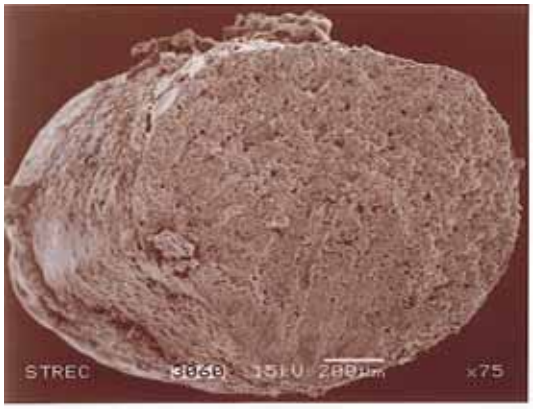

Figure 1 SEM micrograph of kaolin coated with chitosan chitosan:acetic acid ratio of 1.5:1

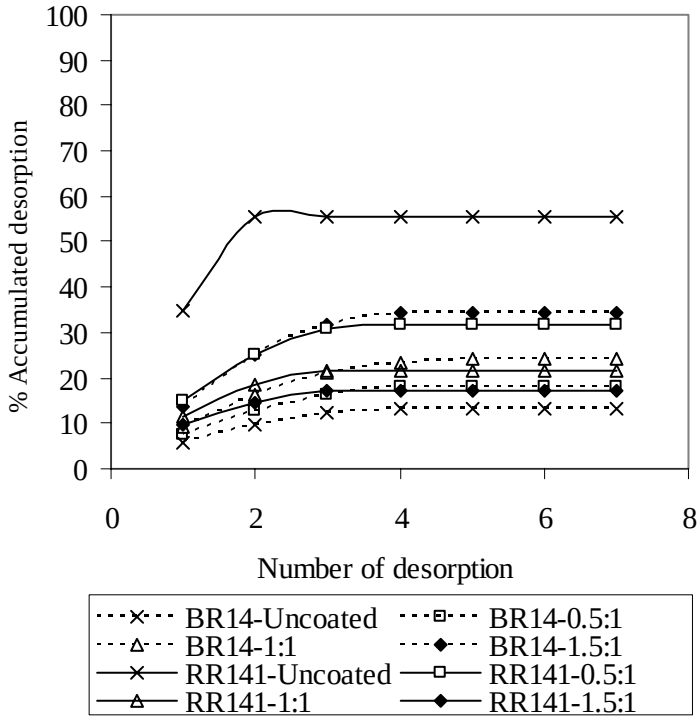

Figure 2 Desorption of sorbed dyes in buffer solution

*soydoa.vin@kmutt.ac.th

P025

Prediction of plant availability of radioactive ^{137}Cs by using radiocesium interception potential

H. Tsukada[1]*, A. Takeda[1], S. Hisamatsu[1], A. Nakao[2]

[1]*Department of Radioecology, Institute for Environmental Sciences, 1-7 Ienomae, Obuchi, Rokkasho-mura, Kamikita-gun, Aomori 039-3212, Japan*

[2]*Laboratory of Soil Science, Graduate school of Agriculture, Kyoto University, Sakyo-ku, Kyoto 606-8502, Japan*

It is important to estimate the internal radiation dose from radionuclides through food ingestion. Therefore, it is necessary to predict the concentration of radionuclides in agricultural plants. Radioactive ^{137}Cs is one of important radionuclides for the assessment of radiation exposure to the public, because of its high fission yield, long-half life (30.2 y) and transferability in the environment. In the present study, soil and potato tuber samples (26 sites) were collected throughout Aomori Prefecture, Japan and the concentration of fallout ^{137}Cs in the samples were determined. The specific retention of radiocesium in soils is associated with Cs^+ selective sorption on frayed edge sites (FES) located at the edge on the mineral particles. The FES abundance can be estimated by the radiocesium interception potential (RIP), which is defined as the selective coefficient of $^{137}Cs^+$ against K^+ in the FES abundance. When $^{137}Cs^+$ is adsorbed on the FES, the concentration of ^{137}Cs in plant can be written under the assumption of a constant K concentration in soil solution as follows:

$$C_{137Cs}^{BPlant} = \alpha\, C_{137Cs}^{BSoil} / RIP$$

where α is a constant value dependent on a kind of plant, and the C_{137Cs}^{BPlant} and C_{137Cs}^{BSoil} are the concentration of ^{137}Cs in plant and soil, respectively. The range of observed RIP value was 410-5,600 μmol g^{-1}. Abundance of soluble ^{137}Cs in soils, i.e. the ratio of ^{137}Cs concentration in the soils against RIP, was well correlated with the concentration of ^{137}Cs in the potato tubers (Fig. 1). Therefore, the RIP value was a useful parameter for predicting soil-to-plant transfer of ^{137}Cs. This work was performed under contract with the Aomori Prefectural Government, Japan.

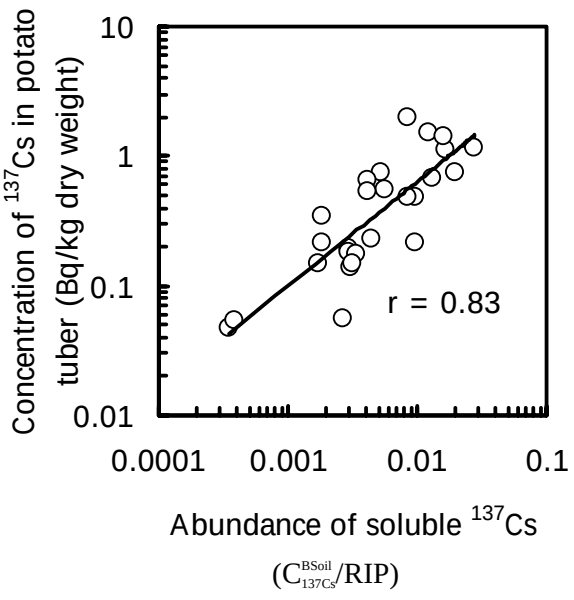

Fig. 1 Relationship between concentration of ^{137}Cs in potato tuber and abundance of soluble ^{137}Cs which is the ratio of ^{137}Cs concentration in soil against RIP.

*hirot@ies.or.jp

P026

Effect of pore size on colloidal transport phenomena in porous media

Koichi SUTO[1*], Yasuhiko YOSHINO[1], and Chihiro INOUE[1]
[1]*Department of Environmental Studies, Tohoku University,*
6-6-20, Aramaki, Aoba-ku, Sendai, 980-8579, JAPAN

Since the colloidal transport in porous media was affected from pore size, colloidal particle flowed faster than liquid solutions and ions. It has been suggested that size exclusion effect caused the transport phenomena. However, the details of the phenomena have still unknown and no suitable mathematical model has been established. The objective of this study was to clarify the colloidal transport phenomena in porous media. Colloidal transport experiments were carried out using one-dimensional columns consisted of several particle size distributions of spherical glass beads or silica sand. In these experiments polystyrene particles, diameter 1, 2 or 3 μm, were used as colloids injected into columns. Concentrations of colloidal particles in the effluent from the columns were measured using spectral photometer. Also tracer experiments using KCl solution were carried out under the same condition with colloidal transport experiments. Some results were summarized in Table1 and 2. In the case of glass beads used for the column materials, the phenomena were confirmed in the case of 500 - 710 and 710 - 990 μm glass beads used as the column materials although not confirmed in the column used smaller glass bead, 350 - 500 μm. Therefore faster flow of colloid occurred in case of bigger pore size. This fact suggested that the reason that colloidal transport became faster than tracer was not able to be explained by only the size exclusion effect. On the other hands, in the case of silica sand, the phenomena which colloids flowed faster than tracer were confirmed in all experiments. Although the size distributions on silica sands and glass beads were almost same, the results were different. By several calculations, it was clear that pore size distributions used silica sand was much wider than glass bead because these shapes were different. It was estimated that pore size distribution was much important for the colloidal transport phenomena than pore size in porous media.

Table 1 Results of colloidal transport phenomena in glass bead porous media. Flow rate : 8cm/h, colloidal particle diameter : 2μm. Result of tracer experiment are shown in parentheses.

Size distribution[μm]	Time of start flowing out[-]	Time of peak[-]	Recovery rate[-]
350 - 500	0.73 (0.73)	1.06 (1.06)	1.16 (1.16)
500 - 710	0.58 (0.64)	0.81 (0.94)	1.06 (0.88)
710 - 900	0.69 (0.81)	0.90 (1.08)	1.11 (0.97)

Table 2 Results of colloidal transport phenomena in silica sand porous media. Flow rate : 8cm/h, colloidal particle diameter : 2μm. Result of tracer experiment are shown in parentheses.

Size distribution[μm]	Time of start flowing out[-]	Time of peak[-]	Recovery rate[-]
300 - 425	0.61 (0.73)	0.97 (1.08)	0.85 (1.03)
600 - 850	0.53 (0.70)	0.74 (0.95)	0.79 (1.25)

*suto@mail.kankyo.tohoku.ac.jp

P027

Anion Exchange Properties of Hydrous Metal Oxides. Analysis Based on Surface Coordination with Stability Constant Data Base

K. Ooi*

National Institute of Advanced Industrial Science and Technology, Shikoku Center (AIST-Shikoku)
2217-14, Hayashi-cho, Takamatsu 761-0395

Studies of anion exchange properties of hydrous metal oxides (HMeOs) are important in the field not only of fundamental surface or separation chemistry but also of environmental- or geo-chemistry. Two kinds of anion exchange (adsorption) reactions are known with HMeO,

$$M\text{-}OH + X^- \rightleftarrows M\text{-}X + OH^- \quad \text{(ligand exchange)} \quad (1)$$

$$M\text{-}OH + X^- + H^+ \rightleftarrows M\text{-}OH_2^+\text{-}X^- \quad \text{(protonation)} \quad (2)$$

where M is central metal atom of HMeO. Selectivity sequences on different kinds of HMeO vary depending on the kind of central metal atoms

This paper shows that stability constant (SC) data base compiled by IUPAC is useful to predict the selectivity sequence of anion exchange on HMeO, especially consisting of trivalent and divalent metals. When the random mixing can be assumed for exchanged anions with a constant number of exchange site, the anion exchange reaction can be treated as a homogeneous solution reaction of complex formation. The first stepwize stability constant (K_1) can be written as follows,

$$M^{n+}_{aq.} + X^- \rightleftarrows MX^{n-1} \qquad K_1 = [MX] / [M][X] \quad (3)$$

where metal ion M^{n+} is in a hydrated form. Since metal ions are hydrated before the complexation reaction, the stability constant corresponds to the value of H_2O/X^- legand exchange. The anion exchange reaction of HMeO can be written by two step reaction as follows,

$$\boxed{M}\text{-}OH \xrightarrow[(K_{1,OH}{}^{-1})]{OH^-/H_2O\ \text{exchange}} \boxed{M}\text{-}OH_2^+ \xrightarrow[(K_{1,X})]{H_2O/X^-\ \text{exchange}} \boxed{M}\text{-}X \quad \text{(inner sphere complexation)}$$

$$\boxed{M}\text{-}OH_2^+ \xrightarrow[(K_{1,X})]{+X^-} \boxed{M}\text{-}OH_2X \quad \text{(outer sphere complexation)}$$

where $K_{1,OH}$ and $K_{1,X}$ are the stability constants given as follows,

$$M^{n+}_{aq.} + OH^- \rightleftarrows M(OH)^{n-1} \qquad K_{1,OH} = [M(OH)] / [M][OH] \quad (4)$$

(stability constant for OH coordination)

$$M^{n+}_{aq.} + X^- \rightleftarrows MX^{n-1} \qquad K_{1,X} = [MX] / [M][X] \quad (5)$$

(stability constant for X coordination)

The selectivity of anion exchange can be evaluated from the value of $K_{1,X}$, since the stability constant ($K_{1,OH}$) of H_2O coordination is constant. The selectivity sequences of anion exchange were correlated comparatively well with the orders of first stepwise stability constants ($K_{1,X}$) of the corresponding metal-ligand complexes. Conditions whether inner sphere or outer sphere surface complex forms could be evaluated by the difference in the stability constant between the OH^-/X^- (X^-: anion) and OH^-/H_2O ligand exchange reactions.

* k-ooi@aist.go.jp

P028

Temperature-Swing Adsorption of Proteins in Water Using Polymer-Grafted Silica Particles

S. Morisada*, S. Suzuki, K. Namazuda, Y. Hirokawa, Y. Nakano

Department of Environmental Chemistry and Engineering, Tokyo Institute of Technology, 4259 Nagatsuta, Midori-ku, Yokohama, Kanagawa 226-8502, Japan

In wastewater treatment using adsorbent, simple processes for adsorption and desorption of the target substances are desirable. If the adsorption amount is controlled only by temperature, recycling of adsorbent and process simplification can be achieved. In the present study, the temperature-swing adsorption of bovine serum albumin (BSA) in water has been achieved using the temperature-sensitive adsorbent. This protein is negatively charged above its isoelectric point of pH 4.8 and has the denaturation temperature around 336 K. As temperature-sensitive adsorbent, therefore, we employed the copolymer-grafted silica particles, where the copolymer consists of vinylbenzyl trimethylammonium chloride (VBTA) and *N*-isopropylacrylamide (NIPA): polyNIPA is a well-known temperature-sensitive polymer having a lower critical solution temperature around 306 K. The adsorption/desorption of BSA on/from such copolymer-grafted silica particles was investigated by the temperature-swing operation at 298 and 313 K, and as a result, we found that the copolymer-grafted silica particles adsorbed BSA at 298 K and released some of BSA adsorbed by increasing temperature to 313 K, as seen in Figure 1. It is worth noting that the copolymer-grafted silica particles can repeatedly adsorb and desorb BSA by the temperature-swing operation. This adsorption/desorption behavior of the copolymer-grafted silica particles is attributed to the temperature-sensitivity of NIPA.

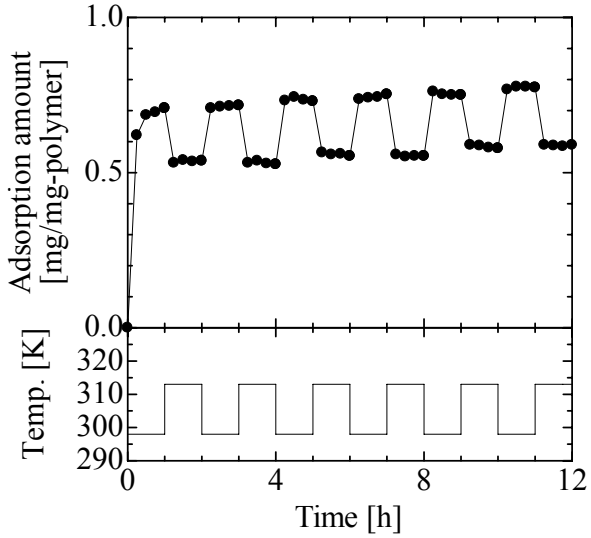

Figure 1. Time and temperature dependence of amount of BSA adsorbed on the poly(NIPA-*co*-VBTA)-grafted silica particles.

smorisada@chemenv.titech.ac.jp

P029

Volatilization of organic compounds from sandy soil

T. Moroizumi[1]*, Y. Sasaki[2], T. Miura[1]

[1]*Graduate School of Environmental Science, Okayama University,*
3-1-1 Tsushima-naka, Okayama 700-8530

[2]*Nikka-Engineering Corp.,*
3-12-4 Namiyoke, Minato-ku, Osaka 552-0001

The volatilization of organic compounds such as TCE (trichloroethylene) and oils from soils and groundwater has become a serious environmental issue. The objective of this study is to experimentally investigate the fundamental characteristics of the volatilization of organic compounds from soils. Batch type experiments for the volatilization of organic compounds were carried out in a laboratory under a constant room temperature. HFE-7100 (hydro-fluo-ether-7100) and ethanol were used for the experiments as the simulated organic contaminants. HFE-7100 (hydro-fluo-ether-7100) and ethanol are non-aqueous and aqueous, respectively. Distilled water was also used for reference. Toyoura sand was applied as the soil material. The volatilization of the organic compounds from sand, which was saturated with the above compounds, was completed after about 35 hours for the HFE-7100 and after 80 hours for the ethanol (Figure 1). The evaporation of the distilled water, on the other hand, was not completed until after about 250 hours. The relationship between the levels of latent heat of volatilization and the volatilization fluxes was approximated in a logarithmic function (Figure 2). The volatilization fluxes were also related to the levels of saturated vapor pressure. The progress of volatilization is closely related to the physical properties of organic compounds such as latent heat and saturated vapor pressure.

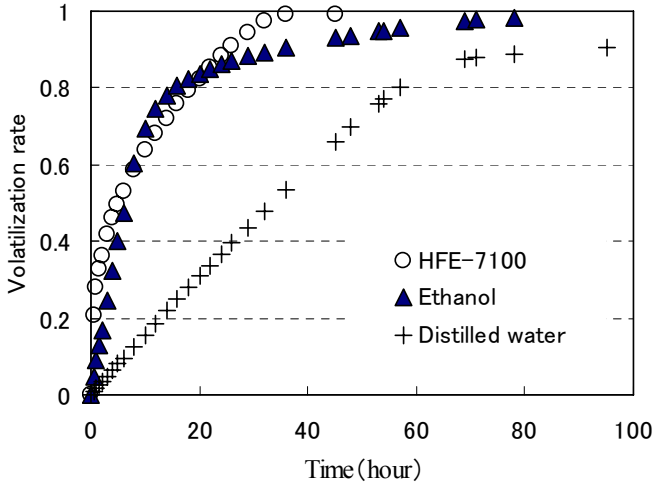

Fig. 1 Volatilization rate of HFE-7100, ethanol, and water from saturated sand.

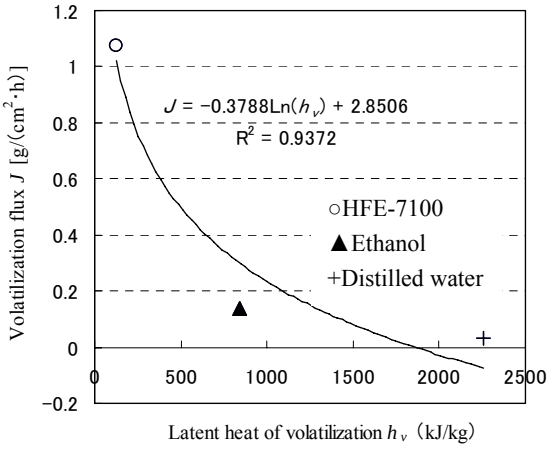

Fig. 2 Relationship between latent heat of volatilization and volatilization flux.

*morot@cc.okayama-u.ac.jp

P030

Microscopic observation of deposition of colloidal particles onto single glass bead: effect of salt concentration

Y. Kusaka*, Y. Yamashita, Y. Adachi
Graduate School of Life and Environmental Sciences, University of Tsukuba
1-1-1, Tennoudai, Tsukuba, Ibaraki, 305-8572 Japan

Deposition of polystyrene latex (PSL) particles onto single glass bead was observed through optical microscopy as a function of ionic strength. The rate of deposition was calculated from the increment of projected area of deposited particles. Glass bead with diameter of 200 μm was fixed on the center of a capillary tube (1mm x 0.2mm x 100mm). The suspension of PSL particles with diameter of 1.04 μm flowed through the capillary tube. Ionic strength of the suspension was adjusted by KCl solution. Zeta potential of glass bead and PSL particle were measured by means of streaming potential method and electrophoresis, respectively. On the other hand, stability ratio of PSL particles was calculated from the rate of Brownian coagulation obtained by turbidity method using spectrophotometer (UV1650PC, Shimazu). Normalized single collector efficiency and stability ratio of PSL particles as a function of ionic strength are shown in Fig. 1. Critical deposition concentration (CDC) is higher than that of critical coagulation concentration (CCC) by one order of magnitude. This discrepancy is considered to be the effect of flow. Normalized single collector efficiency slopes more gently than stability ratio in reaction-limited regime, which qualitatively agrees with the result of shear coagulation [1].

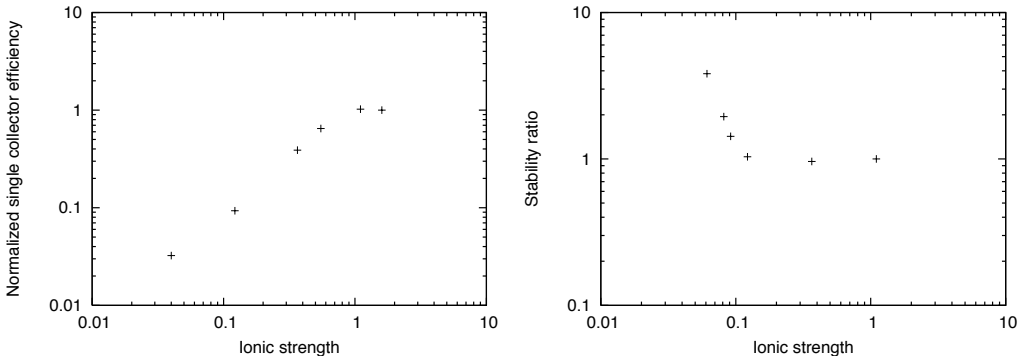

(a) (b)

Fig.1 Normalized single collector efficiency of PSL particles onto single glass bead (a) and stability ratio of PSL particles (b) are plotted against ionic strength.

[1] D.Sato, M.Kobayashi, Y.Adachi, Colloids Surf. A, 266 (2005) 150

* ksaka219@hotmail.com

P031

Prediction of Adsorbed Amounts of Volatile Chlorinated Organic Compounds to Soil

T. Kobayashi[1]*, Y. Shimizu[2], K. Urano[2]

[1]*Center for Risk Management and Safety Sciences, Yokohama National University, 79-5 Tokiwadai, Hodogaya-ku, Yokohama, Kanagawa, 240-8501.*

[2]*Graduate school of Environment and Information Sciences, Yokohama National University, 79-7 Tokiwadai, Hodogaya-ku, Yokohama, Kanagawa, 240-8501.*

The adsorption characteristics of volatile chlorinated organic compounds in soil must be clarified to understand the extent of the contamination and to select an effective cleanup condition. In this study, the adsorption equilibrium model to the soil at any water content was investigated. The model and a prediction method, in consideration of the adsorptions to the dry pore and the wet pore, the adsorption to the soil organic matter and the dissolution to water, were proposed. The adsorption equilibrium relation of each soils and each compounds could be expressed well by the dry pore adsorption ratio γ. γ could be expressed using the water content a. The predicted adsorbed amounts are compared with the measured data in Fig. 1. Both values for the 80% data agree well within ±30%.

Prediction equation：

$$C_{ST} = \gamma\left(5.53\times10^{-4}\times S - 0.00261\right)\times\exp\left[-\left(\frac{RT\ln(p_0/p)}{\beta E_0}\right)^{1.5}\right]\times\rho_L$$

$$+(1-\gamma)0.0005\frac{C_G}{H_{GW}}+0.0073P_{OW}^{0.5}\alpha\frac{C_G}{H_{GW}}+\frac{a}{(100-a)H_{GW}}C_G$$

C_{ST}：Equilibrium adsorbed weight per unit dry weight of soil,
C_G：Concentration of the adsorbate in gas.
γ ：Dry pore adsorption ratio
S ：Surface area
β ：Affinity coefficient.
ρ_L：Liquid density
H_{GW}：Henry's constant
α ：Organic carbon content
a ：Water content

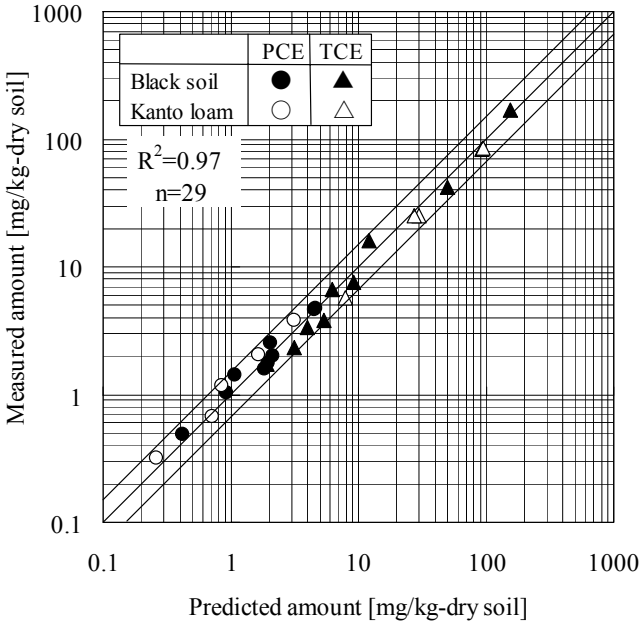

Fig.1 Comparison of the predicted amounts with the measured amounts.

*koba@ynu.ac.jp

P032

Density flow in a porous media caused by salt accumulation

Y. Kihara

Faculty of Life and Environmental Science, Shimane University

1060 Nishikawatsu, Matsue, Shimane 690-8504

The salt accumulation is a serious problem in the semi-arid and arid land agriculture. When the salt accumulation occurs, the solution density at the soil surface is higher than that in the lower zone. This state is called gravitational instability, but it had been considered that the solute doesn't move by this effect. To clarify this effect, two kinds of column experiments were conducted with Tottori dune sand. One is the evaporation experiment using different concentration solutions and another one is non-evaporation experiment which was used close type column. The result from the evaporation experiment showed that the shape of concentration profile was different because the density flow was occurred in high concentration solution. The result from the non evaporation experiment showed that the critical concentration which the density flow occurred existed. The process is governed by the non-dimensional Rayleigh number. The experimental results were agreed with the theory of Rayleigh number.

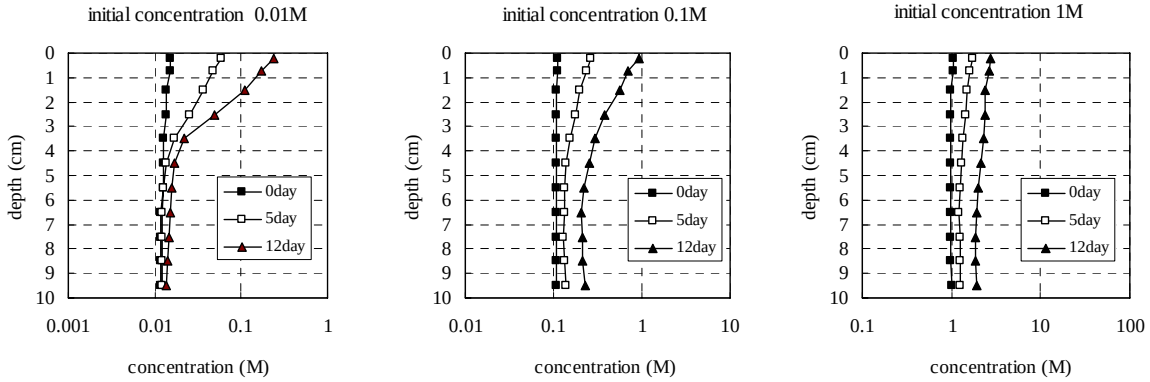

Fig. 1 Concentration profile for evaporation experiments

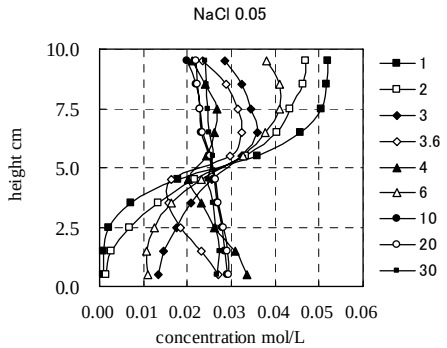

Fig. 2 Concentration profile for non evaporation experiments

kihara@life.shimane-u.ac.jp

IAP08 P033

Transport and Straining of Colloid-Sized Materials in Saturated Porous Media

D.T.K.K Chamindu [1], Ken Kawamoto [1]*, Hirotaka Saito [2], Scott A. Bradford [3], Per Moldrup [4], and Toshiko Komatsu [1]

[1] *Graduate School of Science and Engineering, Saitama University, Japan*

[2] *Institute of Symbiotic Science and Technology, Tokyo University of Agriculture and Technology, Japan*

[3] *USDA, ARS, US Salinity Laboratory, Riverside, CA, USA*

[4] *Department of Biotechnology, Chemistry and Environmental Engineering, Aalborg University, Denmark*

Recent observations of colloid-facilitated transport of sorptive contaminant (e.g., radioneuclides, pesticides, heavy metals, pathogens etc.) into groundwater have spurred research on transport and retention of colloid-sized materials in subsurface environments. Colloid attachment and straining are known as key colloid retention mechanisms in saturated porous media. This study investigated transport and retention of glass beads colloids (diameter 1-10 µm) and soil colloids extracted from volcanic ash soils (less than 1µm) in saturated Toyoura sand at different colloid concentrations and different flow rates by means of a series of column experiments. Deposition profiles of glass beads colloids were also examined. The results showed that glass beads colloids exhibited complete retention (presumably due to straining) at both high and low flow rates. Soil colloids, on the other hand, showed complete retention at low flow rate but showed significant recovery at high flow rate. Particle size distribution analysis of influent and effluent colloids revealed the deposition of smaller colloids (due to attachment) as well as larger colloids (due to straining) in the porous media. Glass beads colloid deposition was nonmonotonic with multiple peaks. The largest peak occurred near the column inlet and two secondary peaks at deeper layers. Particle size distribution analysis of deposited colloids revealed that largest colloids deposited near the column inlet (due to mechanical filtration and straining). Numerical analysis carried out using HYDRUS 1D code assuming first-order attachment, detachment and straining models revealed that straining is the dominant retention mechanism for both colloid types. Moreover, the simulated colloid deposition profiles, however, failed to capture essential multi peaks in the observed deposition profiles.

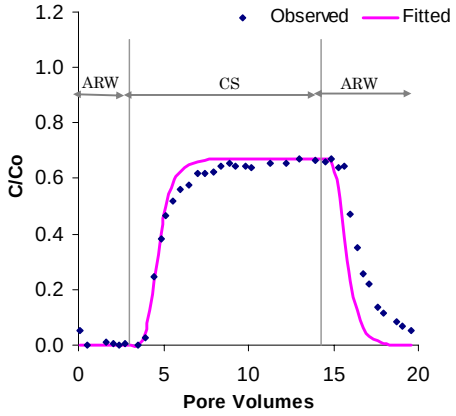

Fig. 1 breakthrough and breakdown curves of soil colloids
Darcy flow rate = 0.60cm/min, Initial concentration = 106mg/L

* kawamoto@mail.saitama-u.ac.jp

P034

Colloid-facilitated and dissolved cadmium transport through layered soils with subsurface cracks

X.-Y. Tang[1,2], H. Katou[1]*, K. Suzuki[1], T. Ohtani[1]

[1]*National Institute for Agro-Environmental Sciences, Tsukuba 305-8604, Japan*

[2]*Zuckerberg Institute for Water Research, Ben-Gurion University of the Negev, 84990 Israel*

Cadmium is among the most toxic heavy metals in soil, but its mobility in contaminated soils is not fully understood. Cadmium is readily sorbed on soil; however, the sorption is weaker than other heavy metals, with a considerable proportion in the exchangeable fraction. Prediction of Cd mobility in soil is further complicated by recent evidence that suspended mobile colloidal particles can substantially enhance the transport of sorbed contaminants. The objectives of this study were (i) to investigate relative contribution of colloid-facilitated and dissolved Cd transport to the total flux in contaminated soils with subsurface cracks which may act as preferential pathways for colloid transport, and (ii) to identify key processes controlling the downward transport of Cd from the contaminated soils. A clayey topsoil, with the clay fraction dominated by smectite, was spiked with 3 or 30 mg kg^{-1} of Cd after incorporating 0 or 25 mmol kg^{-1} of $Ca(OH)_2$. Simulated rainfall experiments were conducted using single-layer columns repacked with the Cd-spiked topsoil and dual-layer columns composed of the repacked topsoil and undisturbed subsurface soil with visible cracks. Distilled water or 5 mM $CaCl_2$ was applied intermittently to the columns at a rainfall intensity of 7 mm h^{-1} for 5 h on 6 consecutive days. The colloid concentration in the column effluent not only showed a quick response to the concentrations of coexisting ions, but was also affected by the remobilization of once-deposited particles after resuming the rainfall. Infiltration of $CaCl_2$ completely suppressed the discharge of colloidal particles and colloid-associated Cd while significantly enhancing dissolved Cd transport. Although Cd transport was predominantly in the dissolved form, colloid-associated transport accounted for 30–80% of the total transport when the ionic strength was lowered by the infiltration of distilled water. The addition of $Ca(OH)_2$ to the soil substantially reduced the dissolved Cd concentration, while the colloid particle transport was not appreciably affected. The colloid-associated Cd can be the main form of total Cd transport in limed soils with subsurface cracks.

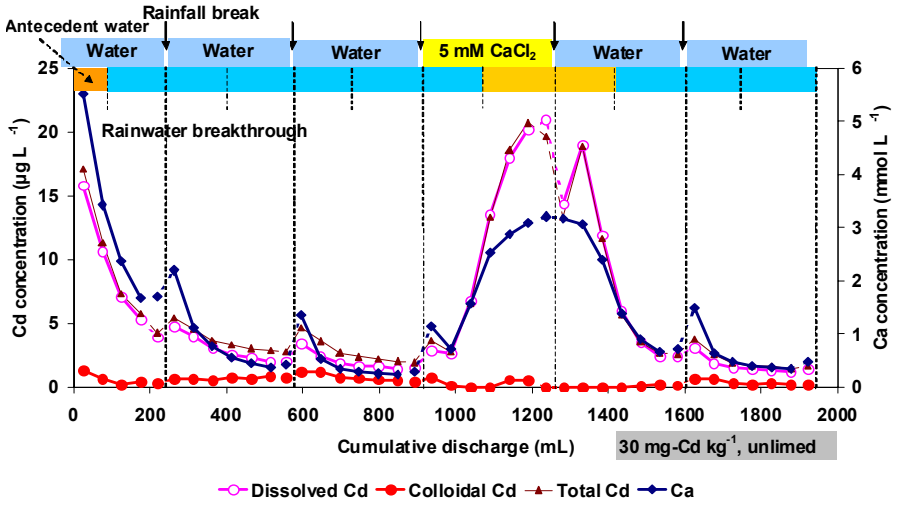

Fig. 1. Breakthrough of dissolved and colloidal Cd from a dual-layer column.

katouh@niaes.affrc.go.jp

P035

The effect of soil compaction on solute diffusion in volcanic ash soil

Shoichiro Hamamoto[1]*, Mandadige Samintha Anne Perera[1], Augustus Resurreccion[2], Ken Kawamoto[1], Toshiko Komatsu[1] and Per Moldrup[3]

[1]*Graduate School of Science and Engineering, Saitama University*

255 Shimo-okubo, Sakura-ku, Saitama 338-8570, Japan

[2]*Department of Engineering Sciences, College of Engineering, University of the Philippines-Diliman*

Quezon City, Philippines 1101

[3]*Department of Biotechnology, Chemistry and Environmental Engineering, Aalborg University,*

Sohngaardsholmsvej 57, DK-9000, Aalborg, Denmark

The unique soil properties of aggregated volcanic ash soil with dual pore system characterize the solute transport in soil-water phase. The diffusion is the dominant mechanism of the solute transport in soils and the solute diffusion coefficient (D_s) is a governing parameter, which is strongly affected by the soil compaction (i.e. bulk density, ρ_b) as well as soil-water content. However, only a few studies on quantifying D_s for volcanic ash soil have been done, especially concerning the effect of ρ_b on D_s. In this study, the D_s of chloride for repacked volcanic ash soils with different ρ_b were measured as a function of soil-water content (θ). The D_s values for volcanic ash soils decreased with decreasing θ and the measured data showed the inflection point at around pF=2.8, where pF is log(ψ: soil-water matric potential in cm H_2O). Furthermore, the magnitude of D_s considerablely decreased with increasing ρ_b at pF < 3.5 (wet condition), and increased with increasing ρ_b at pF > 3.5 (dry condition). Under the wet condition, the solute diffuses basically through larger (inter-aggregate) pore network which causes a decrease in the solute diffusion with compaction, while under the dry condition the solute diffuses through intra-aggregate pore network which causes an increase in the solute diffusion with compaction. With considering these specific D_s behaviors in volcanic ash soils, a new predictive model was developed for D_s, which performed well with available (literature) and measured D_s data for volcanic ash soils.

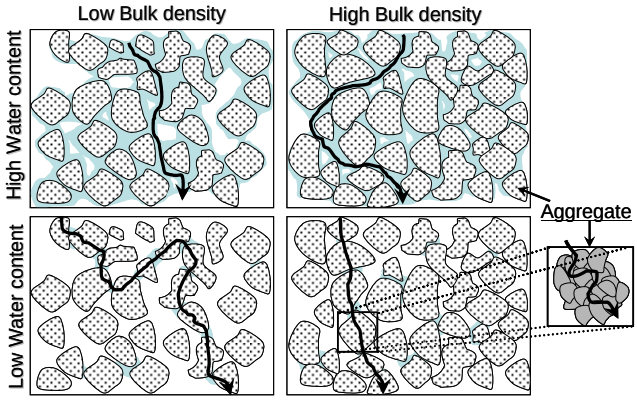

Fig. 1 Schematic diagram of solute movement for aggregated volcanic ash soil.

*s07de004@mail.saitama-u.ac.jp

P036

Experimental study and modeling of europium adsorption onto smectite clay colloids

T. Missana, U. Alonso, M. García-Gutiérrez*, N. Albarrán, T. López-Torrubia
[1]*CIEMAT, Departamento de Medioambiente,*
Avenida Complutense, 22 – 28040 MADRID (Spain)

To establish when the presence of colloids can enhance contaminant migration is a critical task for the performance assessment of a high level radioactive waste (HLRW) repository. Compacted bentonite (mainly formed by the 2:1 clay smectite) is considered a suitable engineered barrier in HLRW repositories to delay radionuclide migration, since it presents high sorption capability for most cations. However, the generation of bentonite colloids at the near field/far field interface, i.e. in the regions in which bentonite comes in contact with the groundwater, has been demonstrated.

The effects of the presence of bentonite colloids on radionuclide elements can be important for those elements that strongly adsorbs (for example tri- and tetravalent elements) but these effects will be limited if sorption onto colloids is not irreversible.

In order to understand the colloid/contaminant interactions and to evaluate their (ir)reversibility, an important preliminary step is to study and to quantify the sorption mechanisms.

In this work, the adsorption of europium onto clay colloids was studied and sorption data were interpreted by using a model which combines surface complexation and ionic exchange processes. The effects of the most important physico-chemical parameters such as pH, ionic strength and radionuclide concentration were independently analyzed. Fig. 1 shows an example of sorption isotherms obtained at two different pHs that present a Langmuir-type behavior.

Europium sorption at low pH (<4) presented a significant dependence with the ionic strength, indicating the importance of ionic exchange processes. The selectivity coefficient obtained from the experimental data is approximately constant in a range of ionic strengths from 0.2 to 0.05 M, but decreases significantly (one order of magnitude) at lower ionic strengths. This might be a consequence of the effect of competitive ions in solution that is not accounted for if Na-Eu exchange is just considered. If this can be related to sorption irreversibility is discussed in the paper.

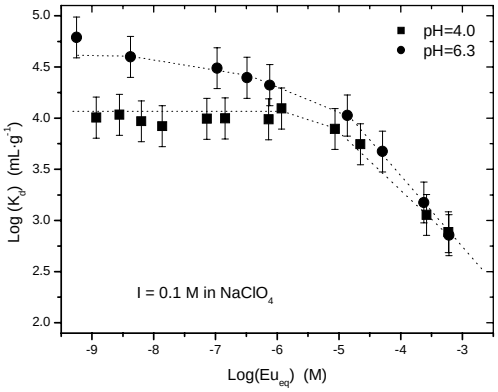

Fig. 1 Sorption isotherms of Eu onto smectite colloids at two different pH. Ionic strength =0.1 M.

Acknowledgements

This work has been partially supported by EC-FUNMIG project and the Spanish Ministry of Education and Science under the grant CGL2005-01482/BTE (PROMICOL).

*miguel.garcia@ciemat.es

P037

Calcium hydroxide leaching process modeling for a well-buffered volcanic-ash soil

D. Chen*, N. Toride
Graduate school of Bioresources, Mie University
1577 *Kurimamachiya-cho, Tsu, Mie* 514-8507, *Japan*

Construction sludge is usually dehydrated with a coagulant material such as lime hydrate for recycling the sludge as a soil foundation. A well-buffered volcanic-ash soil is often used at the bottom of the landfill site to minimize adverse effects of high pH solutions for the surrounding area from the dehydrated sludge. The soil buffering capacity is evaluated with a variable charge model describing the pH dependent charges. Variable cation exchange capacity (CEC) is modeled with a dissociation of hydrogen from the hydroxyl groups at the edge of soil minerals. Variable anion exchange capacity (AEC) is also described with the attachment of hydrogen ions to the surface hydroxyl groups. A titration experiment is conducted for a Kanto loam soil (Japanese volcanic-ash soil) by adding acid and alkaline solutions to a soil-water suspension (Fig.1). Parameter values for the variable charge model are determined based on the titration curve using the PHREEQC geochemical database code (Parkhurst and Appelo, 1999). Furthermore, a leaching experiment of calcium hydroxide solutions is carried out for the Kanto loam soil. Cation and anion concentrations including soil solution pH (Fig. 2) are evaluated with a numerical code HP1 (Jacques and Šimůnek, 2005), which couples the water flow and solute transport code HYDRUS-1D (Šimůnek et al, 2005) and the PHREEQC code.

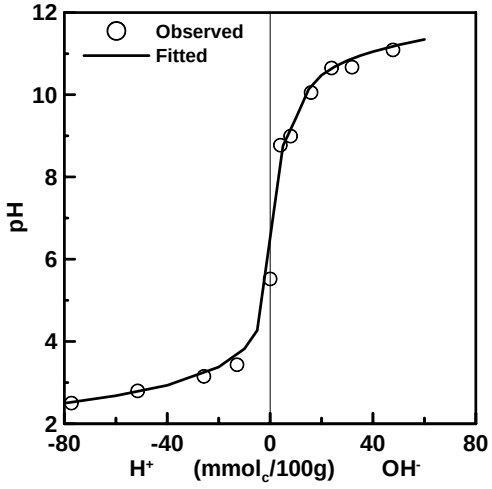

Fig.1 A titration curve for a well-buffered Kanto loam soil

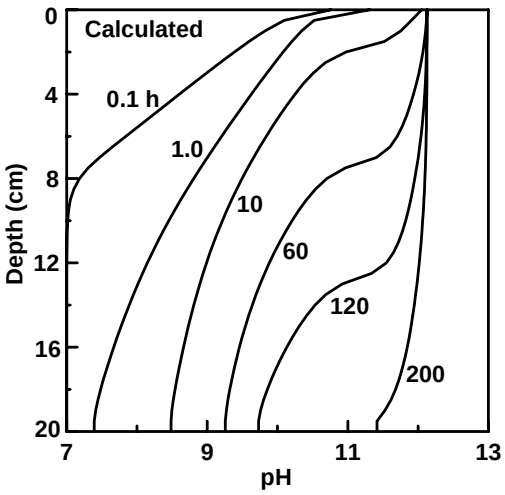

Fig.2 Soil solution pH profiles during a leaching of calcium hydroxide solutions to a Kanto loam soil

*505D506@m.mie-u.ac.jp

P038

Adsorption of selenium on single oxides and natural solids

Charlotte Hurel[1*], Nicolas Marmier[1]
[1]*Laboratoire de Radiochimie, Sciences Analytiques et Environnement (LRSAE)*
University of Nice Sophia Antipolis,
Parc Valrose, 28 avenue Valrose
F-06108 Nice cedex 2 France

Selenium is ubiquitous in the environment and constitutes one of the major component of 40 minerals. The most abundant deposits of selenium are pyrite, chalcopyrite, galena etc. During the erosion process, selenium can be released in the environment, and transported by the ground waters. This study aims at understanding the adsorptive behaviour of selenium at the solid-liquid interface in the geosphere. Experiments were carried out on a single oxide (alumina), clay, and argilite, considering a pH range from 2 to10, in various electrolytic and ionic strengths, and various amounts of Se. The experimental results carried out on alumina have shown that the adsorption of Se depends on the pH value (figure 1). A maximum adsorption is observed for the most acidic pH values. No influence of the ionic strength is observed. Considering these results, a thermodynamic model based on the surface complexation theory was applied in order to propose stoichiometries and equilibrium constants able to describe the behaviour of Se on this single oxide. Finally, the model was applied to the experimental results obtained on clay and argilite, which are more complex solids, supposing that aluminol sites of the argilous materials are the active sites for the sorption of Se.

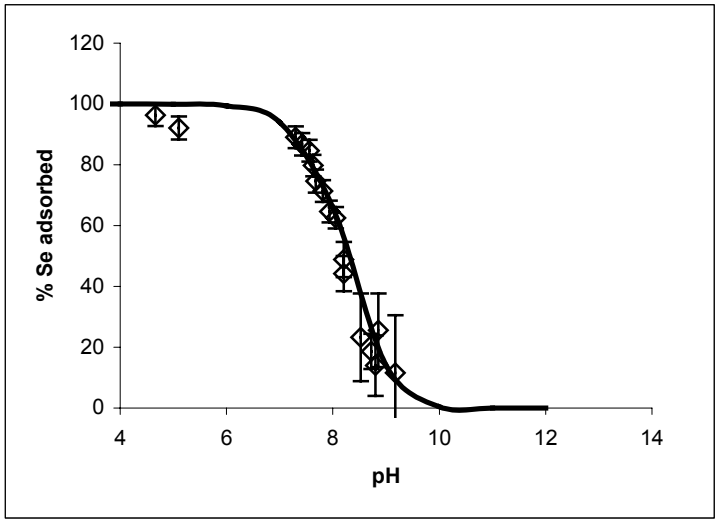

Figure 1 : adsorption of Se on alumina as a function of pH

* charlotte.hurel@unice.fr

P039

Fluorescence Lifetime Imaging Microscopy applied for Eu(III) adsorbed on Granite

K. Ishida[1*], T. Kimura[2], T. Saito[1], T. Toraishi[2], S. Tanaka[1]

[1]*Department of Quantum Engineering and Systems Science, The University of Tokyo, 7-3-1 Hongo, Bunkyo-ku, Tokyo 173-0027*

[2]*Nuclear Science and Engineering Directorate, Japan Atomic Energy Agency, 2-4 Shirane Shirakata Tokai, Ibaraki 319-1195*

The adsorption of toxic metals on minerals is one of the important processes which regulate the migration of toxic metals in subsurface environments. The transport of toxic metals will be hindered by adsorption on immobile rock surfaces or enhanced by binding to mobile mineral colloids. Over decades, numerous studies were performed with various metals and minerals. However, the interpretation of the results obtained in some experiments is not straightforward, when the absorbents are heterogeneous, that is, composed of different constituents, as is the case for granite. Fluorescence lifetime imaging microscopy (FLIM) has been successfully applied for such heterogeneous adsorbents, especially in the fields of biology. This method enables one to observe *in-situ* and local emission from fluorophores or fluorescent probes in samples and to obtain time evolution of the fluorescence if a time-resolved measurement is performed. In this study we applied the FLIM for the adsorption of Eu(III), a known chemical analogue of Am(III) and Cm(III) on Makabe granite.

Figure1 (a) shows the fluorescence image of Eu(III) on the granite with the Eu(III) concentration of 1 mM and at pH 6. The adsorption of Eu(III) reflects underlying mineralogy of the granite. A fluorescence lifetime image of Eu(III) (Fig.1 (b)) was obtained by acquiring a set of fluorescence images with varied delay times and by fitting the decay to bi-exponential function. The lifetime of Eu(III) correlates with the number of water molecules in the first coordination shell and can be used to deduce binding modes of Eu(III) to ligands or surface sites[1]. Figure.1 (b) shows the lifetimes of Eu(III) are distributed from 300 to 400 μs, which indicates that structures of the Eu(III) surface complexes on granite are similar with respect to the number of the sites involved. Further discussion based on the FLIM measurements at different conditions and the comparison with the results of elemental analysis will be made in the conference.

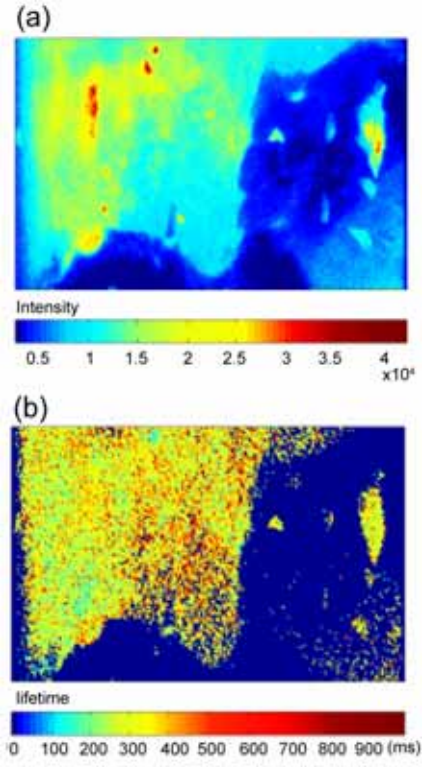

Figure.1 Fluorescence image of Eu(III) on granite (a) and lifetime image (b) ($[Eu^{3+}]_{total}$=1mM, pH 6)

(1) M. Arisaka, T. Kimura, et al. Radiochem. Acta 90 (2002) 193.

*keisuke_ishida@flanker.q.t.u-tokyo.ac.jp

P040

Effects of pore-wall on the transport properties of porous media

S. Ooi

National Institute for Rural Engineering,

2-1-6 Kannondai , Tsukuba, Ibaraki 305-8609

(1) Random networks of capillaries are believed to provide the best model for complicated pore systems. However, the capillary model predicts an erroneous diffusivity for granular beds. Therefore, two mathematical models, one a network of line segments (capillary pores) and the other a network of plane segments (slit-like pores), were proposed. The diffusivities were determined for the two models from the degrees of freedom for local diffusions (line one freedom and plane two). The surface (plane) network model was a better model for diffusion of granular beds. In addition, the surface network model also gave better results for Knudsen diffusion and viscous flow.

(2) In small pores (meso-pores), the effects of the wall on motion of a particle are important. Large particles can not move easily in a small pore. Therefore, diffusive mobility of particles was precisely determined by the measurement of settling mobility (settling velocity). The decreased mobility in the axis of a circular cylinder agreed with the Haberman exact theory(Fig.1). Eccentric effects were also the same as the Bungay-Brenner theory.

(3) In a thin pore, slip velocity on a permeable pore-wall is important. The width of the boundary layer along the permeable surfaces was measured by controlling surface permeability with a thin film and the width was found to be the root of the permeability as theoretically predicted. Furthermore, the slip effect for the flow through a small gap was measured and the slip was confirmed to easily couple the flow-rate.

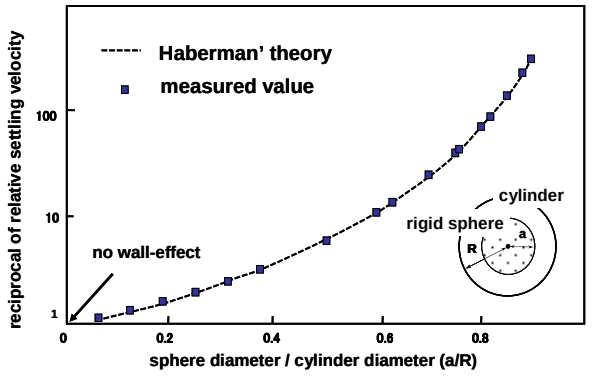

Fig.1 Relative settling velocity in narrow cylinders

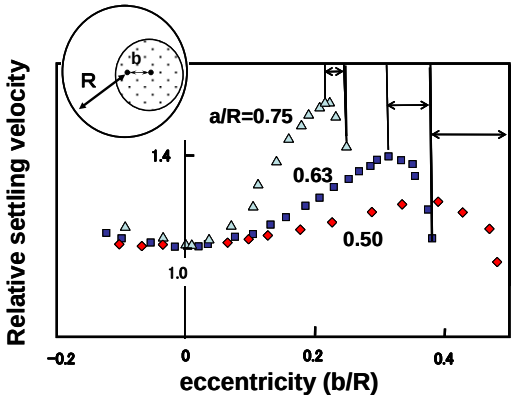

Fig.2 Eccentricity effect on settling velocity

setooi@affrc.go.jp

P041

Two-dimensional Arrays of Gold Colloids and the Function of Ionic Liquid on their Stabilization

Om P. Khatri[a]*, Kosaku Adachi[a], Kuniaki Murase[a], Ken-ichi Okazaki[b], Tsukasa Torimoto[b], Nobuo Tanaka[c], Susumu Kuwabata[d], and Hiroyuki Sugimura[a]

[a]*Department of Materials Science and Engineering, Kyoto University, Sakyo-ku, Kyoto 606-8501,Japan*
[b]*Department of Crystalline Materials Science, Graduate School of Engineering, Nagoya University, Chikusa-ku, Nagoya 464-8603, Japan*
[c]*EcoTopia Science Institute, Nagoya University, Chikusa-ku, Nagoya 464-8603, Japan*
[d]*Graduate School of Engineering, Osaka University, Suita, Osaka 565-0871, Japan*

Ionic liquids are considered as an "environmental-friendly solvent" or "green solvent", and have drawn much attention because of their ability to disperse several kinds of nanomaterials. The enhanced surface to volume ratio and loosely coordinated protective layer of 1-*n*-butyl-3-methylimidazolium hexafluorophosphate (BMI-PF_6) ionic liquid, push gold colloids for potential utilization in fabrication of catalytic devices. In this study, we demonstrate the formation and immobilization of ultra-fine gold colloids (ϕ = 2.6 nm) using BMI-PF_6 ionic liquid as a stabilizing media. Figure 1 shows 2D arrays of gold colloids on (3-mercaptopropyl)trimethoxysilane (MPS) functionalized silicon surface. The scattered organization is determined by the intrinsic charge and steric hindrance provided by superamolecular structure of BMI-PF_6 aggregates, which surrounds the gold colloids. It was observed that loosely coordinated BMI-PF_6 aggregates on gold colloids are replaceable with dodecanethiol (DDT), resultant Au-S bonding. The XPS, FE-SEM, and contact angle measurements suggest that the immobilization of gold colloids is based on (a) strong affinity between gold and mercapto (-SH) group of MPS monolayer and (b) physisorption of BMI-PF_6 aggregates, which holds the gold colloids. The DDT treatment advances the detaching of physisorbed gold colloids and the chemisorbed colloids remain pristine because of strong Au-S linkage. The synthesis of gold colloids using elegant and green methodology followed by their immobilization on silicon surface is expected to promise potential applications for the developments of catalytic and electronic devices.

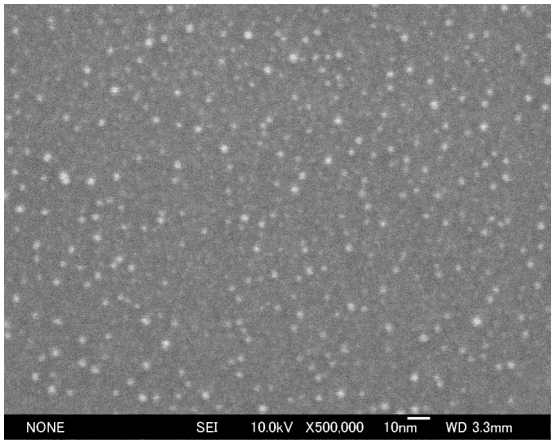

Fig. 1: 2D structural organization of BMI-PF_6 stabilized gold colloids on MPS functionalized silicon surface

*E-mail: khatriopk@gmail.com

P042

Speciation Characterization of Hydrolyzed Fe(III) during Fenton Reaction by Ferron Assay

Gao Yianxin* Yang Min Wang Dongsheng Zhang Yu
State Key Laboratory of Environmental Aquatic Chemistry, Research Center for Eco-Environmental Sciences, Chinese Academy of Sciences,

Abstract In this paper, the speciation of hydrolyzed Fe(III) under typical Fenton reaction conditions was investigated by ferron assay. It is found that the factors such as coexisting Fe(II) and H_2O_2 under normal Fenton process has little effect on the Fe(III)-ferron colorimetric reaction. Experimental results show that hydrolysis of Fe(III) exhibits some difference between the normal ferric salts and that formed during the Fenton process. By applying the modified hydrolyticity, B*, the difference of hydrolysis under various conditions could be compared effectively. Increasing the B*, the Fenton process is dominated by the formation of a large part of polymeric ferric species in the initial period. The H_2O_2/Fe ratio in Fenton process has also some effect on the Fe(III) hydrolysis. With the increase of H_2O_2/Fe, Fe_a and Fe_b increase gradually while Fe_c decreases. The speciation results show also that the polymer species are produced mostly in-situ depends on the hydrolyticity and undergo rapid transformation with aging. It is indicative of a possible optimum coagulation condition for the application of Fenton process.

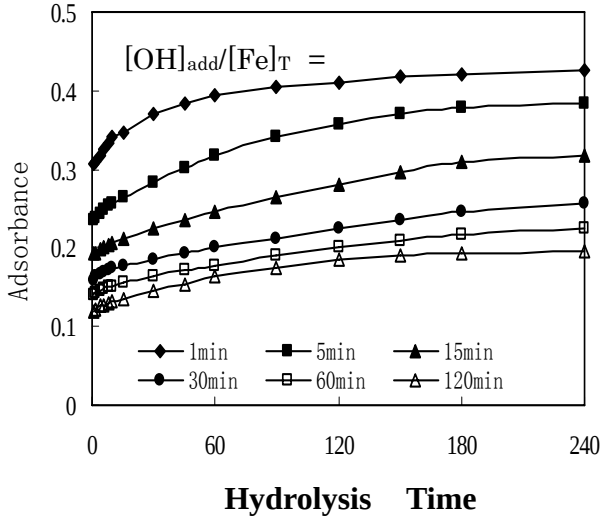

Fig. 1. Effect of hydrolysis on speciation of polyferric sulfate solutions $[Fe^{3+}]_0$=1.0mM

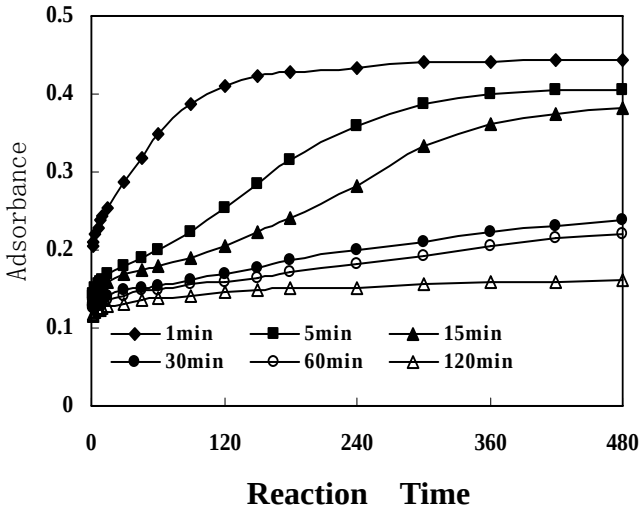

Fig. 2. Effect of Reaction Time on Fe^{3+} Species Produced in Fenton reaction $[H_2O_2]_0$: 25mM;

*longwisher@yahoo.com.cn

P043

INTERACTION BETWEEN ENZYME TREATED RED BLOOD CELLS

A. Hyono[1]*, J. F. L. Duval[2], F. Gaboriaud[3], T. Mazda[4], H. Ohshima[1]

[1]*Faculty of Pharmaceutical Science, Tokyo University of Science,*
2641 Yamazaki, Noda, Chiba 278-8510, Japan

[2]*Laboratory Environment and Mineral Processing, Nancy-University, CNRS,*
15 avenue du Charmois, B.P. 40, 54501 Vandoeuvre-lès-Nancy cedex, France

[3]*Laboratory of Physical Chemistry and Microbiology for the Environment, Nancy University, CNRS*
405 rue de Vandoeuvre 54600 Villers-lès-Nancy, France

[4]*Japanese Red Cross Central Blood Institute,2-1-67 Tatsumi, Koto-ku, Tokyo 135-8521, Japan*

Background: Proteolytic enzymes are commonly used in blood group serology. Red blood cells treated with these enzymes render them agglutinable by otherwise non-agglutinating anti-bodies. Van Oss et al. described the effect of the enzyme treatment of red blood cells as reducing the cell zeta potential and thus allowing red blood cells to be separated by a distance less than that between the antibody binding sites in an IgG molecule. However, neuraminidase, which removes only sialic acid and is the most efficient of all enzymes in reducing the surface charge of red cells, is not as effective as protease in increasing red blood cell agglutinability with certain antibodies. Therefore, Stratton et al. suggested that the second mechanism is a removal of structures on the cell surface by proteolytic enzyme activity which sterically inhibits access of the antibody molecule.

Aims: To estimate the interaction energy between red blood cells using ‘soft particle models’

Methods: Electrophoretic mobilities of red blood cells were analyzed with “a theory of a soft particle”. This theory assumes that a soft particle is covered with an ion-penetrable polyelectrolyte layer, in which dissociated groups of valence Z and number density N are uniformly distributed. We can obtain two parameters, the surface charge density ZN and a “softness” parameter $1/\lambda$, which has the dimension of length. To estimate repulsive forces between erythrocytes, we solved the Poisson-Boltzmann equation and obtained the disjoining pressure between two erythrocytes.

Results: The surface charge densities are estimated to be ZN = -0.055 M and $1/\lambda$ = 1.2nm (untreated), ZN = -0.030M and $1/\lambda$ = 0.8nm (5units papain-treated), and ZN =-0.013M and $1/\lambda$ = 1.1nm = 1.1nm (0.1units neuraminidase-treated) from analyzing the electrophoretic data with ‘a soft particle theory’. Although an explicit relation between the charge densities and titers are not obtained, the softness may probably affect their agglitinability. By assuming that the distance between the two binding sites of IgG molecule is 12 nm, the soft layer thickness is greater than 6nm when cells are untreated or treated with neuraminidase, while it is less than 6nm when they are treated with papain.

*craftsmanship@hotmail.co.jp

P044

Effective interaction between colloidal particles with grafted polyampholytes

T. Terao*, T. Kuze

Department of Mathematical and Design Engineering, Gifu University,
Yanagido 1-1, Gifu 501-1193

Polymer brushes are eliciting interest to regulate the stabilization of colloidal suspensions. In many applications, effective interaction between colloidal particles is a fundamental problem, and a lot of studies on polymer brushes grafted onto surfaces have been performed to avoid flocculation. However, most of these studies have devoted to electrically neutral or uniformly charged polymer brushes, and there are no detailed investigations on polyampholyte brushes. Especially, the effect of added salt on these systems is not clarified yet.

We have investigated the effective interaction between colloidal particles with grafted polyampholytes by Monte Carlo simulations. In this system, each colloidal particle is composed of a spherical core and flexible AB-diblock polyampholytes grafted onto the surface of the core (Figure 1). The diblock polyampholyte consists of positively charged monomers (A segments) and negatively charged ones (B segments), and the A end of the diblock copolymers is grafted onto the surface of the core. Our calculated results show that the effective interaction between colloidal particles with grafted polyampholytes is repulsive with smaller screening length. On the contrary, the effective interaction becomes attractive with larger screening length. A comparison with charged colloidal suspensions in an aqueous solution is also discussed.

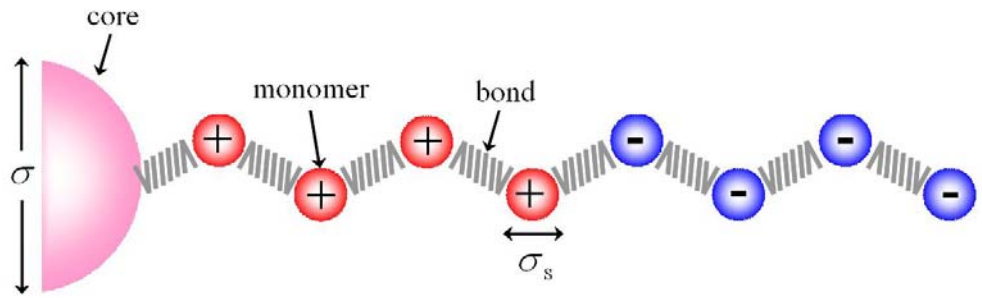

Figure 1 Model of colloidal particle with grafted polyampholytes.

*terao@gifu-u.ac.jp

P045

Effect of Counterion on Colloid Vibration Potential in Aqueous Surfactant System

Y. Takata*, T. Nagahashi, T. Miyayama, A. Hyono, H. Ohshima
Faculty of Pharmaceutical Sciences, Tokyo University of Science,
2641 Yamazaki, Noda, Chiba 278-8510, Japan

When the ultrasonic wave is propagated into the various solutions, the ultrasonic vibration potential is generated due to the vibration of species (electrolyte ions, colloidal particles, and so on) in the solution. The colloid vibration potential is very useful in the respect that it is deeply related to the electrostatic properties of colloidal particles, such as surface charge density or ζ-potential. In this study, we measured the ultrasonic vibration potential of the aqueous solution of dodecyltrimethylammonium bromide (DTAB) and dodecyltrimethylammonium chloride (DTAC) for the purpose of shedding light on the influence of the micelle formation and counterion on the colloid vibration potential.

In the DTAB system, the vibration current increased linearly with increasing the molarity, and then, a break point appeared near the critical micelle concentration (CMC), as shown in Figure 1a. In the DTAC system, on the one hand, no break point was observed (Figure 1b). Comparing both systems in the regime above the CMC, it was found that the slope of the DTAC system is larger than that of the DTAB system. Taking into consideration that the chloride ion has a smaller binding constant to the micelle surface than the bromide ion, it is suggested that the differences in the charge density or ζ-potential of micelle surface affect the colloid vibration potential.

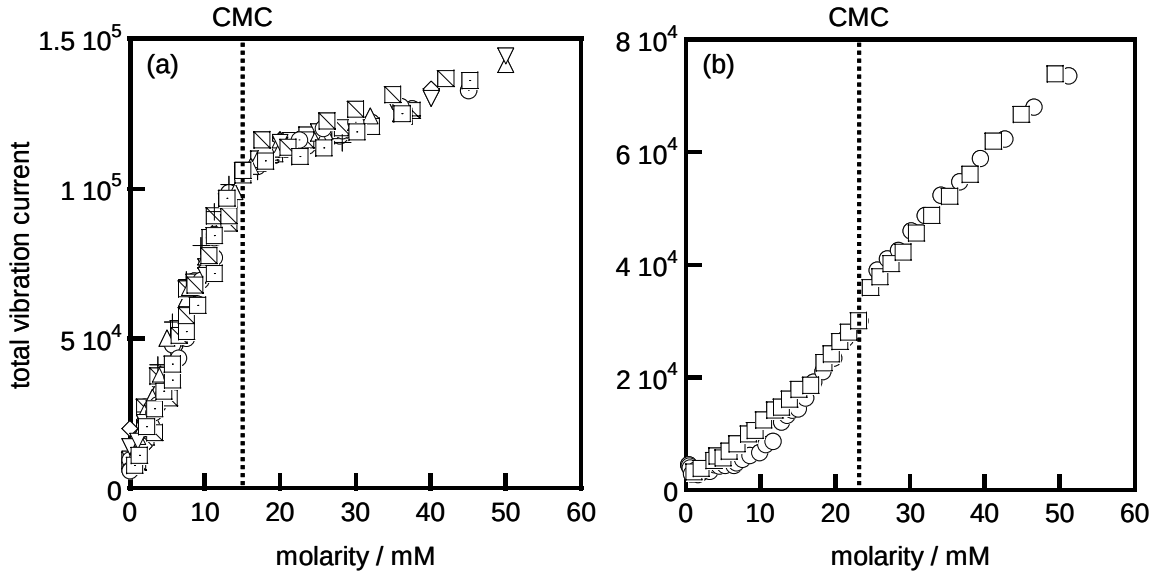

Figure 1. Plots of total vibration current against molarity: (a) DTAB and (b) DTAC system. Total vibration current stands for the sum of ion and colloid vibration currents.

*yoichit@rs.noda.tus.ac.jp

P046

Sorption of U(VI) on granite: Application of a surface complexation model

J.K. Lee[1]*, M.H. Baik[1], S.Y. Lee[1], Y.C. Seo[2]

[1]*Divition of HLW Disposal Research, Korea Atomic Research Institute,*
150-1 Deokjin-Dong, Yuseong, Daejon, Korea 305-353

[2]*Department of Environmental Engineering, Yonsei University,*
234 Maeji Heungup, Wonju, Gangwon-Do, Korea 220-710

The mobility of U(VI) in a geological media is mainly influenced by the reaction between metals and the surrounding geological materials. In this study, batch type experiments on U(VI) sorption by Korean granite were conducted as a function of pH and carbonate concentration. Chemical sequential extraction procedure was also conducted to evaluate the effect of mineralogical contribution to U(VI) sorption on granite. The fraction of U(VI) associated with clay minerals and refractory minerals in granite was about 19% from the study of a sequential chemical extraction procedure and the XRD pattern identified that it was chlorite. Though chlorite contents in granite was below 1%, its contribution to U(VI) sorption on granite was relatively high. A non-electrostatic model was used to interpret the U(VI) sorption by granite. Several U(VI) surface species including $SOUO_2^+$, $SOUO_2OH$, $SOUO_2CO_3^-$, and $SOUO_2(CO_3)_2^{3-}$ were assumed and at least two types of surface binding sites (strong and weak) were considered to describe U(VI) surface reactions with granite surface. From the model calculation, it was suggested that UO_2^{2+} and $UO_2CO_3^0$(aq) would dominantly react with the granite surface and the strong binding sites were 1% of total binding sites.

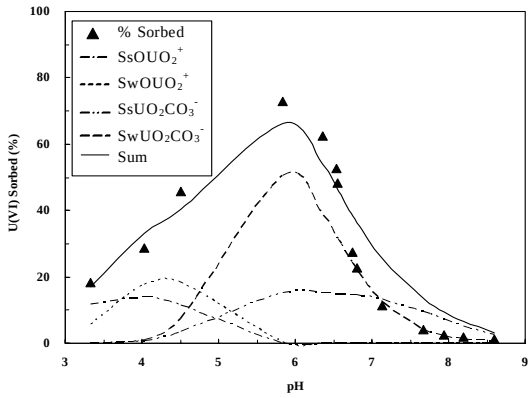

Fig. 1 Experimental(symbols) and model simulation (lines) results of U(VI) sorption onto crushed granite particles. [U(VI)]tot =10^{-6}M, [CO_3^{2-}] = 0.01M $NaHCO_3$, I = 0.01M $NaClO_4$

*jklee1@kaeri.re.kr

P047

Surface Charge and Coagulation of Bentonite Colloids: Effects of the pH and Ionic Strength

M. H. Baik[1], J. H. Park[2], J. K. Lee[1]*

[1]*HLW Disposal Research Division, Korea Atomic Energy Research Institute, 150 Deokjin-dong, Yuseong-gu, Daejeon 305-353, Republic of Korea*

[2]*Papa Inc., 2-1, 644-3 Ssangsong-Ri, Mado-Myeon, Hwaseung-Si, Gyeonggi-Do 445-861, Republic of Korea*

Surface charge and coagulation properties of bentonite colloids were investigated in order to study the colloidal stability of the bentonite colloids in a solution depending on the pH and ionic strength. The bentonite colloids were found to be composed of only montmorillonite from the XRD measurement. It was observed from the potentiometric titrations that a zero net proton adsorption occurred at about pH 8.2 (pH_{PNZPC} ~ 8.2). Surface charges of the bentonite colloids mainly carrying structural negative charges revealed a very small dependency on the pH. The same behavior was also observed in the zeta potential measurements. The zeta potential measurements for the bentonite colloid showed that the bentonite colloids were stable at lower ionic strengths of 0.01 M and 0.001 M $NaClO_4$ but unstable at a higher ionic strength of 0.1 M $NaClO_4$ within the whole pH range studied. A coagulation of the bentonite colloids was observed at pH 4.2 even at a lower ionic strength, and this coagulation was considered to be due to the contribution of the positive charges developed at the edge sites of the montmorillonite. An enhanced stability of the bentonite colloids was also observed, even at the higher ionic strength of 0.1 M $NaClO_4$, particularly at a higher pH > 9.2. This enhanced stability of the bentonite colloids is considered to be due to the increased negative surface charge of the edge sites over a pH_{PZNPC} of 8.2.

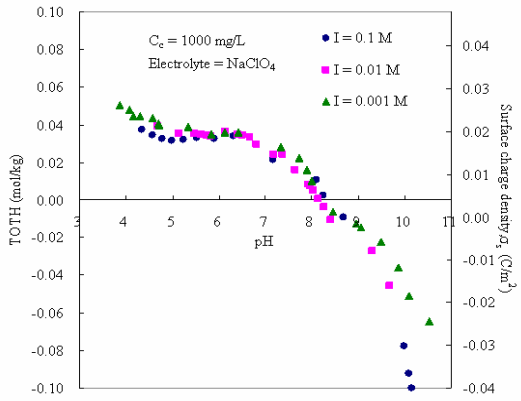

Fig. 1 Surface charge of the bentonite colloids.

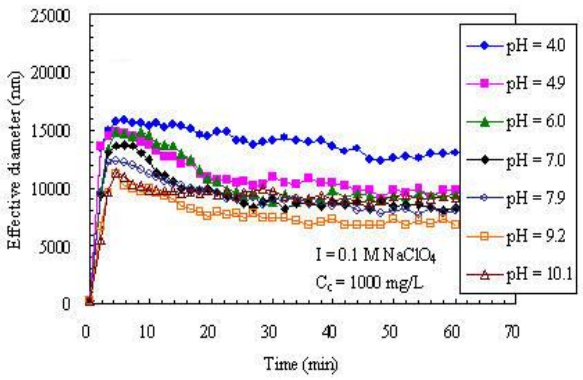

Fig. 2 Coagulation of bentonite thecolloids.

*jklee1@kaeri.re.kr

P048

Initial deposition rate of latex particles in the packed bed of zirconia beads

M. Kobayashi*, H. Nanaumi, and Y. Muto
Faculty of Agriculture, Iwate University
Ueda 3-18-8, Morioka, Iwate020-8550, Japan

Transport of colloidal particles in a packed bed of collector beads depends on the deposition kinetics of the particles onto the collector surface. The deposition is governed by the hydrodynamic and colloidal interactions between the particle and the collector. The colloidal interaction is controlled by the electric potentials of surfaces of collectors and particles. While many experiments have been carried out on the deposition with repulsive electric double layer (EDL), not so many studies have been conducted on the deposition in a packed bed in the presence of attractive EDL, where collector beads and colloidal particles are oppositely charged. Also, systematic experiments to examine the effect of surface potential on the deposition with attractive EDL are still lacking. In this context, we have decided to carry out the deposition experiment of sulfate latex particles, bearing a constant negative charge, in a packed bed of zirconia beads, having pH-dependent surface charge and an isoelectric point around pH 7. Deposition experiments were performed as a function of KCl concentration and pH of background solution to clarify the influence of surface potential on deposition in the presence of attractive EDL. Dimensionless deposition rates were evaluated from the breakthrough of latex suspension from the packed bed of zirconia. Experimental results demonstrated that deposition rates increase with decreasing salt concentration, and that the values of pH, that is, surface potential, have minor effect on deposition kinetics (Fig. 1). The thickness of diffuse part of EDL is more important in the presence of attractive EDL force.

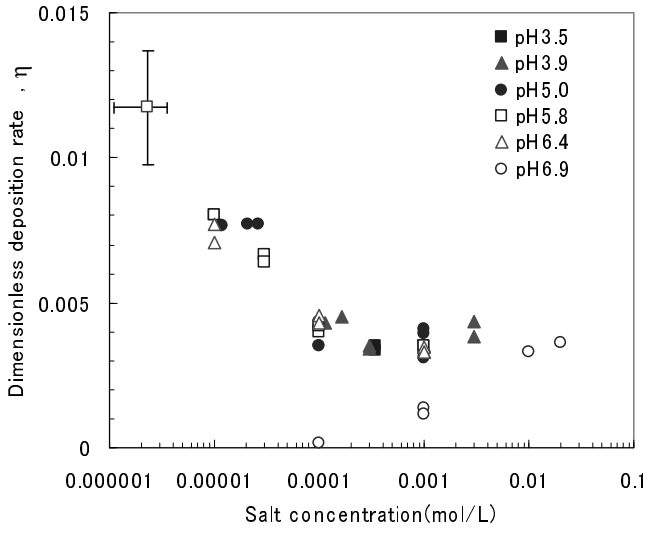

Fig.1 Deposition rate against salt concentration.

*mkoba@iwate-u.ac.jp

P049

Surface charging, polyanionic coating and colloid stability of magnetite nanoparticles

A. Hajdú*, E. Illés, E. Tombácz

University of Szeged, Department of Colloid Chemistry, H-6720 Szeged, Aradi vrt. tere 1. Hungary

Synthetic magnetite (Fe_3O_4) was prepared by alkaline hydrolysis of iron (II)- and iron (III)-salts. The pH-dependent surface charge formation in protonation ($\underline{Fe}$-OH + H^+ ⇔ $\underline{Fe}$-OH_2^+) and deprotonatation ($\underline{Fe}$-OH ⇔ $\underline{Fe}$-O^- + H^+) processes, particle charge and aggregation were characterized. The point of zero charge (PZC) was identified at pH~8. The net proton surface excess amount ranges from +0.3 to –0.2 mmol/g. The electrophoretic mobility measurements showed that the charge of pure magnetite nanoparticles decreases significantly over the whole range of pH and reverses from positive to negative at pH~8, which may consider as isoelectric point (IEP). Colloidal stability of naked magnetite nanoparticles showed significant pH-dependence, and the resistance against electrolytes was limited even far from the pH of PZC/IEP. [1]

In the present work, the formation of small and large molecular polyanionic coating and their role in stability enhancement of magnetite nanoparticles are compared. Magnetite was stabilized with citric (CA) and humic (HA) acids [2]. The macromolecular HA, a notable fraction of the natural organic matter (NOM), contains mainly carboxylic groups similarly to the CA, and both acids are able to form surface complexes on $\underline{Fe}$-OH sites of iron oxides. The pH dependence of overcharging effect and particle aggregation was quantified, and the enhanced salt tolerance of stabilized systems was studied. The dynamic light scattering (DLS) method was used to characterize colloidal stability under different conditions. The average particle size and electrophoretic mobility were measured in a NanoZS apparatus (Malvern, UK), and the electrolyte tolerance was tested in coagulation kinetic measurements. The colloidal stability depends sensitively on the dose of organic acids and the pH. These polyanionic organic complexants can modify the surface charge properties of magnetite entirely or in a certain degree depending on the amount adsorbed. The presence of trace amount of HA only neutralizes the positive charges of magnetite at pH lower than its pH PZC ~8, and so it promotes the aggregation between the particles having both positive sites and negative humate patches on the surface. Above the adsorption saturation, the complete surface coverage causing a sign reversal of particle charge and overcharging of nanoparticles. The magnetite nanoparticles are stabilized in a way of combined steric and electrostatic effects. The thicker layer of macromolecular HA provides better electrosteric stability than that of CA coating. The magnetite was well stabilized by both CA and HA, meanwhile its dissolution was enhanced due to the complexation of Fe ions in aqueous medium.

[1] Tombácz E., Illés E., Majzik A., Hajdú A., Rideg N., Szekeres M. : Ageing in inorganic nanoworld: an example for magnetite nanoparticles in aqueous medium, Croat. Chem. Acta, 80, 2007, 503-515.

[2] Illés E., Tombácz E.: The effect of humic acid adsorption on pH-dependent surface charging and aggregation of magnetite nanoparticles. J. Colloid Interface Sci., 295, 2006, 115-123.

*hajduangi@chem.u-szeged.hu

P050

Effect of colloid volume fraction on the rate of Brownian coagulation

T. Fukasawa* and Y. Adachi

Graduate School of Life and Environmental Sciences, Tsukuba University,

1-1-1 Tennoudai, Tsukuba, Ibaraki 305-8572, Japan

Many experimental data showed that the rate of coagulation qualitatively agrees with the prediction of Smoluchowski theory. However the rate constant obtained by experiment is reduced to 40-60% of theoretical prediction. This effect is usually described by the collection factor, α_B, so-called the coagulation coefficient. The reduction of correction less than unity has been ascribed to the effect of hydrodynamic interaction between colliding particles. However, from this theory, the dependence of initial particle concentration on the rate of coagulation cannot explain.

We have been investigating the effect of excluded volume of flocs on the rate of Brownian coagulation[1]. In the present study, we focus on the effect of initial volume fraction on the rate of Brownian coagulation. Direct counting of flocs formed of polystyrene latex particles undergoing rapid Brownian coagulation as a function of elapse time was performed through optical microscope changing the diameter of primary particle and the initial number concentration to verify the effect of initial volume fraction on the rate of Brownian coagulation. The obtained result indicated that the coagulation coefficient gradually increases in accordance with the increase of initial volume fraction (Fig.1).

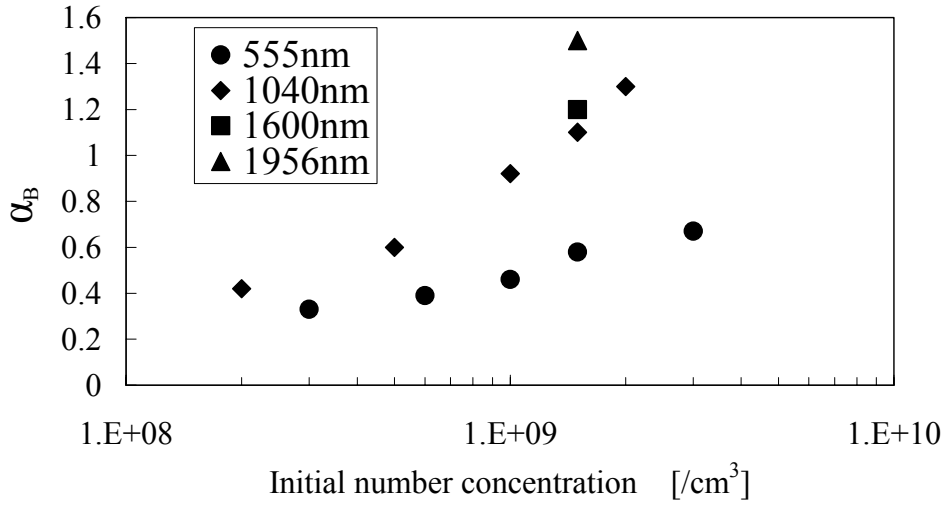

Fig.1 Coagulation coefficients as a function of initial number concentration of primary particles.

REFERENCE

[1] T. Fukasawa, Y. Adachi, J. Colloid Interface Sci. 304 (2006) 115.

*s0730537@ipe.tsukuba.ac.jp

P051

Dynamic study of colloid retention mechanisms in a granite fracture.

N. Albarrán*, T. Missana, U. Alonso, M. García-Gutiérrez, T. Lopez-Torrubia
CIEMAT, Departamento de Medioambiente,
Avenida Complutense, 22 – 28040 MADRID (Spain)

Contaminant migration can be significantly affected by the colloid presence in groundwater. Colloids generated from the engineering barriers of a high level radioactive waste repository (HLWR) emplaced in crystalline rocks (i.e. bentonite colloids) are of concern, since they can play a significant role in radionuclide transport.

To understand the main mechanisms affecting the colloidal transport in a crystalline medium, in this work, colloid migration in a granite fractured column was studied in dynamic conditions. In particular, we focused the attention on colloid recovery, varying the initial conditions of the experiment. We studied the effects of the water chemistry, in particular pH, of the water velocity and of colloid properties (size) on the colloid retention in the fracture. Gold colloids of different size and bentonite colloids were used in this study, the first were selected as model system, because of these colloids present similar characteristics to bentonite colloids (charge and zeta potential), are available in different size. The stability of colloids was evaluated before the column tests.

Results showed that, even when colloids are stable in the water in static conditions, colloid mobility is significantly affected by water flow rate. In general, the higher the water flow rate, the higher the recovery. Additionally, the hydrodynamic behavior was observed to be dependent on the colloid size.

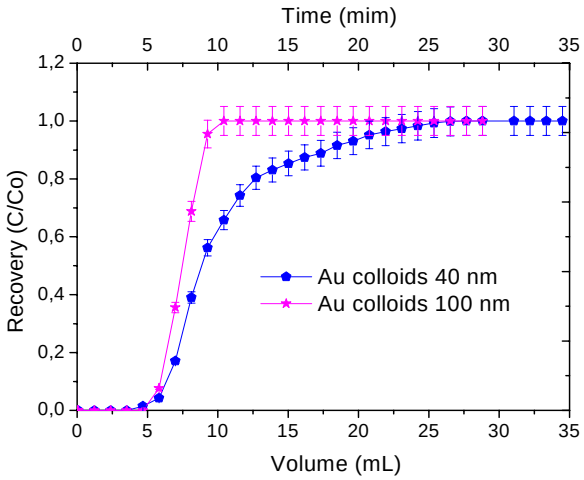

Fig.1 Comparative of recovery curves obtained for 100 nm and 40 nm Au colloids in granitic column (Q = 1.15 ml/min).

Acknowledgements

This work has been partially supported by EC-FUNMIG project and the Spanish Ministry of Education and Science under the grant CGL2005-01482/BTE (PROMICOL).

*nairoby.albarran@ciemat.es

P052

Investigation of Air/solution Interface by a Small Bubble

T. Murata[1], M. Sakai[1]*, K. Mukae[1], A. Yamauchi[2], and Y. Moroi[2], Willem Norde[3]

[1]*Department of Industrial Chemistry, Faculty of Engineering, Kyushu Sangyo University, 2-3-1 Matsukadai, Higashi-ku, Fukuoka 813-8503*

[2]*Graduate School of Sciences, Kyushu University, Fukuoka 812-8581*

[3]*Laboratory of Physical Chemistry and Colloid Science, Wageningen University, POB 8038, 6700EK Wageningen, the Netherlands*

A small air bubble is formed in *n*-alkylammonium chloride solution in a cylinder of 30 mm in diameter and 600 mm in length, which is rotating in order to keep the bubble on a line of rotating axis of the cylinder. Electric voltage of 45 volts is applied to the solution through two electric terminals at both sides of the cylinder, and the electrophoretic mobility of the bubble was determined. The bubble size was changed from 0.02 cm to 0.06 cm in diameter, and then, the values of the maximum mobility and the corresponding diameter of the bubble determined the apparent surface charge density at the air/solution interface. The surface charge density was found to be negative for the solution of all *n*-alkylammonium chlorides whose carbon atoms were 1, 2, 3, and 10 in number and to decrease in magnitude with increasing the carbon number as shown in Fig. 1. *n*-Decylammonium chloride (DAC) is a typical cationic surfactant, and nevertheless, the surface is still negative, which strongly suggests that DAC molecules are not adsorbed at the air/solution interface. The zeta potential of the bubble was also evaluated from both the solvent viscosity and the bubble velocity and found to increase from a certain negative value with increasing concentration. The change of surface charge density with the salt concentration was analyzed by the Langmuir adsorption isotherm as shown in Fig.2 and as a result, DAC could trace the adsorption isotherm.

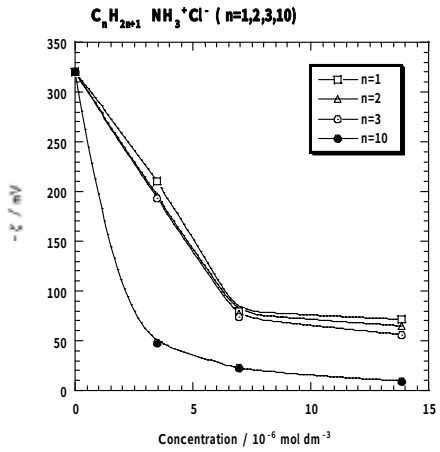

Fig. 1 Surface charge density

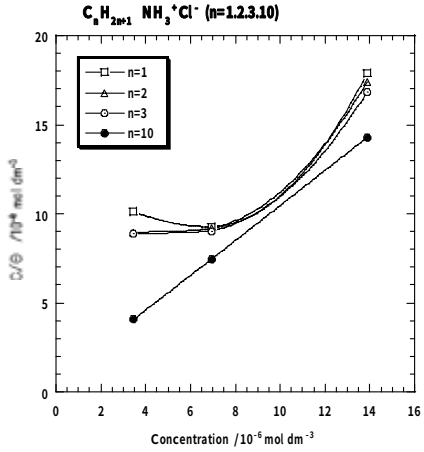

Fig.2 Langmuir adsorption isotherm

*mashi@ip.kyusan-u.ac.jp

P053

Influence of nanosized bubbles on the stability of disperse systems

N. Mishchuk[1]*, J. Ralston[2], D. Fornasiero[2]

[1] *Institute of Colloid and Water Chemistry of the National Academy of Sciences of Ukraine*
pr. Vernadskogo, 42, Kyiv, 03680, Ukraine

[2] *Ian Wark Research Institute University of South Australia*
Mawson Lakes Campus, Adelaide, SA 5095, Australia

One of a number of factors which strongly affects surface characteristics and interparticle interaction, is the presence of very small bubbles of gas or vapor on the surface of particles and/or in the interparticle gap.

There are several explanations for the presence of these gas bubbles: incomplete wetting of a hydrophobic surface; air trapped in surface microfissures; dissolution of atmospheric air in liquid; capture of air during mixing of components of disperse systems; capture of air during emulsification; dissolution of gas and appearance of tiny bubbles during electroflotation; cavitation between hydrophobic particles; chemical reactions caused by interaction of their double layers.

The size, shape and location of these bubbles and, consequently their influence on the electrostatic characteristics of interface and surface forces depend upon the history of their origin. There are three main types of nanobubbles distribution between solid particles: nanobubbles in liquid between particles; nanobubbles on the surface of particles and bubbles that bridge the gap between particles. The theoretical analysis of interparticle interaction for each type of nanobubbles distribution was carried out.

Results from this study have shown that tiny bubbles in the gap between particles or on their surfaces modify the van der Waals and electrostatic interactions. An especially strong influence of nanosized bubbles could be obtained for heterocoagulation between solid particles and macrobubbles under the condition of microflotation. In this case, a thin layer of nanobubbles at the particle surface can lead not only to the change of the absolute value of the van der Waals force, but also to the change of the sign of interaction. This is why the interparticle interaction in the presence of the nanobubbles looks similar to the action of long-range hydrophobic forces.

Nanosized bubbles considerably affect the stability both natural and artifical disperse systems. The role of nanosized bubbles in coagulation or heterocoagulation can be evaluated by joint analysis of the van der Waals and electrostatic forces with simultaneous account of other forces. For example, the efficacy of heterocoagulation between particles and floating bubbles under condition of microflotation depends not only on the size, surface charge and distribution of nanosized bubbles, but also on the solution electrolyte concentration, hydrodynamic regime and other factors.

*nataliya@mis.kiev.ua

P054

Physico-chemical properties of functionalised carboxymethyldextran macromolecules in the presence of metallic cations: an electrokinetic and dynamic light scattering study

Jean-Pierre SAGOU*, Fabien THOMAS and Jérôme F.L. DUVAL
Laboratory Environment and Mineral Processing, Nancy-University, CNRS
BP 40-F-54501 Vandoeuvre - lès- Nancy Cedex, France

The transfer of metals from soil matrix to plant roots occurs through the so-called mucilage, which is the biofilm built by microorganisms around the roots from exsudated glucidic material. The chemical interactions between metal ions and polysaccharides, and their influence on the conformational properties of the macromolecules are of great importance in the understanding of biodisponibility and phytotoxicity of metals.

The present work was focused on the identification of the molecular mechanisms underlying the interactions between an anionic polysaccharide and divalent cadmium ($Cd^{2+)}$ and calcium (Ca^{2+}) ions. To that aim, dextrane, a biopolymer of bacterial origin, was chemically functionalized by carboxymethyl grafting, yielding carboxymethyl dextrane (CMD) of molecular weight 670 kDa.

The modulations of the physico-chemical properties of that CMD have been investigated in aqueous $NaNO_3$ electrolyte, containing Cd^{2+} and Ca^{2+} at various concentrations. The dependence of the electrokinetic and conformational properties of CMD on the ratio metal concentration over charged carboxylate ligand concentration has been thoroughly examined using dynamic light scattering, electrophoresis and electrical conductivity increment measurements. For sufficiently large amount of metallic cations Cd^{2+}, analysis of the data reveals important shrinking of CMD, thus illustrating the formation of intramolecular bridges giving rise to a collapse of inner constituting polymer chains. On the opposite, the presence of Ca^{2+} did not lead to significant change as compared to the situation where metallic cations are absent from solution. For such situation, the size of CMD under conditions where electrostatics is nearly suppressed (high background electrolyte concentration) is predominantly controlled by the subtle variations in solvent quality with increasing CMD concentration. Following the observation of the different responses of CMD when exposed to Cd^{2+} and Ca^{2+}, the electrokinetic signatures of these interacting systems were measured. Like dynamic light scattering technique, electrokinetics is sensitive to variations in conformational and accompanying electrostatic/intramolecular hydrodynamic properties of CMD in the presence of metals. More in detail, we observed a reduction (in magnitude) for the electrophoretic mobility of CMD with increasing metal content in solution. Doing so, Cd^{2+} leads to the most pronounced mobility variation as compared to Ca^{2+} and to the situation of CMD in the absence of metals. Modulations of the electrokinetic properties of CMD by metals are interpreted by (i) a neutralization of carboxylate charges by metallic cations, which results in a decreasing CMD volumic charge density and (ii) a reduction of the CMD hydrodynamic permeability as a result of shrinking and increased compactness. These conclusions were also supported by electrical conductivity measurements.

* jean-pierre.sagou@ensg.inpl-nancy.fr

P055

Capillary Viscosity of Dilute Montmorillonite Suspension under Electrostatically Dispersed State in the Limit of Low Pressure Gradient

N. Sakairi[1*], K. Saito[2], Y. Adachi[2]

[1] *Graduate School of Systems and Information Engineering, University of Tsukuba, 1-1-1, Tennnoudai, Tsukuba-shi, Ibaraki, 305-8573, Japan*

[2] *Graduate School of Life and Environmental Science, University of Tsukuba, 1-1-1, Tennnoudai, Tsukuba-shi, Ibaraki, 305-8572, Japan*

The viscosity of dilute suspensions of Na-Montmorillonite was measured using originally developed spiral-type capillary viscometer(Fig. 1), which enables to measure viscosity of low shear stress region compared with conventional Ostwald viscometer. Suspensions of electrostatically dispersed state are focused, to analyze the influence of EDL on the rheological properties of colloidal suspensions.

Experiments were performed under dilute limit of suspensions, i.e. volume fraction, $\phi < 10^{-3}$, and smaller limit of ionic strength, where EDL are fully developed.

With measuring the difference of water levels of two graduated cylinders, h, against time, t, viscosity of suspensions, μ_s, is estimated by,

$$\log\left(\frac{h(t)}{h_0}\right) = -\frac{\alpha}{\mu_s}t. \tag{1}$$

Where, h_0, and α denotes initial difference of water levels, and experimental coefficient which is determined with geometrical shape of viscometer.

Reduced viscosity of suspensions against ionic strength are shown in Fig. 2. In the figure, reduced viscosity showed higher value than results obtained with conventional method. This shows that strong dependency of viscosity on shear stress in the vicinity of zero shear limit. Furthermore, reduced viscosity showed rapid decrease with the increment of ionic strength, which is ascribed to compression of EDL. This bihaviour is the same as that of yield stress of Na-Montmorillonite dispersion(N. Sakairi *et al.*, JCIS, *vol.* 283, (2005) *pp.* 245-250).

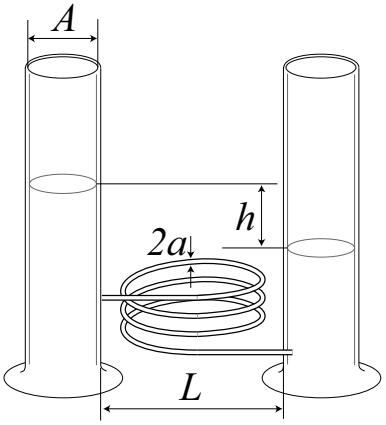

Figure 1: Schematic illustration of spiral-type viscometer.

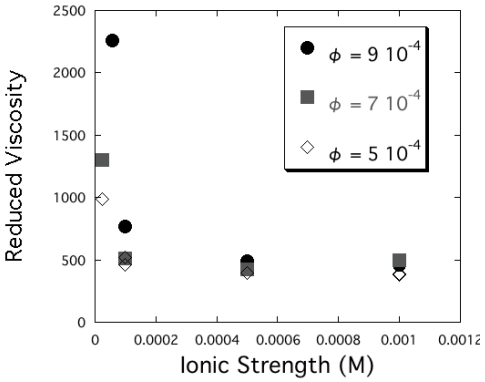

Figure 2: Reduced viscosity against ionic strength.

* nsakairi@surface.kz.tsukuba.ac.jp

P056

On-Chip Cell Electrophoresis to Evaluate Cell's Condition

Takanori Akagi[1,2] * and Takanori Ichiki[1,2]

[1]School of Engineering, [2]Center for NanoBio Integration, University of Tokyo

2-11-16 Yayoi, Bunkyo-ku, Tokyo,113-8656 Japan

Physical measurements of the optical and/or electrical properties of cells have been attracting considerable attention as noninvasive cell evaluation methods that are essential for the future of cell-based application technologies such as cell-based drug screening and cell therapy. Cell electrophoretic mobility (EPM), which can be measured in a noninvasive manner by a cell electrophoresis experiment, reflects the electrical and mechanical properties of the cell surface. We developed a cell electrophoresis system using a microcapillary electrophoresis (μCE) chip and successfully measured cell EPM changes associated with some important biological phenomena including cell cycle, apoptosis, enzymatic treatment and immune reaction. The close correlation between cell EPM and the cell conditions was revealed [1]. In this paper, the study of cell EPM changes throughout the cell cycle is described.

The cell cycle is one of the basic functions of all living thing. Since gene expression and response to drugs are known to be different depending on the cell cycle phase, an accurate evaluation of the cell cycle is a key issue. Hence, we studied cell EPM changes throughout the cell cycle. The EPM of human leukemia (HL-60) cells treated with various synchronizing drugs was measured and compared with that of untreated cells. The EPMs of nonsynchronized cells were distributed between 0 and -2.75 ($\times 10^{-4}$ $cm^2V^{-1}s^{-1}$). In contrast, the EPMs of the cells synchronized at the G_1 phase of the cell cycle using leptomycin B were distributed between -0.25 and -1.5 ($\times 10^{-4}$ $cm^2V^{-1}s^{-1}$) (Fig. 1). When similar experiments were carried out using other synchronizing drugs that induced S or G_2/M cell cycle arrest, their EPMs were distributed within a range narrower than that of nonsynchronized cells. Moreover, it was revealed that the peak value of the EPM distribution differs depending in the synchronizing drug used. These results suggest that the cell cycle phase can be determined using the cell EPM as an index.

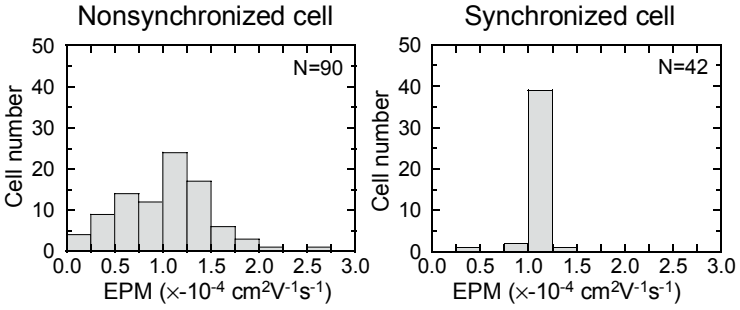

Fig. 1 EPM histograms of cells after treatment with PBS (left) and leptomycin B (right) for 24 h.

[1] T. Akagi and T. Ichiki, "Cell electrophoresis on a chip: What can we know from the changes in electrophoretic mobility?" *Anal Bioanal Chem*, submitted. [2] T. Akagi, M. Suzuki, and T. Ichiki, "Application of On-Chip Electrophoresis of Cell to Evaluation of Cell Cycle Stages of HL-60 Cells" *Jpn J Appl Phys* **45**:L1106-L1109 (2006).

*akagi@sogo.t.u-tokyo.ac.jp

P057

Low-swelling smectite in Ariake marine clay and its role in quick clay development

M. Ohtsubo*, T. Higashi and M. Kanayama
Faculty of Agriculture, Kyushu University,
6-1-1 Hakozaki, Higashi-ku, Fukuoka 812-8581

Sensitive marine clays with pyroclastic origin 15 to 40 m thick extend in the coastal plain around Ariake Bay in Kyushu, Japan. The sensitivity (ratio of undisturbed to remolded shear strength) of the clays is mostly in the range of 8 to 40, but is greater than 40 and occasionally as high as 1000 at reduced pore-water salinity, like quick clay in eastern Canada and Scandinavia. Quick clay behaves as a liquid once it is disturbed though it possesses rather high strength in an undisturbed state, which causes natural disasters such as landslide and subsidence. Ariake marine clay consists mainly of smectite while illite and primary minerals are predominant in the quick clay of eastern Canada and Scandinavia. The presence of a swelling clay mineral (smectite) normally inhibits or prevents the development of quick clay. Ariake clay with smectite-dominated mineralogy, however, developed to quick clay by salt leaching. This unusual behavior has been assessed in terms of the swelling nature of smectite in Ariake clay using the sediment volume tests for Na- and Ca-clay. Paddy soil and Wyoming montmorillonite were employed as reference samples since smectite in those samples is of high-swelling type. For the paddy soil and Wyoming montmorillonite, the sediment volume was grater for Na-clay than for Ca-clay at 0.04 N, indicating that smectite in these clay materials is high-swelling type. On the other hand, the sediment volume for Ariake clay was almost equal for Na- and Ca-clay, indicating that smectite in Ariake clay is low-swelling type. The low-swelling smectite was found to be a beidelite-nontronite mineral, and the low-swelling characteristics of the smectite was ascribed to the considerable substitution of Fe^{2+} for Al^{3+} in the octahedral layer.

Table 3. Sediment volume of the <2-μm clay fractions.

Locality	Sample	Sediment volume (cm³/100 mg) at 0.04 N salt concentration Na-clay	Ca-clay	at 1.0 N salt concentration Na-clay	Ca-clay
Yama-ashi	Y-2	3.08	2.97	3.06	2.81
	Y-6	2.63	2.69	2.82	2.62
	Y-8	2.49	2.50	2.69	2.46
	Y-13	2.43	2.37	2.40	2.31
	Y-15	2.41	2.37	2.48	2.32
Higashi-shiroishi	S-3	2.56	2.93	3.20	2.97
	S-6	2.50	2.66	n.d.[1]	n.d.[1]
Ariake-kantaku	A-8	2.32	2.78	3.07	2.97
	A-12	1.61[2]	2.77	2.69	2.78
Saga Agricultural Experiment Station	W-179-3	4.10	2.58	4.09	2.49

P058

Preparation of W/O/W microcapsule containing enzyme without alcohol

T. Narita*, T. Kishigawa, Y. Tagami, and Y. Oishi
Department of Chemistry and Applied Chemistry, Saga University
1 Honjo, Saga 840-8502 Japan

Immobilization of enzyme into microcapsules is of interest for application to wastewater treatment because it allows us not only degradation but also recuperation of valuable components from effluent streams. As typical enzymes are react in water, preparation of water-in-oil-in-water (W/O/W) type microcapsules is required to keep the enzyme activity. When O/W type microcapsule is converted into W/O/W type one, alcohol is usually used to exchange oil into water. However, alcohol is unsuitable for the preparation of the microcapsule containing enzymes because of the enzyme deactivations. In this study, we propose a novel method for preparing the enzyme-containing W/O/W microcapsule with a high catalytic ability by using a gas phase as substitute for alcohol to exchange oil into water, and also investigate activity of the encapsulated enzymes. As a model system for the study, we prepared a glucose-oxidase-containing O/W/O microcapsule whose volume is changed by the glucose oxidation of immobilized glucose-oxidase, and observed its volume change to confirm the ability of the encapsulated enzymes.

For preparing W/O/W type microcapsules, first, an aqueous solution of L-lysine, $NaCO_3$ and glucose oxidase was added to a (cyclohexane/chloroform) mixed solvent to form W/O emulation. Then, a cyclohexane solution of terephthaloyl dichloride was mixed with the emulsified solution to induce the polymerization, resulting in formation of W/O type microcapsules. The dried microcapsules by a removal of cyclohexane were dispersed into glucose solutions at pH 8 to obtain W/O/W type microcapsules. The shape of the microcapsules was observed with an optical microscope.

Optical microscopic observation confirmed that the W/O/W microcapsule with an average diameter of about 0.25mm is successfully obtained. Dispersing of the capsules into glucose solution, they began to shrink after about 10min, and then reached an equilibrium state with about half size of the initial one at 30 min (Fig. 1). This result indicates that the immobilized glucose-oxidase remains high active and the use of gas phase as a substitute for alcohol in the solvent exchange is available for improving the catalytic ability of enzyme that immobilized by microencapsulation.

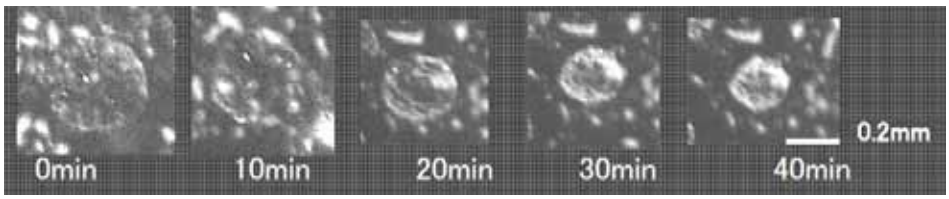

Fig. 1 Micrographs of microcapsule containing glucose oxidase at certain times after dispersing into glucose solution.

*naritat@cc.saga-u.ac.jp

P059

Quickened sedimentation for dense suspensions by the formation of vertical-channels

K. Nakaishi[1], S. Ooi[2], Y. Suzuki[1]
[1]*Faculty of Agriculture, Ibaraki University,*
3-21-1 Chuo, Ami, Inashiki, Ibaraki 300-0393
[2]*National Institute for Rural Engineering,*
2-1-6 Kannondai, Tsukuba, Ibaraki 305-8609

The solid-liquid separation by the sedimentation is difficult for the dense suspensions. Therefore, the method of quickened sedimentation by the formation of vertical channels is investigated.

Channeling has already been an observed phenomenon that often occurs during settling. However, the effect of channeling on the settling velocity has not been clarified yet. In this study, the settling velocity and the diameter and number-density of channels are measured. On this data, the flow rates through a channel are computed and compared with Hagen-Poiseuille flow. The results are as follows.

(1) Two types of channels, one self-organized channel (fine particle) and the other external-force channel (large floc), were found. Self-organized channel were formed by ultra-sonic radiation and external-force channel by bubbling.

(2) Photographic methods were used to measure diameter and number-density of channels (Fig.1). The diameter of channels increased as the concentration increased (Fig.2). On the other hand, the number-density decreased (only for external-force channel) (Fig.3). As a result, there was a peak settling velocity at 2.2% volume fraction (bubbling) (Fig.4).

(3) The flow-rate through a channel was estimated from the zone-settling velocity. On the other hand, the maximum flow–rate was computed on the hypothesis that excess pore-pressure is equal to net self-weight pressure. For dilute suspensions (below 2.2% volume fraction, bubbling), measured flow-rate agreed well with the computed maximum rate (Fig.5).

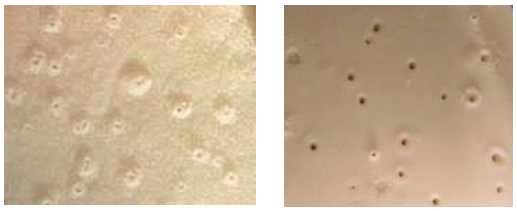

(self-organized) (bubbling)

Fig.1 Outlets of channels at the interfaces

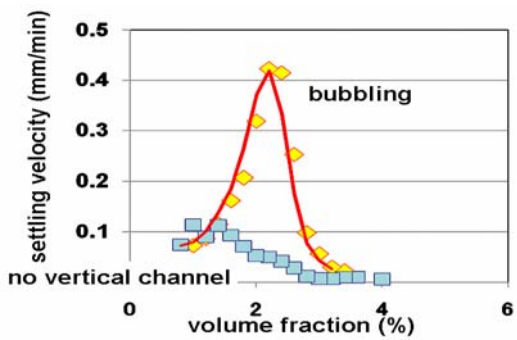

Fig.4 quickened settling velocity due to vertical channel

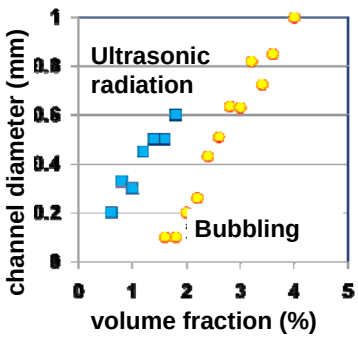

Fig.2 Channel diameter

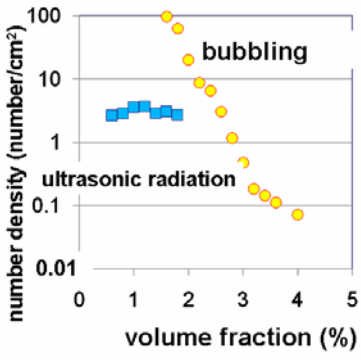

Fig.3 Cannel number density

Nakaishi@mx.ibaraki.ac.jp

P060

THE COAGULATION FEATURES OF LATEX NANOPARTICLES

S. Aidarova*, N. Tusupbayev, K. Musabekov, A. Sharipova
Innovation Laboratory of Petroindustrial and Colloid chemistry,
Kazakh-British Technical University,
Tole bi 59, 050000 Almaty, Kazakhstan

The creation of water stabilized latex base of nanodimensional protective coatings is actual mission of paint and varnish technology because of its environmental friendliness.
The aims are: scientifically-proved development technologies of getting ultramicrogeterogeneous nano emulsion and nano dispersion for increase the quality of paint and lacquer materials in order to protect metal surfaces from the corrosion; the formation and development theoretical and practical bases of forecasting of processes and regularity in nanodisperse systems; the creation of nanodimensional protective coatings of various purposes on the base of water stabilized latex nanoparticles.
The technologies of nanoparticles synthesis in connection with their colloid chemical parameters are investigated.
Model of positively charged polystyrene latex is synthesized by emulsion polymerization of styrene at the presence of emulsifier – cetyl pyridine bromide. The average sizes of latex particles are estimated by optical method. The features of latex coagulation which contain ion groups at the end of polymer chains and ion groups of anionactive surfactants are investigated by spectrophotometry method. It is established, that the process proceeds on the mixed neutralization concentration mechanism which is connected with the specificity of surface structure of latex particles.
The influence of weak polymer acids and surfactant ions on the stability of negatively charged monodisperse polystyrene latexes is investigated. On the basis of Fisher theory the energies of the repulsion and the attraction are calculated. These energies compose potential interaction curves of polystyrene particles covered by adsorption layer, surfactants and their associates with polyelectrolytes. It is established, that on rather small interpartial distances the significant role is played the osmotic effect which is caused by increase of the concentration of segments of adsorbed macromolecules and surfactants in the region of overlap. On father distances the basic role is played the configuration effects which are connected by change conformation of polymer chains in the region of overlap because of the restriction degrees of their freedom.
On the basis of the measurements of spectrophotometric, viscosimetric, electrokinetic characteristics of negatively charged polystyrene latex it is established, that infringement of stability of latex occurs due to reduction of the charge and potential of particles, and due to the formation of the bridge connections and heterocoagulation.
The investigation of this problem has theoretical and practical interests. It allows to forecast the properties of polymer – surfactant composition on interphase boundary because of the development of nano scientific basic knowledge which allows to determine area of their application.

*s.aidarova@kbtu.kz

P061

Adsorption studies for the removal of basic dyes from wastewater by activated sludge biomass

Hawn-Chung Chu[1*], Keng-Ming Chen[2]
[1]Department of Chemical & Materials Engineering, Lee-Ming Institute of Technology
4F, #8, Lane 126, Section 1, Nan-Chang Road, Taipei, Taiwan
[2]Department of Polymer Engineering, National Taiwan University of Science & Technology
#43, Section 4, Keelung Road, Taipei, Taiwan

Adsorption studies were made in treating basic dyes wastewater by using activated sludge biomass as an adsorbent. The experimental results of COD removal (%) show that the biomass is highly effective in adsorbing basic dyes from wastewater. The results of comparing the data of contact time experiments indicate that the molecular weight of basic dyes has a great influence on the equilibration time of adsorption and the adsorption capacity of biomass. The results of analyzing equilibration data show that for the adsorption equilibriums of Basic Red 29 dye adsorbed by biomass, the Langmuir adsorption isotherm is a better fit than the Freundlich isotherm and the maximum adsorption capacity is found to 214.09 mg/g at 30℃. Various thermodynamic parameters such as $\Delta G°$, $\Delta H°$, and $\Delta S°$ were calculated indicating that this adsorption system was a spontaneous and exothermic process.

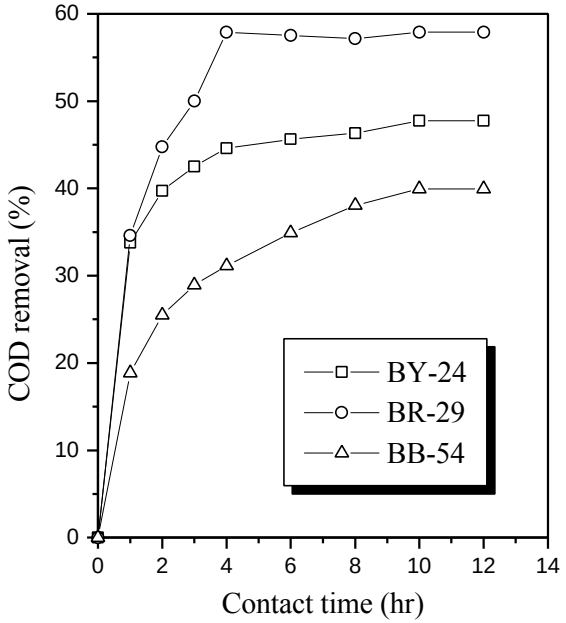

Fig.1 COD removal(%) against contact time(hr) in treating various basic dye wastewater (0.03%) by activated sludge biomass at 30℃

*Corresponding author: chu40523@ms49.hinet.net

P062

ECOLOGICAL ASSESSMENT OF OIL-GAS PRODUCING AREA IN KAZAKHSTAN ZONE OF CASPIAN SEA AND USING THE BIOREMEDIATION TECHNOLOGY FOR CLEANING OF HIGH LEVEL OIL POLLUTED SITES

A.A. Bigaliev, N.E. Ishanova, A.B.Bigaliev*
Al-Farfby Kazakh National University, Republic of Kazakhatan, 71, Al-Faraby ave., BOX 050038, Almaty, H. Dosmuhambetov Atyrau State University, Atyrau

A significant part of mineral raw material resources of Kazakhstan placed in the depth of the Caspian region, where more than 90% extracting of oil and natural gas, 100% balance store rare ground, 3,2 % uranium ore 0,3 %, 90,5% sawn store concentrated. Last years, it takes intensive works by extraction of carbon raw materials in Kazakhstan's sector of the Caspian sea. It brought to exceeding of coastal pollution at the North and middle the Caspian coastal pollution with oil products in average till, 0,282 mg/l. Maximum meaning oil product pollution reaches 0,56 mg/l (which means exceeding of limited concentration on 11 times). How much money need to cover cost of remediation in real sites? Develop of assessment and monitoring procedures based on fate mechanisms for most of representative hydrocarbons in polluted soils. Step 1 - Collection of heavily polluted portions of soils, separation of hydrocarbons by cost efficient mechanical procedures and send HC rich material (HC>95%) to prepare of alternative fuel. Return of low HC content sand to project area (<5.0%). Step 2 - Development of low cost bioremediation procedures in areas transformed to moderately polluted site (HC<5% after removing of heavily polluted portions) with uniform HC content. We are needed to develop of coust efficiency approach for cleaning of high level oily polluted sites around urban areas in Kazakhstan new methodology to estimate polluted area and recover of pollution history, Low cost bioremediation.

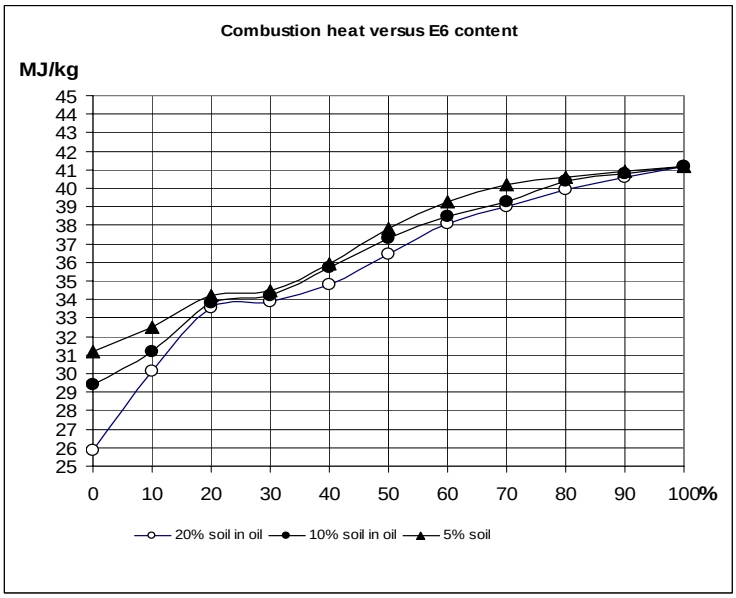

Figure 1.Development of combustible mix preparation techniques

*bigaliev@kazsu.kz

P063

CeO_2 surface induced bromate reduction during ozonation of bromide-containing water

T. Zhang, Z. Qiang*

Research Center for Eco-Environmental Sciences (RCEES), Chinese Academy of Sciences, Beijing 100085, China

Bromate formation is a hindrance of the application of ozone in water treatment for the aim of pollutants destruction. In order to minimize the bromate formation potential (BFP) during ozonation, former researches focused on several treatment options such as ammonia addition, pH depression, ·OH scavenging, and scavenging or reduction of HOBr. Since catalytic ozonation with metal oxides received increasing interests in recent years to improve the oxidation of organic pollutants in water, this work investigated whether BFP could be reduced in catalytic ozonation of bromide-containing water. Results indicate that CeO_2 could most effectively reduce the BFP among the selected metal oxides (i.e. α-FeOOH, α-Fe_2O_3, γ-FeOOH, and CeO_2) taking ozonation alone as control. The BFP reduction by O_3/CeO_2 favored a relatively low Br^- concentration (i.e., < 1.0 mg L^{-1}) and pH < 7. Water temperature ranging from 5 to 25 °C had no insignificant impact on the percent reduction of BrO_3^-. Further investigation indicates that neither the surface adsorption of BrO_3^- and Br^- on CeO_2 nor the surface reduction of BrO_3^- to HOBr/OBr^- by CeO_2, but the inhibition of surface Ce(IV) sites on the oxidation of HOBr/OBr^- to BrO_3^- accounted for the effective BFP reduction. O_3/CeO_2 produced a much lower concentration of H_2O_2 and a higher concentration of HOBr/OBr^- throughout the reaction course than ozonation alone. Therefore, the BFP reduction by CeO_2 may be ascribed to the reduced contribution of H_2O_2 to BrO_3^- formation and the possible surface enhanced formation of OBr^- in the disproportionation of BrO·.

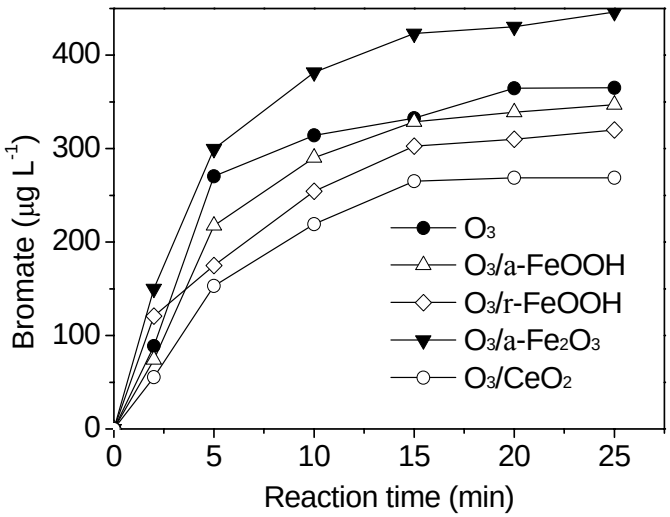

Fig. 1 Bromate formed in ozonation and catalytic ozonation. Conditions: $[Br^-]_o$ = 2.0 mg L^{-1}, $[O_3]_o$ = 4.51 mg L^{-1}, pH_o = 6.20, catalyst dose = 100 mg L^{-1}, T = 15 °C.

*qiangz@rcees.ac.cn

P064

Preparation of carbonaceous sulfur-impregnated adsorbent for removal of heavy metal in aqueous solution

T. Wajima[1]*, K. Sugawara[1]

[1]*Faculty of Engineering and Resource Science, Akita University, 1-1, Tegata-gakuen-cho, Akita, 010-8502*

A novel carbonaceous adsorbent for heavy metal removal was prepared from raw coal using sulfur impregnation. The raw coal was impregnated with sulfur using two methods; K_2S method and H_2S method. In K_2S method, raw coal was mixed with K_2S powder, and the mixture was heated at 800 ^oC for 30 min in nitrogen to produce K_2S-char. In H_2S method, raw coal was pyrolyzed at 800 ^oC for 30 min in nitrogen, and then sulfurized by 6 % of H_2S gas in nitrogen to produce H_2S-char. The sulfur contents of K_2S-char and H_2S-char were determined, and the properties of the sulfur-impregnated chars to adsorb heavy metals, Zn^{2+}, Cd^{2+} and Pb^{2+}, were examined.

The sulfur content of K_2S-char was higher than that of H_2S-char, due to the effective sulfur impregnation using K_2S method, and the ability of K_2S-char to adsorb Zn^{2+} in 2.4 mM of Zn^{2+} solution was higher than those of raw coal and H_2S-char (Fig. 1). K_2S-char also adsorbed Pb^{2+} and Cd^{2+} in 24 mM of Pb^{2+} and Cd^{2+} solution (Fig. 2), and the removal ratios of Pb^{2+} and Cd^{2+} were 97 % and 35 %, respectively. The elution extents of adsorbed Pb^{2+} and Cd^{2+} were zeros in distilled water and 27 %s in 0.1 M HCl solution. The results indicated that the effective heavy metal ions adsorbent could be prepared from coal using K_2S sulfur impregnation and the adsorbed metals could be strongly retained in K_2S-char.

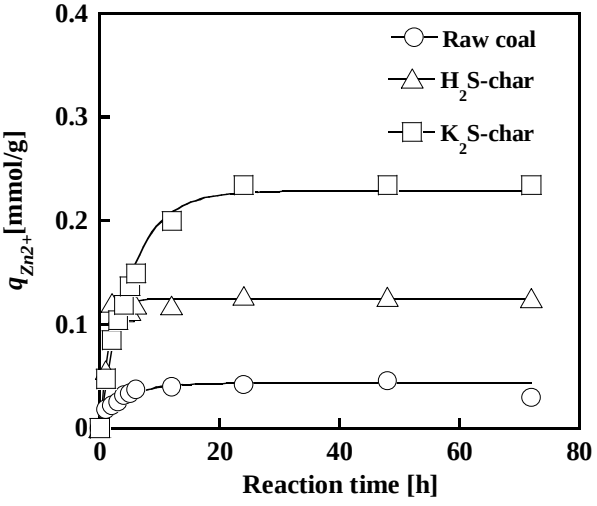

Fig. 1 Adsorption amounts of Zn^{2+} by raw coal, H_2S-char and K_2S-char as a function of reaction time.

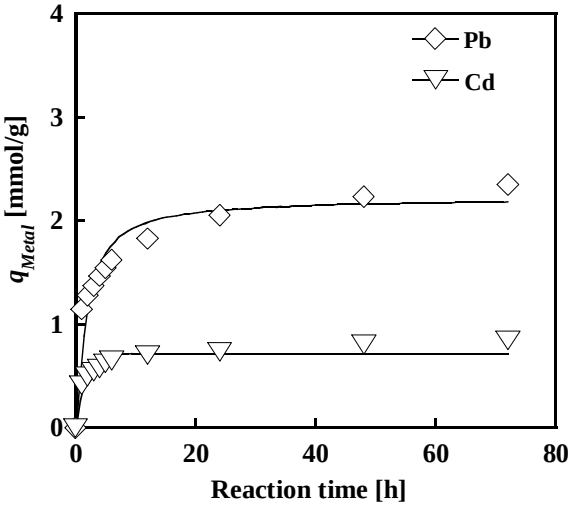

Fig. 2 Adsorption amounts of Pb^{2+} and Cd^{2+} by K_2S-char as a function of reaction time.

*wajima@gipc.akita-u.ac.jp

P065

Adsorption behavior of fluoride ion by titanium hydroxide-derived adsorbent

T. Wajima[1], Y. Umeta[1]*, K. Sugawara[1]
[1]*Faculty of Engineering and Resource Science, Akita University,*
1-1, Tegata-gakuen-cho, Akita, 010-8502

Removal behavior of fluoride ions was examined in aqueous sodium fluoride solutions by using newly designed, titanium hydroxide-derived adsorbent. The adsorbent was prepared from titanium oxysulfate ($TiOSO_4$•xH_2O) solution, and was characterized by TG-DTA, XRD, SEM and microtrac laser particle size analyzer. Bachwise adsorption test of the prepared adsorbent was carried out in aqueous sodium fluoride solutions.

The absorbent was the amorphous material, which was different morphology from raw material, titanium oxysulfate (Fig. 1), and the average particle size is 3.6 um. The adsorption of fluoride by the adsorbent was saturated within 1 h in the solution with lower than 200 mg/L of fluoride ion, together with increasing pH of the solution, due to the ion exchange between fluoride ion (F^-) in the solution and hydroxide ion (OH^-) in the adsorbent. The maximum adsorption of fluoride could be obtained in the solution at around pH 3 (Fig. 2). Fluoride ions were adsorbed selectively in the solution containing high concentration of chloride, nitrate and sulfate ions, and were adsorbed even in low concentration, e.g., < 5 mg/L. The adsorbent after fluoride adsorption could easily desorb fluoride ion using high pH solution, and was completely regenerated for adsorption of fluoride ion in low pH solution.

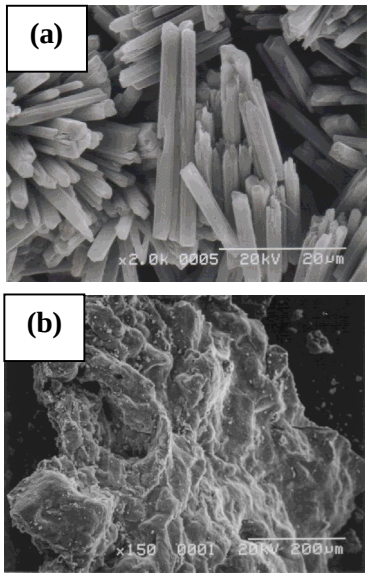

Fig. 1 SEM photographs of (a) titanium oxysulfate ($TiOSO_4$·xH_2O), and (b) titanium hydroxide-derived adsorbent.

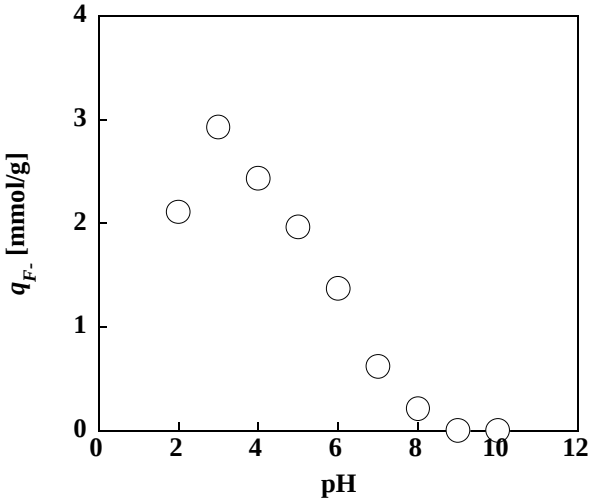

Fig. 2 Amount of fluoride ion adsorbed to titanium hydroxide-derived adsorbent in 50 mg/L of fluoride ion solution at various pH .

*m9007023@wm.akita-u.ac.jp

P066

DNA adsorptions on andosols and allophane minerals

M. Sakai[1], A. S-I. Wada[2], K. Saeki[3]*
[1]*Faculty of Agriculture, Kagoshima University, Koorimoto, Kagoshima 890-0065, Japan*
[2]*Faculty of Agriculture, Kyushu University, Hakozaki, Higashi-ku, Fukuoka. 812-8581. Japan*
[3]*Biotron Institute, Kyushu University, Hakozaki, Higashi-ku, Fukuoka. 812-8581. Japan*

With the rapid development in commercial production of genetically modified microorganisms and plants, great emphasis has been put on the security of the genetically modified organisms (GMOs). Some extrinsic genes of genetically modified crops, and antibiotic resistant genes could be excreted to the soil by plant roots or released from decaying plant tissues, which resulted in changes of the microorganism populations and various properties of the soil (Oger and Dessaux, 1997). Understanding the adsorption of DNA on soil particles is helpful for the study for soil biodiversity and for risk assessment for release of GMOs. Many researches have used 2：1 type layer phyllosilicate such as montmorillonite as adsorptive particle to understand the DNA adsorption on soils (*e.g.* Khanna et al.,1998; Pietramellara et al., 2001). However, only results of DNA adsorption on phyllosilicate is hardly enough to study the DNA molecule behaviors in variable-charge soils such as andosol spreading in Japan. Therefore, our study reports on the DNA adsorption on andosol particles and allophane minerals, using a salmon sperm DNA (molecular size < 2000 bp) supplied by Invitrogen LTD.

The DNA adsorption on an andosol used in this study was much larger than those on a fluvisol and an acrisol. The decrease in organic matter contents from the soils hardly fluctuated DNA adsorption per unit weight on the H_2O_2 treated soil particles, implying that soil organic matters may not be related to DNA adsorption on soil. The inorganic minerals such as allophane or amorphous oxides including in andosols may be play an important role as main adsorbents for DNA molecules. In next, DNA adsorption on a synthetic allophane was compared with those on the other variable-charged minerals (goethite and gibbsite). The effects of solution pH on DNA adsorption were observed on the allophane minerals (Fig.1). The DNA adsorption decreased with the increase in solution pH in pH > 5, implying that the adsorption of DNA molecules is similar to those of inorganic anions such as phosphate. The competition of phosphate against DNA adsorption on the allophane minerals was observed in some extent, meaning that DNA adsorption mechanism on the allophane minerals could not be explained only by similar reacions to phosphate sorptions.

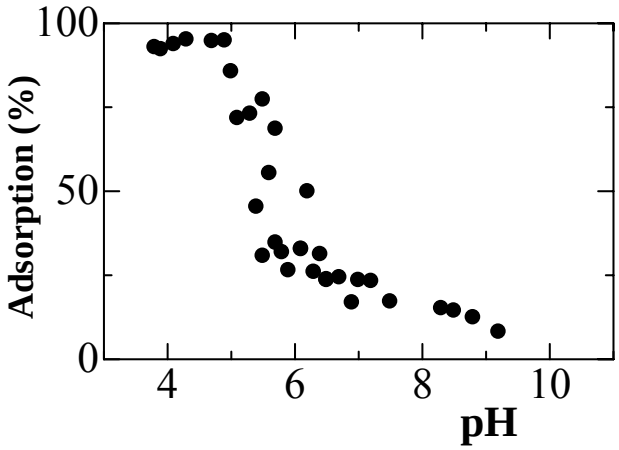

Fig.1 The effect of pH on DNA adsorption on a synthetic allophane.

Solid: 10mg
Solution vol.: 1.0mL
DNA: 200uL of 1mg/mL
Background: 0.1 M NaCl
Reaction time: 2 hrs

*ksaeki@agr.kyushu-u.ac.jp

P067

Extraction of PCBs from River Sediment Using Liquid Dimethyl Ether as Extractant

K. Oshita*[1], M. Takaoka[1], S. Kitade[1], N. Takeda[2],
H. Kanda[3], H. Makino[3], T. Matsumoto[1], and S. Morisawa[1]

[1] *Department of Urban and Environmental Eng., Graduate School of Eng., Kyoto University, C-cluster, Kyotodaigaku-katsura, Nishikyo-ku, Kyoto, JAPAN, 615-8540*

[2]*Eco-technology Research Center, Ritsumeikan University, 1-1-1, Nojihigashi, Kusatsu, Shiga, JAPAN, 525-8577*

[3]*Energy Engineering Research Laboratory, Central Research Institute of Electric Power Industry, 2-6-1 Nagasaka, Yokosuka, Kanagawa, JAPAN, 240-0196*

River and harbor sediments are sometimes contaminated with PCBs that originate from illegally dumped devices such as electric condensers and transformers. It is necessary to remove these PCBs from the sediments. Since river and harbor sediments are large in volume and have a high water content, the removal process has to be efficient and economical.

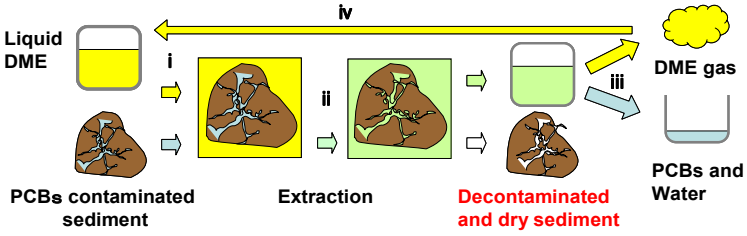

i PCBs Contaminated sediment is mixed with Liquid DME
ii PCBs and Water in the PCBs contaminated sediment is extracted by the DME, and is formed mixture DME, PCBs and water.
iii DME in the mixture is vaporized by decompression. DME and PCB in the water are easily separated by flash distillation, because of large difference of boiling point between DME and PCB in water.
iv DME vapor is compressed and cooled by a heat exchanger. Latent heat of the condensation is reused to vaporize the DME in the heat exchanger.
Liquid DME is reused as extractant.

Fig1. Concept of PCBs extraction method using DME

Therefore, we focus on solvent extraction as a removal method for PCBs from sediments using liquid dimethyl ether (DME) as an extractant. Solvent extraction using liquefied DME for treating the sediment has many potential advantages including high removal efficiencies for organic contaminants and water, the potential to operate at a moderate pressure of 0.6–0.8 MPa at room temperature, and the ability to separate the extract from the extractant and recycle the extractant (Fig.1).

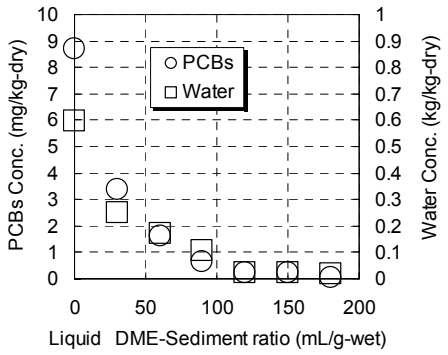

Fig2. Relationship liquid DME-Sediment ratio and PCBs and water concentration in sediment. (Liquid DME linear velocity: 2.85 m/h)

This study evaluated the extraction characteristics of PCBs from contaminated sediments by using a DME flow-type experimental apparatus. It was found that 99.1% of PCBs and 96.6% of water in the sediment were simultaneously extracted by DME under conditions of a linear velocity of 2.85 m/h and a liquid DME–sediment ratio of 180 mL/g (Fig.2). It was evident that a high PCB extraction ratio was achieved by increasing the liquid DME–sludge ratio and by lowering the linear velocity.

Further, the PCB extraction rate was expressed using the first-order reaction-type model and the extraction rate constant of high-chlorinated PCBs was found to be larger than that of low-chlorinated PCBs.

* kazu_oshita@mbox.kudpc.kyoto-u.ac.jp

P068

Sonochemical reduction of MnO_4^- and formation of MnO_2 particles in aqueous solutions in the presence and absence of alcohols

Kenji Okitsu*, Masaki Iwatani, Ben Nanzai, Rokuro Nishimura
Graduate School of Engineering, Osaka Prefecture University,
1-1 Gakuen-cho, Naka-ku, Sakai, Osaka, 599-8531, JAPAN

High intensity ultrasonic irradiation of a liquid provides interesting chemical effects due to a locally formed cavitation bubbles with high temperature and high pressure. Such cavitation bubbles have been actively researched in the field of material science and environmental science [1, 2]. In this study, we report the rate control for the reduction of MnO_4^- and formation of MnO_2 particles by high intensity ultrasonic irradiation. MnO_4^- is a strong oxidant and one of the hazardous chemicals, while MnO_2 is one of the useful materials for the application to Li-batteries and sensors, catalysts, etc. Here, we have tried to control the sonochemical reduction of MnO_4^- to produce MnO_2 particles in the presence of various types of alcohols.

An argon saturated aqueous solution (60mL) containing MnO_4^- was sonicated (Kaijo 4021type, 200 kHz, 200 W) in the presence and absence of various types of alcohols. The concentration of MnO_4^- and MnO_2 in the irradiated solution was determined by a spectrophotometric method.

Fig. 1 shows the rates of MnO_4^- reduction as a function of alcohol concentration. It was found that the rates of reduction are dramatically dependent on the types and concentration of the added alcohols. It was also suggested that the amounts of the reducing spices for MnO_4^- reduction increase in the order of methanol < ethanol < 1-propanol < 1-butanol at 100mM concentration. The obtained results suggested that the rates of sonochemical reduction of MnO_4^- could be accurately controlled by the addition of alcohols.

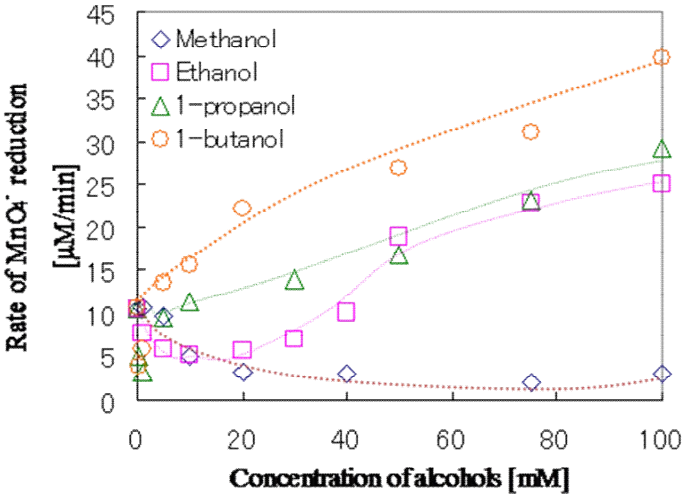

Fig. 1 Rate of sonochemical reduction of MnO_4^- as a function of alcohol concentration.

[1] K. Okitsu, et al., *J. Phys. Chem. B*, 109, 20673-20675 (2005).
[2] B. Nanzai, et al., *Ultrason. Sonochem.*, 15, 478-483 (2008).
*okitsu@mtr.osakafu-u.ac.jp

P069

Estimation of acoustic cavitation bubble temperatures in aqueous anion surfactant solutions

Ben Nanzai*, Kenji Okitsu, Norimichi Takenaka, Hiroshi Bandow

Graduate School of Engineering, Osaka Prefecture University,

1-1 Gakuen-cho, Naka-ku, Sakai, Osaka, 599-8531

Introduction

It is well-known that powerful ultrasonic irradiation in a liquid brings about the formation, growth and collapse of micro gas bubbles. During the collapse, local reaction site of extremely high temperature (several thousand degrees) and pressure (several hundred atmospheres) are produced due to the quasi-adiabatic collapse,[1] while the bulk liquid temperature hardly changes. This process is known as cavitation which induces some local reactions at gas-liquid interface and/or inside of these bubbles. There is, however, little information about the interface region temperature of these acoustic bubbles. In this study, from the sonolysis of linear alkylbenzene sulfonates (LASs), average temperatures of the cavitation bubble interface were measured using a methyl radical recombination (MRR) method.[2] This method is based on the competitive reactions in the recombination of methyl radicals.

Experiment

Aqueous solution of anion surfactants, sodium p-octylbenzenesulfonate (LAS C_8), sodium p-decylbenzenesulfonate (LAS C_{10}) and sodium p-dodecylbenzenesulfonate (LAS C_{12}), were irradiated by high power ultrasound (200 kHz, 200 W). The yields of ethane, ethylene and acetylene were detected by GC/FID. Average bubble temperatures were measured using the MRR method.

Results and Discussion

Since LASs have no volatility, they were decomposed only at the gas-liquid interface region. From the results of the MRR method, the average temperatures of acoustic bubble interface were measured as shown in Fig. 1. The temperatures were estimated as 3100-3900 K in all LASs aqueous solutions. They were little difference from the previous reports of the temperatures inside the acoustic bubbles.[2] From these results, it was suggested that methyl radicals were recombined at the interface region of acoustic bubbles.

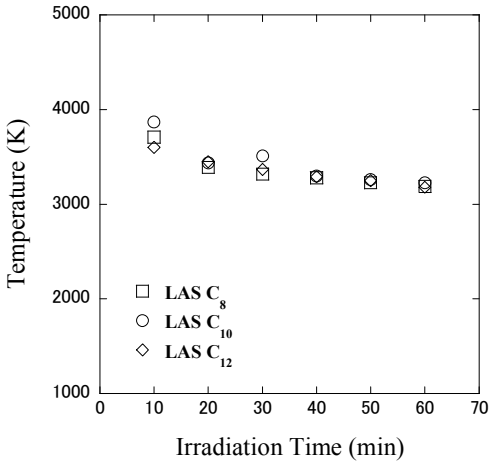

Fig. 1 Temperatures of acoustic bubble interface.

1) Leighton, T.G. *The Acoustic Bubble*; Academic Press: London, 1994.

2) Tauber, A. et al., J. Chem. Soc., *Perkin Trans. 2* **1999**, *2*, 1129.

*nanzai@chem.osakafu-u.ac.jp

P070

Colloidal behavior of acetate-utilizing methanogens in the anaerobic digester

T. Nomura[1*], A. Yoshihara[1], Y. Konishi[1]

[1] *Department of Chemical Engineering, Osaka Prefecture University,*
1-1 Gakuen-cho, Naka-ku, Sakai, Osaka 599-8531

Upflow anaerobic sludge blanket (UASB) reactor has been employed in wastewater treatment. However, the long start up period required for the application of this technology. The mechanism for anaerobic granulation should be understood to shorten the start up period. Surface physico-chemical properties can be treated as an indicator of the adhesion properties of microbial cells. In this study, we evaluated the surface physico-chemical properties of acetate-utilizing methanogens, *Methanosarcina barkeri* JCM 10034 and *Methanosaeta concilii* DSM 3671. *Methanosaeta* and *Methanosarcina* species are the only known methanogens that are capable of acetate catabolism. The surface potential and surface tension of microbial cells were analyzed by the measurements of electrophoretic mobility and contact angle. *M. barkeri* was hydrophobic and negatively charged. By contrast, *M. concilii* was hydrophobic and uncharged. It is a unique result because the majority of microbes are negatively charged. ATR-FTIR measurements were performed to investigate the molecular level of functional groups on cells. The peak levels of the carboxyl and phosphoric group of *M. concilii* are much lower than those of *M. barkeri*. The difference of surface potential between these methanogens was also confirmed by the acid-base titration. Furthermore, the microbial coadhesion agreed well with the prediction by the extended DLVO theory using the parameters (surface potential and surface tension) obtained in the study.

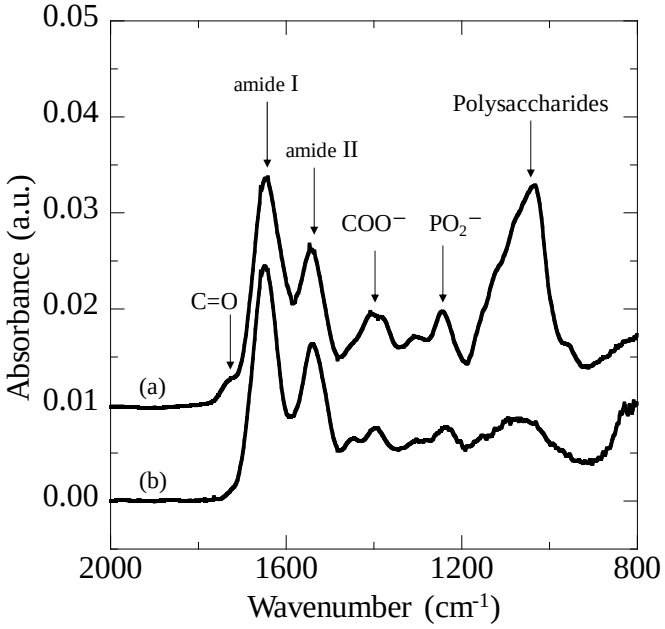

Fig. 1 ATR-FTIR spectra of (a) *M. barkeri* and (b) *M. concilii*.

*nomura@chemeng.osakafu-u.ac.jp

P071

CROSSFLOW ULTRAFILTRATION OF DISSOLVED HUMIC ACID SOLUTIONS USING COAGULATED HUMIC ACID CAKE FORMED ON POROUS FINE CERAMICS

H. Nakakura*, K. Yamashita

Graduate school of Science and Engineering, Yamaguchi University,

2-16-1 Tokiwadai, Ube, Yamaguchi 755-8611

The crossflow ultrafiltration processing of dissolved humic acid solutions was investigated in laboratory experiments. Formation of filter cake of coagulated humic acid on porous fine ceramics was effectively utilized as a self-rejecting dynamic membrane. Commercially produced polyaluminium chloride (PAC) was used as a coagulant. In Fig.1, the experimental results of reciprocal filtration rate ($d\theta/dv$) and humic acid rejection (R) vs. filtrate volume per unit membrane area (v) are plotted for crossflow microfiltration of coagulated humic acid suspension (first step, MF), and crossflow ultrafiltration of dissolved humic acid solution (second step, UF). Crossflow velocity, u_c, and applied filtration pressure, p, were held constant during both filtration steps. The observed rejection of humic acid is defined by $R = 1 - s_f / s_0$, where s_f is the mass fraction in filtrate and s_0 is the mass fraction in the feed solution. The cake structure of coagulated humic acid forming on the ceramic membrane plays a significant role in rejection of humic acid in crossflow ultrafiltration of dissolved humic acid solution. Since coagulated humic acid cake behaves as a highly compressible cake (compressibility coefficient of cake, n=0.56), the internal structure of the filter cake varies considerably with the filtration pressure. An increase in filtration pressure was demonstrated to produce a more compact cake structure, leading to a marked increase in rejection of humic acid. Coagulated humic acid cake with a loose structure was swept away from the ceramic membrane surface due to high shear force produced by the crossflow sweeping effect. The capture mechanisms may be interpreted in the same way as deep bed filtration, that is, Brownian diffusion, interception, physical adsorption, inertia, gravity, and hydrodynamics. The new dynamic membrane filtration system proposed in this study is effective in drinking water treatment processing.

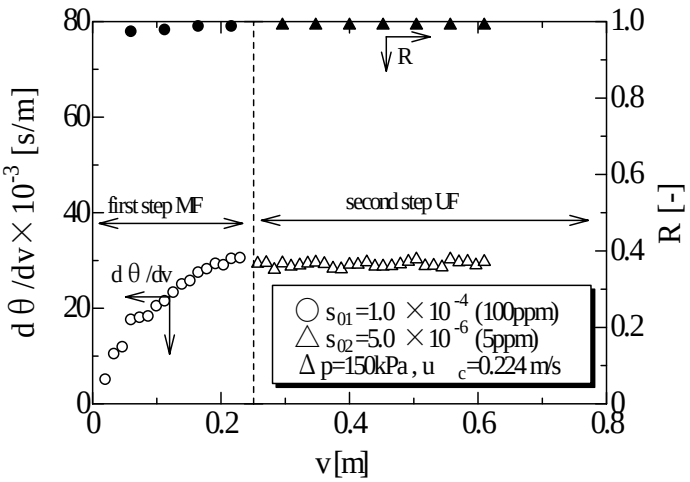

Fig.1 Relation between $(d\theta/dv)$, R and v

*nakakura@yamaguchi-u.ac.jp

P072

Deoiling and Dewatering Processes for General Purposes by Using Liquefied DME

Hideki Kanda* and Hisao Makino

Energy Engineering Research Laboratory, Central Research Institute of Electric Power Industry, 2-6-1 Nagasaka, Yokosuka, Kanagawa 240-0196, JAPAN

The proposed technology is a new concept that aims at energy-efficient drying and cleanup for general purposes by the use of liquefied DME (dimethyl ether) gas. This technology reduces the energy required for water-removal to half the latent heat of water [1, 2]. We almost completely removed water and other oily materials by using DME [3]. DME was completely recycled and none of it remained in these materials. Moreover, low-temperature waste heat recovery enables the circulation of DME as a zero-input-energy operation. Ground pollution is a significant environmental concern. However, large amounts of energy are required for the cleanup of the ground since the water contained in the soil hinders the extraction processes that use hydrophobic organic solvents. Therefore, we focus on the use of liquiefied DME, which is eco-friendly, as an extractant. The saturated pressure of DME is moderate—0.51 MPa at 20°C and 0.68 MPa at 30°C. Liquefied DME resolves high volume organic contaminants and water. Moreover, water can be easily separated from DME by flash distillation. The world's first prototype of a DME deoiling/dewatering process is shown in Fig.1. The capacity of this system is 10 L. Because of the low normal boiling point (–25°C) of DME, it does not remain in the soil and it can thus be reused as an extractant (Fig.2). In this presentation, we show the general purpose deoiling and dewatering processes for several materials. We will now be collaborating with a team from Kyoto University (Dr. Takaoka and Dr. Oshita) for the cleanup of river and harbor sediments polluted with PCBs.

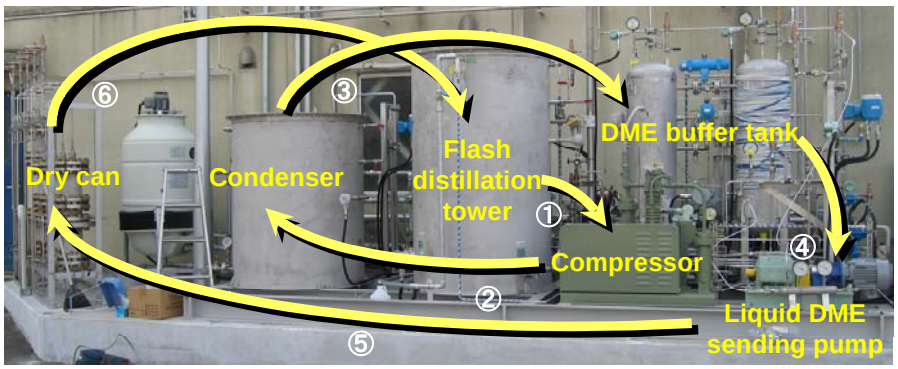

Fig.1 Prototype of the DME deoiling/dewatering process.

Fig.2 Deoiling and dewatering of soil polluted with heavy oil by DME.

References:

1) Hideki Kanda and Hiromi Shirai, *Chinese Patent*, ZL03812777.6; *Indonesian Patent*, ID0018953 (2002).
2) Hideki Kanda, Hisao Makino and Minoru Miyahara, *Adsorption*, in press (2008)
3) Hideki Kanda, *Pending Japanese Patent*, JP237129A (2007).

* kanda@criepi.denken.or.jp

P073

Molecular analysis of a bacterial nanofiber of the highly adhesive bacterium, *Acinetobacter* sp. Tol 5

M. Ishikawa[1*], S. Takada[1], K. Hori[1, 2]

[1]*Department of Materials Science and Engineering, Nagoya Institute of Technology*
Gokiso-cho, Showa-ku, Nagoya 466-8555, Japan

[2]*PRESTO, JST,*
4-1-8 Hon-cho, Kawaguchi, Saitama 332-0012, Japan

Acinetobacter sp. Tol 5 shows high adhesiveness mediated by long adhesive nanofibers. To elucidate the adhesion mechanism of this bacterium, we have obtained a less-adhesive mutant, T1, by transposon mutagenesis. T1 cells lack the adhesive nanofibers. To identify the gene involved in adhesion and producing the nanofibers, we analyzed the region disrupted by the transposon insertion. By southern hybridization and inverse PCR, we have succeeded in cloning of the DNA fragment containing the structural gene inserted by the transposon. The disrupted gene was homologous to genes encoding trimeric autotransporter adhesin (TAA). The whole gene of the TAA homologue was revealed by cloning of several DNA fragments, and its DNA sequence (10,950bp) was determined.

Members of the TAA family form themselves into non-fimbrial adhesive nanofibers exposed on the cell surface of Gram-negative pathogens, and play crucial roles in the infection. *Yersinia enterocolitica* adhesin A (YadA), the representative protein of the TAA family, forms into lollipop-shaped structure with a head-neck-stalk-anchor architecture on the bacterial surface. C-terminal anchor domain forms β-barrel structure by twelve β-strands through the outer membrane and the head-neck-stalk domain (passenger domain) is transported to the bacterial surface via the central pore of the β-barrel.

The TAA homologue of Tol 5 named AadA (*Acinetobacter* adhesin A) comprises 3,630 amino acids. Head, neck, stalk, and anchor domains were present in AadA sequence like other members of the TAA family, and the 3-D structure of the anchor domain, which defines this family, was deduced to be conserved. However, AadA has some unique features unshared with other members of the TAA family. The primary structure of AadA has second head domain to the C terminus region as well as the normal one at the N terminus, several neck domains, and a long stalk domain containing several long and highly conserved repeat sequences. Consequently, AadA is predicated to be a novel TAA.

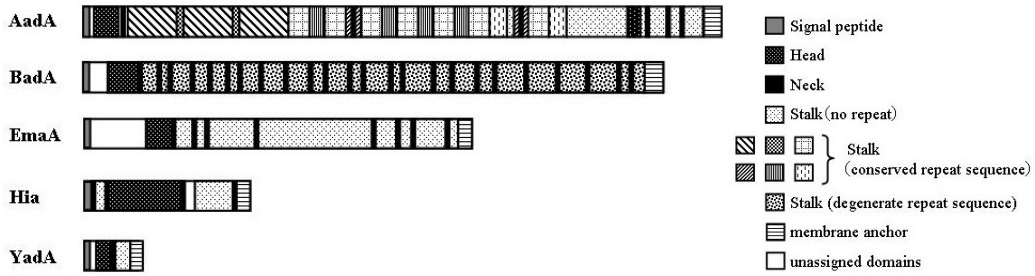

FIG. 1. Schematics of the primary structure of AadA and members of the TAA family

*hori.katsutoshi@nitech.ac.jp

P074

Population analysis of denitrifiers inhabit the biofilm on submerged reed surface through molecular biological protocol targeting denitrifying genes, *nir*S and *nir*K

I. Yoshinaga*, T. Nakamura, T. Amano, Y. Sako

Gradute School of Agriculture. Kyoto Univeresity,

Kitashirakawa, Kyoto 606-8502 Japan

Considerable denitrification activity and abundance of denitrifying bacteria were observed in the biofilm (BF) on submerged reed (*Phragmites australis*) surface, indicating reed community might supply a “hot spot” for denitrifying bacterial population in aquatic environments. In this study, species compositions of denitrifying bacterial population inhabit the BF on submerged reed surface was estimated through the culture-independent, clone library protocol targeting nitrite reductase genes, *nir*S and *nir*K. Genomic DNA was extracted and purified from the BF on reed surface, the BF on rocks, sediments and lake water, respectably, which were collected around a reed community grown at the east coast of Lake Biwa (Japan) on June 18, 2007. Partial fragments of *nir*S (the component gene of cytcrome cd[1] type nitrite reductase) and nirK (the component gene of Cu-including type nitrite reductase) were amplified by selective PCR, respectively, from the purified genomes. After cloning, more than 40 clones of each gene from each sample were sequenced and analyzed phylogenetically. As the result, most of the *nir*S and *nir*K genes from reed band were novel and un-deposited sequence in gene databases, indicating the reed community should be a good source for isolating new microbial resources, useful denitrifying bacteria for environmental managements. Interestingly two phylotypes of *nir*S gene and three phylotypes of *nir*K gene were dominantly isolated only from the BF on reed surface. In conclusion, BF on the submerged reed surface should be a unique habitat for some denitrifying population and detail investigation on the physicochemical characteristic, the microbial community structure, and the interaction between reed and denitrifying bacteria in the BF on reed surface should be needed in the future.

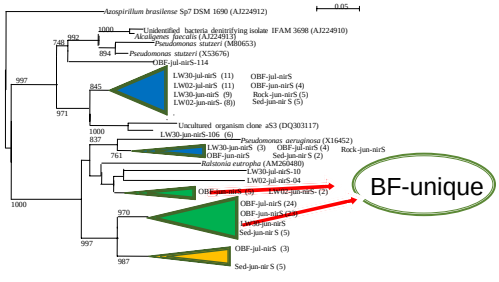

Figure 1 Phylogenetic tree inferred from *nir*S genes including PCR amplified fragments (Partial) from biofilms developed on the submerged reed (*Phragmites australis*) surface.

* iyoshina@kais.kyoto-u.ac.jp

P075

Root endophytes isolated from a native species *Clethra barvinervis* Sieb. et Zucc. in Hitachi mine increase the seedling growth and control the heavy metal absorption

K. Yamaji[1]*, Y. Watanabe[1], K. Kobayashi[1], T. Kozaki[2]
[1]*Graduate school of Life and Environmental Science, University of Tsukuba, 1-1-1 Tennoudai, Tsukuba, Ibaraki 305-8572*
[2]*Graduate school of Engineering, Hokkaido University, Kita 13, Nishi 8, Kita-ku, Sapporo, Hokkaido 060-8628*

Though Hitachi mine was bare land because of smoke injury, the mine has been successfully green by tree planting. *Clethra barvinervis* Sieb. et Zucc.was not a selected species for tree planting but a native species. *C. barvinervis* seems to be tolerant of the high concentration of heavy metals, Cu, Ni, Zn, Cd, and Pb that were highly included in the Hitachi mine soil (Kubota et al., 1986). Our purpose of this study is to clarify the ability of *C. barvinervis* that could be suitable for the severe environment such as highly polluted place with heavy metals, considering the interaction with root endophytes. We examined 1) heavy metal contents of rhizosphere soil, leaves, and roots collected from mature *C. barvinervis* in Hitachi mine from June in 2006 to May in 2007, isolated 2) endophytes from surface-sterilized root segments in June, August, and October 2006, and examined 3) the growth, and heavy-metal and nutrient absorption of *C. barvinervis* seedlings growing in gamma-ray sterilized mine soil with or without root endophytes.

The rhizosphere soil of *C. barvinervis* highly included Pb (492.3~779.4 mg/kg), Cu (435.8~644.4 mg/kg), and Zn (131.5~386.4 mg/kg) compared with Ni (8.82~13.3 mg/kg) and Cd (3.32~6.61 mg/kg). Though the roots highly included Pb (ave. 517.1 mg/kg), Zn (219.9 mg/kg) and Cu (ave. 212.9 mg/kg), the leaves highly included only Zn (304.0 mg/kg) (the others; less than 22 mg/kg). The contents of Pb and Cu in the *C. barvinervis* roots were significantly higher than those in *Prunus speciosa* (Koidz.) Nakai and *Camellia japonica* L. that were tree species for planting in Hitachi mine. These results indicate that *C. barvinervis* was a tolerant tree species for high contents of Pb, Cu and Zn. Three endophytes frequently isolated from mature tree roots were considered as dominant endophytes. Inoculation results showed that *C. barvinervis* seedlings with the root endophytes grew significantly compared with those without the endophytes. The seedlings inoculated with the root endophytes significantly absorbed higher amount of K, and much lower amounts of Cu, Ni, Zn, Cd and Pb than the seedlings without the endophytes.

Our results indicate that *C. barvinervis* is tolerant tree species for high contents of heavy metals because the root endophytes increase the seedling growth through nutrient uptake as well as control of the excess absorption of heavy metals into roots.

Kubota et al. Japanese Journal of Soil Science and Plant Nutrition, 57, 142-148 (1986).

*yamajik@sakura.cc.tsukuba.ac.jp

P076

Influence of Biofilm Formation on Stainless Steel Corrosion

T. Urakami*[1], A. Ikoma[1], H. Morisaki[1], J. Liao[2], H. Fukui[2], K. Hojo[2]

[1]*Graduate School of Science and Engineering, Ritsumeikan University, 1-1-1 Noji-higashi, Kusatsu, Shiga 525-8577,* [2]*Kurimoto Ltd., 2-8-45 Suminoe-ku, Osaka 559-0021, Japan*

Two model lines consisted of SUS304 stainless steel pipes varying in diameter and inside smoothness were constructed on a float in a dam lake. The lake water (pumped up from the depths of 2 and 8 m, respectively) was flowed continuously through the two lines. The vertical profiles of temperature, dissolved oxygen concentration and light intensity of the lake water were measured at 2 months interval through a year. Various features of BF (thickness, ion concentrations, microbial flora) were analyzed and their relation with the metal corrosion was examined. Potentials of the stainless steel pipes were measured with an Ag/AgCl reference electrode.

The lake water separated into two layers during hot season (aerobic and warmer upper-layer vs. anaerobic and cooler lower-layer), although the two layers disappeared during cool season.

At the early period of the experiment, the potentials of the pipes increased to a high level due to the formation of BF inside the pipes. Corrosion occurred at welded part of the pipes of both the two lines after 1 to 3 months (Fig. 1), accompanied by a dramatic drop of the potentials. The concentrations of nutrient ions (ammonium, nitrate, nitrite, phosphate) in the BF interstitial-water were several hundred times higher than those in the lake water. The thickness of BF was greater at welded part of the pipe than non-welded part. The BF at the corroded part showed greater nutrient ion concentrations compared with the BF at non-corroded parts. The microbial floras were different between BF and lake water, however few distinct microbes was identified as causal agent of the metal corrosion.

From the above findings it was assumed that BF at a certain level of maturation (in respects of thickness and nutrient salt concentrations) could form a micro-scale environment where the metal may be easily corroded compared to the part free from the matured BF.

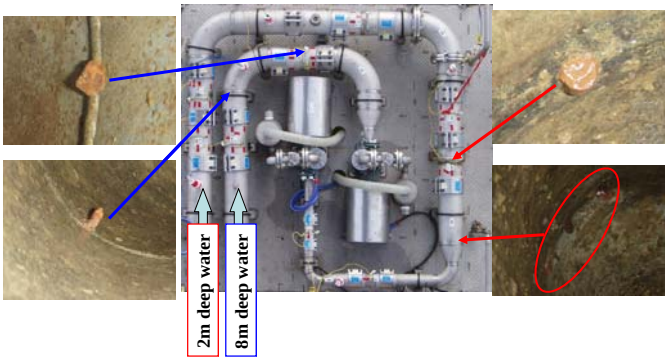

Fig.1. Two pipe lines for corrosion experiment and the corroded parts inside the pipes (after 1 year).

* rb001034@se.ritsumei.ac.jp

P077

Viable spores on solid surfaces: adhesion characteristics and alkaline cleaning effect

Yusuke Nanasaki*, Tomoaki Hagiwara, Hisahiko Watanabe, Takaharu Sakiyama
Department of Food Science and Technology, Tokyo University of Marine Science and Technology Tokyo 108-8477 Japan

Endospores are resistant to heat and chemicals. Thus adhesion of endospores to food contact surface leads to a high risk of cross contamination in food manufacturing. Understanding the characteristics of adhesion and removal of endospores has significance in food safety. In this study, adhesion and removal of *Geobacillus stearothermophilus* JCM12216 spores were analyzed. Substrates employed were stainless steel (SS) of type 304 and polypropylene (PP).

First, the effect of dehydration on the adhesion was studied. Spore suspension was made contacted with a plate of SS or PP (50×50 mm) under a high humidity for 60 min. The spores remaining on the plate after soaking in sterile water for 10 min were taken as adhered. Result showed that approximately half of spores in the suspension adhered to SS and PP plates. When similar experiments were conducted under a low humidity condition, where the spore suspension was allowed to dry for 60 min, almost all spores in suspension adhered to SS and PP plates. Thus dehydration increased the adhesion of the spores.

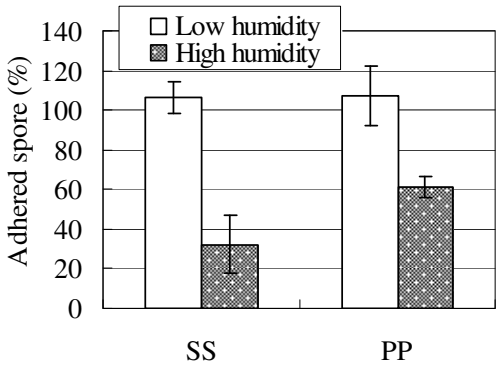

Fig1. Adhesion of spores to SS and PP plates under different humidity conditions.

To study the removal characteristics of spores adhered under the low humidity condition, the plates with spores adhered were subjected to washing in stirring tank for 10 min. Washing with sterile water and 1% NaOH at 25℃ removed very few spores from the plates. Washing with 1% NaOH at 75℃ reduced viable spores: 50% remaining on PP and 3% on SS. However, survival of spores suspended in 1% NaOH at 75℃ for 10 min was less than 1%. Thus spores on solid surfaces, especially on PP, showed higher resistance against alkali than those in suspension.

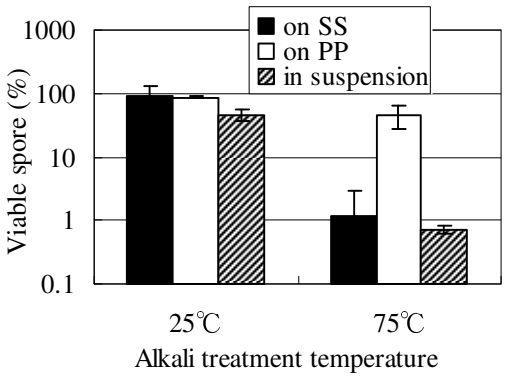

Fig2. Percentage of viable spores on SS (■) and PP (□) plates after washing treatment in 1% NaOH. For comparison, free spores (▨) were suspended in 1% NaOH.

*lucifer772000@yahoo.co.jp

P078

Penetration behavior of *Vibrio cholerae* hemolysin into a mixed monolayer of DMPC and Cholesterol

Y.Tagami[1], T.Narita[1], H.Ikigai[2], and Y.Oishi[1]*

[1]*Dept. of Chem. & Appl. Chem., Saga Univ., Saga, 840-8502, Japan*

[2]*Dept. of Chem. & Biochem., Suzuka Natl. Coll. of Technol., Suzuka, 510-0294, Japan*

There are many kinds of pathogenicity proteins produced by bacteria. *Vibrio cholerae* hemolysin (VCH, molecular mass 65 kDa) is one of the proteins, which forms a transmembrane oligomer in target cell membrane to induce a strong cytotoxicity. However, the assembly mechanism of VCH in membrane is not yet clear. In this study, the formation of VCH oligomer in mixed monolayer of dimyristoylphosphatidylcholine (DMPC) and cholesterol (Chol) was studied by an atomic force microscopy (AFM).

Chloroform solution of (DMPC/Chol) with a molar fraction of 70:30 was prepared at a concentration of 1.0×10^{-3} mol/l. The monolayer was prepared by compression to a surface pressure of 3.0±0.1 mN/m at an area change rate of 2.6×10^{-3} nm^2/molecule s. With maintaining the surface pressure, water or aqueous VCH solution was injected into subphase. The concentration of VCH in subphase by the injection was 0.55 μg/ml. After standing for 12h, the monolayer was transferred onto a freshly cleaved mica by the horizontal drawing up method at a transfer rate of 1 mm/min. Topographic images of the monolayer surface on mica were obtained by AFM in air.

Figure 1 shows LB curves of (DMPC/Chol) mixed monolayer with different injection solutions. The monolayer rapidly shrank to be an equilibrium state after 4×10^3 sec in the case of water injection. On the other hand, the monolayer gradually expanded when the VCH solution was injected into subphase. This suggests that VCH induced a change in monolayer state. Figure 2 shows an AFM image of (DMPC/Chol) mixed monolayer which was prepared in the presence of VCH. Larger domains with a diameter of about 40 nm, dots with that of about 10 nm and matrix region were observed on the monolayer surface. Dots were not observed on the monolayer prepared in the absence of VCH. It is, therefore, reasonable to consider that VCH molecules penetrate into the monolayer from the hydorophilic group side and appear as dots with a diameter of 10 nm at the hydrophobic group side.

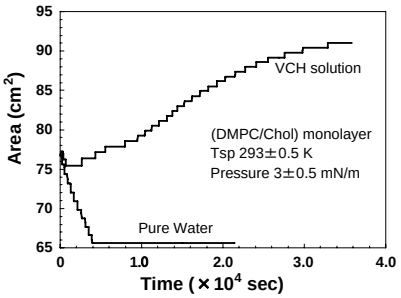

Fig. 1. LB curves of the mixed monolayer with different injection solutions.

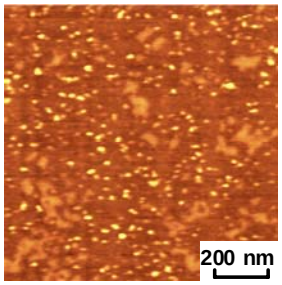

Fig. 2. AFM image of the mixed monolayer by VCH addition.

*oishiy@edu.cc.saga-u.ac.jp

P079

Microscale Environment and Microbial Flora Inside of Biofilm

Y. Tsuchiya*, A. Hiraki, T. Arakawa, R. Kusakabe, M. Yamamoto, H. Morisaki

Graduate School of Science and Engineering, Ritsumeikan Univeresity

1-1-1 Noji-higashi, Kusatsu, Shiga 525-8577

The nutrient salt concentrations in the interstitial water of biofilm (BF) formed on the surfaces of reeds (*Phragmites australis*) and stones in Lake Biwa were investigated during several years. The microbial flora of the BFs was also analyzed to examine the correlation between the flora and the microscale environments inside BF.

Reeds and stones were sampled at northern and southern basin of Lake Biwa once a month. The BFs formed on their surfaces were taken and suspended in distilled water and filtrated. The suspension was used for the analysis of microbial flora by PCR-DGGE method. The filtrates were used to analyze the concentrations of various ions colorimetorically.

The concentrations of nutrient ions (ammonium, nitrate, nitrite, phosphate) in the BF interstitial-water were several hundred times higher than those in the lake water regardless of seasons. The concentrations of these ions showed characteristic seasonal change. Interestingly, the concentrations of the ions in the lake water showed similar seasonal change with those in the BF interstitial-water, i.e., high in winter and low in summer (Fig. 1). The microbial flora of the BFs was different from the lake water and changed seasonally.

Above results suggest that BFs may concentrate various ions from surrounding environment (lake water in the present study), so that show a similar seasonal changing pattern of the nutrient salt concentration with the lake water. This seasonal change seemed to result in the development of microscale environments inside BF hence to microbial flora characteristic for the BF at each season.

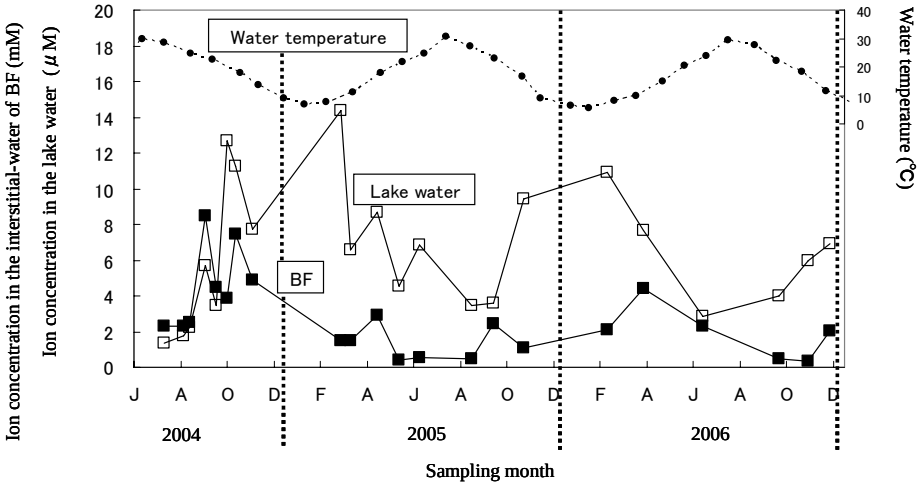

Fig.1 Seasonal change of nitrate ion concentration in reed-BF(■) and lake water(□) with showing the change of water temperature(●) at the southern basin of Lake Biwa.

* rb005028@se.ritsumei.ac.jp

P080

Effect of cathodic protection on biofilm attached to carbon steel

K. Miyanaga*, Y. Tanji

Department of Bioengineering, Tokyo Institute of Technology,

4259 J2-15 Nagatsuta-cho, Midori-ku, Yokohama 226-8501

Biofilm formed on carbon steel causes serious problems such as microbiologically influenced corrosion (MIC) of steel, choking of flow in the pipe, deterioration of the heat-transfer efficiency and so on. Cathodic protection (CP) is known to be a reliable method for protecting carbon steel from corrosion.

In this study, CP was applied to the carbon steel soaking the artificial seawater with bacterial consortia or phosphate buffer solution containing *Pseudomonas aeruginosa* PAO1, a biofilm constituent. The aims of this study were to evaluate the inhibition effect of CP on biofilm proliferation, the initial bacterial adhesion and bacterial viability. The change of bacterial surface charge revealed that electrostatic repulsion between the surface of carbon steel and bacterial cell wall was enhanced by the CP. Consequently, the enhanced electrostatic repulsion also contributed the inhibition of bacterial adhesion to carbon steel in the CP process. In addition, to evaluate the inhibition effect of CP on bacterial viability in the biofilm, CP was applied to an artificial biofilm containing PAO1 on carbon steel. The viability of PAO1 in artificial biofilm of 5-mm thickness on cathodically protected steel decreased to 1% of the initial cell concentration but did not decrease any more for 24 hours. Analysis of pH distribution in the artificial biofilm by pH microelectrode revealed that pH in proximity to carbon steel increased to approximately 11 after CP for 5 hours (Fig.1). Moreover, 99% of region in the artificial biofilm was under the pH conditions of over 9. A simulation of pH profile derived from diffusion model of hydroxide ion was shown to correspond to experimental values. These results indicate cells in most part of artificial biofilm were killed or damaged by CP due to pH increase. Survived bacteria are thought to exist in only thin layer (50 μm) from the bulk solution.

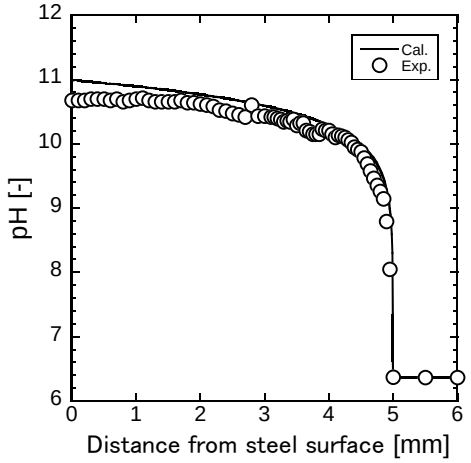

Fig.1 pH profile in the artificial biofilm on the carbon steel during cathodic protection. Open circles and solid line indicate experimental values and simulation result, respectively.

*kmiyanag@bio.titech.ac.jp

P081

Denitrification in the biofilm developed on submerged reed surface

T. Nakamura[1]*, T. Amano[1], T. Yamagishi[2], Y. Suwa[2], Y. Sako[1], I. Yoshinaga[1+]

1. Gradute School of Agriculture. Kyoto Univeresity, Kitashirakawa, Kyoto 606-8502 Japan

2. National Institute of Advanced Industrial Science and Technology (AIST), 16-1 Onogawa, Tsukuba, Ibaraki 305-8569 JAPAN

Denitrification is a key process for removing excess nitrogen compounds from aquatic environments through the N_2 gas production. In this study, we investigated the possibility that biofilm (BF) developed on reed (*Phragmites australis*) surface under the water can be "hot spot" for denitrifying bacterial population since the micro-anaerobic condition, rich nitrogen oxides and abundant organic carbon sources available for the denitrifying bacteria. The submerged stems of reed were collected three times, May, June and July in 2007, at a site in southern basin of Lake Biwa, which is the biggest lake in Japan, and the denitrifying activities in the BFs on reed surface were determined by a ^{15}N-tracer experiment. The intact stems of reed (OST), removed BF with a teeth brush (OBF), and the reed stems free from the BF (OST-BF-free) were incubated with $^{15}NO_3$ under He atmosphere and the $^{30}N_2$ in the head space gas was measured with GC-MS. At the same time, total bacteria and denitrifying bacteria were enumerated through a direct counting method and MPN method, respectively. As the results, denitrifying activities in BFs on the reed surface per total bacterial counts attained to the value in the sediments, indicating BF on the reed surface is an appropriate habitat for the denitrification. The MPN of denitrifying bacteria estimated a MPN protocol also suggested that BF on the submerged reed surface could be a "hot spot" for the denitrifying bacterial population. Interestingly, denitrifying activity remained on the reed stem after scraping BF by a toothbrush in May, but the activities on the stems in June and July diminished after scraping. This observation suggests that the microbial community structure and physicochemical structure of BF on the reed surface might changeable seasonally and effect on the denitrifying bacterial population and their activity.

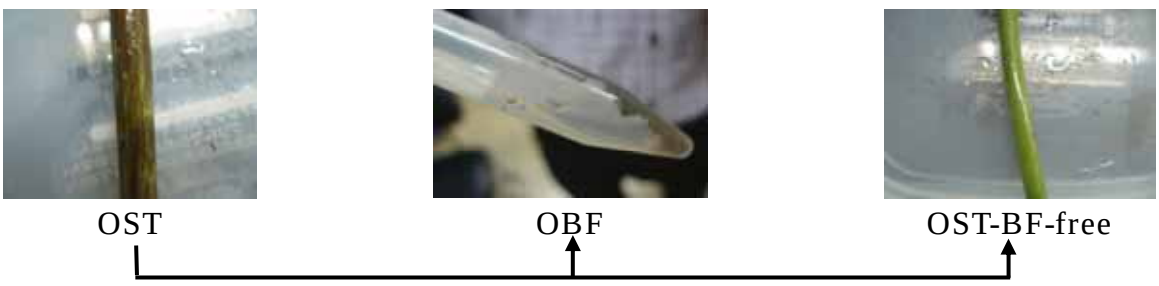

+ Corresponding author: iyoshina@kais.kyoto-u.ac.jp

P082

Adsorption and desorption of Sulfadiazine on different soil components

N. Meng, H. Lewandowski, H.-D. Narres, E. Klumpp*, H. Vereecken

Agrosphere, ICG-4, Forschungszentrum Jülich GmbH, D-52425 Jülich, Germany

The adsorption and desorption behavior of ^{14}C labeled sulfadiazine (^{14}C-SDZ) was investigated with different inorganic soil components including Al_2O_3, goethite, illite and compared with air-dried and heated topsoil. The batch sorption experiments were performed according to the OECD test Guideline 106. All experiments were conducted in natural pH-values of the different sorbents. For Al_2O_3, goethite and the soils these pH-values range from 7.5 to 8.2, causing negatively charged amphoteric SDZ; for illite the natural pH-value was about 4, where SDZ is neutral. For comparability adsorption experiments on illite were also done in a buffered solution of about pH 8.

The adsorption isotherms on all sorbents are strongly nonlinear and can be fitted well by the Freundlich equation. From the initial slope of the isotherm the partition coefficient K_d could be determined. The adsorption of SDZ on illite at pH 4 has a higher K_d-value than at pH 8, which demonstrates that the negative charge of SDZ obstructs the adsorption.

The desorption isotherms show hysteresis effects for all adsorbents. Whereas for goethite and illite a strong hysteresis was found, for Al_2O_3 a low effect indicates the weak bonding of the adsorbed SDZ. The properties of the inorganic matrix and especially the charges of the inorganic compounds in relation to the charge of SDZ are important parameters for the sorption process.

To analyze the importance of the organic matter (OM) for the sorption behavior of a hydrophilic organic molecule on natural sorbents the ad- and desorption isotherms of SDZ on a soil with about 1% OM and a heated soil without OM are compared.

* e.klumpp@fz-juelich.de

P083

Analysis of Biofilm Formation Process on Reed Surface

A. Hiraki*, Y. Tsuchiya, T. Arakawa, R. Kusakabe, H. Morisaki

Graduate School of Science and Engineering, Ritsumeikan Univeresity

1-1-1 Noji-higashi, Kusatsu, Shiga 525-8577

The formation process of biofilm (BF) on reed (*Phragmites australis*) surface was examined in natural environment.

The BFs on reeds were removed (May 19, 2007) at a site in southern basin of Lake Biwa. Then, the reeds were sampled at 3, 10, 17, 31 and 59 days after the BF removal day. The BFs formed on the reed surface were suspended in distilled water and filtrated. The suspension was used to determine total cell count and colony forming unit (CFU) on agar medium and was used for the analysis of microbial flora by PCR-DGGE method. The filtrates were used to analyze the concentrations of various ions colorimetorically.

The following dynamic aspects of BF formation process were revealed for the first time (Fig. 1).

1) The BF thickness was very small until 10 days of formation process but began to increase rapidly after 10 days and reached ca. 40 μm at 17 days, then remained almost constant.

2) The number of CFU in BF (10^7〜10^8CFU/wet-g BF) was higher (ca. 10^3 times) than that of lake water and increased at an early stage (during 3 to 10 days) then decreased at later stage. The ratio of CFU/total cell count was highest at 10 days of the formation process. Thus, the early stage BF seemed to contain many more active microbes than the later stage BF.

3) Extracellular polymeric substances (EPS) covering BF were observed microscopically at later stage BF. It seemed that the microbes increased their cell number at the early stage (until 17 days) then turned to produce EPS at the later stage.

The bacterial flora and nutrient salts concentration in BF along its formation process are being investigated and will be discussed.

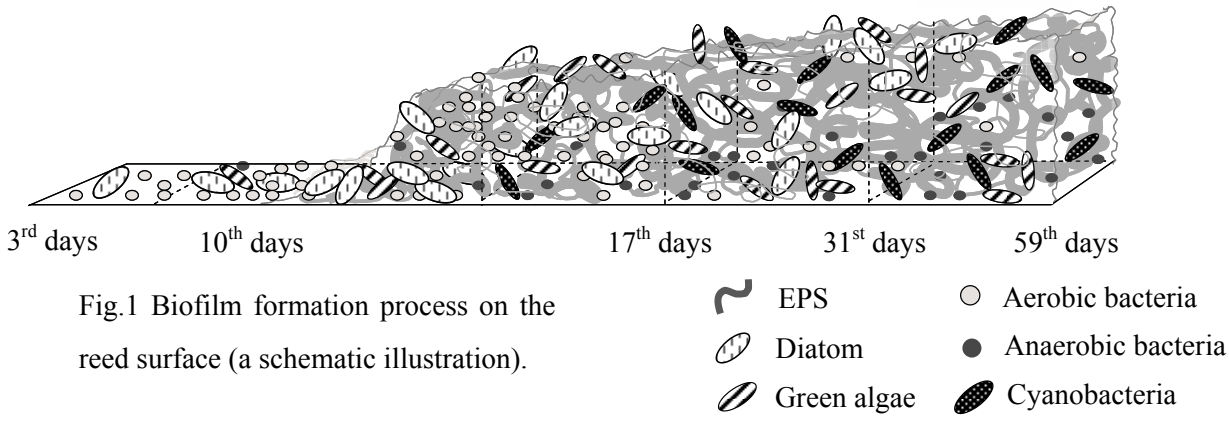

Fig.1 Biofilm formation process on the reed surface (a schematic illustration).

* rb007040@se.ritsumei.ac.jp

P084

Morphological analysis of bacterial nanofibers on *Acinetobacter* sp. Strain Tol 5 by electron microscopy.

A. Higuchi[1]*, Y. Hotta[2], K. Yamamoto[2], K. Hori[1, 3]

[1]*Department of Materials Science and Engineering, Nagoya Institute of Technology, Gokiso-cho, Showa-ku, Nagoya 466-8555, Japan*

[2]*Department of Operative Dentistry, Asahi University, 1851 Hozumi, Mizuho,Gifu 501-0296, Japan*

[3]*PRESTO, JST, 4-1-8 Honcho Kawaguchi, Saitama 332-0012, Japan*

Acinetobacter sp. Tol 5, which was isolated as a toluene-degrading Gram-negative bacterium, shows high adhesiveness to solid surfaces and self-agglutinates. FE-SEM revealed that Tol 5 cells have at least two types of adhesive nanofibers. An anchor-like nanofiber extends straight to the substratum without branching and tethers the cell body at its end at distances of several hundred nanometers. The other, a pili-like nanofiber, attaches to the substratum in multiple places, fixing the cell at much shorter distances. *Acinetobacter* sp. Tol 5 can grow on various carbon sources, for example, toluene, lactic acid, ethanol, and triacylglycerol (TAG). Tol 5 cells scarcely produce the nanofibers in the absence of surface areas sufficient for adhesion, but start to produce them when carrier with a large surface area and toluene are given. In the study, we investigated the effects of carbon sources on the adhesiveness and the production of the nanofibers in Tol 5 cells.

The adhesion tests using polyurethane foam about the cells grown on toluene, lactic acid, and TAG revealed that Tol 5 cells from toluene are the most adhesive and are followed by the cells from lactic acid. While almost all of the cells grown on toluene adhered to the polyurethane, only half of the cells grown on TAG did. Then, these cells were observed by FE-SEM and TEM. FE-SEM revealed that cells from toluene and lactic acid produce a lot of the pili-like nanofibers to adhere to the polyurethane surface, but cells from TAG hardly produced these nanofibers (Fig. 1). TEM observation indicated the similar results.

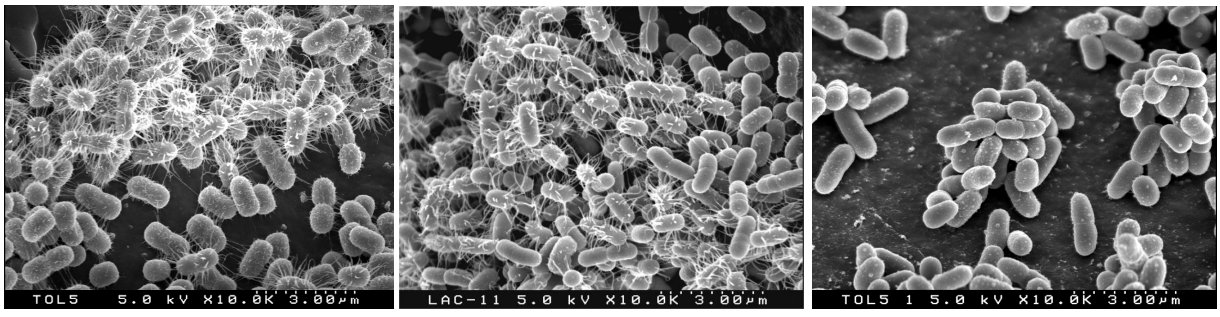

Fig. 1. FE-SEM images of Tol 5 cells grown on toluene (left), lactic acid (middle), or TAG (right) on the surface of polyurethane foam.

* hori.katsutoshi@nitech.ac.jp

P085

Colloids fractal dimension

P. Le Coustumer[1]*, S. Galaup[1], M. Masson[3], J. Schäfers[1], G. Blanc[1] **&** M. Baalousha[2]

[1] *Earth & Sea UFR, Bordeaux1 University, B.18 Av Facultés, 33405 Talence*

[2] *Department of Environmental Health, University of Birmingham, Edgbaston, Birmingham, B15 2TT, United Kingdom*

The role of the colloids in the diffusion of mobile trace elements (MET) is well known, however the mechanisms and parameters which govern their capacity to trap and to carry MTE are more or less understood. Recent research studies clearly put in evidence that along a natural system, like rivers, some parameters (*e.g.* ionic strength, pH, temperature and time) have an important impact on the speciation mechanisms. In a previous work, we have developed the concept of physical speciation. The concept of physical speciation developed by M. Baalousha & al suggests that the texture and size of natural nanoparticles strongly influence the transport of pollutants. This work presents an experimental plan to illustrate this concept. It is based on a sampling campaign done along the Garonne river (south west part of France). From samples collected along the downstream chemical flux gradient, colloidal fraction has been extracted by ultrafiltration procedure and study by TEM. Micrography of the texture of the fractionated samples has been collected and Image Analysis performed to determine the fractal dimension of colloids like Humic Acid (HA). The results, allows us to conclude that natural colloids such humic acid have a fractal dimension influenced by parameters operating into the river (charge, Ph, IS, bacteria). The fractal parameter can act as a fingerprint of the colloids of natural system and reflects the evolution of several parameters as figure 1 illustrated it. The quantification by fractal approach helps to understand and describe complex mechanisms at the interface of the sciences.

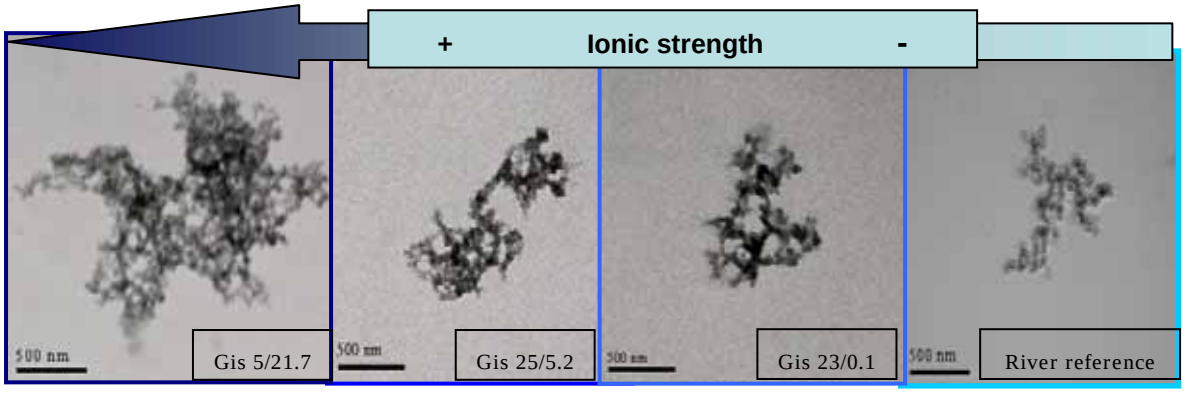

Fig.1: Evolution of the size & morphology of HA of the Garonne river by TEM.

* plc@lnet.fr

P086

Chemical composition of suspended matter and particulate phosphorus discharged to tile drains in a clayey field

K. Suzuki[1]*, K. Adachi[2], T. Sekiguchi[2], S. Yoshida[2], K. Nakano[3], H. Katou[1]

[1] *National Institute for Agro-Environmental Sciences, Tsukuba 305-8604, Japan,*

[2]*Hokuriku Research Center, National Agricultural Research Center, Joetsu 943-0193, Japan,*

[3]*National Agricultural Research Center for Kyushu Okinawa Region, Chikugo 833-0041, Japan*

Subsoil cracks in clayey fields can act as a major pathway for discharge of suspended matter and associated phosphorus (P) to tile drains. Sources of particulate P discharged from the fields are, however, poorly understood. The objective of this study was to investigate chemical composition of discharged suspended matter and associated P to infer their sources in a clayey field. The experimental site was a converted "ex-paddy" field of the Hokuriku Research Center, cropped with soybean. The soil was classified as a Mottled Gley Lowland soil, with the clay fraction dominated by smectite. During rainfall events, tile drainage as well as perched water at the topsoil–plowsole boundary was collected, and Fe, Al, Si and P contents of the suspended matter were determined. Sequential extraction with 2.5% CH_3COOH, 1 M NH_4F, and 0.1 M NaOH was conducted to determine Ca-bound P (P_{Ca}), Al-bound P (P_{Al}), and Fe-bound P (P_{Fe}), respectively, in the suspended matter. Poorly crystalline Fe ($Fe_{c\text{-}a}$) and associated P ($P_{c\text{-}a}$) contents were also determined by extraction with 0.2 M sodium citrate–0.05 M sodium ascorbate. Except for the initial stage of discharge, elemental composition as well as Fe and $Fe_{c\text{-}a}$ contents of suspended matter in the tile drainage was similar to that in the perched water (Fig. 1). This suggests that the main source of the suspended matter in the tile drainage was the dispersed topsoil particles rather than secondary precipitates in the tiles. At the peak and recession stages of discharge, $P_{c\text{-}a}$ accounted for 72–75% of total P, whereas P_{Fe}, bound to the surface of iron oxides, was less than 10–25%. The results suggest that 50–60% of particulate P was occluded in weakly-crystallized Fe oxides transported from the topsoil layer. P_{Al}, bound to the surface of Al oxides or clay minerals, accounted for 33–44% of the total P. At the initial stage of discharge with high Fe and $Fe_{c\text{-}a}$ contents, $P_{c\text{-}a}$ constituted 95% of total P, implying that a considerable fraction of P was occluded in the poorly-crystalline Fe oxides precipitated in the tile drains in this case.

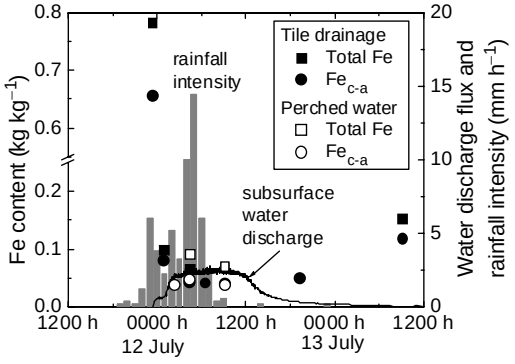

Fig. 1. Fe contents in the suspended matter during a rainfall event on 11 July 2005.

Table 1. Chemical form of P in the suspended matter in the tile drainage during a rainfall event on 11 July 2005.

	P_{Ca}	P_{Al}	P_{Fe}	$P_{c\text{-}a}$	Total P
	g kg^{-1}				
23:20 on 11 July	0.21	3.34	2.07	10.10	10.61
4:20 on 12 July	0.03	0.52	0.38	1.14	1.53
9:05 on 13 July	0.08	0.88	0.20	1.45	2.01
Bulk topsoil	0.04	0.25	0.22	0.30	1.18

*suzukatu@affrc.go.jp

P087

Effect of water extraction on soil water repellency of a forest soil

M. Kobayashi[1*], H. Matsui[1]

[1]*Forestry and Forest Products Research Institute, 1 Matsunosato Tsukuba, Ibaraki 305-8687, Japan*

Forest soils often exhibit water repellency (WR), which is an important soil property because of its effects on water and nutrient dynamics in the soil. Soil WR is caused by organic compounds on soil particles or aggregates, and occurs when a soil becomes dry; it breaks down or disappears when the soil is moist. A possible mechanism of the moisture-dependency of WR is thought to be the adsorption and desorption of water-soluble amphiphilic organic compounds, although this has not been verified directly. With this background, we examined the effect of water extraction on the degree of WR and the surface chemical composition of a water-repellent forest soil.

Distilled water was passed through the sample soil 5 or 15 times. To confirm the amphiphilicity of the substances extracted from the soil, the relationship between the concentration of dissolved organic carbon (DOC) and the surface tension of the extract was examined. The WR of the sample soils at various controlled moisture levels was measured using the ethanol percentage (EP) as an index. Then, using X-ray photoelectron spectroscopy (XPS), the atomic composition and bonding status of the outer surface of the soil aggregate before and after the extraction treatments were determined.

The sample soil showed a single peak of WR with water content. Initially, the EP increased with decreasing water content until it reached a maximum (EP_{max}). Then, it decreased until the air-dry moisture condition was achieved (EP_{air}). EP_{max} and EP_{air} were lower for the samples subjected to water extraction than for the untreated samples. The relationship between DOC concentration and surface tension showed a critical micelle concentration (CMC), indicating that the solute in the extract was amphiphilic. The atomic ratio of a carbon component with a small chemical shift to oxygen (C1/O) on the outer surface of the soil aggregate decreased with extraction treatment. This carbon component corresponded to nonpolar functional groups (C-C or C=C), and might be the agent that causes WR.

These results indicate that a water-soluble amphiphilic organic compound contributes to the WR of a soil. In the field, after a period of high rainfall, such organic matter would be washed off the soil, and when re-established the WR would be weaker than it was before the rain.

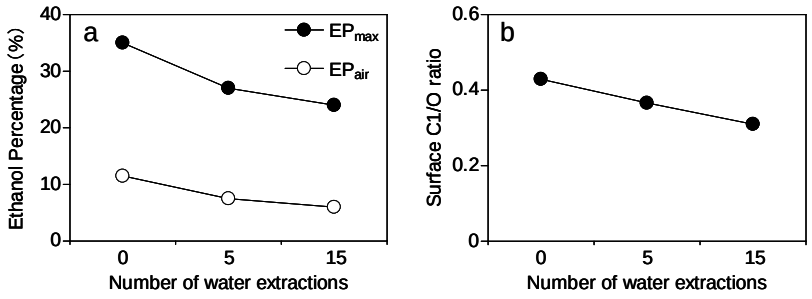

Figure Effect of water extraction treatment on water repellency (a) and surface atomic ratios (b) of the sample soil

* kbmasa@affrc.go.jp

P088

Absorption of The Trees and Shrubs to Sulfur Dioxide and Heavy Metal in Greenbelt of Beijing

F. Qian, Y. Tian*, Q. Wang, and X. L. Liu

School of Chemical and Environmental Engineering, Beijing Business and Technology University, Beijing, P. R. of China. Beijing100037

The In order to explain the availability of trees and shrubs in urban greenbelts in environmental purification, an experiment was carried out during March to May, 2007, in urban of Beijing, using four plants, which are Holly(*Ilex chinensis*), Poplar tree(*Populus. x beijingensis W Y. Hsu*), Littleleaf Box(*Buxus. microphylla s. et Z.*), and Chinese Pine(*Pinus. tabulaeformis*). These plants scattered in three different contaminated areas. The absorption of the trees and shrubs to sulfur dioxide and heavy metal was measured. The results showed that the contents of S in the leaves of the plants have positive relations to air pollution index. The amount of S and heavy metals in the leaves in the industrial zone was higher significantly than that in the cultural zone and residential areas. For the same tree or shrub, the amounts of heavy metals accumulated in the leaves of the plant were deferent, the order of the amounts from high to low was: Zn＞Cu＞Cr＞Cd＞Pb＞Ni. The dynamics of the accumulation of the heavy metals in the leaves was much higher in the spring season than that in the early of summer season.

*tianyuan@th.btbu.edu.cn

P089

FOR PUBLIC ADMINISTRATION ISSUES OF CASPIAN SEA ECOLOGICAL POBLEMS

Zhanburshin E.T.
Department "Marine engineering and technology",
Aktau branch,
Kazakh Academy of Transport and Communication named after Tinishpayev M,
130000, Aktau, microdistrict 9, building 24

The end of 20th century for Kazakhstan oil industry is marked by detection of unique hydrocarbon fields in northern part of Caspian Sea. Preliminary estimates show that oil reserves make about 10 billion ton and up to 2 trillion m^3 of gas. Many world transnational companies take part in oilgas fields development in Caspian shelf: "Eni", "Royal Dutch Shell", "Exxon Mobil", "Total", "ConocoPhillips", "Impex", "Lukoil" and KazMunaiGaz. But at the same time uniqueness of near caspian basin is consisted not in oil and gas only, but in it's natural bioresources also, which are valued at more than 500 billion US dollars. Approximately 130 kinds and varieties of fish inhabit in water basin of Caspian Sea, including sturgeon, forming 90% of world stock of these fish. There are many species of fish in Caspian Sea, and the only one sea mammalian inhabiting in these waters is Caspian seal. Caspian region is important for life of more than 100 kinds of birds, inhabiting here, and also for million of migratory birds, flying over region territory. One more geographical characteristic of this sea is that it is not connected with Open Ocean and it is drainless water body.

As of today anthropogenic load for Northern Caspian Sea, basically run in three directions.

Firstly. Pollution by different toxic materials, bringing in by inflowing into sea stream flows, especially by rivers Volga and Ural.

Secondly. This entering of oil products into marine environment, afterwards of leakage and shipwrecks, and also of different harmful substances, contained in ballast waters, discharging by water transport.

Thirdly. Sea Pollution, in a result of offshore oil production and in nearshore zones. Many nearshore oil fields of Northern Caspian Sea are located in flood water zone. Development of sea shelf increased the development pressure on ecosystem of Caspian Sea. Within recent years thousands of seals and birds died in nearshore zone.

All that requires the further improvement of public administration system for solution of undermentioned ecological problems of Caspian Sea.

Firstly, there is no scientifically based analysis of how much oil and gas is necessary to be produced offshore in order to save the ecosystem integrity. For example, there is no data about what negative influence does conducting geophysical survey exert on bioresources of Caspian Sea.

Secondly, until now there is no regulatory and legal framework and goal oriented government program on issues of Caspian Sea biodiversity protection, the method of economic disbenefit determination is not formulated yet in case of oil spill into sea aquatory and etc. That is, existing controlling mechanism of management of water environment problems is imperfect, that creates the conditions for ecological risk increase during large-scale realization of petroleum operations on Caspian Sea.

Thirdly, there is no system, continuous, independent monitoring of Caspian Sea ecological environment. From the part of appropriate state bodies the effective control of harmful substances emission and disruption is not organized during performance of offshore oil operations. Besides, the material and technical basis of controlling unit is not correspond to those requirements, which are presented in modern conditions, and it requires the serious improvement.

Ecological problems of Caspian Sea is not the problem separate government only, but it is a problem of international level., and all abovementioned problems are should be solved within the framework of cooperation and interaction of Caspian Governments and interested international institutes.

---

edilzh@rambler.ru

P090

Influence on concentration and molecular size distribution of uranium in soil solution by plant growth

A. Takeda[1]*, H. Tsukada[1], Y. Takaku[1], S. Hisamatsu[1]

[1]*Department of Radioecology, Institute for Environmental Sciences, 1-7 Ienomae, Obuchi, Rokkasho-mura, Kamikita-gun, Aomori 039-3212*

Uranium is a naturally occurring long-lived radionuclide, which is known to have both radio- and chemical toxicity. Since a small quantity of U is contained in phosphate fertilizers, the U levels in agricultural soils could be elevated by a long-term application of phosphate fertilizers. Andosols, which are found in almost half of upland fields in Japan, have generally received large amounts of phosphate fertilizers for long time, because of their intrinsic low phosphate fertility and high capacity of phosphate retention. The studies on the distribution and transfer of U in the soil–water–plant system are necessary for predicting its behavior in agricultural fields. The influence on concentrations and molecular size distribution of U in soil solution by plant growth is reported in this paper.

The soil collected from an arable field in Aomori was used for a pot cultivation experiment. Soil samples of 400 g dry each were put into plastic pots, where the rhizosphere zone (R) was separated from the non-rhizosphere zone (NR) by a nylon net screen. *Brassica rapa* nothovar. was cultivated for ca. one month. Soil solution samples were collected by a high-speed centrifugation method occasionally during the cultivation period. The concentration of U in the soil solution was measured by an ICP-MS. In addition, the molecular size distribution of U in the soil solution after the cultivation was analyzed with a size exclusion chromatography (SEC) combined with an ICP-MS system.

The concentrations of U in the R soil solution increased with plant growth, while those in the NR soil solution did not significantly change throughout the cultivation period. Concentration of UV absorbing organic substances with large molecular size was higher in the R soil solution than that in the NR soil solution. A peak of U associating with the organic substances was found in the R soil solution. Those results suggested that plant growth enhanced dissolution of U adsorbed with organic matters from the solid phase in soil at the rhizosphere.

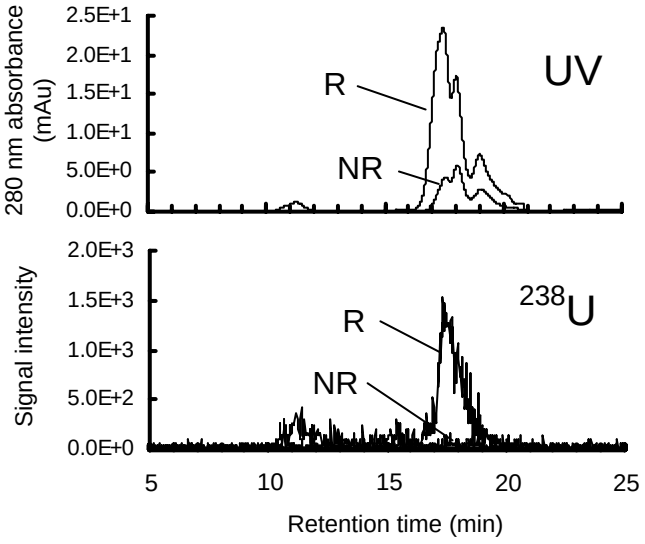

Fig. 1 The SEC-ICP-MS chromatograms in soil solution samples.

This study was conducted under contact with Aomori Prefectural Government.

*takeda@ies.or.jp

P091

Simultaneous Measurement of Surface Potential and Viscosity in a Capillary Channel

Takeshi NASHIMA*
National Metrology Institute of Japan, AIST
1-1-1 Umezono, Tsukuba 305-8563

As a capillary channel is used for both measurements of streaming potential and viscosity, they can be carried out simultaneously. The viscosity is expressed by $P = 8\eta Lq / \pi r^4$ and the zeta potential by $j = \pi r^2 \varepsilon\zeta P / L\eta$. Introducing the relation $dV/dt = -q$, if $P = AV$ is concluded, the flow profile $q(t)$ at the starting or stopping section is written with an exponential decay function, the time constant of which is proportional to the viscosity. As to the steady state, the streaming current, instead of the streaming potential, is independent of the viscosity, as is expressed as $j = 8\varepsilon\zeta q / r^2$.

The measurement system consists of an airtight vessel, a plunger pump, a capillary channel which is made of fused silica, and an open-air vessel (Fig.1). And, a couple of Ag/AgBr electrodes and an electrometer are used for measurements of streaming current.

To verify this system, aqueous solutions of CTAB(cetyltrimethylammonium bromide) were measured. As CTAB adsorbs onto silica surfaces and forms a threadlike micelle with addition of salicylate, the measurements were carried out with several concentrations of salicylate. Figure 2 shows the result. It is found, for example, that the viscosity of the CTAB solution increases according to the sufficient addition of salicylate. And the zeta potential also varies at the same time.

[Nomenclature] P: pressure difference, η: viscosity, L, r: length and radius of capillary, q: flow rate, ζ: zeta potential, j: streaming current, ε: dielectric constant, V: volume, t: time, A: constant.

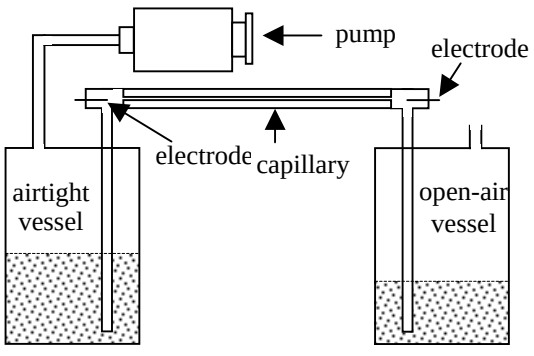

Fig.1 Schematic diagram of the system

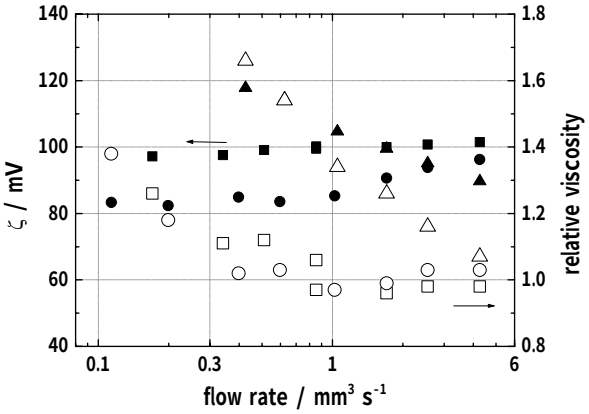

Fig.2 Zeta potential (filled symbols) and relative viscosity (open) vs. flow rate; CTAB 0.3 mM, salicylate conc.: ■□ 0 mM, ●○ 0.12, ▲△ 0.36.

* t.nashima@aist.go.jp

P092

Surface-Assisted Laser Desorption/ionization Mass Spectrometry of Environmental Pollutants with Nanostructured Surfaces

H. Kawasaki*, T. Sugitani, Y. Shimomae, T. Watanabe, and R. Arakawa

Department of Applied Chemistry, Kansai University, Suita, Osaka 564-8680, Japan

A surface-assisted laser desorption/ionization mass spectrometry (SALDI-MS) without the aid of an organic matrix has seen major improvements in simple sample preparation, low noise background, efficient soft ionization, high salt tolerance, fast data collection, and flexibility as the result of nanomaterials-coupled MS techniques. Compared to the traditional MALDI-MS and GC-MS, SALDI may be a promising analytical technique in the area of small molecule analysis. In this study, we have investigated the SALDI-MS of pyrene and dimethyldistearylammonium chloride(DDAC) as environmental pollutants, using layer-by-layer (LBL) multilayer films [$(AuNPs/PAH)_n$] consisting of alternating depositions of ammonium citrate capped AuNPs and poly(allylamine hydrochloride)(PAH) on silicon. Pyrene is one of polycyclic aromatic hydrocarbons (PAHs), and it is toxic and carcinogenic. The longer the alkyl chain length the lower the solubility of the cationic surfactant, so that the surfactant is less bioavailable for biodegradation and also toxic interaction with resident organisms. Thus, it is important to detect PAHs and DDAC in the environment with high sensitivity.

Figure 1 presents the SALDI mass spectra of DDAC obtained from the $(AuNPs/PAH)_5$ multilayer film without the extraction experiment (i.e. direct deposition of the sample solution of 0.5 μL on the film)and (b) with the extraction experiment(i.e. adsorption of analytes into the film). The peak appearing at *m*/*z* 550 corresponds to a DDAC molecular ion without the counter-ion. We obtained enhanced signals for the DDAC ion with the extraction experiments. It is evidence that the detection limit significantly increased from 10^{-7} g/L(10 ppm) to 10^{-17} g/L(10^{-5} ppt) by the extraction experiment. It seems that the surfactant can diffuse into the LBL multilayers, and the cationic surfactants bind to the surface of negatively charged gold nanoparticles through the electrostatic and hydrophobic interactions between the citrate anions on the surface of the gold nanoparticles and the cationic surfactants. The enhanced detection limit of pyrene with the multilayer films was also found by the extraction experiment. Furthermore, the SALDI-MS of perfluorooctane sulfonats(PFOS) on the porous silicon surface was examined, and we could quantitatively identify the PFOS in the concentration range of 2～10 ppb. Thus, SALDI-MS have potentials for the application in tracing possible pollution sources from very dilute aqueous solutions with high sensitivity.

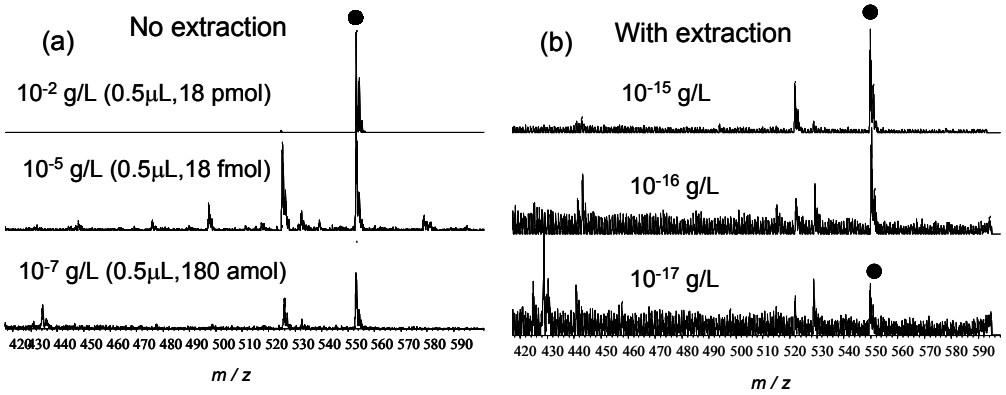

Fig. 1. SALDI mass spectra of DDAC from the multilayer film

hkawa@ipcku.kansai-u.ac.jp

P093

Contact angle effects of sand on the fingered flow under non-ponding infiltration

T. Annaka*, S. Hanayama
Faculty of Agriculture, Yamagata University,
1-23 Wakaba-machi, Tsuruoka, Yamagata 997-8555

Fingered flow can develop even in macroscopically homogeneous sand during downward infiltration whether the sand is water repellent or water wettable. However, effects of sand wettability on the fingered flow formation have not been sufficiently investigated. We conducted two-dimensional, non-ponding infiltration experiments using sand samples with different contact angle (from 43 to 91º, estimated by capillary rise method). The experiments were conducted in an acrylic chamber of 32-cm high, 10-cm wide and 0.6-cm thick. Water was applied from five drip needles spaced 1-cm interval, with applied fluxes of 0.5, 5, and 10 % of the saturated hydraulic conductivity. Infiltration process was observed and photos were taken with a digital video camera, from which properties of fingered flow, such as the fingertip velocity and finger width were estimated.

Results obtained were as follows:

(1) When a finger began to develop from the induction zone, velocity of the fingertip increased rapidly and became constant before the finger length grew 5-cm long independently of apparent contact angles.

(2) Time-averaged fingertip velocity was almost the same in the sand layer with apparent contact angle from 50 to 75°, and spatially-averaged finger width showed the minimum value when the apparent contact angle was about 72°.

(3) As the applied flux increased, time-averaged fingertip velocity also increased, but spatially-averaged finger width only slightly increased.

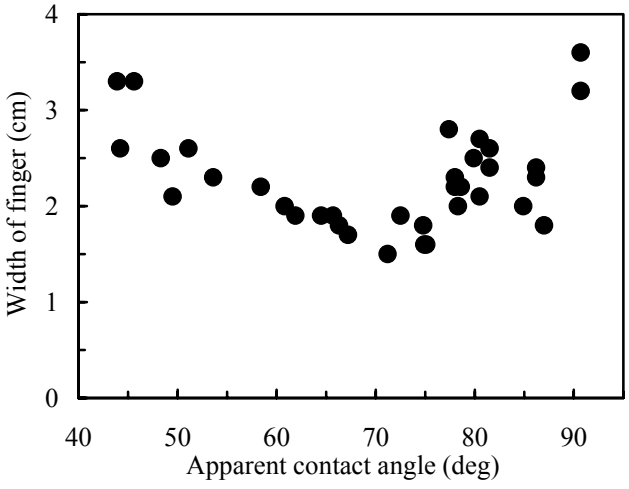

Fig.1 Apparent contact angle vs. width of finger (for the flux of 5 % of the hydraulic conductivity)

*annakt@tds1.tr.yamagata-u.ac.jp

P094

Bactericidal activity of Ag-Ce/$AlPO_4$ catalyst using molecular oxygen in water

Q.Y. Chang[1], H. He[1*], J.C. Zhao[2], M. Yang[1], J.H. Qu[1]
[1]*Research Center for Eco-Environmental Sciences, Chinese Academy of Sciences, Beijing, China 100085*
[2]*Institute of Chemistry, Chinese Academy of Sciences, Beijing, China 100080*

Pathogenic microbes are contaminants of major concern in drinking water, thus disinfection of water is very important to provide a sanitary environment. However, the commonly used disinfection methods have been found to have potentially adverse effects on human health and the environment. Though increasing attention has been given to catalytic oxidation involving reactive oxygen species (ROS), the methods of catalytic disinfection by molecular oxygen at room temperature without extra light or electric power input were seldom reported yet. In this study, the catalytic inactivation of *E. coli* in water by Ag-Ce/$AlPO_4$ catalyst using molecular oxygen was investigated. It was found that molecular oxygen catalyzed by Ag-Ce/$AlPO_4$ catalyst exhibited good bactericidal activity against *E. coli* cells, resulting from the high oxygen storage capability of surface ceria and desirable dispersion of Ag particles on the catalyst surface. ROS with strong oxidative properties, such as •OH and $\bullet O_2^-$, were successfully detected by ESR at room temperature without extra light or electric power input, which provides direct evidence for the catalytic inactivation of *E. coli* cells by the Ag-Ce/$AlPO_4$ catalyst using molecular oxygen. The formation of H_2O_2 as an important intermediate was confirmed by addition of catalase, thus strongly supported the proposed catalytic oxidation mechanism. This may provide a novel approach for the efficient disinfection of drinking water. Further study of the interaction of surface metal species and ROS with bacteria is currently in progress.

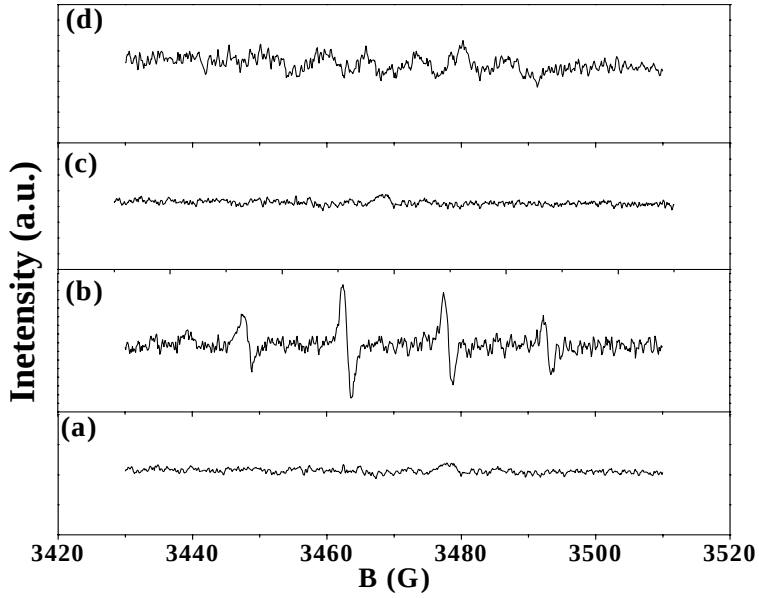

Fig. 1 DMPO spin-trapping ESR spectra recorded at ambient temperature in aqueous dispersion (for DMPO-OH• adduct) (a) before and (b) after the addition of Ag-Ce/$AlPO_4$ catalyst; and in methanol dispersion (for DMPO-O_2^-• adduct) (c) before and (d) after the addition of Ag-Ce/$AlPO_4$ catalyst

* honghe@rcees.ac.cn

P095

Complete mineralization of the recalcitrant cyanuric acid substrate by ozonation in aqueous TiO_2 suspensions

T. Oyama*, I. Yanagisawa, T. Koike and H. Hidaka
Frontier Research Center for the Global Environment Science, Meisei University, 2-1-1. Hodokubo, Hino, Tokyo 191-8506

Water pollutants coming from herbicides and pesticides cause considerable problem. Pesticides bearing a triazine heteroring are widely used and accumulate in nature without biodegradation. The degradation of triazine type agrochemicals has been investigated by advanced oxidation technologies. Degradation of atrazine generates cyanuric acid as a final product which was never mineralized by photocatalytic method[(1)].

We have found that cyanuric acid were completely mineralized by catalytic ozonation. Cyanuric acid is a mixture of tautomer bearing the keto and enol forms (Scheme 1). The oxidation were carried out in alkaline solution (pH 12) using TiO_2 (Degssa P25) in the presence of H_2O_2. In a quartz reactor, O_3 was continuously bubbled into the suspension during UV-irradiation. In alkaline solution, cyanuric acid exists in the enol form. The enol form is preferable for the cleavage of triazine ring having conjugated double bonds. O_3 and TiO_2 synergistically oxidize cyanuric acid via formation of $O_3^{\bullet -}$ and ultimately $OH^{\bullet}$ radicals. UV-light more than 250 nm was irradiated with a high-pressure Hg lamp (400W) which caused direct photodissociation of O_3 to give $OH^{\bullet}$ radical. The decrease of total organic carbon (TOC) and increase of NO_3^- ion formed during the degradation under different conditions are illustrated in Fig. 1. Under the optimimal condition of H_2O_2 concentration, cyanuric acid can be mineralized completely after 24 h of irradiation. Degradation mechanisms are discussed in detail.

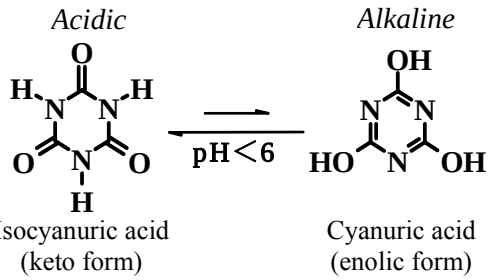

Scheme 1. Tautomerization of cyanuric acid at different pH values

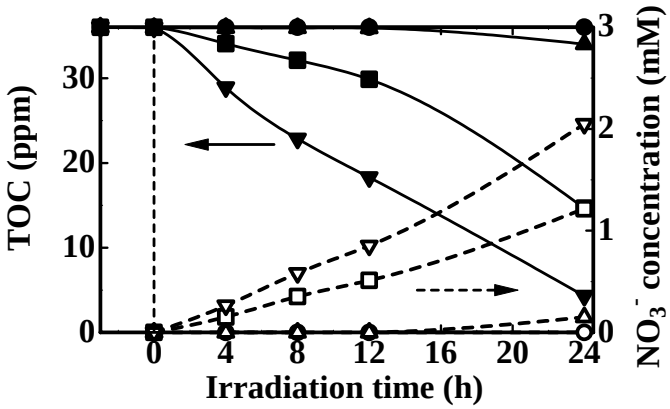

Fig. 1 Temporal TOC changes and formation of NO_3^- ion in the photodegradation of cyanuric acid. ●: O_3/UV pH 5.6, ■: O_3/UV pH 12.0 + H_2O_2, ▲: O_3/TiO_2/UV pH 5.6, ▼: O_3/TiO_2/UV pH 12.0 + H_2O_2

Ref. (1) E.Garcia-Lopez, G. Marci, N. Serpone and H. Hidaka, *J. Phys.Chem. C,* **111**, 18025 (2007).

*oyama@epfc.meisei-u.ac.jp

P096

Catalytic properties of Fe-containing imogolite in cyclohexane oxidation

M. Ookawa*, Y. Nagamitsu, M. Oda, Y. Takata, T. Yamaguchi, T. Maekawa
Graduate School of Science and Engineering, Ehime University,
Bunkyo-cho 3, Matsuyama, 790-8577

Imogolite is a naturally occurring, aluminosilicate clay mineral with typical chemical composition of $(OH)_3Al_2O_3SiOH$. The imogolite has an outer diameter of ca. 2 nm and an inner diameter of 1 nm. Although imogolite is expected to have a shape-selective character similar to zeolites, few investigations have been carried out to use natural imogolite as a catalyst. Recently we synthesized Fe-containing imogolite (Fe-imogolite) and found that the synthetic material played as oxidation catalyst. It is noteworthy to point out that phenol was obtained directly by the oxidation of benzene with H_2O_2 using this catalyst [1]. H_2O_2 is widely used in the oxidation of organic compounds as a clean oxidant. The application of Fe-imogolite catalyst with H_2O_2 is expected as one of the environmentally-friendly technology. In this study, we attempted the oxidation of cyclohexane with H_2O_2. The Fe-imogolite was synthesized using the mixture of aqueous solutions of $FeCl_3$ and $AlCl_3$ (molar ratio of Al / Fe = 19) and Na_4SiO_4 aqueous solution. The detail of synthetic method is shown in previous literature [1]. These products were characterized by XRD, FT-IR, UV-VIS, XRF and AFM. The reaction was carried out using 2 mmol of cyclohexane, 10 mmol of H_2O_2 (30 wt%) and 30 ml of acetonitrile as a solvent with 50 mg of catalyst under stirring at 60 °C for 3h. The products were analyzed by GC-MS and FID-GC. The AFM image of Fe-imogolite is shown in Fig. 1. The fibrous morphology was observed in this sample similar to the synthetic imogolite. It was found that the diameter is 2.2 nm as a result of section analysis. The results of oxidation reaction of cyclohexane are summarized in Table 1. The oxidation products were hardly detected without catalysis. The cyclohexyl hydroperoxide (Cy-OOH) was produced with Fe_2O_3 or α-FeOOH as a catalyst. With Fe-containing imogolite, three oxidation products, cyclohexanone (Cy-one), cyclohexanol (Cy-OH) and Cy-OOH were produced under this reaction condition. It was found that Fe-imogolite played as oxidation catalyst of not only aromatic hydrocarbon but also cycloalkane.

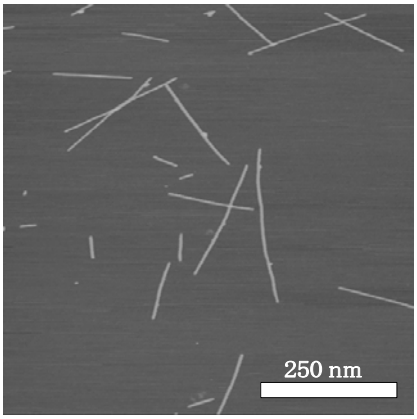

Fig.1 AFM image of Fe-containing imogolite

Table 1 Results of oxidation reaction

Catalyst	Yield / %		
	Cy-one	Cy-Ol	Cy-COOH
None	**0.0**	**0.0**	**tr.**
Fe-Imo	**0.3**	**0.9**	**23.4**
FeOOH	**0.0**	**0.0**	**2.2**
Fe_2O_3	**0.0**	**0.0**	**9.4**
Fe_3O_4	**0.8**	**0.8**	**4.5**

Refference
[1] Ookawa et al., Clay Sci., 12 suppl. 2, 280(2006).

*ookawa@eng.ehime-u.ac.jp

P097

Using Fe (III)-substituted hydroxyapatite as an adsorbent and a photo-Fenton catalyst for clarification of stained water

T. Moriguchi[1], S. Nakagawa[2], F. Kaji[2]*

[1]Departmrnt of Chemistry, Saitama Medical University,

38 Morohongo, Moroyama-machi, Iruma-gun, Saitama 350-0495, JAPAN

[2]R & D Division, Taihei Chemical Industrial Co., Ltd.

1-1 Takayasu, Ikaruga-cho, Ikoma-gun, Nara 636-0104, JAPAN

Hydroxyapatite $Ca_{10}(PO_4)_6(OH)_2$ has cationic exchange ability, in which Ca^{2+} is facilely substituted in water with heavy metal ions such as Pb^{2+}, Cd^{2+}, Cu^{2+}, Cr^{3+}, and Fe^{3+}. Metal-substituted hydroxyapatite may have much possibility to exhibit a high functionality attributed to imported metals, more than adsorbable and biocompatible properties as original hydroxyapatite have ever indicated. In order to develop a novel adsorbent and/or catalyst, Fe(III)-substituted hydroxyapatite, HAP-400-Fe, was synthesized from $FeCl_3$ solution and Ca-deficient hydroxyapatite, HAP-400 (Ca/P = 1.47, from Taihei Chem. Industrial Co. & Ltd.). We investigated both adsorption and photo-Fenton reaction of dye compounds, alizarin red S, neutral red, and methyl orange, with HAP-400-Fe under aqueous media.

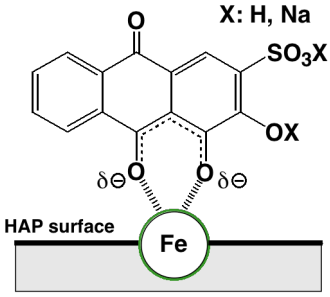

Fig. 1 Adsorption mechanism of alizarin red S on HAP-400-Fe.

Among these dyes, alizarin red S indicated the highest adsorption (99%). From microscopic FT-IR analysis, the adsorption mechanism was elucidated, as shown in Fig. 1, meaning chelation of $C–O^-$ and C=O groups of the adsorbate molecule toward one Fe site of the adsorbent surface. In photo-Fenton reaction, consumption of alizarin red S was improved with increase in Fe content of the HAP catalyst (from 0 to 5 mmol/g), as shown in Fig. 2. The substrate consumption eventually amounted to 99%, and its mineralization was extended to 60%. Under the ultimate condition, consumptions of neutral red and methyl orange were 55% and 42%, respectively, lower than that of alizarin red S. In addition, catalysis of FeOOH, $FePO_4•2H_2O$, or Fe_2O_3 under the same condition was inferior to that of HAP-400-Fe. It was found that the present Fe (III)-substituted HAP catalyst enables dye molecules to be decomposed efficiently in water.

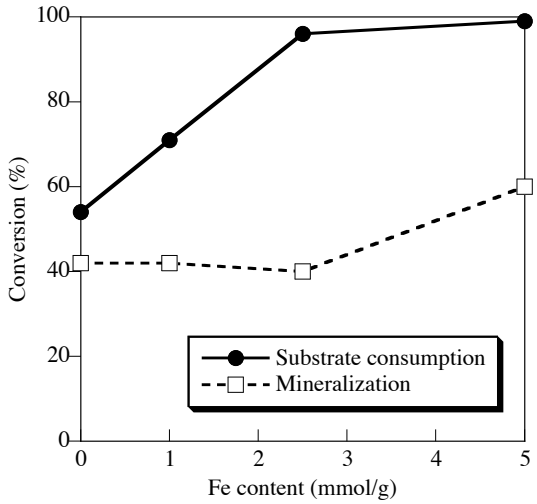

Fig. 2 Photo-Fenton reaction of alizarin red S (23 μM) with H_2O_2 (10 mM) and HAP-400-Fe (0.5 g/L) at 25˚C for 6h under black light irradiation (370 mW/cm^2 at 365 nm).

*tksmorig@saitama-med.ac.jp

P098

Catalytic Diesel Soot Oxidation – Screening Study and Ag/Ceria Catalyst

Hiroshi Kawachi,* Ken-ichi Shimizu, Atsushi Satsuma
Gracuate School of Engineering, Nagoya University
Furo-cho, Chikusa-ku, Nagoya 464-8603

Diesel particle filters (DPF) are effective for removal of soot particulate matter (PM) from diesel engine exhausts. The trapped PM in the DPF has to be removed continuously or periodically by combustion. The light-off temperature of PM is about 600 ^{o}C. To avoid thermal damage of catalytic converters and consumption of excess fuels for heating of DPF, active oxidation catalysts are desired to lower the reaction temperatures. To date, various types of catalysts have been reported such as precious metals, modified ceria, and alkaline-based catalysts. In the present study, through screening tests of various metal oxides, we have found Ag/CeO_2 as highly activity catalyst for soot oxidation.

Catalytic tests were carried out by TG-DTA in a flow of O_2/He =20%/balance at a rate of 100ml mi^{-1}. Carbon black was used to substitute the real diesel soot. A catalyst and carbon black (catalyst/carbon = 40 mg/2 mg) were mixed and grounded in a mortar for 5 min, then the mixture was heated from room temperature to 600 ^{o}C at a rate of 5 ^{o}C min^{-1}.

The activities of various metal oxides (MOx: M = Ag, Ce, Mn, Bi, La, Er, Mo, Fe, Gd, Ni, Tb, Dy, Y, In, Ho, Sm, Sn, Yb, Nb, Ta, Al, Ti, Ga) were evaluated by exothermal change in DTA profile, weight loss in TG profile, and produced CO_2 in gas phase. Ag_2O showed the lowest temperature of exothermal peak at 200 ^{o}C, and that of CeO_2 was the second lowest at 365 ^{o}C. Although the exothermal temperature of Ag_2O became more than 200 ^{o}C higher in the second run, the deactivation of CeO_2 was very small. Then, CeO_2 as rather stable metal oxide was modified with Ag by impregnation of CeO_2 with an aqueous solution of silver nitrate followed by calcination at 500 ^{o}C in air. The amount of supported Ag was 20 wt%.

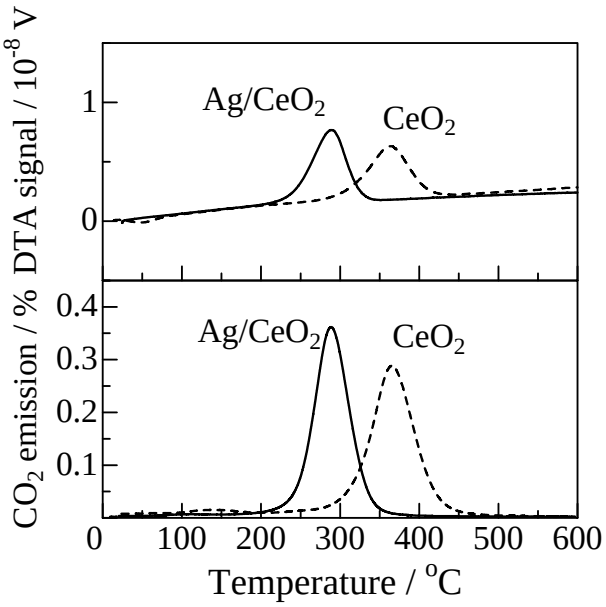

Fig. 1 Profiles of DTA and CO_2 emission of Ag/CeO_2 and CeO_2 during carbon oxidation.

Fig. 1 shows DTA and CO_2 emission profiles of Ag/CeO_2 and CeO_2. Clearly, the carbon oxidation on Ag/CeO_2 was around 80 ^{o}C lower than that of CeO_2. Complete conversion of carbon over these catalysts was confirmed from CO_2 emission profiles. Even in the second run, the shift of the oxidation temperature of Ag/CeO_2 was less than 5 ^{o}C. It was demonstrated that the modification of CeO_2 by Ag is effective for soot oxidation at lower temperatures.

*satsuma@apchem.nagoya-u.ac.jp

P099

Simultaneous HDS and HDN over supported PtSn catalysts in comparison to commercial NiMo/Al2O3

Micheal Okiror, Nakasi Sarah,F.Kamya Walulya*
Tirinyi Institute of Higher Education
Science Department,P.o.box 71157 clock tower kampala,
Uganda East Africa.

Abstract

The performance of platinum-tin catalysts, supported on Al2O3 and SiO2 and subjected to reduction prior to use, has been studied. The catalysts were characterized in reduced forms by X-ray diffraction (XRD) and XPS. The surface properties were determined by N2 BET specific surface area and CO chemisorption. The model compounds were 4,6-dimethyldibenzothiophene (4,6DMDBT) and carbazole. The PtSn catalysts supported on either Al2O3 or SiO2 were characterised by high activity, but the catalyst PtSn/SiO2 was found the most effective, even more effective than the commercial KF848 catalyst. Both PtSn catalysts studied were more effective in the reaction of 4,6DMDBT hydrogenation, the dominant product obtained with the use of PtSn/Al2O3 was methyl-cyclohexyltoluene (MCHT) and with PtSn/SiO2 the dominant product was dimethylbicyclohexyl (DMBCH). The amount of dimethylbiphenyl (DMBPh) obtained was small and practically independent of the contact time. In the HDN reaction of carbazole the most active was PtSn/SiO2. It was also more active in the consecutive reaction of isomerisation of the main product of the HDN reaction, bicyclohexyl (BCH) to methylcyclopentylcyclohexane (MCPCH). The large differences shown in the hydrotreating activity specially in the HDN reaction between PtSn catalysts supported on Al2O3 and SiO2 result from the physicochemical properties of both samples. The significantly higher CO chemisorption for PtSn/SiO2 indicates the presence of larger amount of metallic species and better hydrogenation properties so important for deep hydrotreating process.

Keywords: Hydrodesulphurisation; Hydrodenitrogenation; 4,6-Dimethyldibenzothiophene; Carbazole; Platinum; Tin; Alumina and silica supports; Commercial catalyst-KF848
kyakitech@fastermail.com

P100

Sorption of atrazine (AT) onto humic acids (HAs) coated nanoparticles

Jiajuan Lu[1], Ying Li[2], Baoyou Shi[1], Hongxiao Tang[1], Dongsheng Wang[1]*
[1] *State Key Lab of Environmental Aquatic Chemistry, RCEES, Chinese Academy of Sciences, POB 2871, Beijing 100085, China*
[2]*College of Materials Science and Technology, Beijing Forestry University, Beijing, 100083, China*

With the development of nanotechnologies, a large number of nano-materials with novel properties are poured into the environment. However, little is known about their fate, transport, toxicity and the sorption of their complexes with humic acids (HAs), a category of the most important widely distributed organic matters in nature environment. Nano-SiO_2 and nano-kaolin coated with soil HA and peat HA respectively were used as sorbents. Sorption data of AT onto the complexes under various solution conditions such as different sorbent concentrations, ionic strengths and pHs are fit well by Freundlich models. Sorption capacity increases with increasing concentration of AT and decreases with ionic strength and pH (Fig. 1). Moreover relative change of adsorption with pH is more significant at low pH. Also sorption capacity of AT onto sole nano-particles is larger than the capacity of their corresponding complexes and the trend of nano-SiO_2 is more obvious than nano-kaolin. This may be partly explained by the changes of particle sizes. The size of nano- SiO_2 dispersed greatly after coated with HAs. The surface properties of the complexes are important factors affecting the sorption process and more attention should be paid to it.

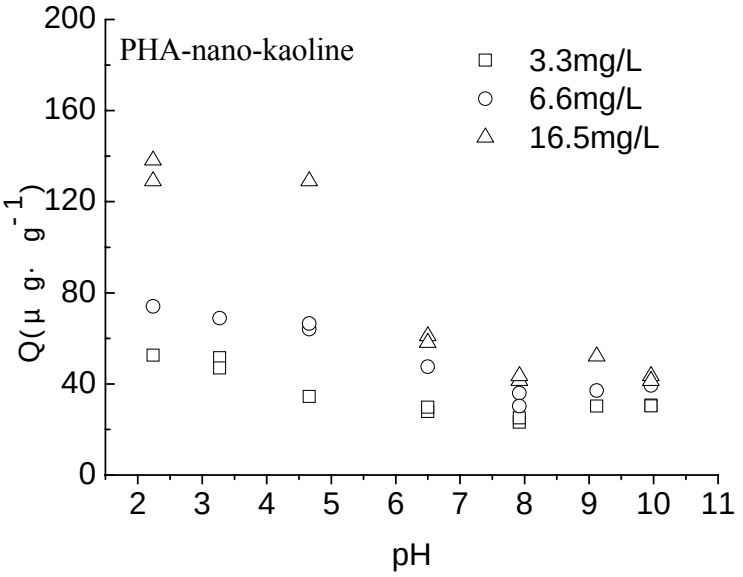

Fig. 1 Sorption isotherms of PHA on nano-kaoline at various pHs. All suspensions contained 5 g /L nano-particle complexes, 100 mg /L NaN_3, 0.01 mol/L $NaNO_3$ and AT concentrations [in mg/L] 3.3(□), 6.6(○), 16.5(△).

* wdgs@rcees.ac.cn

P101

BIODISTRIBUTION OF COLLOIDAL GOLD NANOPARTICLES UP ON INTRAVENOUS ADMINISTRATION: EFFECT OF PARTICLE SIZE

G. S. Sonavane[1,2], K. Tomoda[1,2]* and K. Makino[1,2,3]

[1]*Faculty of Pharmaceutical Sciences, Tokyo University of Science, 2641 Yamazaki Noda Chiba 278-8510, Japan*

[2]*Center for Drug Delivery Research, Tokyo University of Science, 2641 Yamazaki Noda Chiba 278-8510, Japan*

[3]*Institute of Colloid and Interface Science, Tokyo University of Science, 2641 Yamazaki Noda Chiba 278-8510,* Japan

Colloidal gold nanoparticles (NP) are reemerging as a lead candidate in the field of nanotechnology due to their diverse applications. But, for the successful application of nanocarriers, it is essential to understand the biological fate of nanoparticles. The aim of this study was to evaluate the biological distribution to enable their diverse applications in nanotechnology. Gold NP of different sizes, mainly 15nm, 50nm, 100nm and 200nm, were synthesized by modifying citrate ion concentration, a method pioneered by Turkevich *et al.* (1) with certain modifications. Synthesized gold nanoparticles were suspended in sodium alginate solution (0.5 %w/v) and administered to mice (1 g/Kg, intravenously) [n=3]. After 24 h of administration of gold NP, blood was collected under light ether anesthesia, animals were sacrificed by cervical dislocation and various tissues were removed. The tissues were washed with saline, digested with aqua regia and subsequently gold was extracted. The determination of gold was carried out using ICP Mass spectrometry. Results suggested that gold NPs were mainly accumulated in liver and lung, and importantly their concentration was found to be dependent on particle size. 15nm gold NP showed highest accumulation in lung, kidney and brain whereas 200nm gold NP showed highest accumulation in liver and spleen compared to other size particles. Small amount of gold NP was also detected in heart, pancreas and interestingly also in stomach. In conclusion, we observed that smallest size particles (15nm gold NP) could be beneficial for targeting brain, liver and lung whereas 200nm gold NP could be useful for targeting liver, spleen and lung.

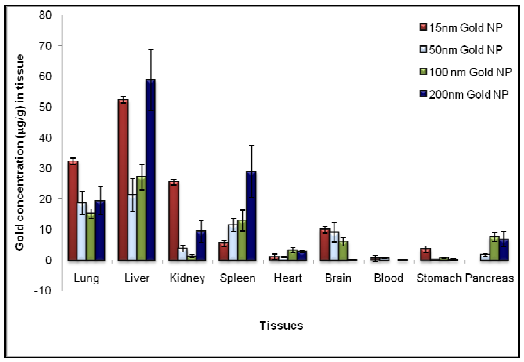

Fig. 1 Comparative Colloidal Gold Distribution [15nm, 50nm, 100nm and 200nm] (µg Au/g of tissue ±S.D.) at the Organ/Tissue Level of albino Mice after 24 h of dose administration.

Reference: (1) J.Turkevich et al, *Discuss. Faraday Soc.* 11: 55 (1951).

*j3105705@ed.noda.tus.ac.jp

P102

Bridged polysilsesquioxane xerogels functionalized with different groups as sorbents of mercury from wastewaters

Mariusz Barczak[1], Andrzej Dąbrowski[1*], Stanisław Pikus[1], Yuriy L. Zub[2]

[1]*Faculty of Chemistry, Maria Curie-Skłodowska University,*
Maria Curie-Skłodowskiej Sq. 3, 20-031 Lublin, POLAND

[2]*Institute of Surface Chemistry, National Academy of Sciences,*
General Naumov Str. 17, 03-164 Kyiv, UKRAINE

Bridged polysilsesquioxanes are a class of hybrid organic-inorganic materials, formed by molecular building blocks: bridges of organic origin that linking two or more Si atoms by forming hydrolytically stable Si–C bonds. By choosing the appropriate precursors in the reaction of hydrolytic polycondensation it is possible to design these materials on a molecular level keeping control over their chemical and physical properties, including adsorption characteristics. The possibility of introduction of the organic and inorganic groups into the structure by co-condensation of different monomers is additional advantage of the sol-gel processing of organosilicas. Schema of such co-condensation is presented on Fig. 1.

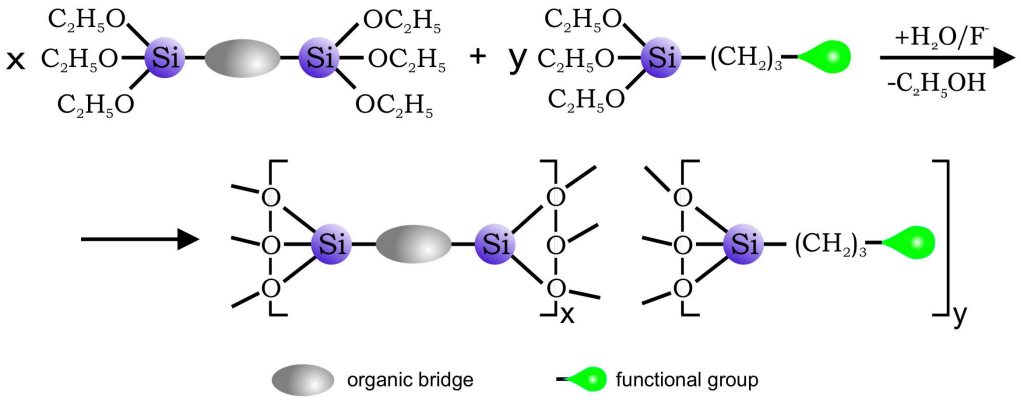

Fig. 1. Schema of co-condensation of organosilica monomers

Amino-, thiol-, phenyl-, and vinyl- functionalized polysilsesquioxane xerogels have been obtained and investigated by several instrumental techniques: ^{13}C NMR, ^{29}Si NMR, FTIR and Raman spectroscopy, termogravimetry, elemental analysis, AFM and TEM microscopy. The parameters of porous structure were evaluated from nitrogen adsorption/desorption measurements.

Thiol-functionalized xerogels exhibited a high adsorption capacity for Hg^{2+} ions what make them potential sorbents for selective and efficient removal of these ions from the wastewaters.

* dobrow@hermes.umcs.lublin.pl

P103

Effect of Infiltration Rate on Denitrification in a Ponded Soil Column

S. Watanabe[1]*, K. Nakamura[1], T. Hama[1], S. Kawashima[1]
[1]*Graduate School of Agriculture, Kyoto University*
Kitashirakawa Oiwake-cho, Sakyo-ku, Kyoto 606-8502

The control of soil infiltration rate by changing groundwater table in agricultural fields is expected to increase the residence time of infiltrated water in soil. And it increases root uptake of nutrients, increases the amount of denitrification, and avoids environmental degradation induced by excessive nitrogen outflow. We demonstrate the effect of infiltration rate on the amounts of denitrification by a laboratory experiment. Paddy soils were packed in soil columns with inside diameters of 10.5cm and lengths of 40cm, and subsequently saturated by ponding. Different infiltration rate was given to each soil column by setting different hydraulic gradient. Top-dressing of KNO_3 solution was given continuously during the experimental period and methanol, which is a hydrogen donor and carbon source for denitrification, was additionally applied from 8 days after the start of the experiment till the end. Concentrations of cations and anions including nitrate in leachate and soil solution at three different depths were measured. We investigated the relationship between the ratio of denitrified nitrogen to nitrate nitrogen input and the infiltration rate. Under the soil condition limited by methanol, the ratio of denitrification to nitrate nitrogen input decreased linearly with increasing infiltration rate from 100 to 450 mm day^{-1}. Below the infiltration rate of 200 mm day^{-1} under rich methanol condition, the denitrification rate was not controlled by the infiltration rate. The relationship between denitrification rate and infiltration rate depended on the amount of carbon in the soil.

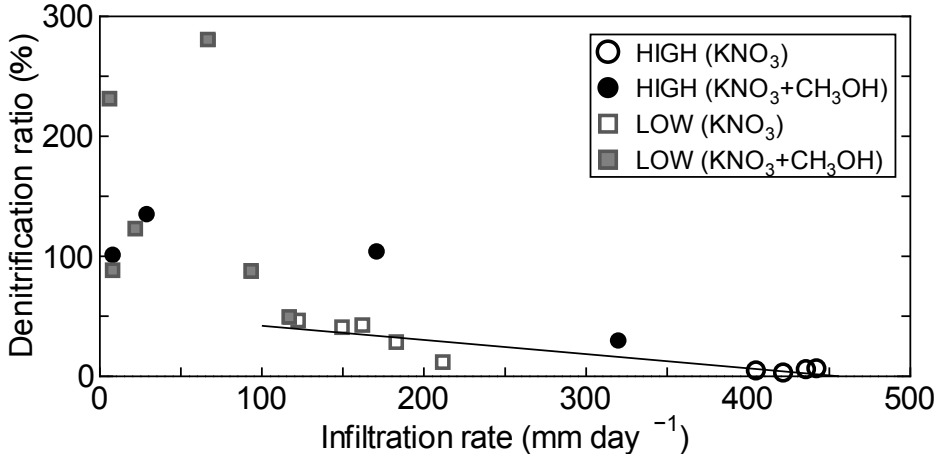

Figure Relationship between the denitrification ratio, defined as the ratio of denitrified N to nitrate N input, and the infiltration rate in a paddy soil. HIGH and LOW mean high and low hydraulic gradient, respectively. Solid line represents the approximate relationship under the condition limited by methanol.

*atokhigh@kais.kyoto-u.ac.jp

P104

Characteristics comparison of fulvic acids extracted from mountain streams in different forest forms.

Hiroki Kodama[1*], Daigo Itoh[2], Naoko Higashi[3], Masaaki Chiwa[3], Kyoich Otsuki[3], Tohru Miyajima[2].

1 Analytical Research Center for Experimental Sciences, Saga University, 1-Honjyo, Saga, 840-8502, Japan

2 Department of Chemistry, Faculty of Science and Engineering, Saga University, 1-Honjyo, Saga, 840-8502, Japan

3 Department of Forest and Forest Products Sciences, Division of Forest Ecosphere Sciences and Management, Kyusyu University, 394 Tsubakuro, Sasaguri, Kasuya, 811-2415, Japan

Coniferous trees such as cedars and Japanese cypress have been tightly planted in large areas of Japan after the war because of large wood demand; in recent years, however, many artificial plantations have been abandoned due to cheep imported lumbers. In such non-managed forests, tree crowns shut out sun light from forest floor; small plants on the forest floor are hard to grow, leading to nude lands. This phenomenon is called "forest desertification", and it is worried about that forest loses its functions such as water shortage and flood restraint. Therefore, transplantation from coniferous trees to broad leaf trees and/or careful management of the artificial plantation are promoted. It is believed that 1) nutrients are transferred to ocean via river from forest by forming composites of inorganic components(clay minerals and metal oxides) with organic components, and that 2) the quality of the organic matter would influence the aggregation ability and the mobility of soil particles.

In this work, humic substances (HSs) of non-colored mountain stream water in different forest forms have been collected and their structural characteristics have been examined. Three kinds of forests in Kyushu island, i.e., broad-leaf forest(B) managed conifer(MC), and non-managed conifer(NMC) have been selected as sampling points, respectively. HSs in the mountain streams were collected by an automatic concentration system, which includes a large column of 900 cm^2 cross section filled with 5kg DAX-8 resin. Though yields of fulvic acids from stream water were always proportional to the TOC values in stream waters, the BOD value in NMC stream water did not correlate to the TOC value (Fig. 1). Bio-degradated organic components in NMC stream water seem to be quite different in nature from MC and B stream waters. This may be probably due to the influences by influxes soil component.

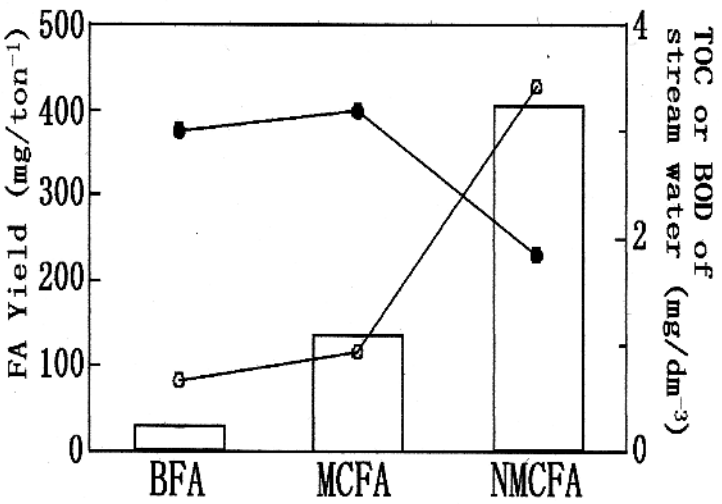

Figure 1. Relationship between FA yield and TOC/BOD. (○); TOC, (●); BOD, Rod; FA yieald.

*kodamah@cc.saga-u.ac.jp

P105

Chemical structures of humic acids on tideland sediment in Ariake sea

N. Hiromatsu and T. Miyajima*
[1]*Faculty of Science and Engineering, Saga University,*
1Honjo, Saga 840-8502

Among several reasonings of Ariake sea environmental problems, low permeability of sea water to bottom sediment seems one of the most fundamental mechanisms. Since sea water is a carrier of oxygen, inteference of sea water to the bottom sediment brings about reductive condition, which activate anaerobic bacteria. Particularly, sulfate reducing bacteria is expected to produce poisonous hydrogen sulfide to kill benthos. Since the mechanism of aggregation/dispersion of the sediment particles is strongly affected by the hydrophlicity/hydrophobicity nature of the surface, it can be said that the water permeability is influenced by the chemical nature of humic acids(HAs) covering the surface. The aim of the present research is to relate the chemical structure of HAs and the colloidal characteristics of the sediment particles. Sample sediments have been collected from 2 different regions of the inner Ariake sea shore, Iida coast and Higashiyoka coast, each represents worse and better environmental conditions, respectively. HAs have been extracted according to IHSS standard procedure. The chemical structures have been determined based on the data obtained by elemental analysis, CP-MAS ^{13}C NMR, and 3-D fluorescence spectrometry. The averaged molecular weights and the distributions have been estimated by used of high performance size exclusion chromatography.

It was found that nitrogen content of Iida HAs was much higher than Higashiyoka HAs. By plotting N/C ratio againt H/C, approximately linear relationship has been obtained, showing decomposition rate of organic matter in Iida coast is much suppressed than Higashiyoka. Similar conclusion can be deduced from the fact that the number-averaged molecular weights of Iida HAs are always higher than Higashiyoka samples. By the careful analysis of ^{13}C NMR spectra (Fig. 1) straightforward evidence for the lower degree of humification of Iida HAs has been gained. Iida HAs samples contain more aliphatic carbon atoms with less aromatic carbon atoms than Higashiyoka, indicating the lower degree of humification than Higashiyoka HAs samples.

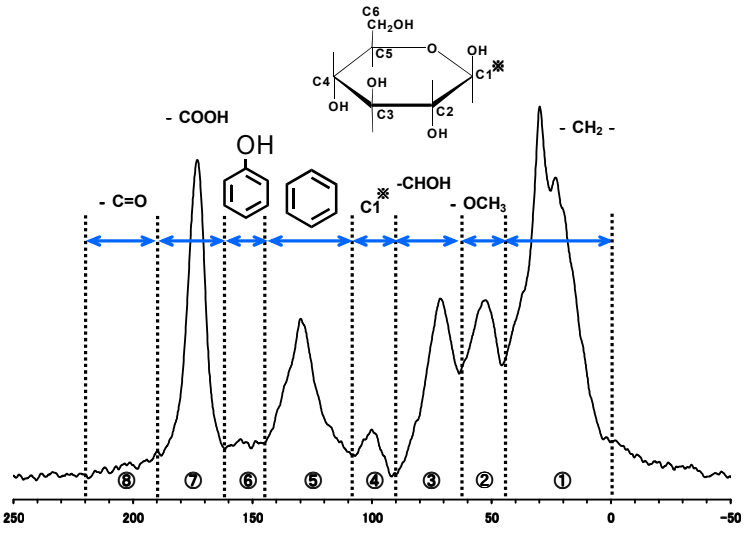

Fig.1 CP MAS-^{13}C-NMR spectrum of Ariake sea tideland sediment HA (2004 /Nov./Iida/0-2cm)

t-miyaji@ cc.saga-u.ac.jp

P106

Adsorption-desorption behavior of heavy metal ions with colloids in Ariake sea esturian area

D. Itoh, M. Kamachi*, and T. Miyajima
[1]*Faculty of Science and Engineering, Saga University,*
1Honjo, Saga 840-8502

Migration behavior of heavy metal ions from terrestrial region to marine is of great interest from pollution and nutrient points of view. It is partly controlled by adsorption-desorption properties of metal ions with colloidal particles, which are composed of inorganic components, such as clay minerals and metal oxides, and natural organic matter, such as humic substances. Iron is essential for phytoplankton in ocean and its supply from terrestrial region is of particular concern to elucidate the primary production of the esturian area. In this investigation, the change of states of ferric ions in river, esturian area, and ocean have been studied by using Chikugo river-Ariake sea region(Kyushu island, Japan) as an example.

Ferric ions precipitate as hydroxyl complexes at pH of natural water systems. Dissolved ferric ions are usually complexed with natural organic mater(mainly fulvic acid; FA). They also exist at the surface of inorganic-organic composites, probably complexes with humic acids(HA) covering the surface of the colloidal particles. We have extracted FA samples from Chikugo river water, and HA samples from Ariake sea sediments according to IHSS standard method. By the chemical analysis of the FA and HA samples, it has been revealed that these organic ligands are able to strongly complex with ferric ions in natural water systems.

The concentration of ferric ions gradually increased from upper to lower stream, in parallel with the concentration of FA. However, it increased rapidly at the mouth of the river in accord with the turbidity increase. In order to understand the behavior of sediment particles in the esturian area, a portion of Ariake sea sediment was taken and washed with sodium chloride solutions of various concentrations. The TOC value as well as the concentration of ferric ions in the aqueous phase drastically decreased with the an increase in the salt concentration level(Fig. 1) The intercept of the plots appearing at 0.5 mol dm^{-3} indicates the weak complexing ability of natural organic matter.

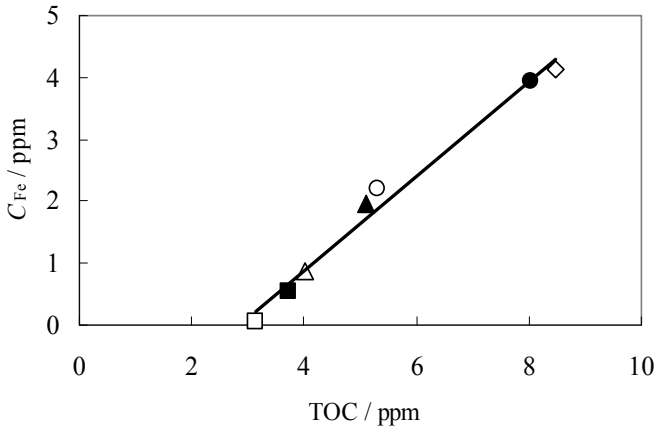

Fig.1 The decrease in Fe and TOC with salt concentration level.
C_s(mol dm^{-3}) : 0(◇), 0.001(●), 0.005(○), 0.01(▲), 0.05(△), 0.1(■), 0.5(□).

04631302@edu.cc.saga-u.ac.jp

P107

Unfrozen water in a bundle of capillaries filled with solution

K. Watanabe*
Graduate School of Bioresources, Mie University
1577 Kurima-Machiya,Tsu, Mie 514-8507

In porous media, such as soil, some water remains unfrozen at subzero temperatures. Understanding how solute affects the amount and flow of unfrozen water in frozen soil is important when utilizing soil freezing techniques for soil remediation or as a waste disposal barrier. In this study, we apply the capillary bundle model, in which soil pores are treated as a bundle of capillaries of varying sizes, to frozen saline soil, and derive the soil freezing characteristics (the relationship between unfrozen water amount and temperature) with different solute concentrations.

When a capillary with radius r filled with solution at concentration C is at subzero temperature T, the surface forces cause a film of unfrozen water on the capillary wall with thickness d while, as cylindrical ice forms at the center of the capillary, the ice excludes the solute, resulting in a higher concentration of $Cr/2d$ in the film. The relationship between the temperature and thickness is given by

$$T_m - T = \frac{T_m}{\rho_l L_f}\left[\frac{iRT_m Cr}{2d} - \frac{A}{6\pi d^3} - \frac{\Delta\gamma}{2}\sqrt{\frac{iCr}{2d}}\left(1+\frac{\sigma}{d}\right)\exp\left(-c\sqrt{\frac{iCr}{2d}}\left(d-\sigma\right)\right)\right] \quad (1)$$

where T_m is the melting temperature of bulk water, ρ_l is the density of water, L_f is the latent heat, i is the dissociation constant, R is the gas constant, $A = 12\pi\sigma^2\Delta\gamma$ is the Hamaker constant, σ is the short-range cutoff of the order of molecular diameter, $\Delta\gamma$ is the surface energy difference between the dry and wet surfaces, and c is a constant. During nucleation, only aggregates larger than a critical size are stable and grow to reach the solid phase. The critical radius r_{GT} is given by

$$r_{GT} = \frac{\gamma_{iw}}{\rho_s}\left(\frac{T_m - T}{T_m}L_f - \frac{Rc}{\rho_l}\right)^{-1} \quad (2)$$

Frozen soil is regarded as a mixture of ice-free capillaries [$r - d(T,C) < r_{GT}(T,C)$] and ice-containing capillaries [$r - d(T,C) \geq r_{GT}(T,C)$]. Using an analogue of the capillary bundle model for unfrozen soil with soil water characteristics, such as the van Genuchten equation, we can calculate the freezing characteristics from equations (1) and (2). Figure 1 shows the calculated (lines) and measured (plots) freezing characteristics for Fujinomori silt with different solute concentrations; the calculation agreed well with the observations.

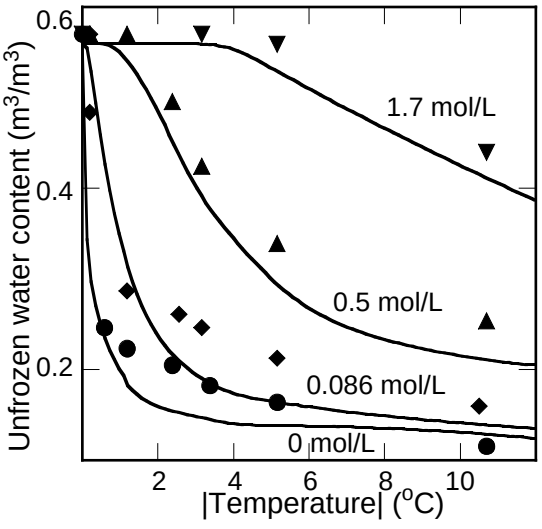

Fig. 1 Soil freezing characteristics of silt.

*kunio@bio.mie-u.ac.jp

P108

Restoration of cadmium-contaminated paddy soils by washing with ferric chloride: -An increase of soil sediment volume during washing procedure-

Yoshifumi Kodani[1], Tomoyuki Makino[2*], Takashi Kamiya[3] and Hiroyuki Takano[3]
[1] *Fukui Agricultural Experiment Station, Fukui, 918-8215 Japan*
[2] *Soil Environmental Division, National Institute for Agro-Environmental Sciences, Tsukuba, 305-8604, Japan*
[3] *Research & Development Center, Taiheiyo Cement Corp, Sakura, 285-8655, Japan*

Rapid industrialization in Japan caused serious soil pollution by Cadmium (Cd) and various other heavy metals. We have newly developed an on-site soil washing technology to restore Cd-contaminated paddy soil. However, soil sediment volume increased during the water washing, which deteriorated the drainage efficiency of washed wastewater and Cd removal efficiency from soils. The aim of this study is to clarify the mechanism of the sediment volume increase.

Materials and methods

①**On site washing**: A soil-washing procedure was applied on a paddy field (Fine-textured gley soils) in Fukui prefecture, which consisted of three steps, i.e., (1) chemical washing with $FeCl_3$; (2) water washing; and (3) on-site treatment of the wastewater by a portable purification apparatus with a chelating material. ②**Soil properties:** Unwashed and washed soils were sampled from whole Ap-horizon (0-15cm in depth) and every 2 cm of B-horizon (15-25 cm in depth) of the experimental paddy field. The clay contents and the clay mineral compositions of the soils were analyzed by the pipette method and X-ray diffractometry analysis, respectively.

③**Soil sediment volume in a lab experiment**: The unwashed soils were placed in graduated cylinders and added 25 mM $FeCl_3$ to attain the ratio of solution to soil; 1.5:1, which was almost as same as, the ratio observed in the on-site washing. After we sealed the cylinders, shaken them for 1 hr, let stand for 6 hrs and measured soil sediment volume, the supernatants of the cylinders were drained. Then, we added pure water in equal proportions to the drained supernatants and repeatedly performed the washing procedure with water. Distributions of soil particle size at each washing process were measured by laser scattering method（HORIBA LA-920）.

Results and discussion

Concentrations of Cd in the treated wastewater were below Japan's environmental quality standard (0.01 mg Cd L^{-1}), and Cd removal efficiency from the paddy soil was approximately 23 %, suggesting the effectiveness of our soil-wash method in remediating Cd-contaminated paddy fields. However, the Cd removal efficiency substantially lower than that in other experimental site (50-70 %), as soil sediment volume increased which deteriorated the drainage efficiency of wastewater and Cd removal efficiency from soils.

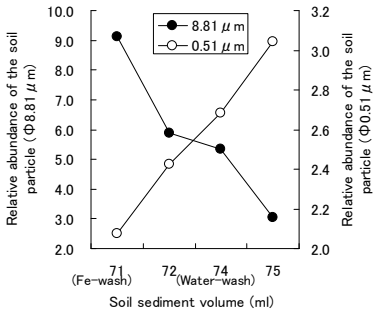

Clay contents and clay mineral compositions were almost equivalent between Ap horizon-soil and B horizon-soil. Although carbon contents of unwashed B horizon-soils gradually decreased with each 2cm of depth, those of the washed soils changed little between 0 and 23 cm in depth. These results indicate soils were agitated to 23 cm during on-site washing.

Sediment volume of Ap horizon-soil was relatively low compared to that of B horizon. The sediment volume of B horizon was gradually increased with the increase of washing times, indicating the agitation of B-horizon is one of the reasons of the sediment volume increase. On the other hand, laser scattering method revealed two peaks in soil particle distribution (ϕ 0.5 and 8.8 μm) of Ap horizon-soil. Relative abundance of the soil particle of ϕ 0.5 μm was gradually increased with increase of washing times, while that of ϕ 8.8 μm decreased (Fig). These results suggest soil settlement was changed to aggregated form (edge to edge, coarsely packed by fine particle) with the washing procedures, which could also increase the soil sediment volume in situ.

e-mail: *michiai@affrc.go.jp

P109

Estimation of constrictivity relevant to diffusion in sedimentary rocks based on X-ray CT image

Hiroaki Takahashi*, Yoshimi Seida, Kaname Miyahara, Mikazu Yui
Geological Isolation Research and Development Unit, Japan Atomic Energy Agency,
4-33, Muramatsu, Tokai-mura, Naka-gun, Ibaraki 319-1194, Japan

Diffusion of radionuclides in natural rock is one of key factors relating to migration of the radionuclides in deep geological disposal system of high level nuclear waste considered in Japan. Average pore characteristics of rock such as porosity, tortuosity and/or formation factor are used in prediction of effective diffusion coefficient, D_e using the relation, $D_e = \varepsilon\delta/\tau^2 \times D_v$ (ε: porosity, δ: constrictivity, τ^2: tortuosity, D_v: diffusion coefficient of ions in bulk water), conventionally. Rocks in general contain variety of micro- to macor-pores in them which affect the diffusivity of rock significantly. Evaluation of pore dimension which influences to D_e is important in retardation performance. However, no methods are available for the direct measurement of those factors in relation to the real pore structure, which are empirical in their definition. The macro-pores will be main diffusion path which directly affects accessibility of nuclides and will contribute the diffusivity largely if the macro-pores percolate throughout the rock for instance. In the present study, direct observation of macro-pore geometry, their distribution and their connectivity in sedimentary rock sampled from Horonobe generic URL site was performed by means of nano-focus X-ray computer tomography (X-ray CT) to identify real formation factor and connectivity of the rock followed by prediction of D_e based on the pore characteristics. Sub-micrometer resolution image of the rock was obtained by using 3D corn-beam CT. The image was processed to extract contour of pore geometry and percolating pores to assess medial axis and connectivity of pores. Radiuses of pore, R(p) and throat, R(t) were calculated based on the medial axes. The connecting pores and their size were visualized through drawing the medial axes of percolating pores and the axis lines colored to distinguish the pore size. Connection of pores and homogeneity of the accessible pore distribution were clarified by using sub-millimeter sample. From the ratio between throat radius and the average of the radius of the two pores the throat separates, which strongly correlates with constrictivity of the rock, was evaluated as shown in Fig.1. The sedimentary rock was found to include accessible connecting micrometer pores with the series of constrictivity. Constrictivity based on the pore characteristics based on this study will be compared with data obtained from separate diffusion experiment.

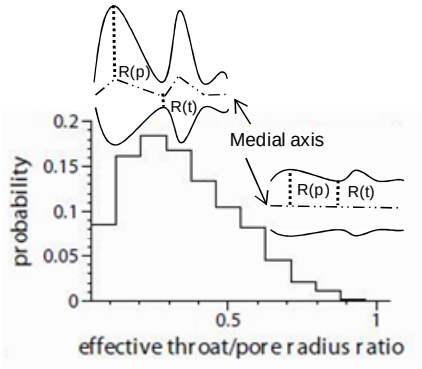

Fig. 1 Distribution of effective throat/pore radius ratio of the sedimentary rock from CT image.

This study was funded by the Ministry of Economy, Trade and Industry of Japan.
*takahashi.hiroaki@jaea.go.jp

P110

Transport and fate of dissolved organic carbon in the vadose zone and shallow aquifer below an Andisol

S. Eguchi*, M. Sawamoto, and M. Shiba

Carbon and Nutrient Cycles Division, National Institute for Agro-Environmental Sciences, Kannondai 3-1-3, Tsukuba, Ibaraki 305-8604

Dissolved organic carbon (DOC) is important as an energy source for the heterotrophic denitrification reaction in the shallow aquifer where the groundwater is contaminated by nitrate. The study was conducted to elucidate the changes in the DOC concentration in the vadose zone and shallow aquifer below an agricultural field of Andisol.

The DOC concentration in the soil water taken by the suction porous cup method at the depths of 1, 1.5, and 2 m, and that in the shallow groundwater were determined with an interval of a few to several weeks. The water table fluctuated usually around the depth of 2 m.

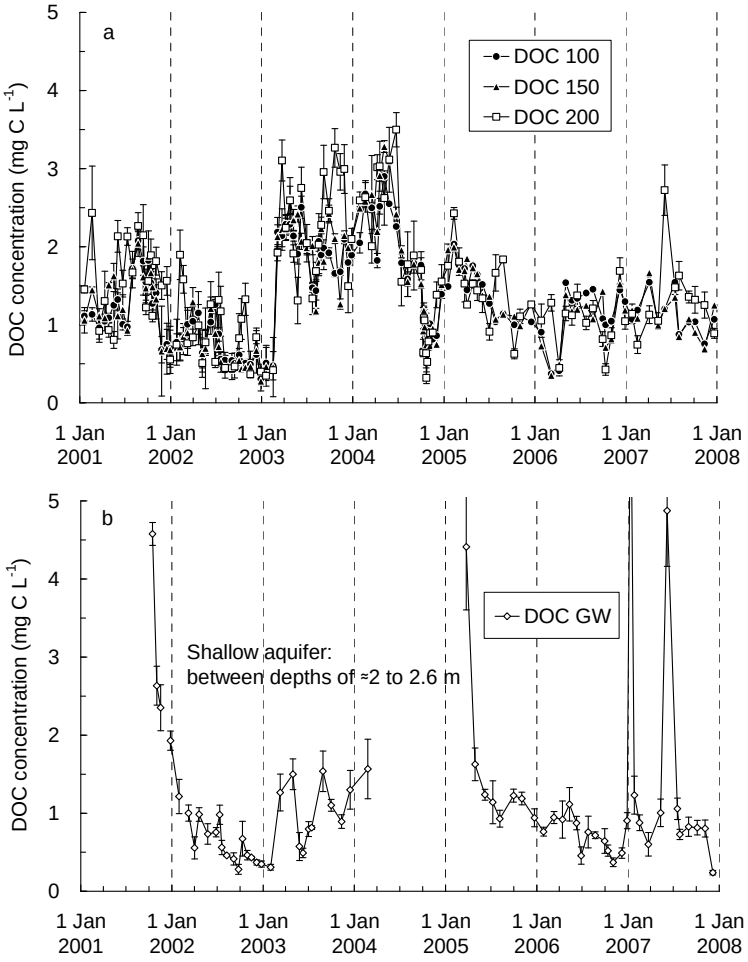

Fig. 1 Changes in the liquid-phase DOC concentrations (a) at depths of 1, 1.5, and 2 m, and (b) in the shallow aquifer.

The DOC concentrations at the depth of 2 m (Fig. 1a) and in the shallow aquifer (Fig. 1b) fluctuated more widely and drastically than those at the depths of 1.5 and 2 m, regardless of much lower carbon contents at these depths. Higher DOC concentration peaks were observed in the shallow aquifer a few times per year, generally several days or weeks after the end of the groundwater recharge processes that were caused by heavy rain events following dry periods. This indicates that the higher DOC concentration peaks were mainly due to the DOC production in the shallow aquifer. These results suggest that non-dissolved or colloidal organic carbon was supplied from the vadose zone to the shallow aquifer via preferential flow paths, and that it was important as a major DOC source in the shallow aquifer below this Andisol.

*sadao@affrc.go.jp

P111

Effectiveness and Mechanism of Priority Pollutant Nitrobenzene Adsorption by Incinerated Rice Husks

Zhi-Sheng Liu[1]*, Jun Yin[2], Yu-Juan Yu[2], Jian-Hui Wang[2], Gui-Bai Li[3]

[1]Department of Municipal Engineering, Changchun Institute of Urban Planning and Designning, 1893 Tongzhi Street, Changchun 130021, P.R. China

[2]Department of Environmental Engineering, Jilin Architectural and Civil Engineering Institute, Changchun 130021, P.R. China

[3]School of Municipal and Environmental Engineering, Harbin Institute of Technology, 202 Haihe Road, Harbin 150090, P.R. China

Effect of nitrobenzene on human health has been well known, and nitrobenzene toxicology have been widely reported in many aspects. Because of its toxicity, nitrobenzene has been placed as one of the 129 priority pollutants by USEPA. There are several methods for removing nitrobenzene from waters, such as advanced oxidation, membrane filtration, ion exchange, and adsorption. High capital and regeneration costs of them, however, have encouraged researchers to look for other types of adsorbents that are less expensive.

The Songhua River nitrobenzene accident of 2005 led to serious fateful water pollution including groundwater, which reason is that about 100t chemical was leaked out into Songhua River. In this study, the feasibility of nitrobenzene removal using incinerated rice husk as an adsorbent was investigated, for the purpose of constructing the emergent drinking groundwater treatment process in rual areas. Furthermore, the adsorption mechanism and the comparative cost were also examined.

Rice husk was prepared by simple incineration. Water samples artificial containing nitrobenzene were prepared by typical groundwater along Songhua River in Jilin province. Kinetics of adsorption represents the adsorption efficiency of the nitrobenzene and determines their potential applications further. The result illustrates the initial adsorption rate is relatively high and adsorption equilibrium time is about 30 mins, which follows first order reaction kinetics model. Adsorption isotherm reflects the satisfaction of the Langmuir isotherm model with R^2=0.9719. The maximum adsorption capacity (Q^0) of nitrobenzene by rice husk calculated from the Langmuir isotherm was 204.08ug/g. With initial concentration of 85ug/L nitrobenzene, residual concentration of 5ug/L and 17ug/L were obtained by 0.7g/L and 1.7g/L dosage of rice husk after 30mins contact time, respectively.

It was reported that there were many nano interstitial pores(< 50nm) formed by the packing of nano SiO_2 particles and micron-cellular pores(~10um) in rice husk ash. Honeycomb pores, nano SiO_2 particles and nono pores lead to great specific surface(50~100m^2/g) of rice husk ash. Removal mechanism of nitrobenzene from waters is physical adsorption, chemical adsorption and ion-exchange reaction. Under 15℃ condition in this study, physical adsorption is basic removal factor.

Rice husks are agricultural waste concerning with environment pollution. Rice husk was chosen to be applied as a precursor material due to its granular structure, insolubility in water, chemical stability, high mechanical strength and its local availability at almost no cost. The advantage in the application of these adsorbents is that there is no need to regenerate them because of their low production costs.

The process of rice husk adsorption is a cost–effective technology for the treatment of groundwater polluted by nitrobenzene in rural areas, especially at household level.

*lzs008@sohu.com

P112

Towards a New Conceptualization of Colloid Filtration in Granular Porous Media

N. Ochiai[1*], M. Dragila[1], J. Parke[1]

[1]*Department of Crop and Soil Science, Oregon State University*

3017 Ag Life Science Bldg, Corvallis, OR 98661

Transport of inorganic and biotic colloids through porous media is of concern to numerous scientific and applied disciplines. Colloid filtration theory (CFT), based on the convective-dispersion equation with a first order deposition/reaction term, currently provides the primary framework for understanding of colloid retention and transport in porous media. Underlying CFT is the conceptualization of porous media as an assembly of ideal spherical 'collectors,' enabling estimation of a key model parameter, namely the frequency (η_0) of colloid contact with collector surfaces. A number of recent papers, however, demonstrate that mechanistic analysis of colloid deposition dynamics requires the ability to predict local hydrodynamic forces, which depend largely on pore geometry. Pore-scale hydrodynamics may also contribute significantly to macro-scale phenomena such as early colloid breakthrough, which are not adequately explained by CFT. Given this background, our investigations focus on developing a conceptualization of a 'unit pore' (in contrast to the 'ideal collector'), which incorporates pore-scale features and heterogeneities in the flow field relevant to colloid transport. Based on a series of direct visualization studies of colloids passing through porous media consisting of glass beads or sand, we have identified three hydrodynamic domains within pores associated with distinct colloid behaviors. These are: (i) stagnant zones near grain-to-grain contacts from which colloids are almost always excluded; (ii) low-flow zones near grain walls which are preferentially avoided by colloids. Colloids entering low-flow zones may become associated with the grain surface and permanently or temporarily removed from the general colloid population; (iii) normal-flow zones in pore centers in which colloids primarily travel along fluid streamlines. The macro-scale phenomenon of 'early colloid breakthrough' may in part be a consequence of population partitioning into normal-flow and low-flow zones.

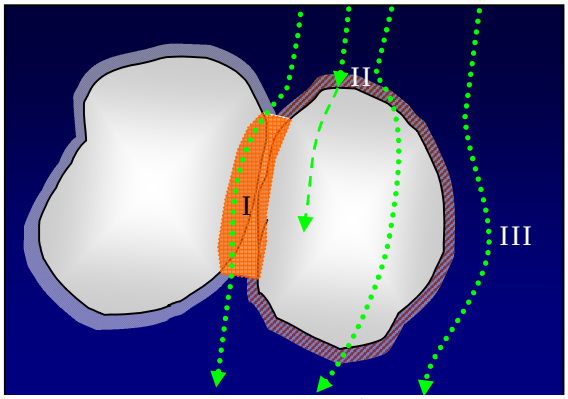

Fig. 1. 'Unit pore' consisting of 2 media grains, showing 3 hydrodynamic domains and associated particle behavior: (I) stagnant zones near grain-to-grain contacts; (II) low-flow zones near grain surface; (III) normal-flow zones in pore centers.

*ochiain@onid.orst.edu

P113

STRUCTURE FORMING COMPONENTS OF SOIL ON THE BASIS OF DERIVATIVES OF CELLULOSE

K.B. Mussabekov [1]*, S.B. Aidarova[2], N.E. Bekturganova[3], N.Sh. Stamkulov [1].

[1]*Faculty of Colloid chemistry. Kazakh National University named by Al-Farabi.*

95a Karasai Batyr str. Almaty. Kazakhstan. 050012

[2]*Almaty Technological University*

[3]*Kazakh-British Technical University*

The condition of soil resources of republic Kazakhstan causes the big alarm and represents a global problem. To unsuccessful regions concern to near Aral, Balkash, Semipalatinsk. Tens thousand hectares represent abandoned lands, ash-disposal area thermal power station, dumps of household and industrial waste products, and also coal and ore career, mountain manufactures, oil-filds. A destructive role in this plan ranges of a military-industrial complex which have deduced from a revolution more than 10 million hectares of an arable land and pastures have played.

In global practice process of structurization of mineral dispersions by synthetic polymers and polymeric complexes is one of effective methods problem-solving of degradation of soil.

We give report about results of systematical research structurization of erosion danger soil of Azgirsk graund by complexes of methyl cellulose and sodium-CMC with polythene.

Soil structurization in concentrated suspensions by sodium-CMC/PEI (polyethyleneimine) MC/PEI complete after 20-24 hours. Slowness of process is connected to slow processes of polycomplexes macromolecules adsorption on the soil particles with formation of polymeric bridges between them and changes polycomplex conformation in adsor ptive layers.

Intensity of a deflation and plastic durability of system: that the increase of concentration PEI in polycomplex at constant values concentration sodium-CMC and MC, decrease deflation intensity on 40-50 % is shown. This phenomenon is interpreted by existence of a polymeric complex as gel hydrophilic associate, which assumes interaction of the associate with superficial of the soil layer, forming water-proof crust.

Experimental data has shown that processing of soil results in formation of water-stronger aggregate, capable to maintain action of a lot of washing away water (on washout of a sample of soil in weight 160 g. it was required 20-30 liters of water).

On the basis of the got results it is possible to do a conclusion that structurization of soil by polymeric complexes sodium-CMC/PEI, MC/PEI results in decrease of a soil erosion in conditions of wind and water erosion. The opportunity of qualitative fastening land is established, that allows solving some problems of preservation of the environment connected to the soil erosion.

*KuanM@kazsu.kz

The influence of different additives on the combustion of water-dispersive polyvinylacetate paints

M.N. Abdikarimov*

Kazakh National Technical University named after K.I. Satpayev 050013,

Republic of Kazakhstan, c. Almaty

In the present time the most topical questions are the questions of high incombustibility of water-dispersive paints for the fire-resistance of metal and wooden surfaces. Fire-resistant paints are mostly needed in oil and gas industry since the abnormal wastes that occur in the oil and gas mining conditions intensify the fire risk situations. Exclusion of toxic solvents from the paint structure will improve the ecological situation and improve the air urban-industrial environment of cities and industrial regions. Many fires are conditioned by the wide usage of synthetic materials that have high level of inflammability and producing toxic gases. The issue of the day is the creation of fire-resistant paints because of the fire inflammability of most wooden materials and synthetic surfaces. Aggregative resistance of water dispersions depends on the size of the particles, emulsifier types, modifiers, stabilizers, surface-active substances (SAS) and other factors affecting surface tension, cohesion and fire-resistant properties of the paints on the metal and wooden constructions. The influence of the nature of polymeric binding agents used in the preparation of water-dispersive paints and other frothing agents - phosphates of metals and other inhibitors on the mechanism and the combustion rate were studied. Temperature distribution during the thermogravimetry, thermomechanic and pyrolysis under the influence of propane-air fire were also studied. The purpose of this research is the study of the inflammability of different water-dispersive paints on the base of polyvinyl acetate (PVA) emulsion, brand mark EKG-26A (GOST 19214-80) and paint and varnish coating on the basis copolymers: vinyl acetate (VA) with vinyl chloride (VCH), vinyl acetate (VA) with (VA) dibutyl maleate (DM), brand mark DPM 50 35B for printing industry (OST 6-05-637-78), with different additives. From the thermogravimetric curves shown on Fig.1 can be seen that copolymer VA-VCH has a loss of mass two times lower than PVA and copolymer VA-DM which is in line with the results of fire tests. As result printing of the study the following resume can be done: It was shown that pentaerythrite, ammonium phosphate monosubstituted, melamine, thricresyl phosphate, dinonilphthalate lead to the decrease of flammability of PVA-paints, flammability speed equals to 2.4-3.6 g/min and the mass loss – 22.5-43%. It was found that the most inflammable effect is reached at the introduction of dinonilphthalate and foaming inhibitors of combustion: ammonium phosphate monosubstitute, melamine and penthaeritrit $CH_2OH)_4$ –fiveatom alcohol, carbonized at the high temperature with the creation of coke layer. The speed of PVA combustion = 2.4 g/min, mass loss – 22.5%. Hardflammable PVA paints compositions for wood with the components such as threebrompropylether of phosphate acid, threethylenglikol, pentaerithrite, sulfonat, ammonium phosphate monosubstituted, additive A – thetramethylanstoffe and phosphotungstic sodium were developed.

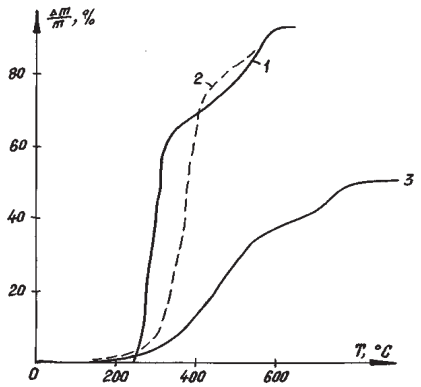

Fig. 1 Temperature dependence of loss of mass of paint samples on the air. Velosity of heating -10 °/minute; 1 – emulsion PVA; 2 – Copolymer VA-DM;3 – Copolymer VA-VCH.

The speed of combustion of the emulsion of vinylacetate and vinyl chloride copolymer at the metal bottom layer is reducing in 5 times at the introduction of 36 mass parts of the 85% additive of the phosphoric acid due to the formation of the hard carbon residue.

mn.abdikarimov@mail.ru

Evaluation through mathematic modelling of the environmental pollution by emissions of aerosols caused the manufacture of thermal phosphoric acid

R.H. Turgumbayeva

Natural geographical faculty, Kazakh National Pedagogical University named after Abai, 050100, Almaty, Republic of Kazakhstan, 8727-2202376

At present there is no generally accepted method of evaluation of impact on the environment which allows characterization of an enterprise construction project as well as an enterprise activity in the period of operation. An unbiased evaluation of the system state rests on the group of indices, having a different physical nature and basing on different methods of measurements and control.Evaluation through mathematic modelling of the environmental pollution by aerosols caused by the manufacture of thermal phosphoric acid is given in the present work. With the aim of quantitative evaluation of atmosphere pollution by aerosols we have used Pasquille-Gifford empiric model based on the assumption of constant interference-free point source of a definite capacity having homogenous characteristics of atmospheric dispersion. This model is based upon the conception of concentration of admixture emitted by a constant point source into atmosphere as of a stream with vertical Gaussian distributions and transverse to wind. In this work we have used the data on technical characteristics of the emission sources and averaged value of aerosols in the conditions of its actual operation. Calculations were made by means of universal integrated suite MATLAB. As the maximum environmental pollution takes place in the conditions of calm, we calculated for the wind velocity of 0.1 m/s, i.e. in conditions close to calm. Is shown that the aerosols is distributed over the whole territory adjacent to the plant gradually decreasing with the distance from the source of emission down to 0,1 fractions of MCL at the distance 20 km. As the emissions contain simultaneously several substances having their own corresponding maximum concentration limits values (MCL) with concentration C_i (i =1,2,3…n), it seems necessary to determine the distribution of the total concentration of aerosols of pollution agents emitted by the enterprise .The model allows prediction of the degree of atmospheric air pollution at different emission capacities and to obtain the data on the distribution of polluting aerosols and determine the zones of danger for human beings. Calculations for the emission capacity of 8.35 fractions of MCL at the mouth of conditional source show that at the situation close to calm, the concentration of aerosols does not exceed MCL. (Fig.1) .

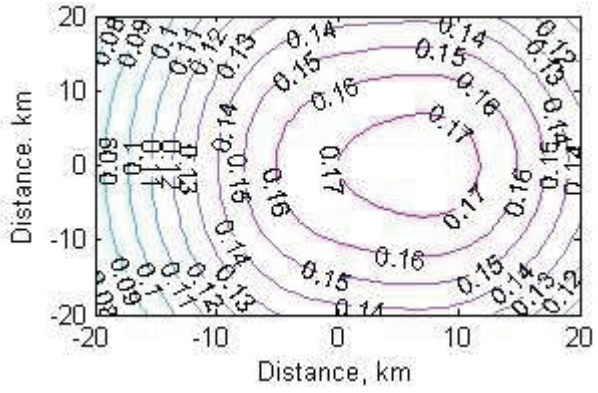

Fig.1 – Aerosols distribution in the near-surface layer of the atmosphere with the indication of areas of danger. On the curves the values of dimensionless total concentration of spray in the fractions of MCL are shown.

Thus, the presented results of the calculation of the aerosols in the near-surface layer of the atmosphere using the empiric model of Pasquille- Gifford allows prediction the distribution concentration of toxic substances of aerosols within the area, and so allows to single out the most sites of the contaminated area. The feasibility of singling out the areas most harmful for human health is realized.

E-mail: rturgumbayeva@mail.ru

Study of Ionic surfactants Binding to Humic Acid and Fulvic Acid by Dynamic Light Scattering and Potentiometric Titration

M. M. Yee, T. Miyajima, H. Kodama, and N. Takisawa*
Department of Chemistry and Applied Chemistry,
Faculty of Science and Engineergin, Saga University,
1 Honjyomachi, Saga 840-8502, JAPAN

Surfactant is a potential probe to study the surface property of humic substances which play a crutial role in environment. The interaction of anionic surfactant, sodium dodecyl sulfate (SDS) with Aso humic acid (AHA) has been studied by dynamic light scattering (DLS) and potentiometric titration methods at two pH regions and ionic strengths. At pH 9.18 and low ionic strength, no binding is observed between SDS and AHA in the investigation by both methods, whereas some interaction is observed at pH 3.98 and at high ionic strength by DLS measurement (Fig. 1) since electrostatic repulsion is suppressed by counterions at this solution condition.

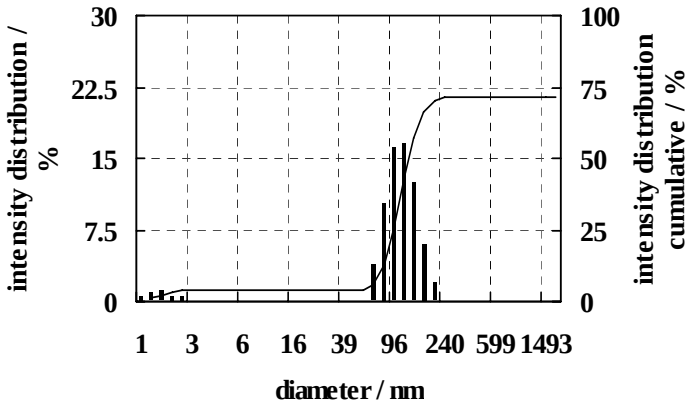

Fig. 1 Representative histogram of the particle size distribution for SDS-AHA system

The binding between cationic surfactant, dodecyltrimethylammonium ion ($DTMA^+$) with Aso fulvic acid (AFA) and AHA has also been investigated by both methods and compared with that of dodecylpyridinium ion ($C12Py^+$). The binding of $DTMA^+$ ions with AFA/AHA is weaker than that of $C12Py^+$ ions, presumably due to the steric hindrance of headgroup of $DTMA^+$ ions and the possible aromatic interaction of $C12Py^+$ ions. The hydrodynamic diameter of $DTMA^+$-AFA or -AHA aggregates is smaller than that of $C12Py^+$-AFA or -AHA aggregates (Fig. 2), which may reflect the interaction strength.

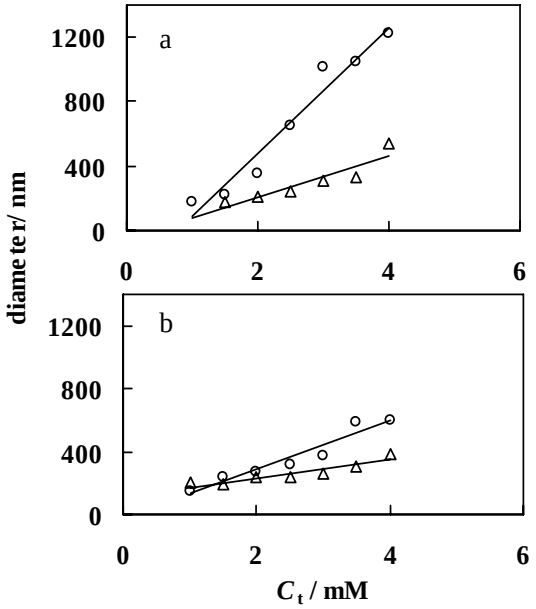

Fig. 2 Concentration dependence of particle size. (a) AFA system, (b) AHA system, and (o) $C_{12}Py^+$, (Δ) $DTMA^+$.

*takisawa@cc.saga-u.ac.jp

Author Index

Hall Map

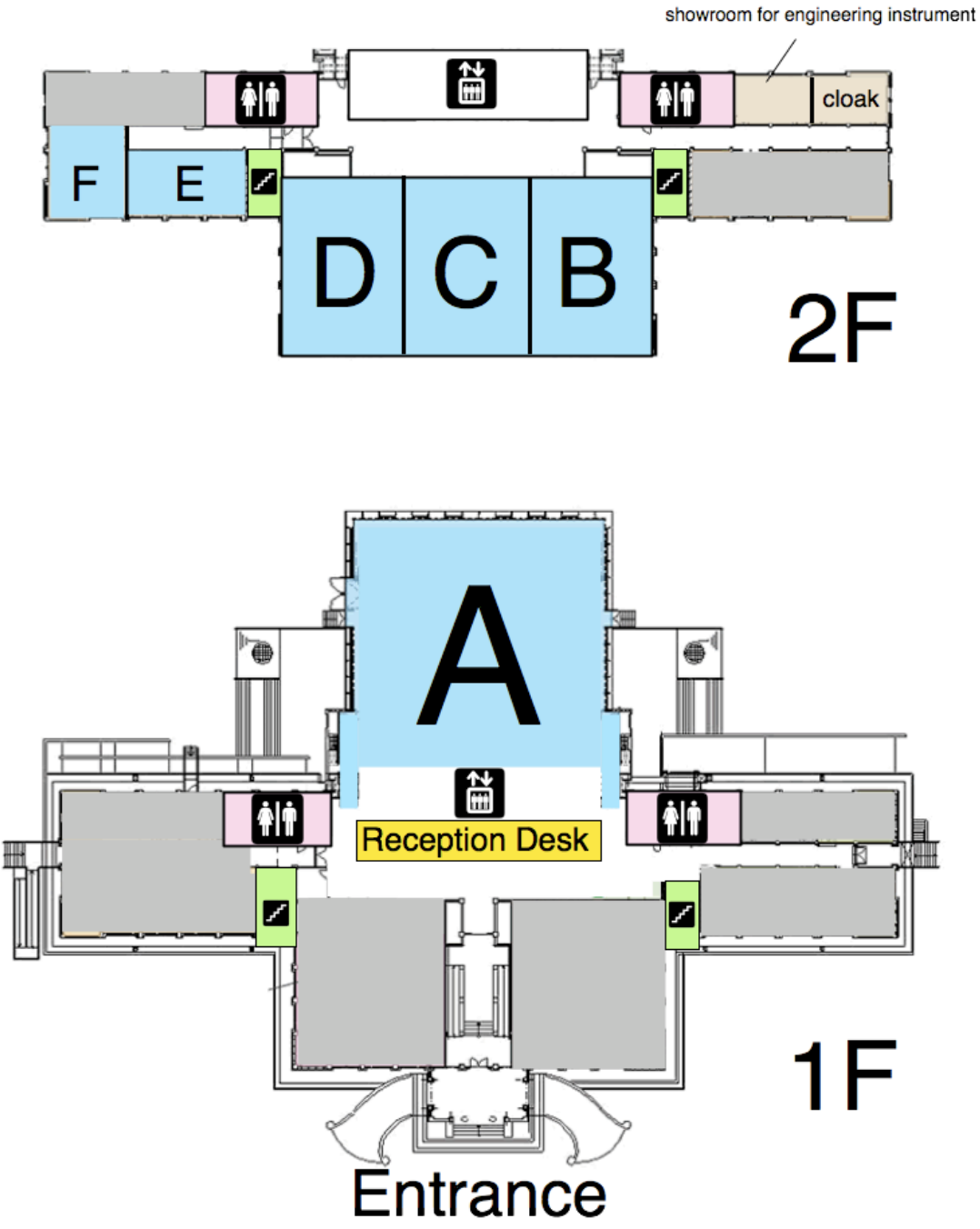
showroom for engineering instrument
cloak
F
E
D
C
B
2F
A
Reception Desk
1F
Entrance

Timetable of IAP2008

June 1

Room A		Room B	Room E	Room F
16:30	*Opening*			
16:40	1A01			
17:10	1A02			
17:30	1A03			
			18:00 *Welcome Mixer*	

June 2

Room A		Room B		Room E		Room F	
9:00	2A01						
9:30	2A02						
9:50	2A03						
10:10	2A04						
10:30	2A05						
10:50	*Break*						
11:10	2A06						
11:30	2A07						
11:50	2A08						
12:10	2A09						
12:30	*Lunch*						
14:00	2A11	14:00	2B11	14:00	2E11	14:00	2F11
14:20	2A12	14:20	2B12	14:20	2E12	14:20	2F12
14:40	2A13	14:40	2B13	14:40	2E13	14:40	2F13
15:00	2A14	15:00	2B14	15:00	2E14	15:00	2F14
15:20	*Break*	15:20	*Break*	15:20	*Break*	15:20	*Break*
15:40	2A15	15:40	2B15	15:40	2E15	15:40	2F15
16:00	2A16	16:00	2B16	16:00	2E16	16:00	2F16
16:20	2A17	16:20	2B17	16:20	2E17	16:20	2F17
16:40	2A18	16:40	2B18	16:40	2E18	16:40	2F18

Room C & D	
17:30	*Poster Session P001 - P112 (Buffet)*

June 3

Room A		Room B		Room E		Room F	
9:00	3A01						
9:30	3A02						
9:50	3A03						
10:10	3A04						
10:30	*Break*						
10:50	3A05						
11:10	3A06						
11:30	3A07						
11:50	3A08						
12:10	*Lunch*						
14:40	3A11	14:40	3B11	14:40	3E11	14:40	3F11
15:00	3A12	15:00	3B12	15:00	3E12	15:00	3F12
15:20	3A13	15:20	3B13	15:20	3E13	15:20	3F13
15:40	3A14	15:40	3B14	15:40	3E14	15:40	3F14
16:00	*Break*	16:00	3B15	16:00	*Break*	16:00	*Break*
16:20	3A15	16:20	3B16	16:20	3E15	16:20	3F15
16:40	3A16			16:40	3E16	16:40	3F16
17:00	3A17			17:00	3E17	17:00	3F17
17:20	3A18			17:20	3E18	17:20	3F18

Room A		Room B & C & D	
18:00	*Cultural Event*		
		18:30	*Banquet*

June 4

Room A		Room B		Room E		Room F	
9:00	4A01						
9:30	4A02						
9:50	4A03						
10:10	4A04						
10:30	*Break*						
10:50	4A05						
11:10	4A06						
11:30	4A07						
11:50	4A08						
12:10	4A09						
12:30	*Lunch*						
14:00	4A11	14:00	4B11	14:00	4E11	14:00	4F11
14:20	4A12	14:20	4B12	14:20	4E12	14:20	4F12
14:40	4A13	14:40	4B13	14:40	4E13	14:40	4F13
15:00	4A14	15:00	4B14	15:00	4E14	15:00	4F14
15:20	*Break*	15:20	*Break*	15:20	*Break*	15:20	*Break*
15:40	4A15	15:40	4B15	15:40	4E15	15:40	4F15
16:00	4A16	16:00	4B16	16:00	4E16	16:00	4F16
16:20	4A17	16:20	4B17	16:20	4E17	16:20	4F17
16:45	*Farewell*						